

Wissenschaftszentrum Weihenstephan  
für Ernährung, Landnutzung und Umwelt  
Lehrstuhl für Ökologische Chemie und Umweltanalytik  
der Technischen Universität München

*Investigation of Tobacco Pyrolysis Gases and Puff-by-puff Resolved Cigarette  
Smoke by Single Photon Ionisation (SPI) – Time-of-flight Mass Spectrometry  
(TOFMS)*

**Thomas Adam**

Vollständiger Abdruck der von der Fakultät Wissenschaftszentrum Weihenstephan für Ernährung, Landnutzung und Umwelt der Technischen Universität München zur Erlangung des akademischen Grades eines

**Doktors der Naturwissenschaften (Dr. rer. nat.)**

genehmigten Dissertation.

Vorsitzender: Univ.-Prof. Dr.-Ing. Roland Meyer-Pittroff

Prüfer der Dissertation:

1. Univ.-Prof. Dr. rer. nat., Dr. h.c. (RO) Antonius Kettrup
2. Univ.-Prof. Dr. rer. nat., Dr. agr. habil., Dr. h.c. (Zonguldak University/Türkei) Harun Parlar
3. Univ.-Prof. Dr. rer. nat. Ralf Zimmermann,  
Universität Augsburg

Die Dissertation wurde am 07.03.2006 bei der Technischen Universität München eingereicht und durch die Fakultät Wissenschaftszentrum Weihenstephan für Ernährung, Landnutzung und Umwelt am 12.06.2006 angenommen.



**FÜR MEINE ELTERN**

**IN GEDENKEN AN RAINER MINIGSHOFER**

„Die Forschung ist immer auf dem Wege, nie am Ziel.“

Adolf Pichler

# Contents

<b>1. INTRODUCTION.....</b>	<b>4</b>
1.1. HISTORY OF TOBACCO CONSUMPTION .....	6
1.2. HISTORY OF HEALTH-RELATED TOBACCO RESEARCH .....	7
1.3. STATUS QUO OF TOBACCO SMOKE RESEARCH TODAY .....	9
1.4. CIGARETTE SMOKE CHEMISTRY .....	19
1.4.1. INFLUENCE OF TEMPERATURE AND OXYGEN LEVEL ON SMOKE FORMATION .....	19
1.4.2. FORMATION PATHWAYS OF TOBACCO SMOKE CONSTITUENTS .....	24
1.4.2.1. CARBON MONOXIDE AND CARBON DIOXIDE.....	24
1.4.2.2. NITROGEN OXIDES, AMMONIA, HYDROGEN CYANIDE, AND AMINES .....	24
1.4.2.3. HYDROCARBONS .....	25
1.4.2.4. CARBOXYLIC COMPOUNDS .....	27
1.4.2.5. PHENOLIC COMPOUNDS .....	27
1.4.2.6. ACIDS .....	27
1.4.2.7. N-HETEROCYCLIC COMPOUNDS .....	27
1.4.2.8. NITROSAMINES .....	29
1.4.2.9. METALS.....	31
1.4.2.10. FREE RADICALS .....	31
1.5. MOTIVATION .....	33
<b>2. METHOD AND INSTRUMENTATION.....</b>	<b>34</b>
2.1. PRINCIPLE OF THE SINGLE PHOTON IONISATION PROCESS .....	35
2.2. TIME-OF-FLIGHT MASS SPECTROMETRY .....	41
2.3. CHARACTERISATION OF THE SPI-TOFMS INSTRUMENT .....	44
<b>3. PYROLYSIS EXPERIMENTS OF TOBACCO.....</b>	<b>54</b>
3.1. INTRODUCTION TO PYROLYSIS .....	54
3.2. EXPERIMENTAL SET-UP OF PYROLYSIS EXPERIMENTS .....	56
3.3. SAMPLE PREPARATION.....	58
3.4. RESULTS AND DISCUSSION OF PYROLYSIS EXPERIMENTS .....	60
3.4.1. SPECTRA PROCESSING AND MASS ASSIGNMENT .....	60
3.4.2. INFLUENCE OF TEMPERATURE AND REACTION GAS COMPOSITION ON TOBACCO PYROLYSIS.....	64
3.4.3. INTRODUCTION TO THE THREE MAIN TOBACCO TYPES .....	82

---

3.4.3.1. BURLEY TOBACCO .....	83
3.4.3.2. VIRGINIA TOBACCO .....	84
3.4.3.3. ORIENTAL TOBACCO.....	85
3.4.3.4. DISCRIMINATION OF TOBACCO TYPES BY SUM PARAMETERS .....	86
3.4.4. DISCRIMINATION OF TOBACCO TYPES BY ADVANCED STATISTICAL METHODS .....	87
3.4.4.1. DIFFERENCE SPECTRUM.....	88
3.4.4.2. FISHER-RATIOS .....	93
3.4.4.3. PRINCIPAL COMPONENT ANALYSIS .....	99
3.5. CONCLUSION OF THE PYROLYSIS EXPERIMENTS.....	104
<b>4. PUFF-BY-PUFF RESOLVED MEASUREMENTS OF CIGARETTE SMOKE .....</b>	<b>105</b>
4.1. INTRODUCTION TO SMOKING EXPERIMENTS.....	105
4.2. EXPERIMENTAL SET-UP OF SMOKING EXPERIMENTS.....	108
4.3. SAMPLE CIGARETTES .....	111
4.4. RESULTS AND DISCUSSION OF SMOKING EXPERIMENTS.....	114
4.4.1. SPECTRA PROCESSING.....	114
4.4.2. SELECTION OF HAZARDOUS TARGET COMPOUNDS FOR QUANTIFICATION.....	116
4.4.3. CHARACTERISATION OF THE 2R4F RESEARCH CIGARETTE .....	120
4.4.3.1. TOTAL YIELDS OF WHOLE SMOKE AND GAS PHASE.....	120
4.4.3.2. DRAWBACKS OF THE SMOKING REGIME .....	121
4.4.3.3. PUFF-BY-PUFF RESOLVED CHARACTERISATION OF WHOLE SMOKE AND GAS PHASE.....	125
4.4.3.4. QUANTITATIVE EVALUATION.....	126
4.4.4. DIFFERENT TOBACCO TYPES COMPARED TO THE 2R4F CIGARETTE.....	142
4.4.5. DIFFERENT CIGARETTE TYPES COMPARED TO THE 2R4F CIGARETTE.....	152
4.5. CONCLUSION OF THE SMOKING EXPERIMENTS .....	159
<b>5. CONCLUSION AND OUTLOOK.....</b>	<b>160</b>
<b>6. APPENDIX .....</b>	<b>166</b>
6.1. FIGURES .....	166
6.1.1. DIFFERENT TOBACCO TYPES COMPARED TO THE 2R4F CIGARETTE.....	166
6.1.2. DIFFERENT CIGARETTE TYPES COMPARED TO THE 2R4F CIGARETTE.....	178
6.2. TABLES.....	190
6.2.1. CLEANING PUFFS ADDED TO SMOKING PUFFS.....	190
6.2.2. CLEANING PUFFS NOT ADDED TO SMOKING PUFFS .....	197

---

<b>7. REFERENCES .....</b>	<b>204</b>
ABBREVIATIONS .....	241
LIST OF FIGURES .....	243
LIST OF TABLES .....	249
ACKNOWLEDGMENT .....	252
LIST OF PUBLICATIONS .....	253
I. PEER-REVIEWED SCIENTIFIC ARTICLES .....	253
II. POSTER PRESENTATIONS .....	255
III. ORAL PRESENTATIONS AND CONFERENCE CONTRIBUTIONS .....	256
CURRICULUM VITAE .....	257

## 1. Introduction

According to the World Health Organisation (WHO) 32.5 % of the German population between 18 and 59 years smoke (examined time period: 2002 to 2005). This number, which incorporates daily and occasional smokers, is divided into a female fraction of 28.0 % and a male fraction of 37.3 %. At the same time the smokers' fraction of young people was 33.0 %. In this context an adolescent smoker is defined as smoking at least once a week and being 15 years of age or older. The proportion of adult smokers has slightly decreased over the years (1994 – 1998: ca. 40 % smoked) whereas the proportion of adolescent smokers has increased (1993 – 1996: 20 % smoked) [1]. Subsequently about one third of the German population are smokers, two thirds are non-smokers. Different positions often culminate in conflicts between both parties. Non-smokers are affected frequently by the smoking habit of their opponents. In turn, smokers often feel hostility and constriction. Recently, this controversy was present in the media again due to the ban of smoking in pubs and restaurants in Ireland, Norway, and Italy [2]. Detailed information of all European countries regarding the proportion of smokers and related statistics can be found in [1]. It is well-known that active as well as passive smoking damages human health and harmful effects can even lead to death [3]. It is believed that approximately 110,000 people die every year from tobacco smoking related diseases in Germany [4, 5]. In 2002, related economic costs were estimated to be up to 20 billion Euro (€). One third (7 billion €) is caused by health care, whereas the rest is assigned to loss of labour due to illness (13 billion €). Smokers have a shorter life expectancy and it is estimated that, in total, 1.6 million years are lost. Half of these 1.6 million years is related to the employable age of the smokers [4, 6]. A comprehensive overview on estimated costs of tobacco use in the U.S. can be found in [7, 8]. Because of these facts smoking also strongly influences economic work power. On the other hand, besides these long-term negative economic effects, the government profits from enormous income due to tobacco tax which amounted to 13.8 billion € in Germany in 2004 [9]. In addition, the recently passed prohibition of advertising of tobacco products caused sales shortfalls of approximately 100 million € per year [10]. Furthermore, the tobacco industry represents an important employment market sector. In 2000, the total estimated employment in tobacco-related occupations in the European Union (EU) Countries (15 member states) was 190,100 jobs. This represents 0.13 % of total employment. There were about 126,000 jobs in tobacco growing, another 13,400 in tobacco processing, and 50,700 in tobacco manufacturing [11, 12]. Besides cotton, tobacco is the most widely grown commercial non-food crop in the world

[13]. As a consequence, tobacco and tobacco consumption is an important issue of our modern society which affects everyone, regardless if smoker or non-smoker.

Due to this background, many researchers and scientists of various fields are dealing with tobacco science. For the analytical chemist, tobacco and especially tobacco smoke exhibit one of the greatest challenges. On the one hand, tobacco smoke is a highly complex matrix consisting of thousands of substances of which many of them are toxic and their concentrations are at trace levels. On the other hand, this matrix is very dynamic resulting in an ever changing chemical composition [14]. In the past the great majority of studies in this field have dealt with the evaluation and characterisation of the smoke of whole cigarettes. Only very little is known about the chemical composition of the smoke within the smoking process, i.e. the inter-puff and intra-puff behaviour of smoke constituents and the occurring formation and decomposition reactions. The main reason for this lack of knowledge is the difficult analytical task of giving a comprehensive overview of many smoke components combined with a high time-resolution.

The work presented here deals with the application of a recently developed analytical technique, based on photoionisation, to investigate the thermal behaviour of tobacco and give insights into the complex processes taking place in a burning cigarette. The analytical technique employed is single photon ionisation (SPI) combined with time-of-flight mass spectrometry (TOFMS). The experimental part is based on two different approaches, and therefore, it is divided into two sub-sections. In the first one, coupling of the SPI-TOFMS to a pyrolysis furnace is described. The objective is to examine the thermal behaviour of tobacco under various stable and controlled conditions regarding temperature and reaction gas composition. Results help to unravel the complex formation and decomposition reactions taking place when tobacco is heated. In the second part a description is given of how the SPI-TOFMS is, for the first time, connected to a cigarette smoking device to investigate the behaviour of cigarette smoke constituents on a puff-by-puff basis. After a general characterisation of the smoking process, further applications of the analytical set-up are demonstrated by examining the influence of different tobaccos and cigarette types on smoke composition with the main focus on hazardous species. The thesis is structured as follows. In Chapter 1 an overview on the history and status quo of tobacco smoke science is given. It points out the achievements but also the limitations of tobacco smoke analysis and describes the objective as well as motivation for starting this project. In Chapter 2 the analytical technique, SPI-TOFMS, is introduced and characterised in detail. Chapter 3 deals with the first of the two main experimental sections within this work, the coupling of the SPI-TOFMS

to a pyrolysis furnace, and describes and discusses the experiments performed. The second experimental part, the smoking of real cigarettes by coupling the SPI-TOFMS to a smoking machine, is covered in Chapter 4. In Chapter 5 both experimental sections are briefly summarised and an outlook is given on future activities in that field which are based on the achievements gained within this work. The thesis closes with the Appendix in Chapter 6 and the referred literature in Chapter 7.

## 1.1. History of tobacco consumption

It is believed that tobacco began growing in North and South America about 6,000 B.C. The first pictorial record on the smoking of tobacco is depicted in artwork of the Maya people of the Yucatan region of Mexico. A pottery vessel dating from before the eleventh century shows a Mayan smoking a roll of tobacco leaves tied with a string. In this context tobacco consumption was part of political gatherings and religious ceremonies [15].

In 1492, Christopher Columbus and his crew were the first Europeans who encountered tobacco smoking. The form of cigar Columbus had first seen was a thick, long bundle of twisted tobacco leaves wrapped in dried leaves of maize or palm. Besides Columbus, the Spanish explorer Hernando Cortez confirmed in 1519 that tobacco smoking was also practiced by the Aztecs in Mexico. However, it is known that elsewhere on the American continent tobacco was smoked in pipes, chewed, eaten, drunk, or rubbed into the body long before the Europeans arrived [16, 17]. In 1535 the Frenchman Jacques Cartier encountered natives on the island of Montreal, Canada, who smoked tobacco [18, 19].

The first person known to have cultivated tobacco in Europe was Jean Nicot, the French ambassador to Portugal. He introduced tobacco and tobacco smoke at the royal court of Paris, where Catherine de Medici and her son, King Charles IX, used it to treat migraine headaches [20]. From then it rapidly spread and was grown all over Europe [19]. In 1570, the botanist Jean Libault gave the plant the scientific name *Herba Nicotiana*, in honour of John Nicot. The name tobacco is derived from the American Indians' word *tobacco* [18]. The Spanish noun *cigarro* originates from the Mayan verb *sikar*, meaning to "smoke" [18]. The major reason for the plant's growing popularity was its believed medicinal benefit. For instance, in 1571, a Spanish doctor named Nicolas Monardes reported about medicinal plants of the new world

and claimed that tobacco could cure 36 health problems [19]. In the early 17<sup>th</sup> century, English settlers in North America realised the potential of growing tobacco for export [17]. Meanwhile, tobacco was so popular that it was frequently used as money. Consumption and cultivation increased tremendously and the plant became one of the greatest export goods of the United States [21], which also played a role in the initiation of black slavery. In the following centuries only the consumer's preference of consumption of tobacco changed. In the 17<sup>th</sup> century pipes were the most popular, in the 18<sup>th</sup> century snuff held sway. In contrast, the 19<sup>th</sup> century was the age of the cigar. The first cigarette machine patent was granted in 1880 and the growing demand resulted in the foundation of many tobacco processing companies, e.g. Phillip Morris (1847) and RJ Reynolds (1875) (both in the USA), British American Tobacco (1902) and Imperial Tobacco Company (1901) (both in the UK). Technical progress ensured the domination of the machine-manufactured cigarette in the 20<sup>th</sup> century [21]. In the 1950s cigarette manufacturers launched the first filter-tipped cigarettes, similar to the ones we know today [14, 22].

## 1.2. History of health-related tobacco research

For years after the discovery of tobacco by the Spanish conquistadors, the vast majority of consumers considered smoking as a pleasant indulgence which even included medicinal benefits. However, over the years, a growing number of people suspected possible harmful effects, perhaps even fatal effects for the body. In 1604, King James I of England wrote *A Counterblaste to Tobacco* [19, 23] and in 1610, Sir Francis Bacon described that trying to quit the smoking habit was very hard [19]. Probably the first clinical study of tobacco effects was carried out by John Hill in England in 1761. He warned snuff users that they were vulnerable to nasal cancers [1, 19]. Soon afterwards, in 1787, Percival Pott linked cancer of the lip to tobacco snuff [24] and in 1795, Sammuell Thomas von Soemmering reported on cancer of the lip in pipe smokers [1, 21]. In general, tobacco cancers were first recognised in visible organs like the oral cavity. A reason for this was the fact that people rarely inhaled tobacco smoke prior to the invention of cigarettes as it was too harsh [24]. In 1828, the chemists Wilhelm Heinrich Posselt and Ludwig Reimann of the University of Heidelberg, isolated and purified nicotine and described it as the major pharmacologically active ingredient in tobacco [18, 21,

23]. In 1849, Joel Shew attributed 87 different diseases or ill effects to tobacco, including insanity, cancer and haemorrhoids [23]. Moreover, Adolf Pinner revealed the chemical structure of nicotine as 3-(1-methyl-2-pyrrolidinyl)pyridine in 1895 [18]. By the end of the 19<sup>th</sup> century cancer of the lips, tongue, jaw, mouth, pharynx, and nasal cavities were known by physicians as “Smokers’ Cancers” [24, 25]. The increase in smoking world-wide also led to a rising anti-tobacco sentiment accompanied by increased awareness of the dangers of smoking. The invention of cigarettes as well as of a tobacco fermentation process known as *flue-curing* entailed a “smoother smoke” and made it possible to inhale tobacco smoke [24]. In this context, for a long time, lung cancer was not linked to smoking [24]. One reason for this is the possible time lag of smoking and the development of malignancies [26]. In the early stage of the 20<sup>th</sup> century a few but gradually growing number of reports suggested smoking to be a cause of lung cancer and other diseases [24, 26-37].

In 1950, two large-scale epidemiological studies in the USA and the UK demonstrated independently the dose-response relationship between the number of cigarettes smoked and the risk of lung cancer [38, 39]. Thenceforward, within a few years, several reports and publications were released linking smoking to cancer [40-47]. These results were supported by the induction of skin tumours in mice painted with the particulate matter of cigarette smoke [48-50]. Moreover, Cooper et al. identified benzo[*a*]pyrene (BaP) as the first carcinogen in cigarette smoke in 1954 [51]. Furthermore, in 1973, Dontenwill et al. developed a method that exposed Syrian golden hamsters to cigarette smoke diluted with air which led to the formation of tumours in the hamsters’ larynx [52, 53]. These and other scientific reports on the health effects of tobacco smoking resulted in intensive research on the general chemical composition of cigarette smoke as well as on the identification and quantification of toxic and carcinogenic agents in smoke. The rising interest in the chemical and toxicological properties of tobacco smoke is reflected in the progressive identification of smoke constituents. Johnstone et al. listed 600 species in 1959 [54]. In 1968, Stedman extended the number to 1,000 [55]. By 1988, Roberts reported of 3794 chemicals in cigarette smoke [56]. The latest figures (1996) deal with ca. 4800 tobacco smoke constituents [57].

### 1.3. Status quo of tobacco smoke research today

The world-wide greatly increasing number of publications in tobacco science after recognising the severe health effects of smoking entailed standardisation of the analytical smoking process in order to make results of different laboratories comparable [58]. Several institutions and organisations, mainly the Federal Trade Commission (FTC) in the USA in 1966, the UK Tobacco Research Council in 1972, the Deutsche Institut für Normung (DIN), the international operating Centre de Coopération pour les Recherches Scientifiques Relatives au Tabac (CORESTA) in 1969 and the International Organisation for Standards (ISO) in 1977 developed smoking standards. In addition, several authorities, e.g. in Canada, Australia, New Zealand, and Japan established their own standard methods by the late 1980s. Reviews and detailed information about developments of smoking machines, standard smoking conditions, and related things can be found in [58-62]. All these standardisation methods were identical regarding puffing parameters but differed in the type of smoking machine used, the butt length specified, the method of collection of the smoke particulate phase and in some aspects of the analytical methodology of routine measurements. The puffing parameters for all standard conditions are the same, namely a puff volume of 35 mL, puff frequency of one puff per minute, and puff duration of two seconds. All cigarette smoking measurements carried out in this work are adjusted to these standardisations. Concerning further parameters, the conditions established by ISO have been maintained since these regulations are accepted world-wide. These are, for instance, that the filter cigarettes are smoked to a butt length of the filter plus eight mm or to a butt length plus filter tipping overwrap plus three mm, whichever comes first. The cigarettes were stored for several days under controlled conditions of 60 % relative air humidity and 22 °C [60]. The smoking procedure was performed by a custom-made smoking machine based. Separation of the smoke particulate phase from the gas phase, if required, was achieved by application of a quartz fiber filter pad stabilised by an organic binder [63]. This so-called Cambridge filter, since it was originally manufactured by the Cambridge Filter Corporation, Syracuse, New York, was first described in 1959 by Wartman et al. [64]. The filter pad traps particles larger than 0.1 µm present in the cigarette smoke aerosol with 99.9 % efficiency, while gas phase smoke components pass through the filter. Trapped material is usually referred to as total particulate matter (TPM) [60]. In principle, TPM is a simple measurement which can be quantified by the weight of particulate matter collected on the Cambridge pad. "Tar" is defined as the weight of TPM per cigarette less the weight of nicotine and water. Tar values per cigarette measured under ISO conditions are

nowadays routinely printed on cigarette packs in many countries. Figure 1 shows an unused (right) and used (left) Cambridge filter, on which is deposited the particulate phase of a single common research cigarette smoked under ISO conditions.



Figure 1: Photograph of a Cambridge filter pad (diameter 44 mm) before (right) and after (left) the smoking of one cigarette

Humans smoke cigarettes differently to the standardised machine puffing conditions. In this context it is known that no smoker features an identical smoking behaviour and even the same smoker smokes differently in different situations [65-67]. This fact complicates the significance of results achieved by machine smoking and their relevance to human smokers. There have been studies reporting on the phenomenon of compensation whereby the human smoker may increase the puff volume and/or frequency in order to increase the yield of smoke constituents over that obtained using a standardised smoking machine [67, 68]. Furthermore, it has also been reported that the placement of the ventilation holes around the filter could provide the opportunity for the smoker either consciously or unconsciously to block the ventilation holes, thereby obtaining an increased yield of smoke constituents. Both effects are partial for most smokers [69, 70].

Unburnt tobacco contains approximately 2,500 substances. About 1,100 of these constituents are transferred unchanged from tobacco to the generated tobacco smoke. Roughly 1,400 substances are unique to tobacco only, i.e. they are not volatile enough to transfer to smoke and/or decompose when tobacco burns [63]. In contrast, in tobacco smoke more than 4,800

components have been identified. However, advances in chemical analytical techniques showed that more than 10,000 substances might be present [71, 72]. Moreover, estimations of the number of unidentified species have been as high as 100,000 [73]. The highly complex and dynamic smoke matrix is composed of a gas phase (also called vapour phase) and a particulate phase whereas many substances are partitioned between these two phases. The gas phase is comprised of approximately 400 to 500 individual compounds [74] and about 300 can be classified as semi-volatiles [75]. The greater number of smoke constituents appears in the particulate fraction which is often colloquially referred to as *condensate* [63, 76]. The smoke particles are predominantly liquid, with water making up approximately 20 % of the droplet volume and, consequently, they have spherical shapes. There are some  $10^9 - 10^{10}$  particles per  $\text{cm}^3$  fresh mainstream smoke, making it an extremely dense aerosol. Mainstream smoke (MSS) is the fraction of smoke which is inhaled by the smoker. Initially the particles vary in diameter from less than 0.1 to 1.0  $\mu\text{m}$ , having a count median diameter in the range of 0.18 to 0.34  $\mu\text{m}$  [77-81]. These very high concentrations and small sizes are such that the particles will rapidly coagulate, resulting in sizeable decreases in number concentration and increases in average particle diameter within fractions of seconds. The size of smoke particles will also increase in moist environments due to absorption of water vapour. This is particularly important in the respiratory tract [82].

The approximate chemical composition of the whole mainstream smoke from a non-filter American-blend cigarette, smoked under the ISO standard smoking machine conditions, is illustrated in Table 1. The cigarette yielded 500 mg whole smoke, of which the particulate phase weighed 22.5 mg, i.e. 4.5 % by weight of the total smoke. For this cigarette the nicotine amounted to 1.5 mg and the 'tar' yield is 17.5 mg. Thereby, about 76 % by weight of the mainstream smoke is ambient air, nearby 17 % consists of the gases carbon dioxide ( $\text{CO}_2$ ), carbon monoxide (CO), hydrogen ( $\text{H}_2$ ), and methane ( $\text{CH}_4$ ). The water ( $\text{H}_2\text{O}$ ) content amounts to approximately 2 %.

Table 1: Approximate chemical composition of whole mainstream smoke in percentage by weight [63]

<b>Smoke component</b>	<b>%</b>
<i>Air</i>	
Nitrogen (N <sub>2</sub> )	62
Oxygen (O <sub>2</sub> )	13
Argon (Ar)	0.9
$\Sigma$ : 75.9	
<i>Gas phase</i>	
H <sub>2</sub> O	1.3
CO <sub>2</sub>	12.5
CO	4
H <sub>2</sub>	0.1
CH <sub>4</sub>	0.3
Hydrocarbons	0.6
Aldehydes	0.3
Ketones	0.2
Nitriles	0.1
Heterocyclics	0.03
Methanol	0.03
Organic acids	0.02
Esters	0.01
other compounds	0.1
$\Sigma$ : 19.6	
<i>Particulate phase</i>	
H <sub>2</sub> O	0.8
Alkanes	0.2
Terpenoids	0.2
Phenols	0.2
Esters	0.2
Nicotine	0.3
other alkaloids	0.1
Alcohols	0.3
Carbonyls	0.5
Organic acids	0.6
Leaf pigments	0.2
other compounds	0.9
$\Sigma$ : 4.5	

In Table 2, the identified organic smoke components are listed in 15 classes pointing out the complex and diverse composition of tobacco smoke [63]. The table does not contain the numerous metallic and inorganic components.

Table 2: Number of compounds identified in tobacco smoke addressed to different substance classes [63]

<b>Substance class</b>	<b>Number</b>
Amides, imides, lactams	237
Carboxylic acids	227
Lactones	150
Esters	474
Aldehydes	108
Ketones	521
Alcohols	379
Phenols	282
Amines	196
N-heterocyclics	921
Hydrocarbons	755
Nitriles	106
Anhydrides	11
Carbohydrates	42
Ethers	311

After the first carcinogen, benzo[*a*]pyrene, was identified in 1954, the number of detected tobacco smoke constituents thought to be relevant to smoking-related diseases increased steadily. The most comprehensive lists are those published by Dietrich Hoffmann and co-workers of the American Health Foundation in New York [3, 83-86]. Hence, these substances are sometimes colloquially called “Hoffmann analytes” and the list of the compounds is known as the “Hoffmann list”. Within the last few years, additional or revised lists of smoke toxicants have been published by e.g. Smith et al. [87-89]. Depending on the consulted source, more than 80 biologically active species in the mainstream smoke of plain, non-filter cigarettes measured under ISO conditions had been reported by the year 2000 [3, 86]. These biologically active constituents are listed in Table 3, together with their expected range of concentration and the corresponding classification according to the International Agency for Research on Cancer (IARC) categories: 1 – carcinogenic to humans; 2A – probably carcinogenic to humans; 2B – possibly carcinogenic to humans; 3 – not classifiable as to its carcinogenicity to humans.

Table 3: List of biologically active agents in the mainstream smoke of non-filter cigarettes colloquially referred to as 'Hoffmann list' [85, 86]

Smoke components of a non-filter cigarette	Yield	IARC
<i>Polynuclear Aromatic Hydrocarbons</i>		
Benz[ <i>a</i> ]anthracene	20 – 70 ng	2A
Benzo[ <i>b</i> ]fluoranthene	4 – 22 ng	2B
Benzo[ <i>j</i> ]fluoranthene	6 – 21 ng	2B
Benzo[ <i>k</i> ]fluoranthene	6 – 12 ng	2B
Benzo[ <i>a</i> ]pyrene	20 – 40 ng	2A
Dibenz[ <i>a,h</i> ]anthracene	4 ng	2A
Dibenzo[ <i>a,l</i> ]pyrene	1.7 – 3.2 ng	2B
Dibenzo[ <i>a,e</i> ]pyrene	4 – 20 ng	2B
Indeno[1,2,3- <i>cd</i> ]pyrene	0.6 ng	2B
5-Methylchrysene	20 – 70 ng	2B
<i>Heterocyclic Compounds</i>		
Pyridine	16 – 40 µg	
Nicotine	1.0 – 3.0 mg	
Quinoline	2 – 180 ng	
Dibenz[ <i>a,h</i> ]acridine	0.1 ng	2B
Dibenz[ <i>a,j</i> ]acridine	3 – 10 ng	2B
7H-Dibenzo[ <i>c,g</i> ]carbazole	0.9 ng	2B
Furan	18 – 30 µg	2B
Benzo[ <i>b</i> ]furan	Present	2B
<i>Aromatic Amines</i>		
Aniline	360 – 655 ng	
2-Toluidine	30 – 337 ng	2B
2-Naphthylamine	1 – 334 ng	1
4-Aminobiphenyl	2 – 5.6 ng	1
<i>N-Heterocyclic Amines</i>		
2-Amino-9H-pyrido[2,3- <i>b</i> ]indole (Aac)	25 – 260 ng	2B
2-Amino-3-methyl-9H-pyrido[2,3- <i>b</i> ]indole (MeAac)	2 – 37 ng	2B
2-Amino-3-methylimidazo[4,5- <i>b</i> ]quinoline (IQ)	0.3 ng	2A
3-Amino-1,4-dimethyl-5H-pyrido[4,3- <i>b</i> ]indole (Trp-P-1)	0.3 – 0.5 ng	2B
3-Amino-1-methyl-5H-pyrido[4,3- <i>b</i> ]indole (Trp-P-2)	0.8 – 1.1 ng	2B
2-Amino-6-methyl[1,2- <i>a</i> :3',2''- <i>d</i> ]imidazole (Glu-P-1)	0.37 – 0.89 ng	2B
2-Aminodipyrido[1,2- <i>a</i> :3',2''- <i>d</i> ]imidazole (Glu-P-2)	0.25 – 0.88 ng	2B
2-Amino-1-methyl-6-phenylimidazo[4,5- <i>l</i> ]pyridine (PhIP)	11 – 23 ng	2B
<i>N-Nitrosamines</i>		
N-Nitrosodimethylamine	2 – 180 ng	2A
N-Nitrosoethylmethylamine	3 – 13 ng	2B
N-Nitrosodiethylamine	< 2.8 ng	2A
N-Nitroso-di-N-propylamine	< 1.0 ng	2B
N-Nitroso-di-N-butylamine	< 30 ng	2B
N-Nitrosopyrrolidine	3 – 110 ng	2B
N-Nitrosopiperidine	< 9 ng	2B
N-Nitrosodiethanolamine	< 68 ng	2B
N'-Nitrosornicotine (NNN)	120 – 3700 ng	2B
N'-Nitrosoanabasine (NAB)	< 150 ng	
4-(Methylnitrosamino)-1-(3-pyridyl)-1-butanone (NNK)	80 – 770 ng	2B

<i>Aldehydes</i>		
Formaldehyde	20 – 100 µg	2A
Acetaldehyde	0.4 – 1.4 mg	2B
Acrolein	60 – 240 µg	
Crotonaldehyde	10 – 20 µg	
<i>Volatile Hydrocarbons</i>		
1,3-Butadiene	25 – 40 µg	2B
Isoprene	200 – 1100 µg	2B
Benzene	6 – 70 µg	1
Styrene	10 µg	2B
<i>Nitrohydrocarbons</i>		
Nitromethane	0.5 – 0.6 µg	2B
2-Nitropropane	0.2 – 2.2 µg	2B
Nitrobenzene	25 µg	2B
<i>Phenolic Compounds</i>		
Phenol	80 – 160 µg	
Catechol	200 – 400 µg	2B
<i>Miscellaneous Organic Compounds</i>		
Methanol	100 – 200 µg	
Acetamide	38 – 56 µg	2B
Acrylamide	Present	2B
Acrylonitrile	3 – 15 µg	2A
Vinyl chloride	11 – 15 ng	1
Ethylene oxide	7 µg	1
Ethyl carbamate	20 – 38 ng	2B
1,1-Dimethylhydrazine	Present	2B
Maleic hydrazide	1.16 µg	
Methyl isocyanate	1.5 – 5 µg	
Di-(2-ethylhexyl)phthalate	20 µg	
4,4'-Dichlorodiphenyltrichloroethane (DDT)	800 – 1200 ng	2B
Dichlorodiphenyldichloroethylene (DDE)	200 – 370 ng	2B
<i>Inorganic Compounds</i>		
Hydrogen sulphide (H <sub>2</sub> S)	10 – 90 µg	
Hydrazine	24 – 34 µg	2B
Arsenic	40 – 120 ng	1
Beryllium	0.3 µg	1
Cobalt	0.13 – 0.2 mg	2B
Nickel	< 600 ng	1
Chromium	4 – 70 ng	1
Lead	34 – 85 ng	2B
Cadmium	7 – 350 ng	1
Mercury	4 ng	
Polonium-210	0.03–1 pCi	1

The list includes, among others, ten polycyclic aromatic hydrocarbons, four aromatic amines, eleven N-nitrosamines, several heterocyclic compounds, aldehydes, and some inorganic substances. 45 of the components are possibly carcinogenic to humans, eight are probably carcinogenic to humans, and eleven are proven human carcinogens. However, for the majority of known smoke constituents in MSS, no biological data are available since they have not been tested for carcinogenicity. On the other hand, e.g. Rodgman and Green have pointed out that some of these substances have inhibitory or antitumorigenic properties in experiments with laboratory animals [90 and references in there]. For instance, Lee and co-workers [91] have reported that both nicotine and cotinine may inhibit the mutagenicity of several N-nitrosamines. Moreover, the lists mostly refer to non-filter cigarettes and reported yields of hazardous substances often originate from earlier measurements and, therefore, do not necessarily reflect the amounts in filter cigarettes consumed by the majority of smokers nowadays [92]. Substances such as DDT and N-nitrosodiethanolamine are not used in tobacco agronomy anymore and are most likely not as relevant as they used to be [90, 93]. In this context, prioritisation of known toxicants in mainstream smoke would be very helpful in order to focus on the most important species.

At least three such quantitative rankings of cigarette smoke components which are believed to cause health effects have been published in the past. The first one was drawn up by Vorhees et al. [94] in 1997 and was supported by the Massachusetts Department of Public Health Tobacco Control Program. The second ranking by Fowles and Bates was part of a year 2000 report to the New Zealand Ministry of Health [95] and was summarised in [96]. The third paper that addresses ranking, by Rodgman and Green [90], ranked the smoke constituents in various ways according to various toxicological criteria. All the reports contain evaluations of smoke constituents for carcinogenic and non-carcinogenic health effects which are summarised in the following two tables 4 and 5. The substances are ranked due to their expected hazardous potential in smoke in descending order. Fowles and Bates additionally separate non-carcinogenic health effects in cardiovascular and respiratory tract health effects.

Table 4: Three different rankings of smoke constituents by means of their carcinogenic potential in mainstream smoke [90, 94-96]

	<b>Rodgman &amp; Green</b>	<b>Fowles &amp; Bates</b>	<b>Vorhees</b>
1	1,3-Butadiene	1,3-Butadiene	1,3-Butadiene
2	Ethyl carbamate	Acrylonitrile	Acetaldehyde
3	2-Nitropropane	Arsenic	N-Nitrosodimethylamine
4	Acrylamide	Acetaldehyde	Formaldehyde, N-Nitrosornicotine
5	Acetaldehyde	Benzene	Acrylonitrile, Chromium VI
6	Quinoline	Acetamide	Arsenic
7	Acrylonitrile	NNN	Benzene
8	Ethylene oxide	N-Nitrosopyrrolidine	Hydrazine
9	N-Nitrosopiperidine	Chromium VI	Nickel
10	Formaldehyde	Cadmium	Cadmium
11	N-Nitrosodimethylamine	Formaldehyde	N-Nitrosopyrrolidine
12	Hydrazine	Hydrazine	Benzo[a]pyrene, Dibenz[a,i]anthracene
13	Cadmium	NNK	4-Aminobiphenyl, N-Nitrosodiethanolamine
14	N-Nitrosodiethylamine	N-Nitrosodimethylamine	Benzo[a]anthracene, o-Toluidine
15	DDT	DDT	Dibenz[a,h]anthracene
16	Benzene	N-Nitrosodiethylamine	Benzo[b]fluoranthene, Benzo[j]fluoranthene, Indeno[1,2,3-cd]pyrene
17	Polonium-210	Benzo[a]pyrene	Benzo[k]fluoranthene, Vinyl chloride
18	N-Nitrosoethylmethyl amine	N-Nitroso-N- dibutylamine	
19	Acetamine	N-Nitrosoethylmethyl amine	
20	N-Nitrosodi-N-butyl amine	Dibenzo[a,i]pyrene	
21	Di(2-ethylhexyl) phthalate	N-Nitrosodiethanolamine	
22	NNN	N-Nitrosopiperidine	
23	AaC	Urethane	
24	Arsenic	4-Aminobiphenyl	
25	4-Aminobiphenyl	Benzo[j]fluoranthene	
26	Chromium VI	Nickel	
27	MeAaC	Indeno[1,2,3-cd]pyrene	
28	2-Methylaniline	N-Nitroso-N-propylamine	
29	N-Nitrosopyrrolidine	Benzo[k]fluoranthene	
30	5-Methylchrysene	7H-Dibenzo[c,g] carbazole	
31	2-Aminonaphthalene	Vinyl chloride	
32	Carbazole	5-Methylchrysene	
33	Benzo[a]pyrene	Beryllium	

34	Trp-P-1	Chrysene	
35	N-Nitrosodiethanolamine	Dibenz[ <i>a,j</i> ]acridine	
36	Benzo[ <i>j</i> ]fluoranthene	Lead	
37	N-Nitrosodi-n-propyl amine	Dibenz[ <i>a,h</i> ]acridine	
38	Nickel		
39	Glu-P-1		
40	Beryllium		

Table 5: Three different rankings of smoke constituents by means of their toxic but non-carcinogenic potential in mainstream smoke [90, 94-96]

	<b>Rodgman &amp; Green</b>	<b>Fowles &amp; Bates; Cardiovascular</b>	<b>Fowles &amp; Bates; Respiratory tract</b>	<b>Vorhees</b>
1	Acrolein	HCN	Acrolein	Acrolein
2	H <sub>2</sub> S	Arsenic	Acetaldehyde	HCN
3	Acetaldehyde	m + p-Cresol	Formaldehyde	Acetaldehyde
4	HCN	o-Cresol	Cadmium	H <sub>2</sub> S
5	Hydroquinone	CO	Chromium VI	Hydroquinone
6	Nitrobenzene	Benzene	Acrylonitrile	Chromium VI
7	Acrylonitrile	Phenol	Nickel	Formaldehyde
8	Acetonitrile		Ammonia (NH <sub>3</sub> )	Acrylonitrile
9	Aniline			Phenol
10	Toluene			Acetonitrile
11	Methanol			Nickel
12	Chromium VI			Ammonia
13	NH <sub>3</sub>			Benzene
14	Naphthalene			
15	2-Nitropropane			
16	Furfural			
17	Beryllium			
18	Vinyl acetate			
19	Mercury			
20	Styrene			
21	Propylene oxide			
22	Carbon disulphide			
23	Vinyl chloride			

However, there are disagreements among scientists concerning the relevance, accuracy and procedure of establishing the rankings, mainly due to the extrapolation of pure-compound knowledge to the biological properties of a complex and dynamic mixture such as smoke containing them [90]. The assessments are rough calculations and should be considered more as a guideline for prioritisation of target compounds rather than quantifying the true cancer risk probabilities, which are done in the publications. In order to fully prioritise the relative risks of the various smoke components it is necessary to have a robust disease model and a means of verifying that the sum of the individual contributions of the components is equal to the activity of the whole smoke. The reader is referred to the literature for more information.

## **1.4. Cigarette smoke chemistry**

Tobacco smoke is a highly dynamic and complex matrix where many reactions are interrelated and occur in succession and parallel. Therefore, in order to understand the mechanisms taking place, some deeper knowledge about smoke formation and the conditions inside the cigarette with focus on the burning zone is required. This information and related basic definitions are given in the following sections. In addition, possible reaction pathways and precursors of known tobacco smoke constituents are introduced.

### **1.4.1. Influence of temperature and oxygen level on smoke formation**

Cigarette smoke can be divided into two distinct fractions, namely mainstream smoke and sidestream smoke. Mainstream smoke (MSS) is drawn through the cigarette filter or mouth end of the cigarette during a puff and usually inhaled by the smoker. In contrast, sidestream smoke (SSS) is emitted from the cigarette into the atmosphere, both during and between puffs. Between the puffs, SSS is formed by charring in the burning zone, emissions through the mouth piece, and diffusion through the cigarette paper. During the puffing, streams from combustion and effusion are generated. Another form of smoke is environmental tobacco smoke (ETS), which is tobacco smoke present in ambient air. It results from SSS and exhaled

MSS, both greatly diluted by ambient air [14, 97]. The different smoke streams are illustrated in Figure 2.

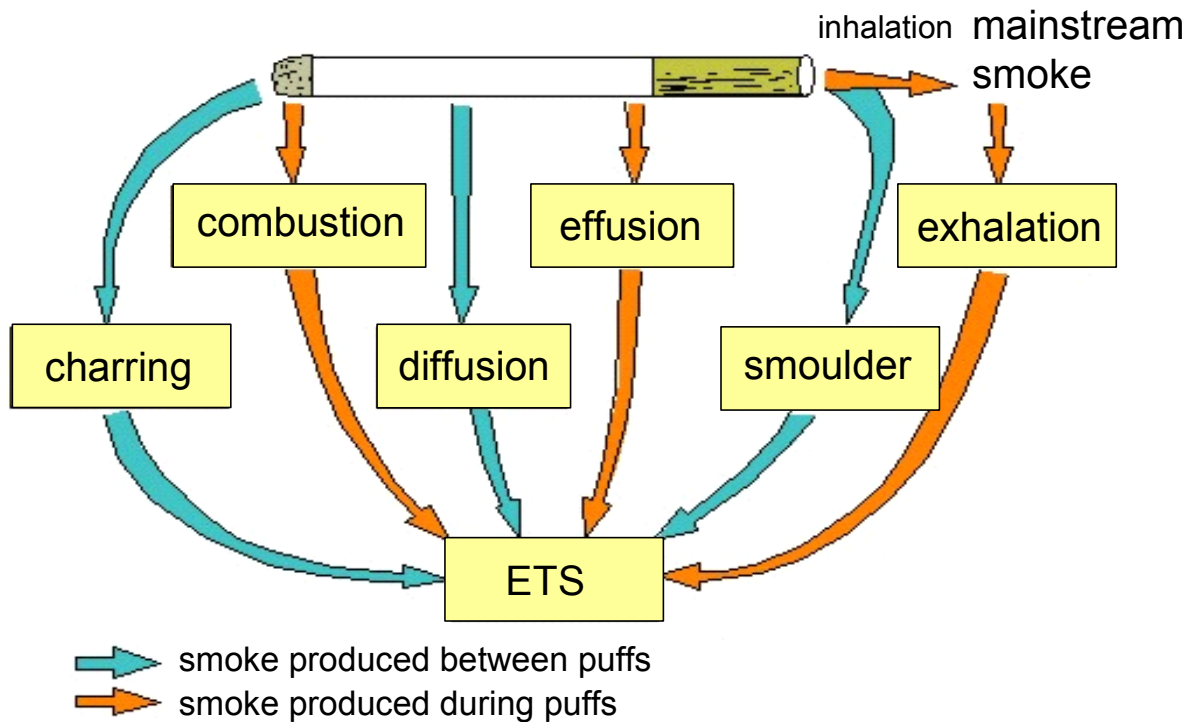
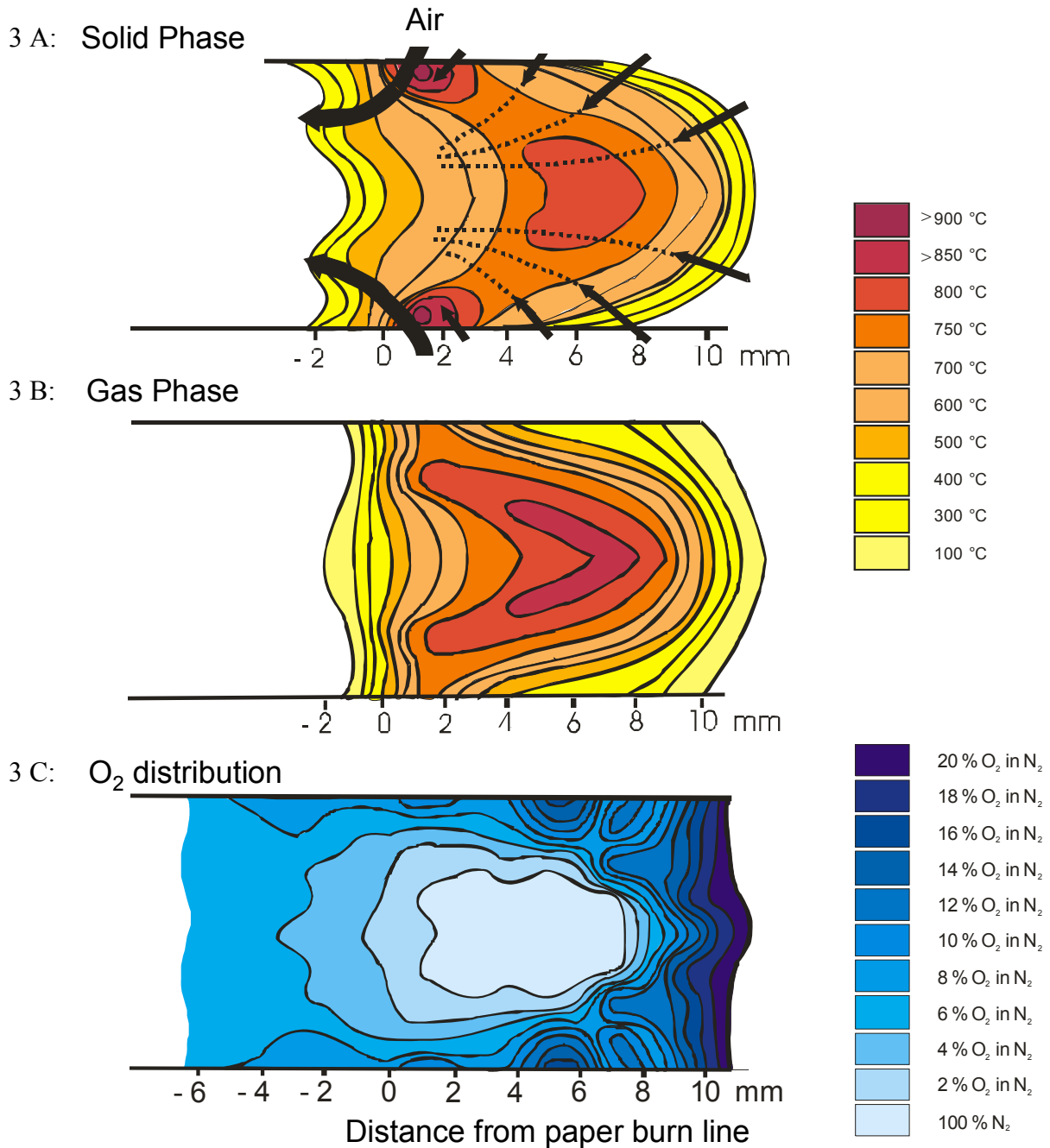


Figure 2: Different smoke streams occurring in a burning cigarette and contributing to mainstream, sidestream, and environmental tobacco smoke [97]

A burning cigarette is a very complex system in which many types of chemical reactions and physical processes occur in parallel. In this context, oxygen concentration as well as temperature and heating rate of tobacco are crucial parameters for the smoke generation process. Typical temperature distributions inside the burning cigarette during the smoking cycle are shown in Figure 3 A for the coal (solid phase) and in Figure 3 B for the gas phase [98, 99]. The figures refer to the third puff, one second after beginning of the puff, with the cigarette smoked under ISO conditions.

In general gas and solid phases are in near thermal equilibrium between puffing, with the highest temperatures of almost 800 °C occurring in the centre of the burning zone (not shown here). However, during the puff the two phases have different temperature distributions near the surface, although they are similar in the central regions. The maximum coal temperature (> 900 °C) occurs at the burning zone periphery, at about 0.2 to 1.0 mm in front of the paper burn line and one to two seconds after the start of the puff. This is where the air flux into the burning zone is the most and, therefore, where the greatest rate of combustion takes place.

The gas temperatures in the same region are lower and vary between 600 °C and 800 °C. After the puff, the solid phase temperatures at the periphery of the burning zone cool from over 900 °C to 600 °C in one second and within about four seconds, the two phases have attained quasi-equilibrium throughout the burning zone again [100, 101].



Figures 3 A, B, and C: Temperature of the coal (Fig. 3 A), temperature of the gas phase (Fig. 3 B) and oxygen contribution (Fig. 3 C) inside the burning zone of a cigarette halfway through a 2 s puff [Arrows in Fig. 3 A indicate influx of air during the puff] [98-103]

In addition, oxygen concentration and distribution are very important regarding smoke formation. Figure 3 C illustrates a typical oxygen distribution inside the burning zone. Like the temperature profiles of the coal and the gas phase, it describes the conditions after one second of the third puff. The centre of the coal is almost entirely devoid of oxygen, and this deficiency remains unchanged throughout the smoking cycle. Thus most of the incoming oxygen is consumed before it can reach the centre, even seven to eight mm in front of the burning line. Subsequently the rate of oxygen consumption is extremely rapid and demonstrates that the rate of tobacco combustion is virtually controlled by the oxygen transport [101-103].

Near the periphery of the coal at about zero to two mm in front of the burning line, the maximum influx of air occurs and oxygen is not entirely consumed because of the complete consumption of the reactant tobacco at this point. The reason for this high airflow (and the highest coal temperature) is that the viscosity and velocity of the gases in the burning zone increase with temperature, so that the burning zone has a relatively high draw resistance to gas flow [104]. Consequently, during a puff, air tends to enter the cigarette at the base of the burning zone near the paper burn line where the draw resistance is lowest. This effect is supported by the paper's increasing permeability to air when it starts to degrade at about 300 °C [105]. Therefore heat release at the base of the burning zone from exothermic combustion is the greatest and the peripheral temperatures of the solid phase exceed 900 °C [106, 107]. On the other hand, since much of the incoming air bypasses the central regions of the burning zone, the gas and solid phase temperatures there increase to a lesser extent during the puff (from just under 800 °C to about 850 °C) [99]. Moreover, as the puff progresses, an increasing fraction of air bypasses the burning zone and enters the cigarette through the paper and, therefore, dilutes the MSS [104, 107]. When the puff ends, there is a greatly reduced transport of oxygen. The periphery of the burning zone cools rapidly due to the radiation of heat to the surroundings. Subsequently, its main source of heat is now the inner core of the coal. Furthermore, relatively high oxygen concentration can be observed at about five to six mm in front of the paper burning line whereby the distance extends during the smoking (not shown here). This oxygen high spot is the position at which air entered the coal in the preceding puff resulting in burnt-out channels in the coal [102, 103].

Considering these factors, the highly complex processes during cigarette combustion can be rationalised and are shown in Figure 4.

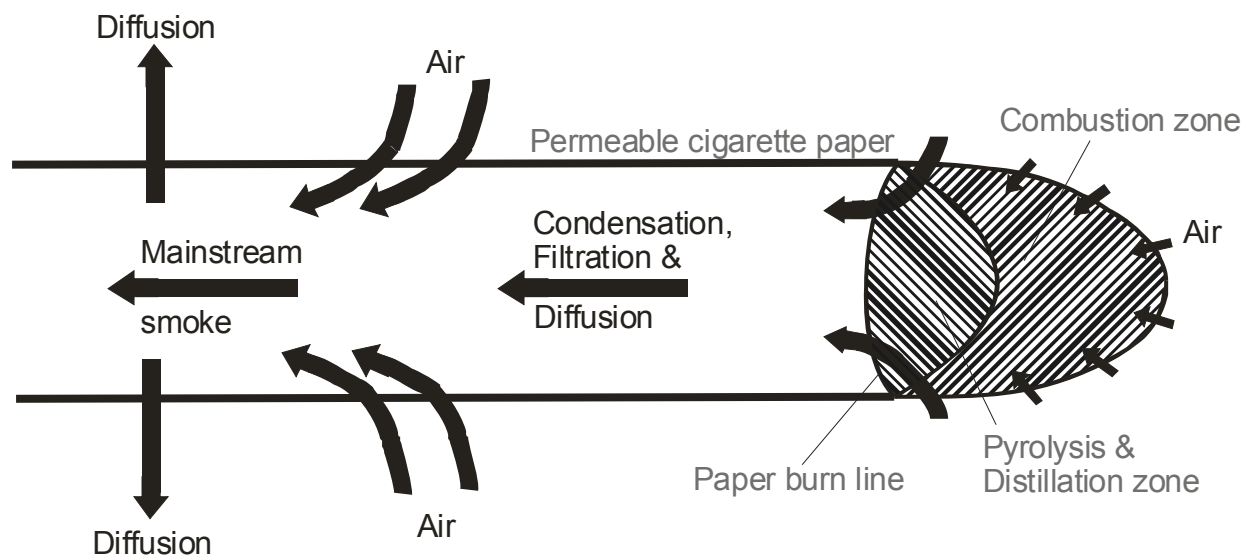


Figure 4: Illustration of combustion zone and pyrolysis/distillation zone inside the cigarette's burning zone, and other effects inside the tobacco rod influencing the composition and concentration of tobacco smoke [14]

There are two main regions inside the cigarette burning zone: an exothermic combustion zone and an endothermic pyrolysis/distillation zone. In the pyrolysis/distillation zone, the temperatures are in the range of 200 to 600 °C and the oxygen levels are relatively low. The vast majority of smoke components are generated in this region by processes which are essentially endothermic [14, 108]. Volatile smoke constituents and moisture distil out of the tobacco and non-volatile substances decompose thermally. This results in the generation of volatile gases and leaves a residual, carbonised char. In the combustion zone oxygen reacts with the carbonised tobacco forming simple combustion gases such as  $\text{CO}_2$ ,  $\text{CO}$  and  $\text{H}_2\text{O}$ , together with the release of heat which sustains the burning process. Temperatures between 700 °C to 950 °C with heating rates as high as  $500 \text{ K s}^{-1}$  are achieved [99]. As a result, a highly concentrated super-saturated vapour is generated and drawn down the tobacco rod. It cools to near ambient temperatures in a few milliseconds in the presence of diluting air entering through the paper. Thereby the vapour condenses into the aerosol particles which make up the smoke. These particles are subjected to various filtration mechanisms as they are drawn through the unburnt tobacco and cigarette filter and make up the MSS finally inhaled by the smoker [109-113].

## 1.4.2. Formation pathways of tobacco smoke constituents

The following section shows possible reaction pathways, which are assumed to be responsible for formation of several smoke components. Many of the suggested precursor-product routes have been obtained from individual pyrolysis studies. Therefore it should be borne in mind that in some of these investigations conditions might have been applied that bear only little resemblance to those inside the burning cigarette. In addition, the smoking of a cigarette is a far more complex process than isolated pyrolysis conditions and the smoke composition much too wide so that most tobacco smoke constituents are not formed from a single precursor but many tobacco ingredients can be the origin.

### 1.4.2.1. Carbon monoxide and carbon dioxide

CO and CO<sub>2</sub> are major products of cigarette smoke. Both are formed by thermal decomposition as well as combustion of all sorts of tobacco constituents such as starch, celluloses, sugars, carboxylic acids, esters, and amino acids [109]. In this context CO is formed to 30 % by thermal decomposition, to approximately 36 % by combustion of tobacco, and to at least 23 % by carbonaceous reduction of CO<sub>2</sub> [114]. Thereby ventilation of the cigarette at the filter reduces the amount of air drawn in through the burning zone leading to a lower temperature during the puff, and consequently, to a lower conversion of CO<sub>2</sub> to CO [109, 115].

### 1.4.2.2. Nitrogen oxides, ammonia, hydrogen cyanide, and amines

Nitrogen dioxide (NO<sub>2</sub>) is formed via oxidation of nitric oxide (NO) in fresh mainstream smoke if the smoke is allowed to age for a few seconds or longer. A principal source of NO is thermal decomposition of nitrates in the tobacco [98, 116-120]. Studies report a more or less linear relationship between yield of NO in mainstream smoke and tobacco nitrate level [117-119]. Furthermore, NO can be formed by oxidation of atmospheric nitrogen [118, 119] and oxidation of organic nitrogenous compounds such as protein and amino acids [119].

NH<sub>3</sub> is formed mainly from the reduction of nitrates and pyrolysis of glycine. The yields in sidestream smoke are much higher than in mainstream smoke (SSS/MSS: 40 to 170) [116].

HCN is also generated from nitrates, glycine, proline and aminodicarboxylic acids but yields in both streams are much more balanced (SSS/MSS: 2.5 to 4.7). The reason for this must be the different pyrolysis and combustion conditions of the smoking puff and the interpuff

smoulder period with emphasis on temperature and oxygen level which either favour the formation of  $\text{NH}_3$  or  $\text{HCN}$  [116, 118].

Most of the almost 200 aliphatic and aromatic amines identified in processed tobacco and tobacco smoke are formed by thermal degradation of alkaloids, protein, and amino acids. [121].

### 1.4.2.3. Hydrocarbons

Tobacco smoke contains a large variety of hydrocarbons. In this context more than 100 alkanes and 150 alkenes have been determined [122, 123]. Their yields decrease drastically with the increasing number of carbon atoms in the molecules which is generally the case for homologue series of many tobacco smoke constituents [75]. Gaseous hydrocarbons featuring a low molecular weight have their origin in the thermal decomposition of many leaf constituents, paraffins, triglycerides, amino acids, aliphatic acids, esters, and aldehydes [121, 124].

In addition to that, hundreds of isoprenoids, including tobacco-specific compounds, have been identified in tobacco and smoke likewise [123, 125, 126]. Isoprenoids have a high contribution to the typical aroma of tobacco leaves. The most predominant acyclic isoprenoids are solanesol, phytone, and neophytadiene, the most prevalent cyclic ones include cembranoids and carotenes. Several isoprenoids are transferred unchanged to the mainstream smoke, however, many of them undergo thermal decomposition reactions, isoprene being one of the major products [127, 128].

More than 75 monocyclic aromatic hydrocarbons, e.g. benzene, toluene, and ethyl benzene are generated from the thermal decomposition of amino acids, fatty acids, cinnamic acid, paraffins and sugars, precursors featuring an aromatic or cyclohexane ring and pyrosynthesis from primary hydrocarbon radicals [121, 124, 129, 130].

Furthermore, a large variety of polynuclear aromatic hydrocarbons (PAHs) are present in tobacco smoke. Regarding combustion processes, investigation of PAHs is often of special interest due to their toxic potential in humans. In the 1970s Snook et al. identified more than 300 individual species [131-133]. Skeletal structures of some of the most important PAH are listed in Figure 5 together with expected yields in plain non-filter cigarettes [75, 134, 135].

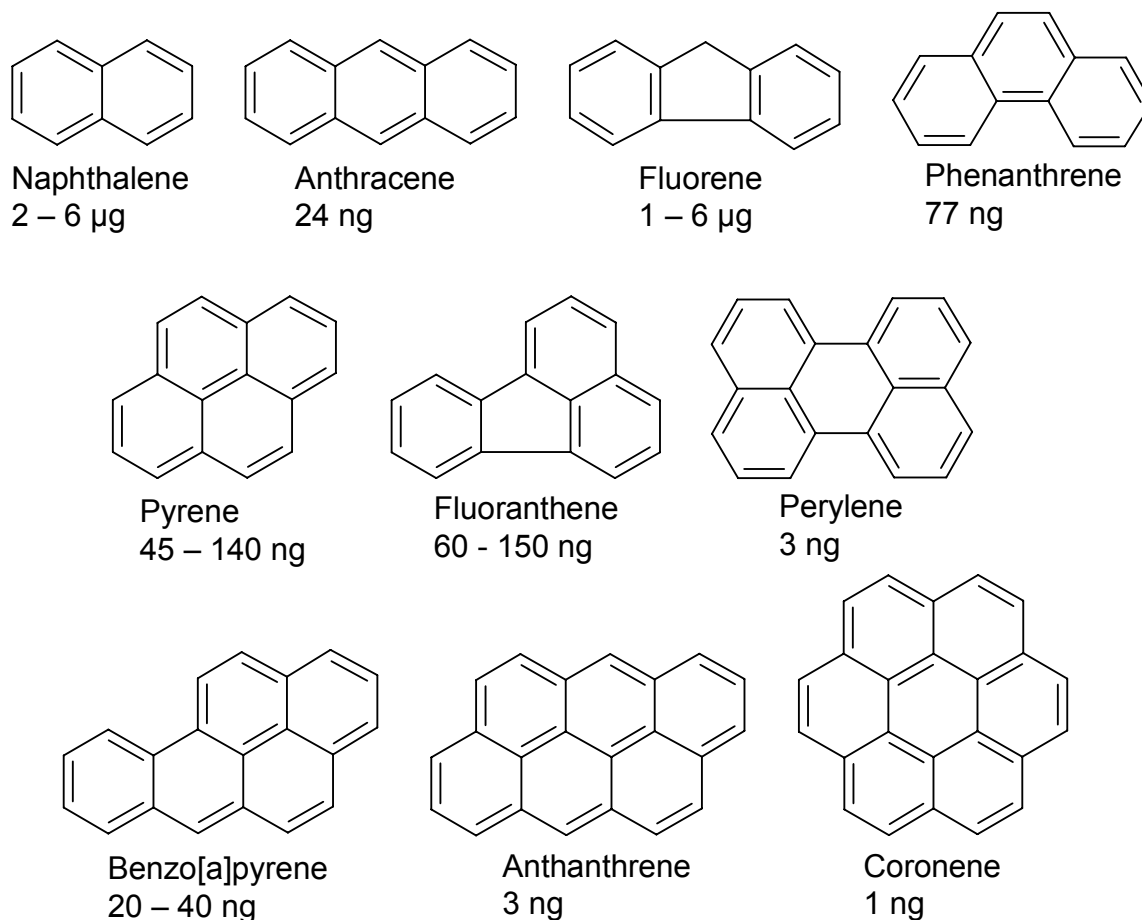


Figure 5: Chemical structures of some important PAHs identified in tobacco smoke and expected yields in non-filter cigarettes [75, 134, 135]

A high number of possible derivatives results in a great number of different PAHs whereby methylated side chains are dominating. For instance, there are at least 80 derivatives of naphthalene present in smoke [75, 135, 136]. In general, PAHs can be generated by pyrolysis and pyrosynthesis of terpenes, phytosterols such as stigmasterol, paraffins, sugars, amino acids, celluloses and many other tobacco constituents [121, 124, 136]. In addition, reactions involving primary hydrocarbon radicals can lead to highly reactive species which, in turn, react via condensation, dehydration, ring-closure mechanisms etc. to stable fused ring systems. In doing so, already existing smaller ring systems can be enlarged [129, 130]. Formation is highly dependent on temperature during tobacco pyrolysis and combustion. It is known that alkanes and alkenes are formed at temperature ranges between 400 °C and 600 °C. Reactions leading to benzene and its alkylated derivatives start above 500 °C and to naphthalenes at approximately 700 °C. PAHs require the highest temperatures for sufficient generation with ca. 800 °C [136-139].

#### **1.4.2.4. Carbonylic compounds**

Non-enzymatic browning reactions in tobacco form aldehydes and ketones, which are transferred from tobacco to smoke by distillation [140]. However, the greatest proportion is generated by the pyrolysis of a number of tobacco constituents, in particular sugars, tobacco lipids and waxes, celluloses, pectins, proteins, amino acids, and triglycerides [98, 121, 124, 141].

#### **1.4.2.5. Phenolic compounds**

The large amounts of phenols in smoke range from simple volatile monophenols to polyphenols. Leaf biopolymers such as lignin and celluloses are the principal precursors of monophenols. In addition, a wide variety of phenols is generated by pyrolysis of other polysaccharides, sugars, protein, amino acids as well as leaf polyphenols such as chlorogenic acid [55, 73, 121, 124]. Many volatile phenols are removed by passing through the plasticised cellulose acetate filter [142].

#### **1.4.2.6. Acids**

Tobacco smoke contains a variety of volatile carboxylic acids ( $C_1$  to  $C_5$ ), long-chain fatty acids ( $C_6$  to  $C_{22}$ ), hydroxycarboxylic acids, dicarboxylic acids and benzoic acids [143]. Long-chain fatty acids originate in tobacco and transfer to smoke. Volatile acids are transferred to smoke from tobacco [55] as well as being generated by pyrolysis of tobacco constituents, e.g. esters, triglycerides, lactic acid salts, starch, pectins, and celluloses [121].

#### **1.4.2.7. N-heterocyclic compounds**

N-heterocyclic compounds significantly contribute to the flavour of tobacco smoke, first and foremost for cigars and pipes. A proportion of these species transfer to smoke by distillation from tobacco where the compounds were generated by non-enzymatic browning reactions involving amino acids and saccharides [140]. Moreover, N-heterocyclic compounds are formed by pyrolytic reactions of nicotine and other alkaloids as well as amino acids, nitrates, saccharides and protein [120, 121, 140, 144, 145]. In this context pyridines (ca. 350) are the largest class of N-heterocyclic compounds. It is assumed that pyridine and its derivatives are partially formed in the cigarette burning zone by pyrosynthetic reactions of  $NH_3$  with, for instance, acrolein [146]. Chemical structures of the most common tobacco alkaloids are illustrated in Figure 6 together with typical yields in the mainstream smoke of plain non-filter cigarettes [134, 143].

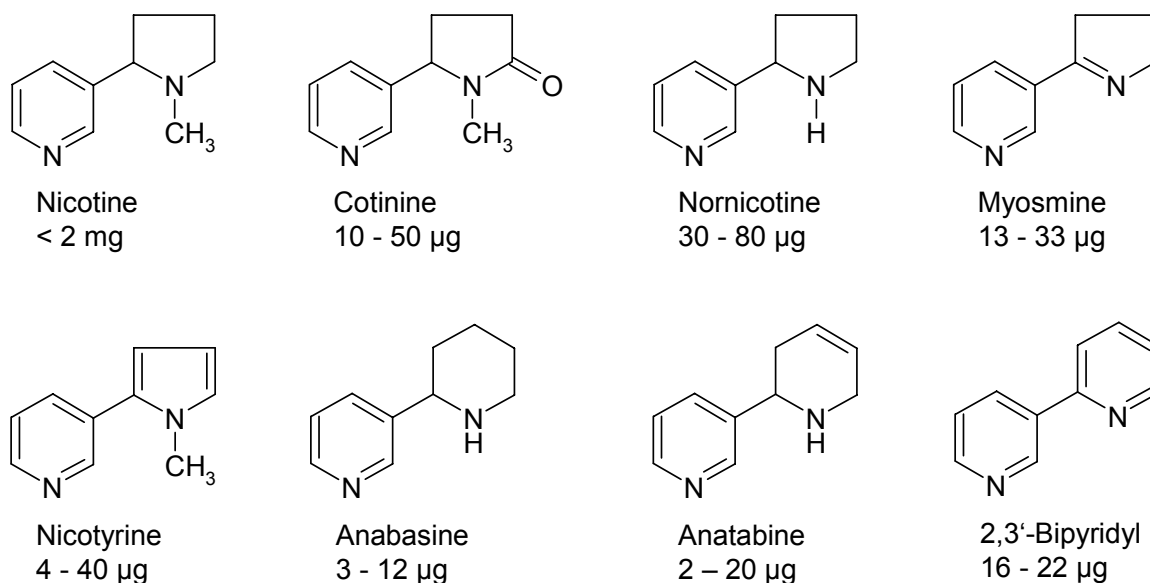


Figure 6: Chemical structures of the most common tobacco alkaloids together with typical mainstream smoke yields of non-filter cigarettes [134, 143]

Nicotine is by far the most abundant tobacco alkaloid accounting for 85 to 90 % of the total alkaloids in smoke. Due to its supremacy in tobacco smoke the fate of nicotine will be treated in more detail. Several studies have dealt with the transfer of nicotine to tobacco smoke, e.g. [124, 145, 147]. The main consistent findings are that the main fraction of nicotine originally present in tobacco transfers intact to tobacco smoke and the higher amount was found in sidestream smoke. In addition, for cigarette smoke all the mainstream and sidestream nicotine was present in the particulate phase only, irrespective of the nature of the tobacco used [14]. About one third of the original nicotine in tobacco underwent pyrolysis or oxidation reactions. The variety of resulting chemicals being formed is rather high in pyrolysis experiments. Schmeltz et al. [145] reported more than 38 different compounds which were identified from the pyrolysis of radiolabelled pure nicotine. However, they found considerably fewer in smoke from a cigarette containing radiolabelled nicotine in the tobacco. This indicates that isolated pyrolysis experiments can generate products that are not actually formed during the smoking of the cigarette. This reflects the high complexity of the burning of a cigarette and the fact that even nowadays there remain a lot of unresolved questions on the chemistry involved. Figure 7 exhibits some formed products together with their percentage fraction of total nicotine in the tobacco leaf separated in mainstream and sidestream smoke according to Schmeltz et al. [145].

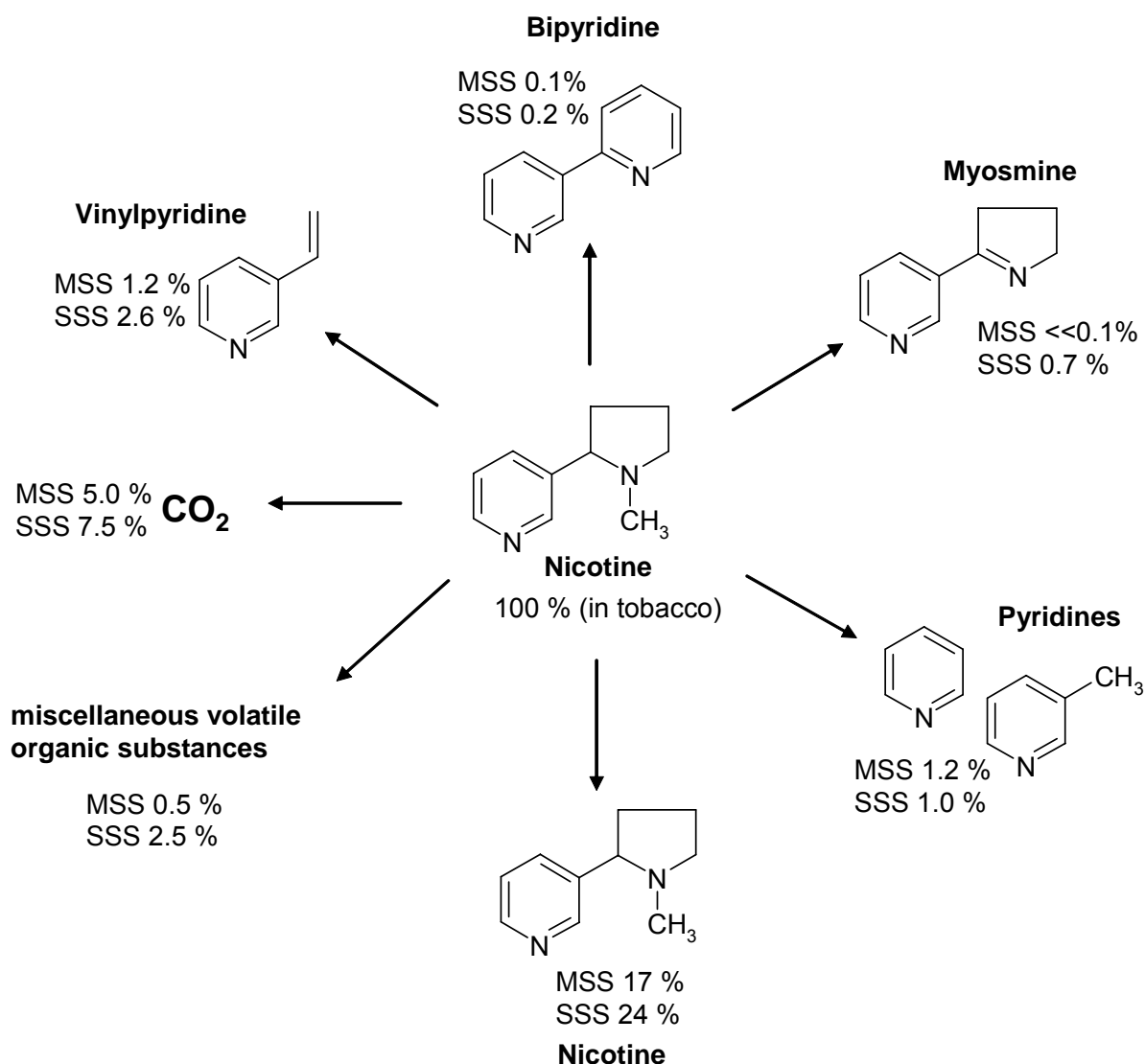


Figure 7: Some possible products of the pyrolysis and combustion of originally present nicotine in tobacco together with percentage fraction and separation in mainstream and sidestream smoke [145]

Much less is known about the fate of the other tobacco alkaloids in a burning cigarette. Nor nicotine transfers to smoke to a lower extent than nicotine but both form generally similar substances when pyrolysed [120].

#### 1.4.2.8. Nitrosamines

Tobacco smoke generally contains two types of nitrosamines, namely tobacco-specific nitrosamines and non-tobacco-specific nitrosamines. Tobacco-specific nitrosamines (TSNAs) are derived from tobacco alkaloids and only occur in processed tobacco and the particulate phase of tobacco smoke i.e. they are non-volatile. In contrast, non-tobacco-specific nitrosamines are also found elsewhere and occur in the vapour phase and particulate phase

likewise [14]. Levels of non-specific nitrosamines are much lower than of TSNAs. Very small amounts have been identified in processed tobacco but it is assumed that their main source in smoke comes from pyrosynthetic reactions [143, 148].

TSNAs are usually not present in freshly harvested green tobacco leaves but are produced during tobacco curing, processing, and storage by nitrosation reactions [148-150]. Figure 8 illustrates the formation pathways of the TSNAs 4-(methylnitrosamino)-1-(3-pyridyl)-1-butanone (NNK), N-nitrosornnicotine (NNN), N-nitrosoanabasine (NAB), N-nitrosoanatabine (NAT), 4-(methylnitrosamino)-1-(3-pyridyl)-1-butanol (NNA), 4-(methylnitrosamino)-4-(3-pyridyl)butanal (NNAL), 4-(methylnitrosamino)-4-(3-pyridyl)-1-butanol (iso-NNAL), and 4-(methylnitrosamino)-4-(3-pyridyl) butyric acid (iso-NNAC) [150].

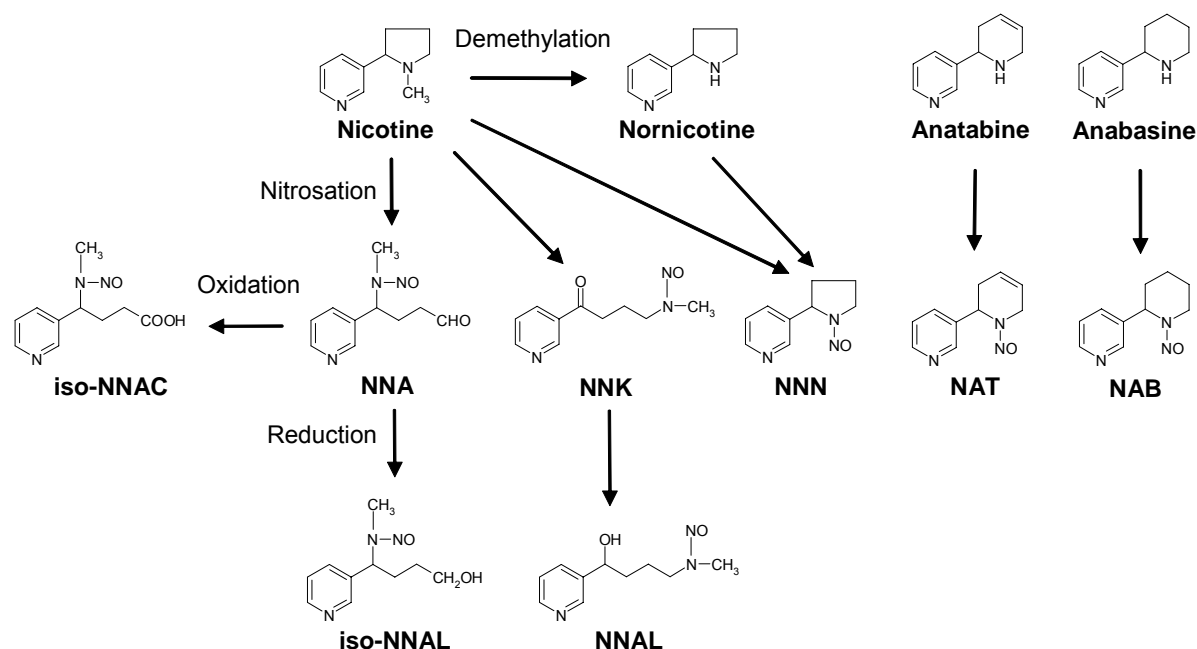


Figure 8: Formation of tobacco-specific nitrosamines NNK, NNN, NAB, NAT, NNA, NNAL, iso-NNAL, and iso-NNAC from common tobacco alkaloids [150]

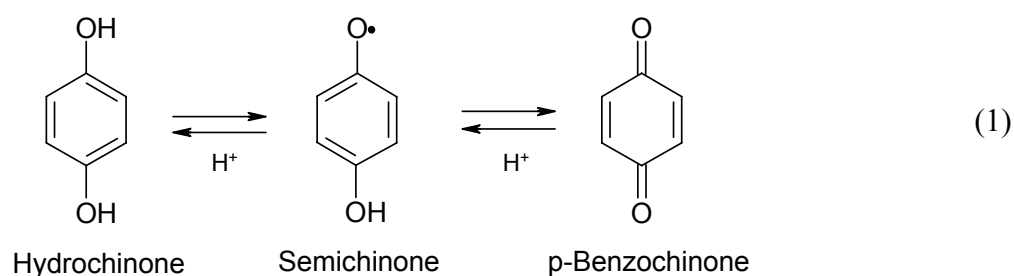
When tobacco burns these TSNAs can either transfer to smoke intact or decompose. Additional amounts of nitrosamines can be generated by pyrosynthetic mechanisms [14]. A review of a variety of nitrogen-containing compounds in tobacco and tobacco smoke covering identified species, precursors etc. is given in [144]. Hoffmann et al. have published a very detailed work on TSNAs involving formation, biochemistry, carcinogenicity, and relevance to humans [150].

### 1.4.2.9. Metals

Tobacco contains minerals and other inorganic constituents like all plant material. Most metals remain in the ash after combustion, only a small fraction appears in the smoke. In total about 30 metals and other elements have been identified in tobacco smoke [151-153].

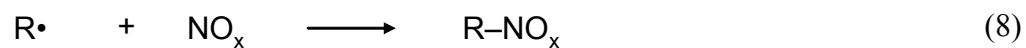
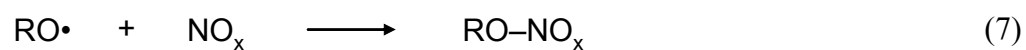
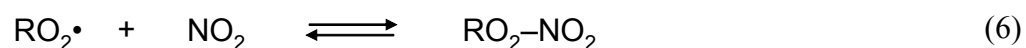
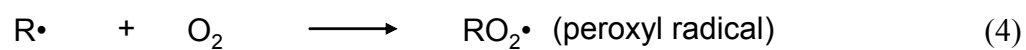
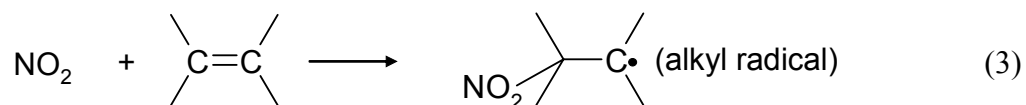
### 1.4.2.10. Free radicals

Tobacco smoke also contains free radicals. According to Pryor and co-workers these free radicals can be classified in two distinct groups: long-lived particulate phase radicals and short-lived gas phase radicals [154, 155]. In the particulate phase there are approximately  $1 \times 10^{17}$  radicals per gram of tar and  $4 \times 10^{14}$  radicals per puff which remain unchanged over several days. Pryor et al. postulated that these are polymers containing a semi-quinone radical associated with quinone and hydroquinone which are illustrated in equation 1. The quinone and hydroquinone species can interconvert by hydrogen atom exchange to produce the charge-transfer complex [154-156].



Equation 1: Hydroquinone/Semiquinone/Benzoquinone charge transfer complex of the long-lived radical in the tobacco smoke's particulate phase [154-156]

The short-lived vapour phase radicals mainly consist of alkyl, peroxy, and alkoxy radicals and are present in amounts of approximately  $1 \times 10^{16}$  radicals per cigarette in mainstream and sidestream smoke, or  $5 \times 10^{14}$  per single puff. Lifetimes of these radicals are usually known to be fractions of a second. However, in cigarette smoke they have apparent lifetimes in excess of five minutes with their concentrations increasing during the first minute of ageing [154, 155]. Therefore Pryor et al. postulated a steady-state mechanism for the continuous formation and destruction of the radicals in smoke, involving the oxidation of NO to NO<sub>2</sub> as driving force. The generated NO<sub>2</sub> reacts with olefinic smoke constituents such as isoprene, butadiene, and acrolein continuously building-up radicals while the smoke is ageing. Equations 2 to 8 illustrate the principal build-up mechanism of the gas phase radicals.



Equations 2 to 8: Illustration of the build-up mechanism of the gas phase radicals of tobacco smoke [154, 155]

Equation (2) shows the initial oxidation of NO to NO<sub>2</sub> and equation (3) the following reaction of the product with a variety of different olefins. Equation (4) and (5) are radical propagation reactions and (6), (7), and (8) are radical termination reactions.

## 1.5. Motivation

More than half a century of tobacco science has led to an immense knowledge about all kinds of related fields such as tobacco plant cultivation, smoke formation, and biological activity of smoke constituents on humans. Regarding analytical smoke chemistry, thousands of smoke constituents have been detected as well as quantified and the number of identified substances is constantly increasing. However, cigarette smoke analysis is mostly done by application of conventional off-line techniques such as liquid chromatography (LC), e.g. [57, 157-160] and gas chromatographic (GC) methods, e.g. [57, 135, 161-168]. These methods can alter the smoke composition during sampling and analytical processing, such as separation, trapping, and derivatisation [169, 170]. In addition, the results obtained are usually for total yields in smoke from whole cigarettes. As a consequence, in most cases short fluctuations and variations in concentration during the smoking process are not resolved. However, this information is essential in order to understand the complex and often interrelated formation and decay mechanisms of various smoke constituents [171], in particular, when public interest focuses on hazardous substances. The analytical task of simultaneously analysing a wide range of compounds at trace levels combined with a high time-resolution is very difficult to achieve. In this context SPI-TOFMS has proven to be well suited for this purpose. In recent times the method has been successfully applied to the analysis and characterisation of organic species in all kind of fields, e.g. waste incineration [172-174], steel recycling [175, 176], exhaust gases [174, 177, 178], and coffee roasting [179, 180]. In the framework of this work, SPI-TOFMS has been used to investigate the thermal behaviour of tobacco and the examination of the cigarette smoking process on a puff-by-puff basis for the first time.

## 2. Method and Instrumentation

Ionisation of the analyte molecules can be carried out by several different ionisation methods. Electron impact (EI) ionisation is one of the standard techniques in this field. With this technique, electrons are emitted from an electron gun and accelerated towards the target molecules. During collision the electrons transfer kinetic energy to these molecules leading to ionisation. Subsequently, the higher the kinetic energy of the electrons the higher is the yield of ionisation of the analytes. However, for sufficient yields, electron energies are required which lead to massive fragmentation of many organic substances. Identification of compounds is carried out by assigning characteristic fragmentation patterns, which is sufficient if only one or a few substances are present. In the case of highly complex samples this might result in superposition of mother ions and fragment ions, making identification of individual compounds difficult or even impossible. Consequently, for these samples soft ionisation techniques are required which cause no or only little fragmentation of the analytes. In this context the single photon ionisation uses photons instead of electrons for ionisation of the target molecules. The principle of this rather new method is explained in Chapter 2.1

In most cases ionisation techniques are combined to mass spectrometry. In the case of pulsed ionisation techniques, time-of-flight mass spectrometry can be applied. This method is very convenient for the analysis of very fast processes and enables the simultaneous investigation of many different compounds in real time. Chapter 2.2 describes the time-of-flight mass spectrometry in more detail.

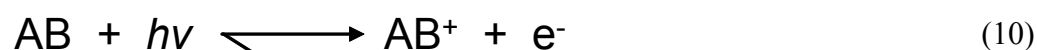
Chapter 2.3 focusses on the introduction and characterisation of the SPI-TOFMS used in the framework of this work. It explains the set-up of the instrument and contains the description of technical details. Furthermore, organic compounds which are accessible by this technique are introduced. In addition to that, detection limits and other related properties of several compounds of interest are discussed, resulting in the development of a sophisticated quantification scheme for a large range of organic molecules.

## 2.1. Principle of the Single Photon Ionisation process

In single photon ionisation (SPI), vacuum ultraviolet (VUV;  $\lambda < 200$  nm) photons are used for the ionisation of molecules. The photons with the energy  $E_{ph}$  are absorbed by the molecules and the molecules are ionised if  $E_{ph}$  exceeds their ionisation potential (IP) [181]. The main advantage of SPI is the low transfer of excess energy beyond the required ionisation energy (IE). This results in low or even no fragmentation of the target molecules and enables the analysis of highly complex matrices containing hundreds of individual compounds.

In general, the probability of photoabsorption, photoionisation, photodissociation, and fragmentation is dependent on the nature of the molecule as well as on the photon's energy.

When a molecule absorbs a VUV photon it is promoted from ground state to an excited state. If the energy is above the IP the molecule dissipates the energy in ionisation (equ. 10) or superexcitation (equ. 10 and 11) which is visualised in the following scheme.



Equations 10 to 12: Processes occurring in a molecule after absorption of a VUV photon having a potential above the molecule's ionisation potential: ionisation (equ. 10), superexcitation (equ. 10 and 11), autoionisation (equ. 11), and dissociation (equ. 12)

The superexcited state is a discrete state with higher energy than the first IP. The superexcited molecule may either autoionise (equ. 11) or dissociate to neutral fragments (equ. 12) [182-184].

In this context the optical oscillator strength  $f_j$  describes the transition probability of the electronic ground state to an excited state by absorption of a photon. The oscillator strength can be expressed in terms of the transition energy  $E_j$  to form the state  $j$  measured in units of the Rydberg energy  $R$ , and of the dipole matrix element squared  $M_j$  as measured in  $a_0^2$  [172, 183, 184].

$$f_j(E_j) = (E_j / R)M_j^2 \quad (13)$$

$$R = m_e e^4 / (2h^2) \quad (14)$$

$f_j$ : oscillator strength

$E_j$ : transition energy for formation of state  $j$

$R$ : Rydberg constant ( $1.097 \times 10^5 \text{ cm}^{-1}$ )

$m_e$ : electron mass ( $9.110 \times 10^{-31} \text{ kg}$ )

$e$ : elementary charge ( $1.602 \times 10^{-19} \text{ C}$ )

$h$ : Planck's constant ( $6.626 \times 10^{-34} \text{ Js}$ )

$M_j$ : dipole matrix element for state  $j$

$a_0$ : Bohr radius ( $5.292 \times 10^{-11} \text{ m}$ )

A set of  $E_j$  and  $f_j$  characterises a discrete spectrum. For discussion of a continuous spectrum, one expresses the oscillator strength in a small region of the excitation energy between  $E$  and  $E + dE$  as  $(df/dE)dE$ , and calls  $df/dE$  the oscillator strength distribution. The total sum of the oscillator strength of all transitions including discrete ( $E_{ph} < IP$ ) and continuous spectra ( $E_{ph} > IP$ ) is equal to the total number  $Z$  of electrons in the molecule [172, 183, 184].

$$\sum_j f_j(E_j) + \int_{IP}^{\infty} (df/dE)dE = Z \quad (15)$$

$df/dE$ : oscillator strength distribution

$Z$ : number of molecule's electrons

Equation (15) is called the Thomas-Kuhn-Reiche (TKR) sum rule. The oscillator strength distribution is proportional to the cross section  $\sigma_a$  for the absorption of a photon of energy  $E_{ph}$  [172, 184].

$$\sigma_a = 4\pi^2 \alpha a_0^2 R \frac{df}{dE} = \frac{eh10^4}{4\epsilon_0 m_e c} \frac{df}{dE} = 1.098 \times 10^{-16} \text{ cm}^2 \text{ eV} \frac{df}{dE} \quad (16)$$

$\alpha$ : fine structure constant (0.007297)

$\epsilon_0$ : dielectric constant of the vacuum ( $8.854 \times 10^{-12} \text{ J}^{-1} \text{ C}^2 \text{ m}^{-1}$ )

$c$ : light velocity ( $2.998 \times 10^8 \text{ ms}^{-1}$ )

Figure 9 shows the valence shell photoabsorption oscillator strength of benzene as a function of the photon energy in the range from 4 to 56 eV[185].

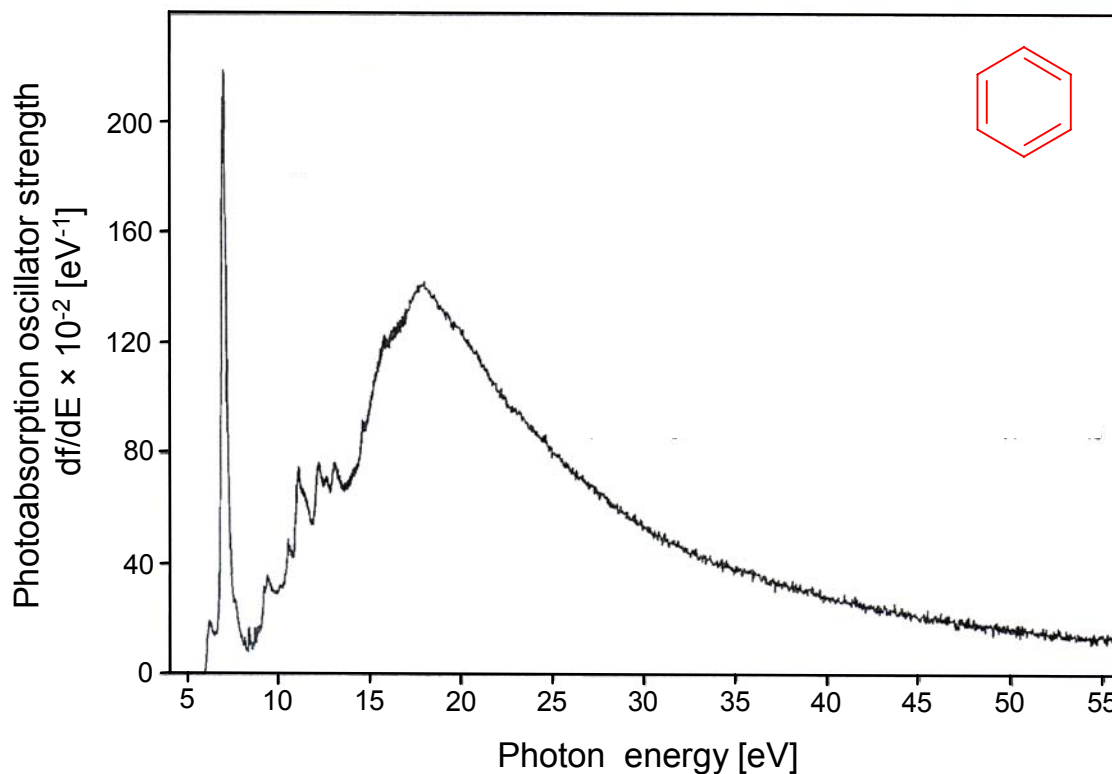


Figure 9: Photoabsorption oscillator strength of benzene as a function of the photon energy in the range from 4 to 56 eV [185]

There is an intense and narrow maximum at about 7 eV and a further broad maximum at about 17 eV. Above the latter threshold the oscillator strength declines and advances to zero for very high photon energies.

Analogous to absorption, there is also a cross section  $\sigma_i$  for photoionisation accounting for the sum of both direct and autoionisation processes. The quotient of the cross sections for photoionisation  $\sigma_i$  and photoabsorption  $\sigma_a$  is called photoionisation quantum yield  $\gamma$  [172, 184].

$$\gamma = \frac{\sigma_i}{\sigma_a} \quad (17)$$

The photoionisation quantum yield describes the ratio of formed ions per absorbed photons. Both photoionisation and photoabsorption cross sections are usually measured in Megabarn (Mb), whereby 1 Mb equals  $10^{-18}$  cm<sup>2</sup>. In general it can be said that molecules are not ionised easily. Although the excitation energy is sufficient for ionisation at close range to the IP, the ionisation quantum yield is much smaller than 1. However, it increases with rising photon energy and attains about 100 % at the energy of IP + 23 eV [172]. Figure 10 illustrates the photoionisation cross section for the formation of the benzene ion ( $C_6H_6^+$ ) from benzene in the range from 9 to 30 eV [186].

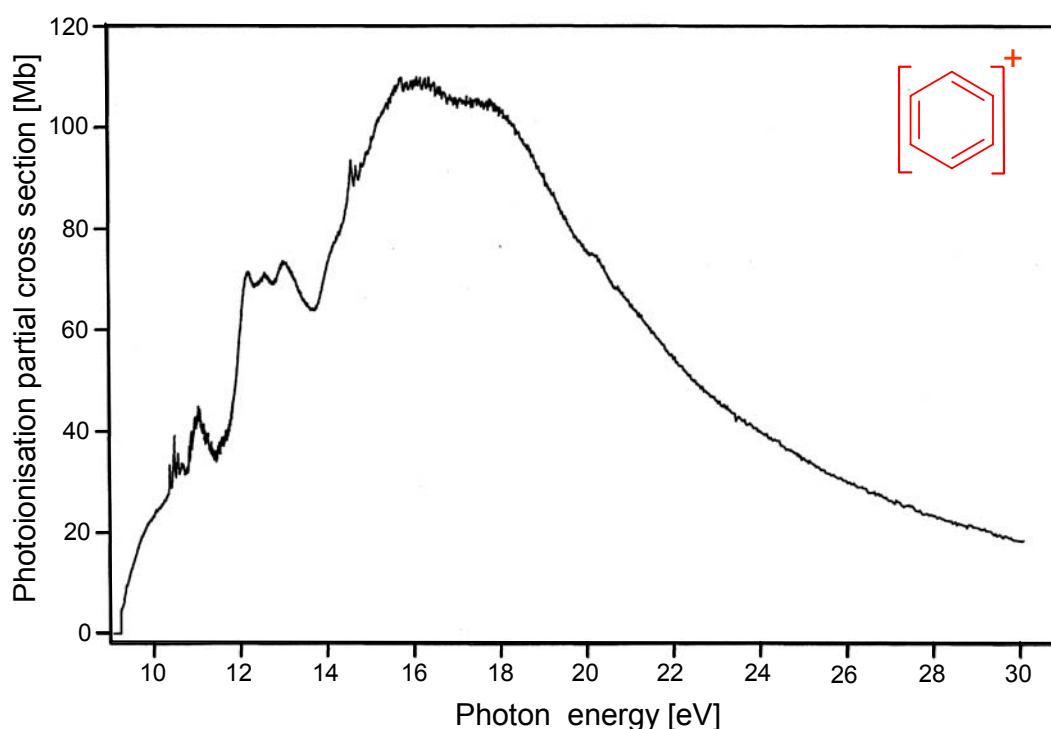


Figure 10: Photoionisation cross section for the formation of  $C_6H_6^+$  from benzene in the range from 9 to 30 eV [186]

Benzene has an IP of 9.24 eV. Above this threshold the photoionisation cross section increases and reaches its maximum at about 16 eV. The curve progression strongly resembles the absorption in Figure 9.

If the photon energy is greater than the required IE, some excess energy is transferred onto the molecule. This excess energy can lead to fragmentation. In this case the fragment with the lower IP usually retains the electric charge. Since the IP of hydrocarbons generally decreases with increasing number of carbon atoms, the electric charge remains on the larger fragment [172]. Holland et al. [186] demonstrated the influence of photon energy on fragmentation of

the benzene molecule by recording time-of-flight spectra at four different photon energies, namely 15.7 eV, 22.4 eV, 31.8 eV, and 35.4 eV, shown in Figure 11.

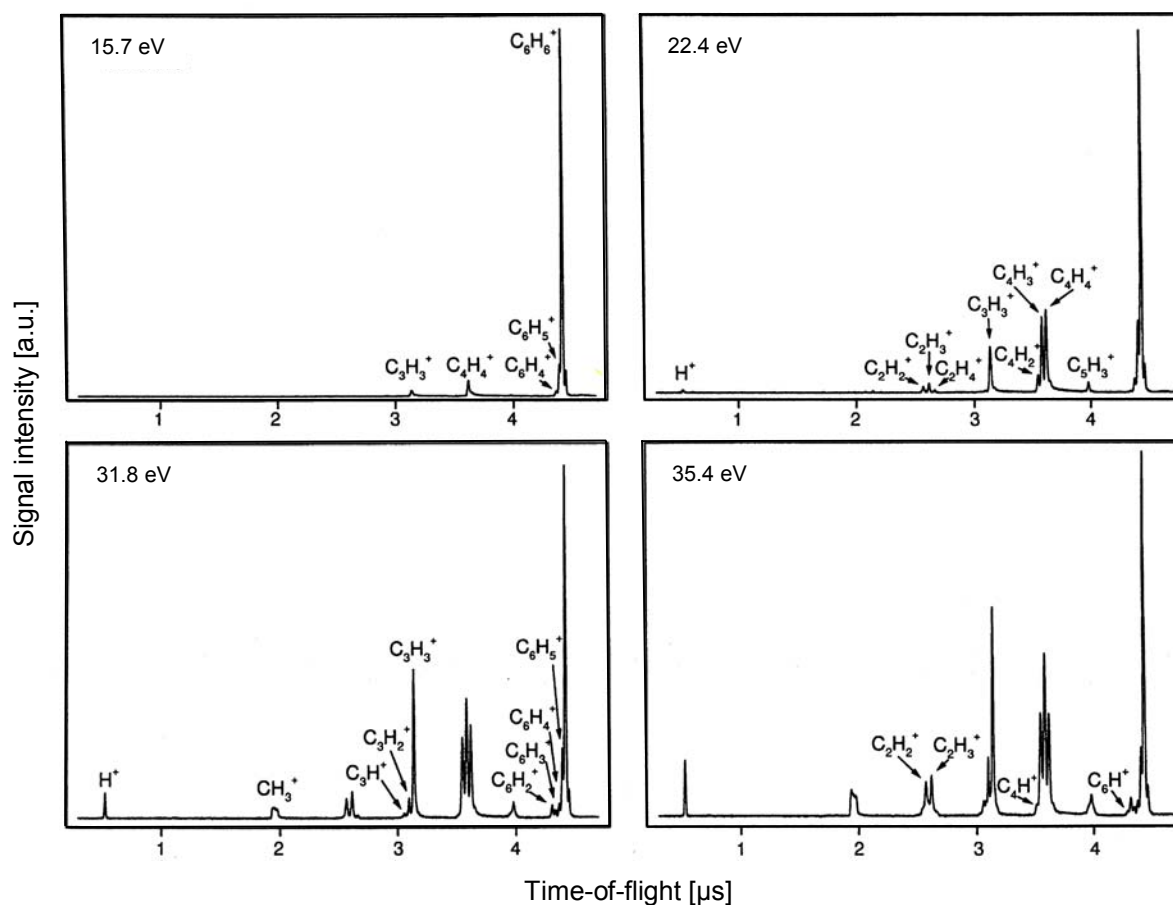


Figure 11: Time-of-flight spectra of benzene after ionisation with four different photon energies of 15.7, 22.4, 31.8, and 35.4 eV

In addition, Holland et al. suggested several reaction pathways for the fragmentation of the benzene molecule [186]. In general, it can be seen that the mother ion of benzene dominates the spectrum at the lowest photon energy of 15.7 eV. However, fragmentation ions gain importance with increasing photon energy. For higher photon energies the mother ion peak might vanish completely, depending on the nature of the original molecule, leaving a more or less characteristic fragment pattern. According to Holland et al., no signals of fragment ions of benzene were observed below 14 eV. Figure 12 illustrates the photoionisation cross sections for the formation of the  $\text{C}_6\text{H}_5^+$ ,  $\text{C}_6\text{H}_4^+$ ,  $\text{C}_4\text{H}_4^+$ ,  $\text{C}_4\text{H}_3^+$ ,  $\text{C}_4\text{H}_2^+$ , and  $\text{C}_3\text{H}_3^+$  fragments from benzene [186], which also reflects the highly challenging task of soft photoionisation. However, since within this work photon energies of 10.49 eV were applied, fragmentation of benzene (and many other organic compounds) is unlikely.

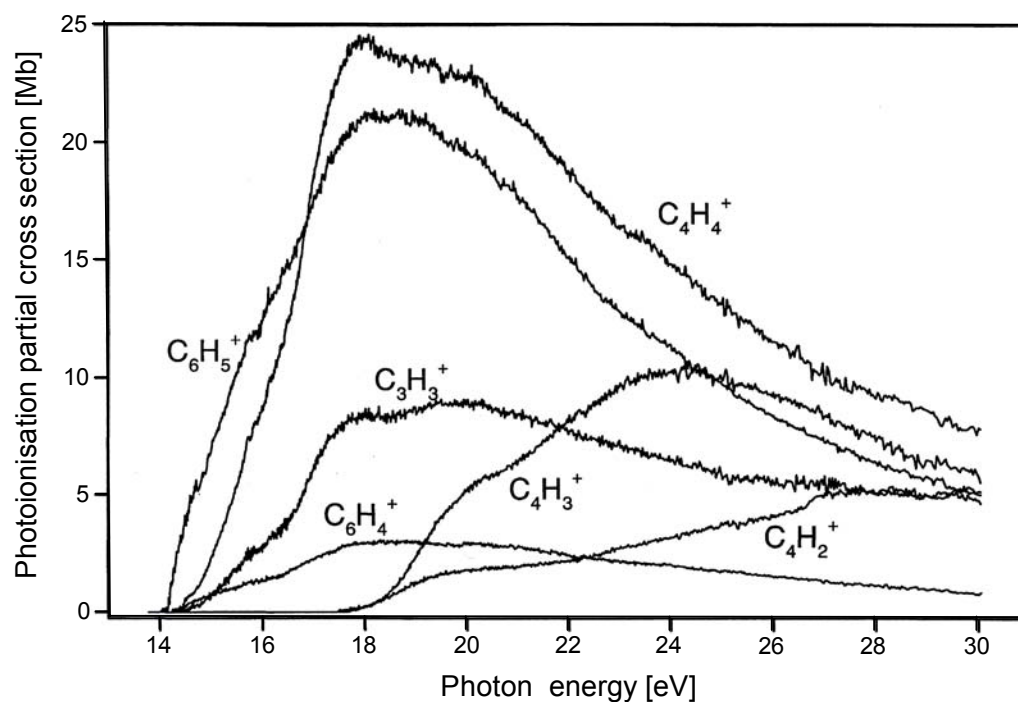


Figure 12: Photoionisation cross sections for the formation of the  $C_6H_5^+$ ,  $C_6H_4^+$ ,  $C_4H_4^+$ ,  $C_4H_3^+$ ,  $C_4H_2^+$ , and  $C_3H_3^+$  fragments from benzene in the range from 13.8 to 30 eV [186]

Over the last decades, numerous works have dealt with the investigation and determination of photoabsorption, photoionisation, photodissociation, and oscillator strengths of many chemical species such as benzene [185-189], other monocyclic aromatic compounds [188, 190-192], PAHs [193, 194], small and long-chained hydrocarbons [182, 183, 195-198], alcohols [182, 199], ether [200],  $NH_3$  [198, 201-203],  $NO$  [204, 205],  $NO_2$  [206], and  $H_2S$  [207].

## 2.2. Time-of-flight mass spectrometry

A time-of-flight mass spectrometer consists of an ion source, a drift tube, and an ion detector. The main advantage of time-of-flight mass spectrometry, in general, compared to most other commonly used types such as quadrupole or sectorfield mass spectrometry, is that a wide mass range of species can be detected at the same time. Subsequently, a fast and comprehensive analysis of highly complex mixtures can be achieved. The basic principle of the technique is that ions are generated between two electrodes with opposite polarity. The static electric field between the positively charged repeller electrode and the negatively charged extraction electrode accelerates the ions, having charge  $z$  and molecular weight (mass)  $m$  towards the extraction electrode. Depending on the existing potential,  $V$ , the ions attain the velocity  $v$ :

$$v = \sqrt{\frac{2zV}{m}} \quad (18)$$

$v$ : velocity  
 $z$ : charge  
 $V$ : potential  
 $m$ : mass

After acceleration the ions pass through the ring-shaped extraction electrode and enter a field-free drift region with the length  $L$ , which is passed with constant velocity  $v$ . At the end of the drift region the ions reach a detector after time  $t$ . In doing so, the time-of-flight of the ions is dependent on the molecular weight and electric charge of the ion, as well as the applied potential and drift length of the mass spectrometer.

$$t = \frac{L}{v} = L\sqrt{\frac{m}{2zV}} \quad (19)$$

$$t \approx \sqrt{\frac{m}{z}} \quad (20)$$

$t$ : time-of-flight  
 $L$ : length of drift region

Consequently, the time-of-flight is proportional to the square root of the ratio of molecular weight and charge ( $m/z$ ). In addition, the differential time-of-flight of two ions with different

molecular weights  $m_1$  and  $m_2$  but the same charge  $z$ , is dependent on the applied potential and the length of the drift region.

For conversion of time-of-flight spectra into mass spectra, equation (20) must be expressed as

$$t = c\sqrt{\frac{m}{z}} + b \quad (21)$$

and, in turn, the resultant equation (21) solved for  $m/z$  (22).

$$\frac{m}{z} = \left(\frac{t-b}{c}\right)^2 \quad (22)$$

In order to calculate the factors  $b$  and  $c$ , the time-of-flights of two  $m/z$  values must be known which can be achieved by measuring two standard substances. The time-of-flights obtained are inserted into equation (23) and (24) to determine  $b$  and  $c$ . Subsequently,  $b$  and  $c$  can be used in equation (22) for the conversion of time-of-flight spectra into mass spectra.

$$c = \frac{t_1 - t_2}{\sqrt{\frac{m_1}{z_1}} - \sqrt{\frac{m_2}{z_2}}} \quad (23)$$

$$b = \frac{\sqrt{\frac{m_1}{z_1 t_2}} - \sqrt{\frac{m_2}{z_2 t_1}}}{\sqrt{\frac{m_1}{z_1}} - \sqrt{\frac{m_2}{z_2}}} \quad (24)$$

A more sophisticated approach is a time-of-flight mass spectrometer based on the two-step extraction principle of Wiley and McLaren [208]. Since the ionisation spot is not punctiform but features a finite diameter, not all ions are generated at exactly the same position, which leads to different starting conditions of the ions. As a result, time-of-flights of ions with the same molecular weight exhibit a time broadening. Thereby two opposing effects play a role.

Ions generated closer to the extraction electrode must pass a shorter distance to the detector than ions generated close to the repeller. On the other hand, the latter ions undergo higher acceleration due to their longer retention time in the static field. At the so-called spatial focal point both effects compensate each other and the broadening of the single mass peaks is minimal.

However, in the case of one-step extraction this spatial focal point is so close to the ion source that the short drift region does not enable a sufficient mass separation. In contrast, the two-step ion extraction according to Wiley and McLaren makes it possible to extend the spatial focal point to a detector positioned further away. With this arrangement, ions are accelerated by two successive extraction electrodes, whereby the second extraction electrode (also called the liner) leads to full velocity of the analyte ion. The following field-free drift region is on the same negative potential as the second extraction plate. After the second extraction electrode, the ion beam passes an electrostatic lens unit as well as an x-y deflection plate unit for controlling the ion trajectories. Moreover, much higher mass resolutions are achieved by the reflectron technique [209]. This method uses the reflection of ions at an ion mirror. Based on the Wiley-McLaren principle, the ion mirror works in two steps and consists of several grids. The first field is used to retard the incoming ions (brems field) into the mirror and accelerates the outgoing ions. The second, much greater field forces the incoming ions to reverse (reflector field). Ions with high kinetic energy penetrate deep into the ion mirror, which leads to a longer residence time in the mirror. This results in a kinetic energy focussing of the slower and the faster ions of the same molecular weight. The potentials of the ion reflector are adjusted in order to focus the ions onto the detector. The kinetic energy compensation and the extended drift region result in a better mass resolution compared to a linear mode time-of-flight mass spectrometer. However, the reflectron technique also entails lower detection limits since a lower yield of generated ions is reaching the detector due to losses during the reflection.

### 2.3. Characterisation of the SPI-TOFMS instrument

The instrument used in the present study was built within the framework of another PhD project [174]. In principle it is able to perform three ionisation techniques in a quasi-parallel mode, namely SPI, EI, and resonance enhanced multiphoton ionisation (REMPI). Detailed technical information and applications can be found in [174]. Since in this work solely SPI was applied, a brief description of the related processes is given here. VUV photons for SPI are generated by frequency tripling of intensive UV laser pulses ( $\lambda = 355$  nm) in a rare gas cell filled with xenon (Xe 4.0;  $p = 12$  mbar). The UV light (225 mJ) is generated by frequency tripling of the fundamental Nd:YAG laser (Surelite-III, Continuum, Santa Clara, USA) wavelength of 1064 nm (pulse duration 3 – 5 ns, repetition rate 10 Hz) by a third harmonic generator (THG). For the set-up used, the 355 nm UV beam is split and only 11 % of the UV light is used for VUV generation. The rest (89 %) can be used for REMPI. The finally resultant VUV photons have a wavelength of 118 nm, which is equivalent to the energy of 10.49 eV. Subsequently, all molecules featuring an IP below 10.49 eV are ionised. Hence, many background gases such as  $N_2$  (IP = 15.58 eV),  $O_2$  (IP = 12.06 eV),  $CO_2$  (IP = 13.77 eV), and  $H_2O$  (IP = 12.62 eV) are not detected as their IP values are above this threshold. Therefore the detector is not oversaturated since these compounds have very high concentrations in many gas phases, such as smoke and ambient air. A detailed description of the generation of VUV can be found in [174, 210-221]. Figure 13 A shows a photograph and Figure 13 B a sketch of the SPI-TOFMS used for the experiments.



Figure 13 A: Photograph of the SPI/REMPI/EI-TOFMS instrument which was used for all the experiments in this work

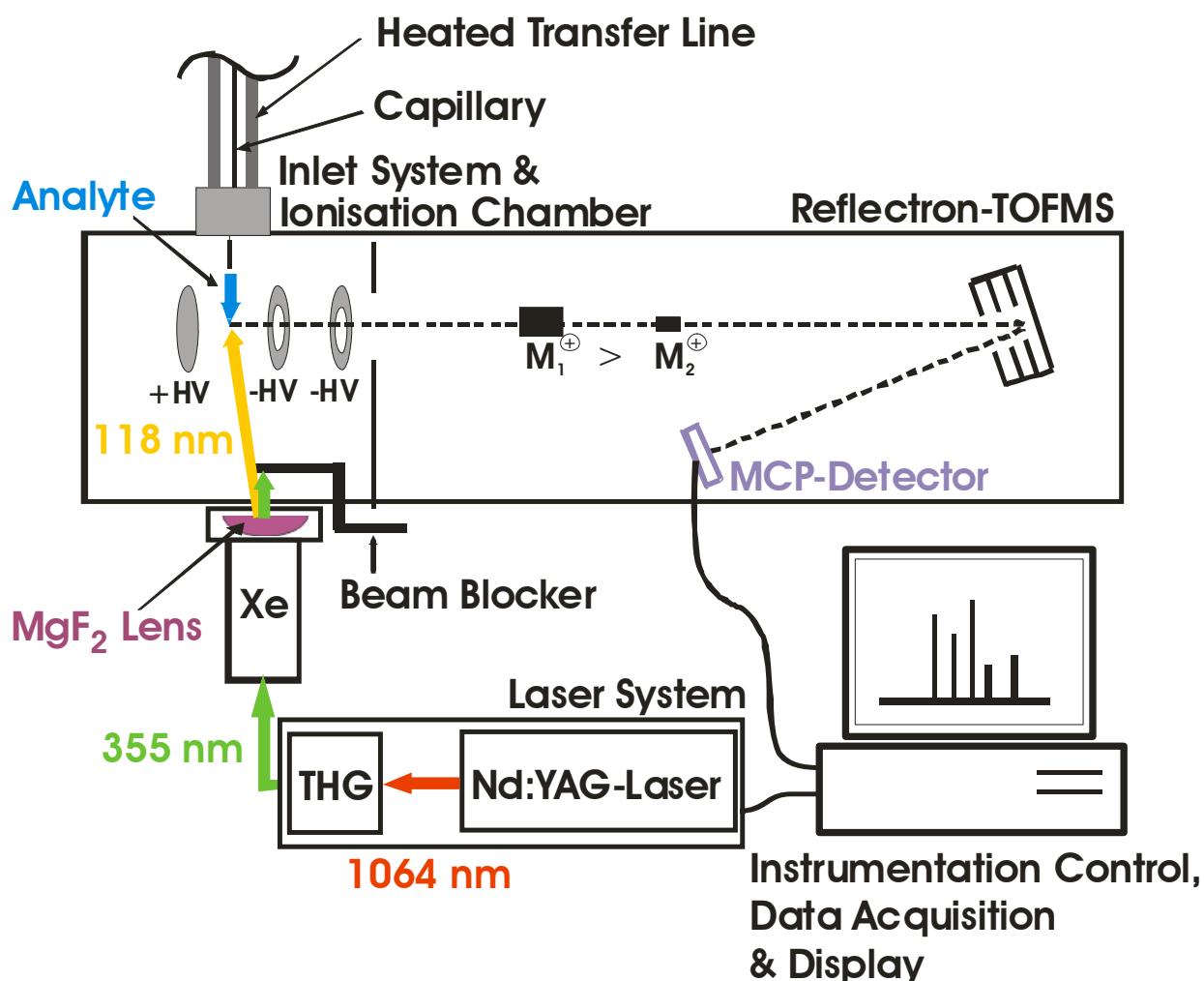


Figure 13 B: Sketch of the set-up of the SPI-TOFMS unit of the instrument

The generation of VUV light is very inefficient, only ca. 0.001 % of the incoming 355 nm beam is converted to 118 nm [213], the remaining 99.999 % of the 355 nm radiation can cause multiphoton ionisation and/or fragmentation by absorption of 355 nm photons. Therefore residual 355 nm light is, firstly, transversely relocated from the 118 nm light by means of different refraction indices  $n$  when passing a MgF<sub>2</sub> lens off-axis ( $\lambda = 355 \text{ nm} \rightarrow n = 1.39$ ;  $\lambda = 118 \text{ nm} \rightarrow n = 1.68$ ) and, secondly, blocked by a beam dump [181, 222-224]. The remaining VUV beam is directed into the ionisation chamber straight underneath the inlet needle of the sampling line and induces single photon ionisation of the organic molecules in the sample. Table 6 lists technical specifications and properties of the laser system used.

Table 6: Technical specifications and properties of the used laser system and the VUV generation unit

Laser type	Continuum Surelite-III
Laser energy (1064 nm)	800 mJ
Laser energy (355 nm)	225 mJ (11 % used for VUV generation)
Laser energy (118 nm)	ca. 0.001 % of incoming 355 nm
Pulse duration	3 – 5 ns
Repetition rate	10 Hz
Xe purity	4.0
Xe pressure	12.0 mbar

Compounds addressable by SPI, with VUV photons generated by the described process, are a wide range of aliphatic and aromatic hydrocarbons as well as heterocyclic and carbonylic species, provided that their IP is below 10.49 eV [225, 226]. Table 7 gives the accessibility of relevant substance classes by SPI by illustrating the first compound of the corresponding homologous series which is ionisable. In general, all the following homologues with higher molecular weight feature a similar or lower IP, and therefore, are accessible. Sieck et al. [227] exhibited this behaviour by plotting the IPs of several aliphatic and aromatic species as a function of their molecular weight, which is illustrated in Figure 14.

Table 7: Relevant substance classes being ionisable by SPI with the VUV wavelength of 118 nm. Listed are the first species of each homologous series which have an IP below 10.49 eV. The IP of species belonging to the same homologue usually decreases with increasing molecular weight [228]

Substance class	Compound	Total formula	MW [g/mol]	IP [eV]
alkanes	pentane	C <sub>5</sub> H <sub>12</sub>	72	10.37
alkenes	propene	C <sub>3</sub> H <sub>6</sub>	42	9.37
alkynes	propyne	C <sub>3</sub> H <sub>4</sub>	40	10.36
aldehydes	acetaldehyde	C <sub>2</sub> H <sub>4</sub> O	44	10.22
ketones	acetone	C <sub>3</sub> H <sub>6</sub> O	58	9.7
alcohol	ethanol	C <sub>2</sub> H <sub>6</sub> O	46	10.48
ethers	dimethyl ether	C <sub>2</sub> H <sub>6</sub> O	46	10.03
esters	methyl acetate	C <sub>3</sub> H <sub>6</sub> O <sub>2</sub>	74	10.25
aromatics	<i>all of relevance</i>	-	-	-
acids	propanoic acid	C <sub>3</sub> H <sub>6</sub> O <sub>2</sub>	74	10.44
amines	methyl amine	CH <sub>5</sub> N	31	8.9
N-heterocyclics	<i>all of relevance</i>	-	-	-

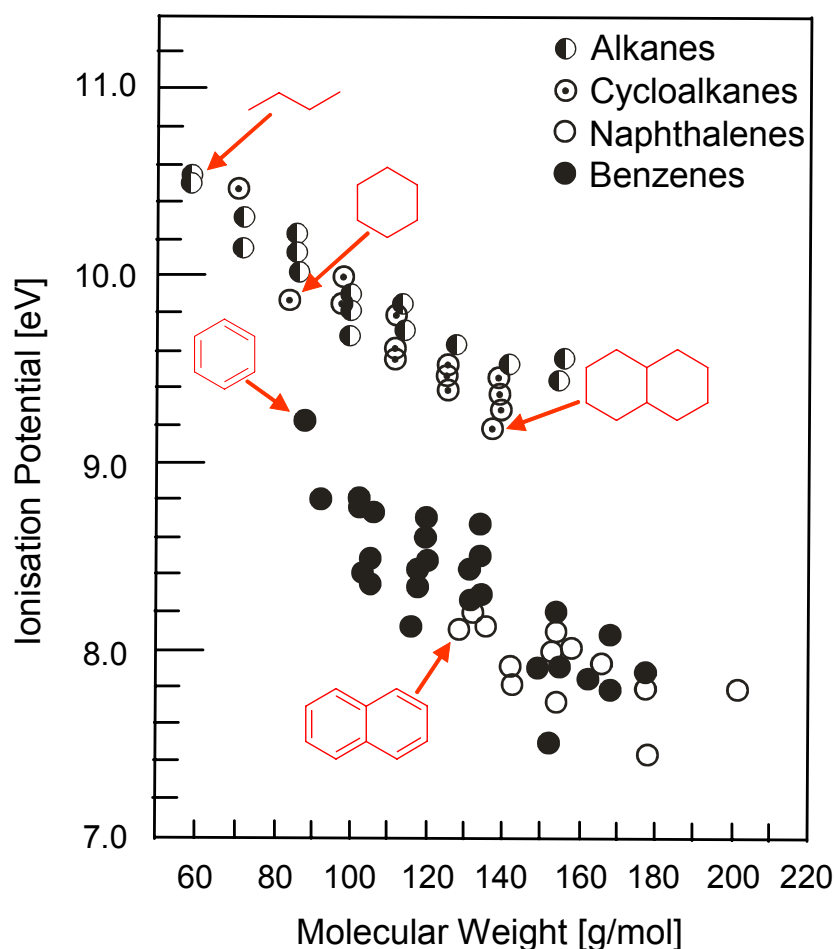


Figure 14: Ionisation potentials of certain classes of organic molecules as a function of their molecular weight [227]

The inlet system consists of a heated, hollow, stainless steel needle, pointing into the centre of the ion source and being located ca. 2 mm above the centre of the ion source. Inside this needle runs a deactivated fused-silica capillary (inner diameter 320  $\mu\text{m}$  (i.d.); outer diameter 450  $\mu\text{m}$  (o.d.)), which is aligned with the tip of the needle. Behind the orifice of the capillary, an effusive molecular beam is formed. This molecular beam is directly hit underneath the capillary tip by the laser pulses for photoionisation [225, 229-231]. The other end of the capillary runs through a heatable transfer line (length 1.5 m). The gas flow through the capillary is ca. 8 mL/min when heated to 220  $^{\circ}\text{C}$ . The technical details of the sampling system are listed in Table 8.

Table 8: Technical details and adjusted parameters of the transfer line sampling system

Capillary material	deactivated fused-silica
Capillary length	1.5 m
Capillary inner diameter	0.32 mm
Capillary outer diameter	0.45 mm
gas flow through capillary	8 mL/min (at 220 °C)
residence time in capillary	ca. 0.7 s (at 8 mL/min)
transfer line temperature range	< 300 °C
Inlet needle material	stainless steel
Inlet type	effusive beam

In principle the time-of-flight mass spectrometer used (Kaesdorf Inc., Munich, Germany) can be operated in linear and reflectron mode but was only used in the latter mode for this work. When operated in reflectron mode, the field-free drift region is 801 mm long, time resolution is 1 ns, and a mass resolution  $R_{50\%}$  of 1800  $m/z$  (determined at 92  $m/z$ ) can be achieved [174]. Mass resolution  $R_{50\%}$  was calculated by means of the full width at half maximum (FWHM) method, see equation (25). Thereby at 1800  $m/z$ , the baseline between two adjacent peaks is not higher than 50 % of the signal intensity of the two peaks, and subsequently, the peaks can be clearly resolved.

$$R_{50\%} = \frac{t}{2\Delta t_{FWHM}} \quad (25)$$

$R_{50\%}$ : Mass resolution according to the FWHM method

$t$ : time-of-flight of known substance (here 92  $m/z$ )

$\Delta t_{FWHM}$ : peak width of known substance at 50 % signal intensity.

The linear range was determined to be greater than three magnitudes [232]. The ion source and the flight tube are differentially pumped by a 520 L/s ( $N_2$ ) and a 210 L/s ( $N_2$ ) turbomolecular pump (TMU521, TMU 261, Pfeiffer Vacuum, Aslar, Germany). The vacuum achieved in the ion source is ca.  $10^{-4}$  mbar and in the flight tube ca.  $10^{-6}$  mbar, when the inlet system is connected to the capillary type described earlier. Ions are detected using a two-stage multichannel plate detector (MCP) in Chevron assembly with 40 mm active diameter. The TOF mass spectra are recorded via a transient recorder card (Aquiris, Switzerland, 250 MHz, 1 GS, signal resolution 8 bit (256 points)). Data processing is done by a LabView (National

Instruments, USA), based on purpose-written software. Table 9 illustrates the applied voltages and instrumental details of the time-of-flight mass spectrometer.

Table 9: Applied voltages and instrumental details of the time-of-flight mass spectrometer

Pressure ionisation chamber	$10^{-4}$ mbar
Pressure TOF tube	$10^{-6}$ mbar
Repeller	+ 600 V
1 <sup>st</sup> Extraction	- 600 V
2 <sup>nd</sup> Extraction (Liner)	- 2990 V
Brems field	- 1080 V
Reflection field	+ 1280 V
Lens	- 1600 V
Multi Channel Plate	< - 2100 V
Detector type	Chevron Typ S3040-10-D Multi Channel Plate (MCP) Detector (Burle Electro-Optics, Inc., USA)
Reflectron TOF drift range	801 mm
Mass resolution $R_{50\%}$	1800 $m/z$ [174]
Linear range	$> 10^3$ [232]

Quantification was carried out by performing external calibration with different commercial standard gases (Linde AG, Germany).

The detection limits of the instrument were determined according to Williams et al. [233] by using equation (26). In this study detection limit calculations refer to a signal-to-noise ratio (S/N) of greater than two.

$$d = \frac{2cs}{(p - m)} \quad (26)$$

d: detection limit

c: standard gas concentration

m: mean value of the noise level (baseline)

s: standard deviation of the noise level

p: signal peak height of standard gas

In Table 10 the limits of detection (LOD) in parts-per-billion [ppb] of a variety of compounds are shown. For all species, six different averages (AVG) of mass spectra (1, 2, 3, 5, 10, and 100 mass spectra averaged) are illustrated, which is equivalent to different time resolutions. Concentrations of the calibration (cal.) gases used in parts-per-million [ppm] are also indicated. Theoretically, the detection limit improves with the square root of averaged spectra [174].

Table 10: Detection limits of a variety of compounds. Six different averages of mass spectra (1, 2, 3, 5, 10, and 100) are tabulated, which represent six different time resolutions

<b>Compound</b>	<b>cal. gas [ppm]</b>	<b>AVG 1 [ppb]</b>	<b>AVG 2 [ppb]</b>	<b>AVG 3 [ppb]</b>	<b>AVG 5 [ppb]</b>	<b>AVG 10 [ppb]</b>	<b>AVG 100 [ppb]</b>
<i>Alkanes</i>							
Pentane	10.2	670	408	393	324	273	105
Hexane	10.5	228	197	170	126	96	38
Heptane	10.2	156	132	110	82	61	23
<i>Alkenes</i>							
Propene	10.8	87	71	45	42	30	10
Butene	10.2	39	30	28	21	15	6
Pentene	9.47	52	42	39	32	22	8
Butadiene	9.2	64	54	37	34	20	8
Isoprene	9.1	93	85	59	45	29	11
<i>Alkynes</i>							
Propyne	9.97	36	26	18	17	12	4
Butyne	9.01	47	36	25	23	16	5
<i>Aromatics</i>							
Benzene	10.0	56	45	46	36	28	16
Toluene	9.3	92	72	66	55	44	25
m-Xylene	9.1	109	89	82	68	53	30
Styrene	9.2	82	71	47	44	27	10
<i>Carbonylic compounds</i>							
Acetaldehyde	11.4	82	92	74	75	43	14
Acetone	10.6	82	92	78	74	39	14
Acrolein	10.5	62	50	38	33	25	8
<i>other compounds</i>							
Nitric oxide	5110	26322	18330	15443	11920	8878	3094
Nitric dioxide	487	2044	1048	1497	1011	751	282

Figure 15 shows the signal intensities of the calibration gases except NO and NO<sub>2</sub> due to their much higher concentration. After compensation of the slightly varying standard concentrations (between 9.1 ppm and 11.4 ppm), all signals were normalised to the signal from benzene for comparison.

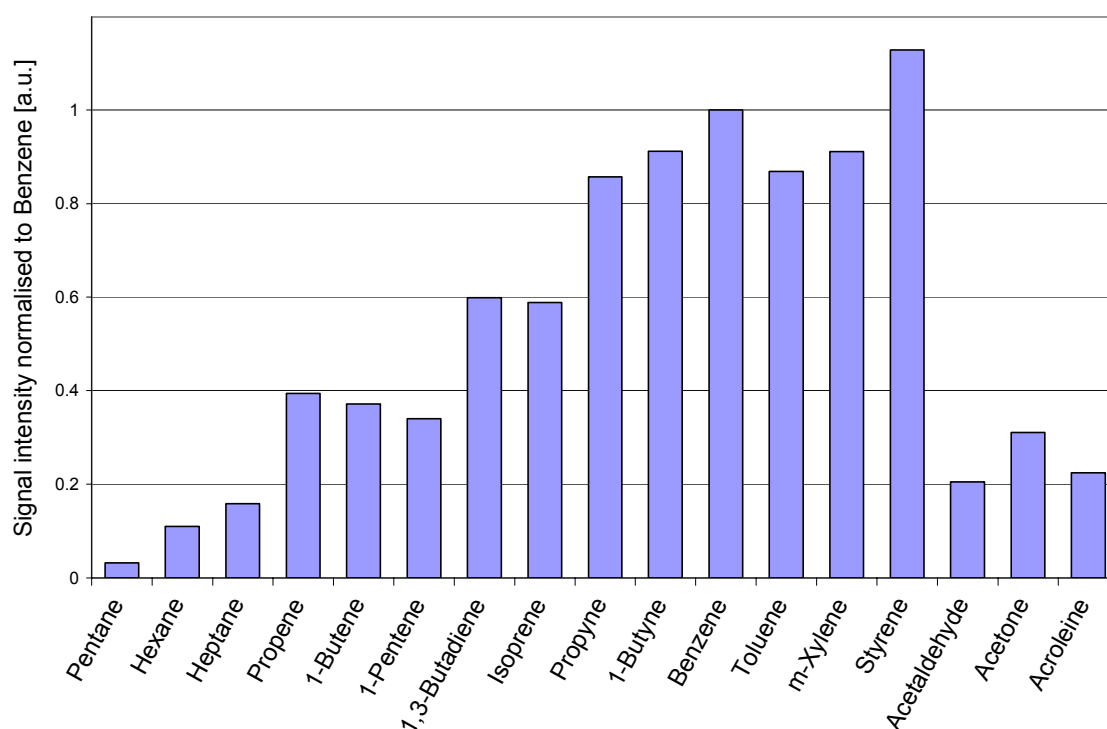


Figure 15: Comparison of the signal intensities of the calibration gases of equal concentration normalised to the signal of benzene

It can be clearly seen that for the photon energy of 10.49 eV the alkanes pentane, hexane, and heptane have the lowest signal intensities. The intensity rises with the carbon atom number within this class. The carbonylic species acetaldehyde, acetone and acroleine also have weak signals. It seems as if ketones result in slightly higher intensities than aldehydes but a greater number of carbonylic compounds must be evaluated for an unambiguous conclusion. The other classes increase in signal intensity in the following order: alkanes (propene, butane, pentene), alkenes with conjugated double-bonds (butadiene and isoprene), alkynes (propyne and butyne), and aromatic species (benzene, toluene, xylene, and styrene). The latter two classes feature very similar values. In this context it seems as if an unsaturated substitute (ethenyl) at the aromatic ring system results in a rise in signal intensity (styrene). In contrast, methyl substitutes lead to weaker signals (toluene and xylene). Table 11 exhibits the photoabsorption and photoionisation cross sections as well as the photoionisation quantum

yields of those chemicals at 10.49 eV, if available in the literature [172 and references therein]. In addition, the difference between the applied photon energy of 10.49 eV and the IP of the corresponding compounds ( $\Delta E$ ) and the relative (rel.) signal intensity normalised to the value of benzene is also given.

Table 11: Photoabsorption cross sections, photoionisation cross sections, photoionisation quantum yields, differences between the applied photon energy of 10.49 eV and the corresponding IPs, and the relative signal intensities of the standard compounds normalised to benzene [172]

Compound	$\Delta E$ [eV]	$\sigma_i$ [Mb]	$\sigma_a$ [Mb]	$\gamma$	rel. signal
Pentane	0.12	-	64	-	0.03
Hexane	0.31	-	76	-	0.11
Heptane	0.59	-	90	-	0.16
Propene	0.76	10 - 11	34 – 40	0.28 – 0.30	0.39
Butene	0.92	10	48	0.21	0.37
Pentene	-	-	-	-	0.34
Butadiene	1.42	18	-	-	0.60
Isoprene	-	-	-	-	0.59
Propyne	0.12	24 - 26	58	0.41 – 0.43	0.86
Butyne	0.31	33	66	0.50	0.91
Benzene	1.25	22	54	0.41	1
Toluene	1.66	-	61	-	0.87
Xylene	1.99	-	-	-	0.91
Styrene	-	-	-	-	1.13
Acetaldehyde	-	-	-	-	0.20
Acetone	-	-	-	-	0.31
Acroleine	-	-	-	-	0.22

The relative signal intensities vary with different photon energies. However, for the same photon energy, here 10.49 eV, every compound has a specific value. Therefore once the relation to an optional compound, here benzene, is known, quantification of all compounds is possible by only calibrating the reference substance. Future work could address the establishment of a comprehensive database of the signal intensities of many different species in relation to a reference compound of choice. This would enable a fast (only one calibration gas needs to be applied) and reliable (database is established under lab conditions) quantification scheme for all sorts of laboratory as well as field applications.

### 3. Pyrolysis experiments of tobacco

The experimental work in this thesis divides into two main approaches. This first one here deals with pyrolysis studies of pure tobacco whereas in the second one, puff-by-puff resolved measurements of complete cigarettes are carried out.

Pyrolysis (Py) is defined as degradation and transformation of materials under the effect of heat [97]. In Chapter 3.1 a brief introduction to pyrolysis in general and the pyrolysis of tobacco is given. It outlines former works in that field and explains the still existing necessity and scientific value of tobacco pyrolysis studies. Chapter 3.2 and 3.3 deal with the description of the experimental set-up and the coupling of the pyrolysis furnace to the SPI-TOFMS as well as the preparation of the tobacco samples. The data processing and discussion of the results is carried out in Chapter 3.4. Therein several tobacco smoke constituents are identified and the influence of temperature and reaction gas composition on their formation and decomposition is shown. Furthermore, it is shown that different tobacco types lead to different smoke compositions. After a detailed characterisation of the single tobacco types it is demonstrated how these tobaccos can be discriminated by focussing on a few key compounds.

#### 3.1. Introduction to pyrolysis

Pyrolysis is roughly divided into two groups, analytical pyrolysis, which is used to identify thermal degradation products of macromolecules, and applied pyrolysis, aimed at the production of advanced materials (e.g. ceramics) from polymer precursors [234].

Pyrolysis experiments in this study refer to analytical pyrolysis. Timeline and history of analytical pyrolysis covering the most important innovations can be found in [235, 236]. Today pyrolysis is a well established method for the investigation of a variety of materials. The following articles give a good overview on several related fields, such as methodology development, pyrolysis mechanisms, and polymeric precursors [234, 237-244].

In this context, tobacco is a very challenging biomatrix because of the large number of substances present in the feedstock and in the generated smoke. In Chapter 1.4.2 an overview on possible precursors of many substances present in tobacco smoke was given. Most of these smoke constituents are at trace levels [14], indicating the importance of highly sensitive analytical techniques. The main reason for pyrolysis studies of tobacco is the fact that several experimental conditions can be adjusted and controlled. The highly complex and changing conditions of varying temperatures and oxygen levels inside a burning cigarette were described in Chapter 1.4.1. These conditions are far too complex to be simulated in pyrolysis studies, however, it was possible to set the furnace and gas supply to several different combustion and pyrolysis conditions. This can give insights into the complex chemistry of many smoke constituents by revealing the preferred formation and decomposition conditions. In the past, a wide range of pyrolysis studies on tobacco, e.g. [98, 124, 127, 128, 245-253] as well as on individual tobacco additives and ingredients, e.g. [254-264] have been undertaken, mainly by application of conventional analytical methods such as gas chromatography (Py-GC-MS) and infrared spectroscopy (Py-IR). A detailed discussion on pyrolysis experiments of tobacco samples can be found in [114, 261 and references therein]. However, in recent years, application of soft ionisation methods, e.g. molecular beam mass spectrometry [265], field ionisation mass spectrometry [246, 251, 266], and resonance enhanced multiphoton mass spectrometry [267, 268], coupled to pyrolysis devices has been of growing interest. The main reason for this trend is the complexity of the matrix tobacco and tobacco smoke since techniques that cause fragmentation further complicate the investigation and evaluation of the pyrolysis gas formed. By applying soft analysis methods a fast and comprehensive characterisation of the resulting pyrolysis gas is possible. In the framework of this work the SPI-TOFMS was coupled to a pyrolysis furnace and applied to the thermal investigation and characterisation of tobacco.

### 3.2. Experimental set-up of pyrolysis experiments

The schematic illustration (Fig. 16) of the Py-SPI-TOFMS system demonstrates the experimental setup.

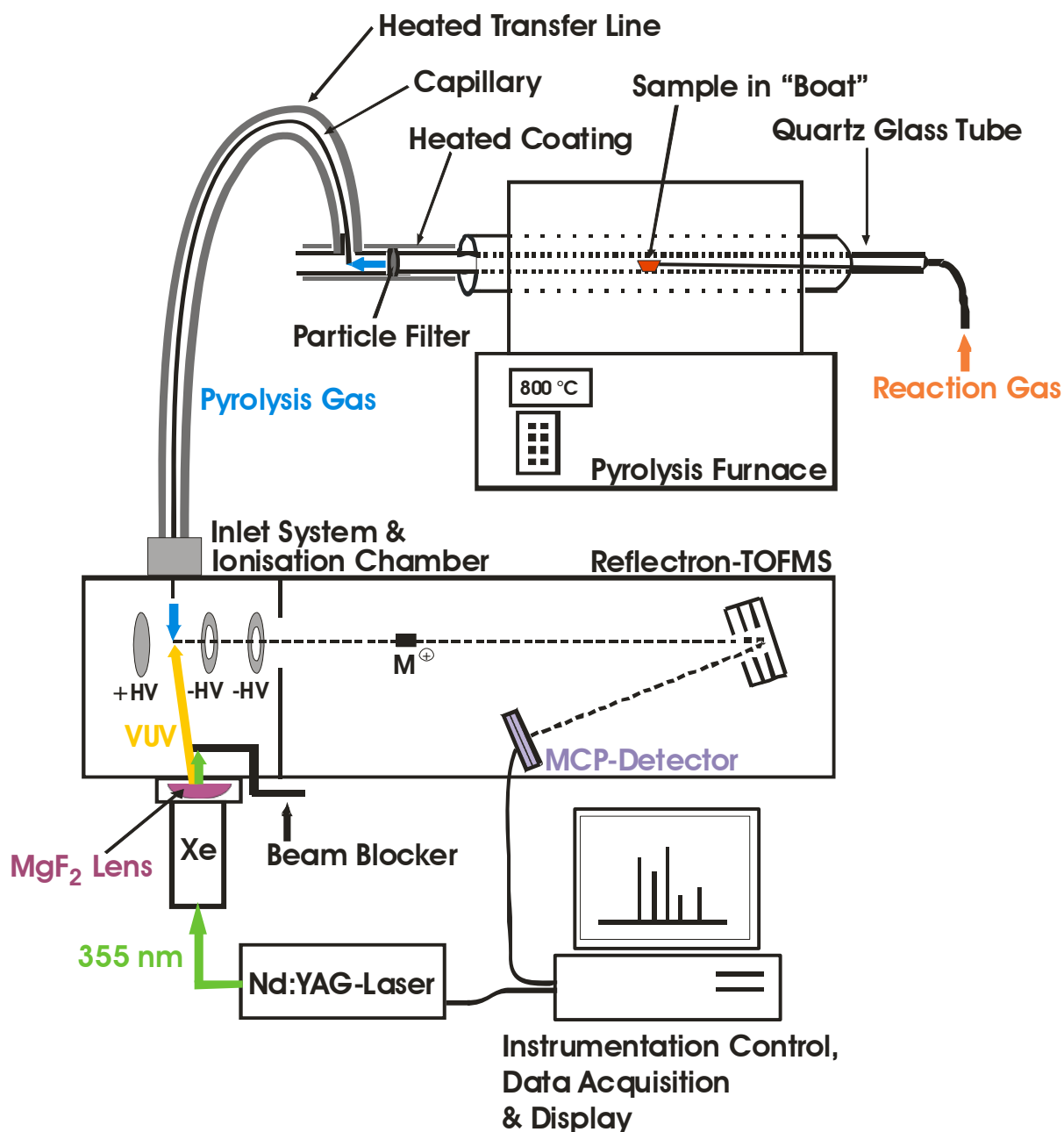


Figure 16: Illustration of the experimental set-up of the SPI-TOFMS system coupled to the pyrolysis furnace

A rotary furnace (Carbolite GmbH, Germany), which was used for the pyrolysis experiments, is connected via the transfer line. Inside the furnace, a quartz glass tube (length 140 cm; 13 mm i.d.) was inserted. At the outlet of the furnace the quartz tube was connected to a filter

holder containing a Cambridge filter to separate particles from the gas stream. That was followed by a glass T-piece connected to the transfer line containing the deactivated fused silica capillary. All devices between the furnace and transfer line such as quartz tube, Cambridge filter holder, T-piece and all connection parts were wrapped with heating mats which were constantly heated to 220 °C to prevent condensation and memory effects. The transfer line was also heated to 220 °C. The capillary was placed orthogonally to the main gas flow inside the T-piece, extracting a small portion of the pyrolysis gas. Figure 17 exhibits the outlet of the furnace with the quartz tube wrapped in heating mats and the transfer line containing the capillary connected to the tube.



Figure 17: Outlet of the pyrolysis furnace with the quartz tube wrapped in heating mats and the transfer line of the SPI-TOFMS coupled orthogonally to the quartz tube

At the other end of the transfer line the capillary is housed inside the heated, hollow inlet needle reaching into the ionisation chamber which was described in Chapter 2.3.

In total, the furnace temperature was set to seven fixed isothermic temperatures of 400 °C, 500 °C, 600 °C, 700 °C, 800 °C, 900 °C, and 1000 °C, respectively. Two measurement series

with different reaction gases, synthetic air (80 % nitrogen, 20 % oxygen) and nitrogen respectively, were carried out. In these experiments a flow rate of 0.5 L/min was adjusted. Figure 18 shows the inlet of the furnace and the quartz tube with the reaction gas line connected to the tube. The Cambridge filter was replaced after every run.



Figure 18: Inlet of the pyrolysis furnace and the quartz tube with the reaction gas line connected to the tube

### 3.3. Sample preparation

The samples were placed in a quartz “boat” and pushed into the middle of the tube by a wire connected to the boat. Simultaneously the data acquisition was started. Tobacco samples have been taken from three different tobacco types: Burley, Virginia, and Oriental. These tobacco types are the main contributors to blended American-style cigarettes sold in the USA and other countries [13, 269, 270]. Cigarettes containing these tobacco types were stored for several days under controlled conditions of 22 °C and 60 % humidity [60]. Before being

pyrolysed the cigarette wrapper was removed and 50 mg of tobacco was placed in the quartz glass boat. One great benefit of the furnace used compared to commercially-available pyrolyser devices is that no further treatment of the sample such as grinding is necessary. The quartz boat containing a sample is illustrated in Figure 19.



Figure 19: Photograph of the quartz boat containing a tobacco sample taken before being pushed into the quartz tube of the pyrolysis furnace

In total, three replicates were measured for each tobacco type, temperature and gas composition. These results were used to account for temperature dependence and reaction gas composition dependence discussed later.

A further series of measurements dealt with the characterisation and discrimination of the three tobacco types by advanced statistical methods. In the experiments the furnace temperature was set to 800 °C. This pyrolysis temperature was chosen because it roughly resembles the conditions in a burning cigarette but, in principle, any temperature could have been adjusted which leads to thermal decomposition. Furthermore, in contrast to the first pyrolysis studies for the analysis of the influence of temperature and reaction gas composition where measurements were carried out in triplicate, the number of analysed replicates for the statistical approach was increased to ten measurements. The reason for this is the general fact

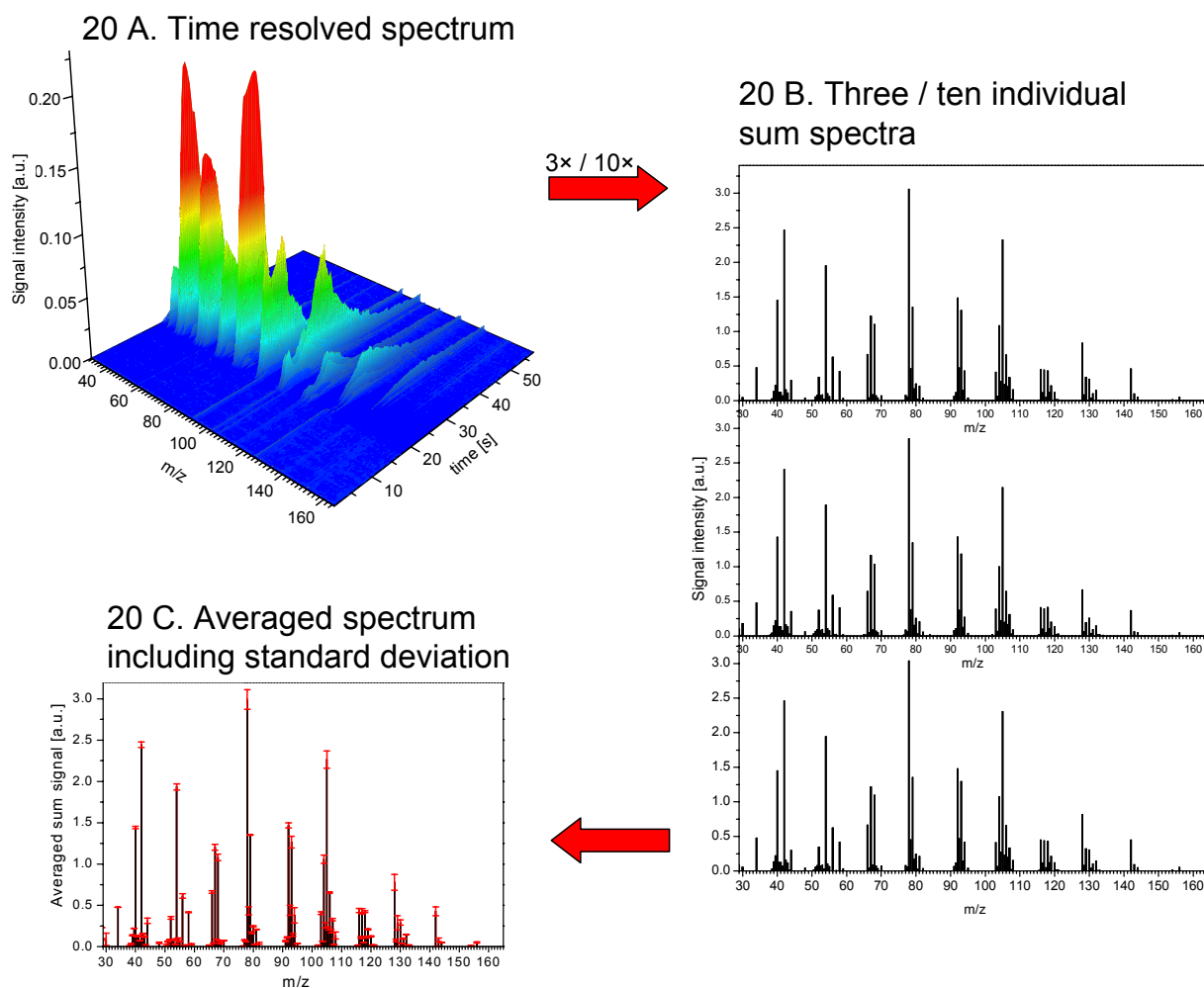
that a statistical evaluation is more reliable the higher the number of measurements. In the framework of this study ten replicates were regarded as a fair compromise. In addition, these pyrolysis experiments were performed in nitrogen, but similarly to the chosen temperature of 800 °C, any reaction gas composition could have been applied. All other experimental conditions were kept unchanged.

### **3.4. Results and discussion of pyrolysis experiments**

This chapter deals with the processing and interpretation of the results of the pyrolysis experiments. In 3.4.1 it is described how the time-resolved time-of-flight spectra are converted to sum spectra accounting for one specific sample and which substances are present in there. In Chapter 3.4.2 the patterns of these spectra are discussed regarding temperature and reaction gas composition. This leads to findings concerning preferred formation and also decomposition conditions of several tobacco constituents in general. In contrast, Chapter 3.4.3 and 3.4.4 deal with the extensive characterisation of different tobacco types and how they can be discriminated by SPI-TOFMS.

#### **3.4.1. Spectra processing and mass assignment**

The recorded time-of-flight spectra were converted into mass spectra as described in Chapter 2.2. Data acquisition was adjusted to average five mass spectra in order to get two complete mass spectra every second by using a 10 Hz laser. Depending on temperature and reaction gas the pyrolysis signals lasted for up to 80 seconds. Since time-resolution did not matter in this experiment, the recorded spectra were added up resulting in a single sum spectrum for each measurement, which is demonstrated for tobacco pyrolysis in nitrogen at 800 °C in Figures 20 A to C. In so doing, Figure 20 A illustrates the online recorded time profile of the occurring pyrolysis process and Figure 20 B describes the resulting sum spectrum after the adding up procedure. The three replicates of the first and the ten replicates of the second measurement series, respectively, were used to calculate mean and standard deviation of each applied condition which is exemplified in Figure 20 C.



Figures 20 A, B, and C: Conversion of time-resolved recorded mass spectra into averaged sum spectra including standard deviation

In general, a definite assignment of all observed masses to chemical compounds and sources is not possible due to the large number of species present in tobacco pyrolysis and the complexity of possible reaction pathways. Table 12 accounts for the most likely options. Component suggestions were made by means of the quoted references which only comprise a part of the literature available in that field.

Table 12: Assignment of observed tobacco masses to most possible chemical compounds in tobacco pyrolysis and cigarette smoke according to listed references

<i>m/z</i>	Most possible compounds	Reference
17	NH <sub>3</sub>	[55, 249]
30	NO	[250, 265]
34	H <sub>2</sub> S	[55, 249]
40	Propyne	[55]
42	Propene	[55, 265]
43	Carbohydrate fragment: C <sub>3</sub> H <sub>7</sub> <sup>+</sup> , C <sub>2</sub> H <sub>3</sub> O <sup>+</sup>	[100, 249, 265]
44	Acetaldehyde	[55, 124, 271]
48	Methanethiol	[55, 249]
52	1-Buten-3-yne,	[55]
54	1,3-Butadiene, 1-Butyne	[55, 265]
56	2-Propenal, Butene, 2-Methylpropene	[55, 114, 124, 265]
57	Carbohydrate fragment, 2-Propen-1-amine	[55, 249]
58	Acetone, Propanal	[55, 124, 249, 271]
59	2-Propanamine	[55]
66	Cyclopentadiene	[55, 124, 265]
67	Pyrrole	[55, 114, 124, 248, 249, 265]
68	Furan, Isoprene, 1,3-Pentadiene, Cyclopentene	[55, 124, 249, 265, 271]
69	Pyrroline	[55, 124, 249, 265]
70	2-Butenal, Methyl vinyl ketone, Methylbutene, Pentene, Butenone, 2-Methyl-2-Propenal	[55, 124, 271]
71	Pyrrolidine	[55]
72	2-Methylpropenal, 2-Butanone, Butanal	[55, 124, 249, 271]
74	Water-eliminated glycerol (C <sub>3</sub> H <sub>6</sub> O <sub>2</sub> ), Tetrahydrofuran	[55, 58, 249]
77	Unidentified fragment	
78	Benzene	[55, 124, 248, 265, 271]
79	Pyridine	[55, 124, 248]
80	Pyrazine	[55]
81	Methyl pyrrole	[55, 249, 265]
82	Methylfuran, Methylcyclopentene, Cyclohexene, 2-Cyclopenten-1-one	[55, 114, 124, 249, 258, 271]
83	Pentanenitrile, 3-Methylbutanenitrile	[55, 249]
84	Nicotine fragment, Cyclopentanone, Dimethylbutene, Hexene, 3-Methyl-3-buten-2-one	[55, 124, 249, 265]
85	Methylpyrrolidine, Piperidine	[55, 249]
86	Methylbutanal, 3-Methyl-2-butanone, Pentanone, 2,3-Butanedione	[55, 124, 249]
92	Toluene	[55, 124, 249, 265]
93	Aniline, Methylpyridine	[55, 58, 114, 124, 248, 251, 265]
94	Phenol, 2-Vinylfuran	[55, 114, 124, 249, 251]
95	Pyridinol, Ethylpyrrol, Dimethylpyrrol	[249, 265]
96	Dimethylfuran, Furfural	[55, 114, 124, 243, 249, 251, 258, 265, 271]
97	Carbohydrate fragment, Hexanenitrile,	[55, 265]

	Methylpentanenitrile	
98	Furanmethanol, Methyl-2-pentenal, 5-Methyl-2(5 <i>H</i> )-furanone, 3-Methyl-2(5 <i>H</i> )-furanone, 1,3-Cyclopentanedione	[114, 124, 249, 258, 265] [243, 251, 258]
102	Phenylacetylene	[124, 249]
103	Benzonitrile	[114, 124, 248]
104	Styrene, 3-Pyridinecarbonitrile	[55, 124, 248, 265]
105	Vinylpyridine	[55, 124, 248, 265]
106	Xylene, Ethylbenzene, Benzaldehyde	[55, 114, 124]
107	Ethylpyridine, Methylbenzeneamine, 3-Pyridinecarboxaldehyde	[55, 114, 249]
108	Anisol, Dimethylpyridine, Methylphenol	[55, 114, 124, 249, 255, 258]
109	3-Methoxypyridine	[249]
110	Dihydroxybenzene, 2-Acetylfuran, Methylfurfural	[55, 124, 249, 251, 258, 265]
112	Acetylcyclopentane, 2-Hydroxy-3-methyl-2-cyclopenten-1-one	[58, 124, 249, 251]
116	Indene	[55, 124, 265]
117	Indole, Methylbenzonitrile	[248, 249, 265, 272]
118	Indane, Methylstyrene, Benzofuran	[124, 265]
119	Indoline, Aminostyrol, Methylvinylpyridin	
120	Methylethylbenzene, Trimethylbenzene	[55, 114, 124]
121	Dimethylaniline, Acetylpyridine, Ethyl-methylpyridine	[55, 249, 251, 265]
122	Benzoic acid, Ethylphenol, Hydroxybenzaldehyde,	[55, 114, 124, 249, 255, 258]
124	Dihydroxymethylbenzene, Guaiacol	[55, 124, 249, 251, 258, 273]
126	5-Hydroxymethylfurfural	[55, 243, 249, 258, 265]
128	Naphthalene	[114, 124, 249, 265]
129	Quinoline, Isoquinoline	[55, 124, 248]
130	Methylindene	[124]
132	Methylbenzofuran, 1-Indanone, Isopropenyltoluene	[55, 124]
134	Isopropyltoluene	[55]
136	Limonene, Methoxybenzaldehyde, 2-Ethyl-5-methylphenol	[55, 58, 114, 124, 251, 255, 258, 265]
142	Methyl naphthalene	[55, 124, 245, 249, 265]
146	Myosmine	[114, 249]
152	Vanillin, 4-ethyl-2-methoxyphenol, 3-Methoxy-2-hydroxybenzaldehyde, Acenaphthylene	[55, 245, 249, 255, 273]
153	Naphthalenecarbonitrile	
154	Dimethoxyphenol, Vinylnaphthalene	[55, 58, 124, 249, 251, 258]
156	Bipyridine, Dimethylnaphthalene	[55, 58, 124, 251]
162	Nicotine, Anabasine	[55, 114, 124, 251]

### **3.4.2. Influence of temperature and reaction gas composition on tobacco pyrolysis**

The occurrence of pyrolysis products strongly depends on pyrolysis conditions, mainly temperature and reaction gas composition. Figure 21 exhibits the total averaged signal SPI mass spectra for pyrolysis temperatures of 400 °C, 500 °C, 600 °C, 700 °C, 800 °C, 900 °C, and 1000 °C for Burley tobacco in nitrogen. For the first evaluations little or no differences of the three tobacco types could be observed by the naked eye. Subsequently, the following interpretation is generally valid for all tobacco types with slight fluctuations only. A detailed characterisation and distinction of the individual tobacco types is given later.

The change of the overall pattern of the mass spectra can be clearly seen. However, the standard deviations are disregarded in Figure 21 in order to keep the illustration simple. Therefore, little peaks and small changes in signal intensities should not be overrated. Scaling of the y-axes (signal intensity) of the individual temperatures is variable because they are adjusted to the highest peak in the corresponding spectrum to enable comparison of the patterns. Absolute signal intensities for different temperatures are discussed later for selected compounds. The same spectra at the different temperatures but in synthetic air are presented in Figure 22 with the same y-axes scaling which makes it possible to compare the patterns of the same temperatures but different reaction gases.

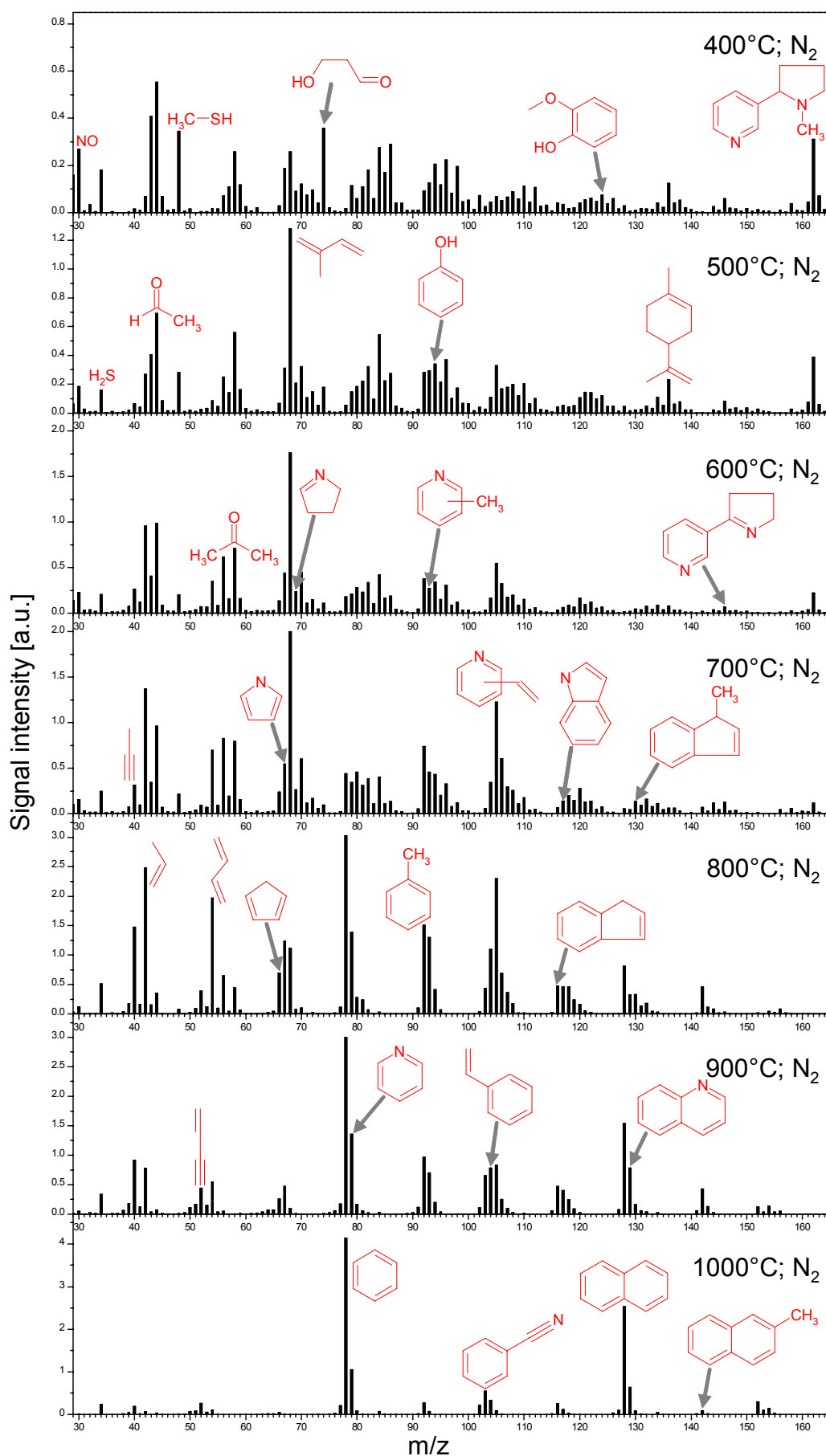


Figure 21: SPI sum spectra of Burley tobacco at 400 °C, 500 °C, 600 °C, 700 °C, 800 °C, 900 °C and 1000 °C in nitrogen

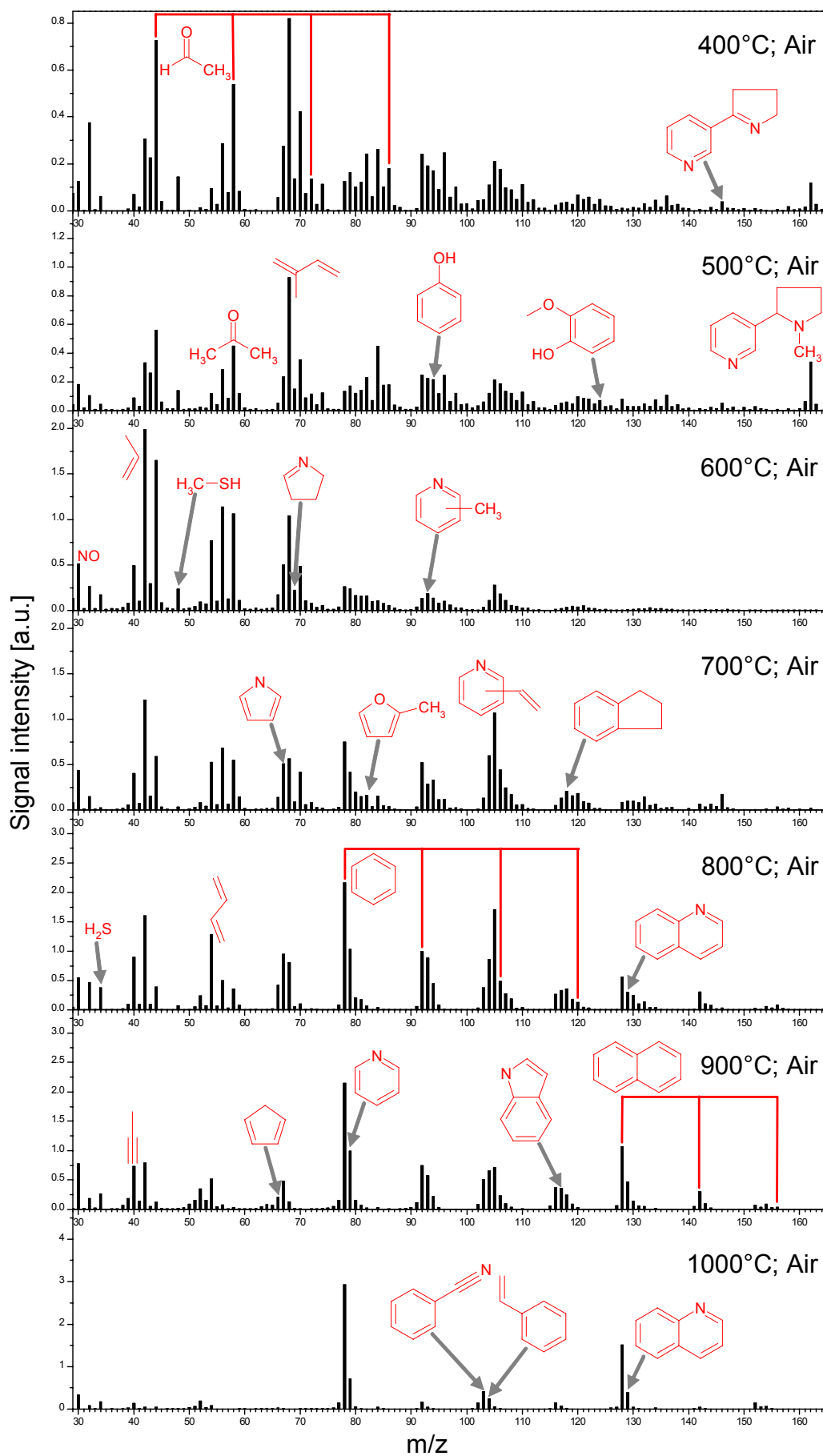


Figure 22: SPI sum spectra of Burley tobacco at 400 °C, 500 °C, 600 °C, 700 °C, 800 °C, 900 °C and 1000 °C in synthetic air

The less severe pyrolysis conditions of 400 °C yield a great variety of species. Besides tobacco components (e.g. nicotine 162  $m/z$  and water-eliminated glycerol 74  $m/z$ , see equ. 27 [58, 114]) decomposition products from thermal degradation of carbohydrates such as cellulose, lignin and sugars (e.g.  $m/z$  43, 44, 56, 58, 72, 82, 86, 96, 98, and 110) as well as proteins and amino acids (e.g.  $m/z$  67, 69, 79, 81, and 93) are present [55, 58, 114, 246, 248, 249, 265, 271]. Signal intensities in synthetic air are mostly higher, especially for 42  $m/z$  (propene), 56  $m/z$  (2-propenal, butene, 2-methylpropene), 58  $m/z$  (primarily acetone), 68  $m/z$  (isoprene, furan), and 70  $m/z$  (crotonaldehyde amongst others). Obviously thermal degradation takes place to a greater extent when oxygen is present at this low temperature. This is supported by higher yields of 48  $m/z$  (methanethiol), 162  $m/z$  (nicotine), and 74  $m/z$  (water-eliminated glycerol) in nitrogen which survive in a non-oxidative atmosphere.

At 500 °C the overall pattern is similar to 400 °C. In synthetic air hardly any differences can be observed. Remarkable are the rise of 68  $m/z$  (isoprene/furan) and the decrease of 74  $m/z$  (water-eliminated glycerol) in nitrogen.

By increasing the temperature to 600 °C the diversity of observed masses is still evident in nitrogen. Thermal degradation products rise, simultaneously 162  $m/z$  (nicotine) is decreasing. In synthetic air, higher molecular mass signals are vanishing, 162  $m/z$  (nicotine) is completely gone. Simultaneously unsaturated and oxygen-containing compounds further increase, especially 42  $m/z$  (propene) 44  $m/z$  (acetaldehyde), 54  $m/z$  (butadiene), 56  $m/z$  (2-propenal, butene, 2-methylpropene), and 58  $m/z$  (acetone).

At 700 °C, most striking is the immense rise of vinylpyridine (105  $m/z$ ) in both atmospheres, which is reported as a decomposition product of nicotine and other nitrogen-containing compounds under severe pyrolysis conditions [55, 248, 265]. This nicotine decomposition includes rupture of the pyrrolidine and the pyridine ring resulting in pyridines (e.g. vinylpyridine, 105  $m/z$ ), aryl nitriles (e.g. benzonitrile, 103  $m/z$ ), and aromatic hydrocarbons (e.g. toluene, 92  $m/z$ ). Schmeltz et al. suggested several pathways and identified more than 38 compounds in the nicotine pyrolyzate [145], demonstrating the complexity of the cracking and pyrosynthetic reactions occurring. 68  $m/z$  (isoprene/furan) is still abundant in nitrogen whereas it does not play a great role in air anymore. Signal intensities in the latter atmosphere become generally lower, indicating rising conversion of compounds into substances not accessible by SPI-TOFMS, e.g. CO and CO<sub>2</sub>.

When increasing the temperature to 800 °C, the pattern changes. In nitrogen, 68  $m/z$  (isoprene/furan) also loses its supremacy and 162  $m/z$  (nicotine) vanished. 78  $m/z$  (benzene) becomes the prevailing peak in both atmospheres. At this severe temperature thermal

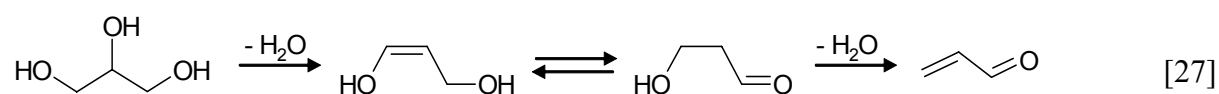
degradation of carbohydrates such as cellulose, lignin and sugars as well as proteins, alkaloids and amino acids with subsequent pyrosynthesis of thermally more stable compounds occurs. Subsequently the spectra shift towards unsaturated components such as 40  $m/z$  (propyne), 42  $m/z$  (propene), and 54  $m/z$  (butadiene) and homologous series of methylated benzenes ( $78 + (n \times 14)$ ;  $n = 0,1,2,\dots$ ) and naphthalenes ( $128 m/z + (n \times 14)$ ;  $n = 0,1,2,\dots$ ) as well as other substituted aromatic species e.g. 104  $m/z$  (styrene), 105  $m/z$  (vinylpyridine), 116  $m/z$  (indene), and 118  $m/z$  (indane). In contrast, oxygen-containing compounds show the opposite behaviour and decrease ( $m/z$  44, 56, 58, 70, 82, 86, 96). Apart from signal intensity hardly any differences between air and nitrogen atmosphere can be observed.

The general trend continues at 900 °C. Predominantly unsaturated species are visible, first and foremost 78  $m/z$  (benzene) and 128  $m/z$  (naphthalene). Substituted aromatic chemicals decrease such as 92  $m/z$  (toluene) and 105  $m/z$  (vinylpyridine). The occurrence of 30  $m/z$  (NO) in nitrogen is depleted whereas in air, it still exists.

Finally, pyrolysis at 1000 °C results in dramatic changes to the pattern of the spectra. Almost all masses are gone or only have little signal intensities. The spectra in both atmospheres are dominated by 78  $m/z$  (benzene) and 128  $m/z$  (naphthalene) together with a few smaller peaks, e.g. 92  $m/z$  (toluene), 103  $m/z$  (benzotrile), and 104  $m/z$  (styrene). The spectrum at 1000 °C clearly shows that at such high temperatures only the most stable aromatic compounds prevail.

Evans and Milne [274] illustrated the nature of the products as a function of pyrolysis severity. Moderate temperatures lead to so-called primary components, which are substantially free of gas phase cracking products. Under more severe conditions these substances undergo subsequent thermal degradation resulting in secondary components. Tertiary components are generated by further decomposition and pyrosynthesis of the secondary compounds [265, 274].

At the high temperatures applied in the pyrolysis experiments, glycerol (1,2,3-trihydroxypropane) immediately eliminates water and finally most likely leads to acrolein, a substance also on the ‘Hoffmann list’, which is demonstrated in equation 27.



Equation 27: Thermal decomposition of glycerol via the water-eliminated intermediate product 3-hydroxy propanal

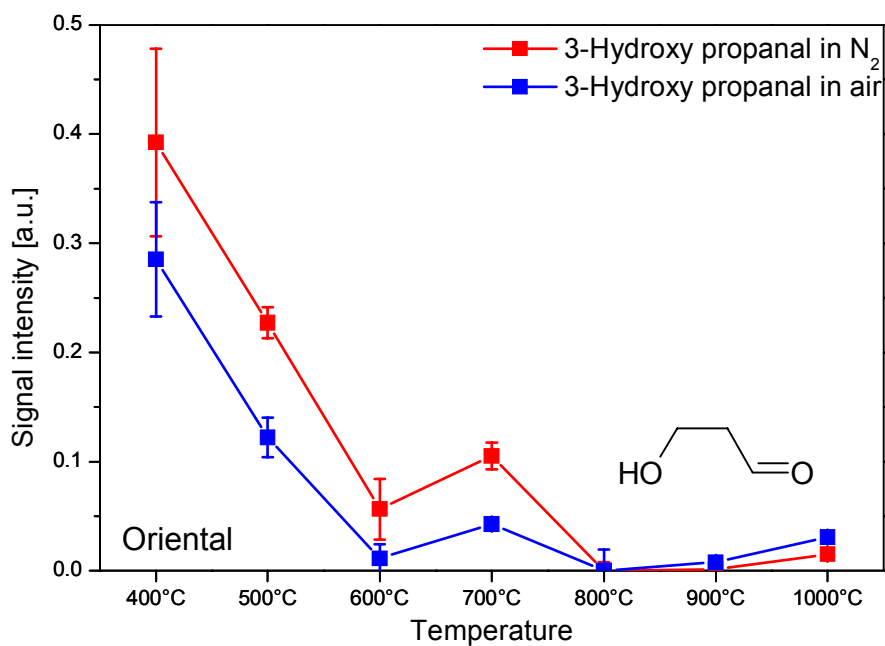
The water-eliminated intermediate product of glycerol, 3-hydroxy propanal ( $C_3H_6O_2$ , 74  $m/z$ ), exhibits the typical behaviour of a primary component which is shown in Figure 23 A. In both reaction gases, nitrogen and air, the highest yields can be observed for the lowest applied pyrolysis temperature of 400 °C. With increasing temperature, their signals tend to decline due to thermal degradation up to almost complete decomposition at 800 °C.

The afore-mentioned behaviour of oxygen-containing and unsaturated compounds for different temperatures is again illustrated in Figure 23 B by means of acetaldehyde (44  $m/z$ ) and cyclopentadiene (66  $m/z$ ) in nitrogen and air, respectively. Both substances show a rise and decline in signal intensity within the temperature range but have their maxima at different temperatures. This behaviour results in their classification as secondary components. The formation of these species depends mainly on prior decomposition reactions. In the case of Burley tobacco, acetaldehyde clearly exhibited the behaviour of a secondary component, having one formation maximum. Higher yields were detected in air as shown. However, this is not universally valid since the other tobacco types featured an ambiguous behaviour in this regard (not shown here). Especially the pyrolysis of Virginia tobacco in air also resulted in greater occurrence of acetaldehyde at 400 °C, already leading to two maxima (400 °C and 600 °C).

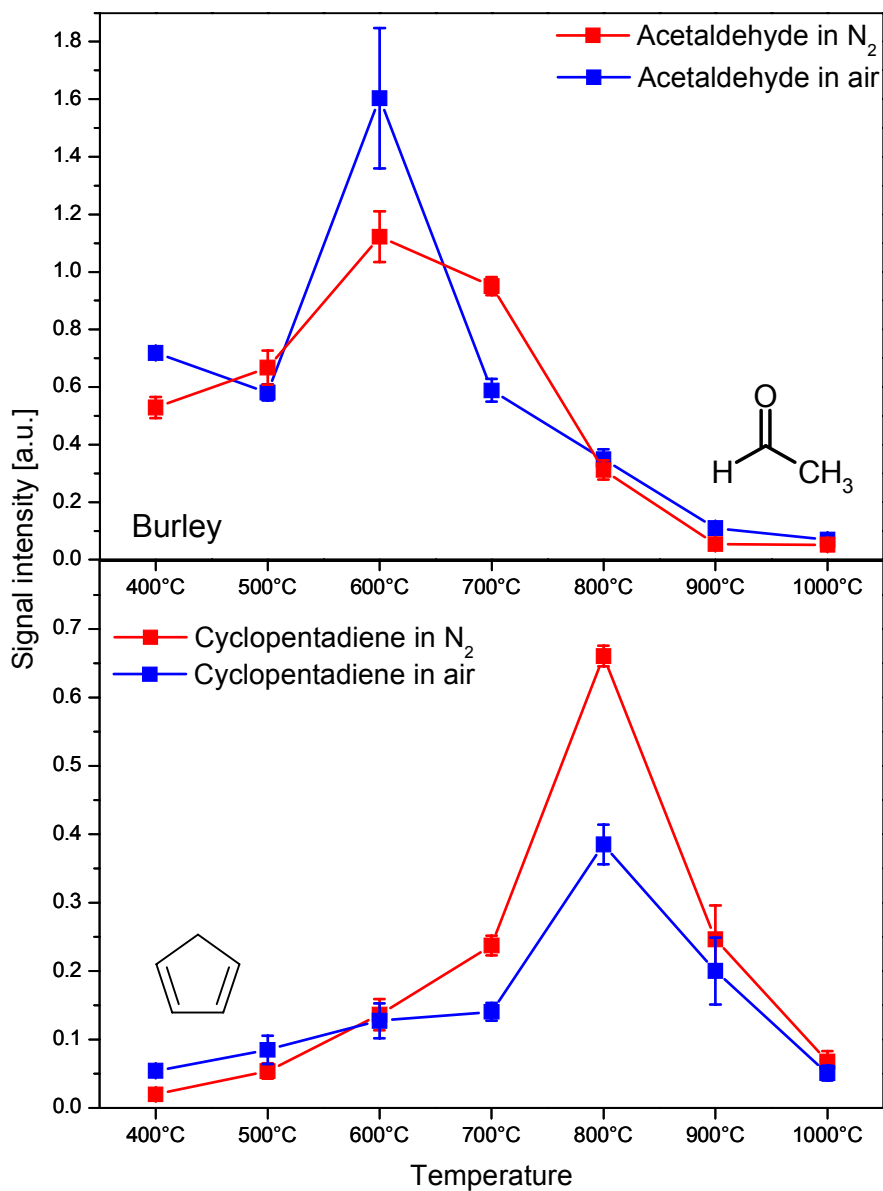
In addition to unsaturated and oxygen-containing compounds, certain aromatics e.g. indene (116  $m/z$ ) and indole (117  $m/z$ ) as well as substituted aromatic compounds e.g. alkylated benzenes (92  $m/z$  and 106  $m/z$ ), can also be classified as secondary components.

In contrast, the group of tertiary components mainly consists of thermally stable aromatic compounds without side chains and a few substituted aromatic species e.g. benzonitrile (103  $m/z$ ). Figure 23 C demonstrates their thermal behaviour by means of naphthalene (128  $m/z$ ).

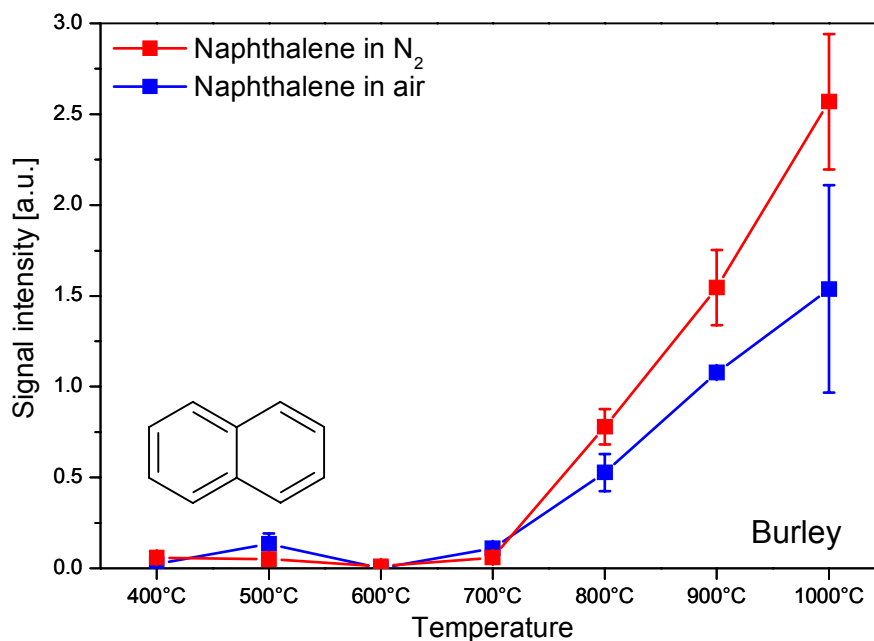
23 A:



23 B:



23 C:



Figures 23 A, B, and C: Behaviour of primary (Fig. 23 A), secondary (Fig. 23 B), and tertiary components (Fig. 23 C) as a function of temperature from the pyrolysis of tobacco in nitrogen and air atmosphere by means of selected compounds and tobacco types

The results achieved enabled an unambiguous classification of a wide range of tobacco smoke substances into either primary, secondary or tertiary compounds which is illustrated in Table 13. Components not listed either showed behaviour of more than one class or differences between tobacco types occurred as explained for acetaldehyde earlier. The reasons for this can originate from different sources for the same compound, e.g. distillation from the tobacco into the smoke (primary component) and formation via pyrolysis/pyrosynthesis reactions (secondary or tertiary product) in similar measures.

Table 13: Classification of observed tobacco masses as primary, secondary or tertiary component

<i>m/z</i>	Compounds present in tobacco pyrolysis gas	Classification
34	H <sub>2</sub> S	Secondary
40	Propyne	Secondary
42	Propene	Secondary
43	Carbohydrate fragment: C <sub>3</sub> H <sub>7</sub> <sup>+</sup> , C <sub>2</sub> H <sub>3</sub> O <sup>+</sup>	Primary
48	Methanethiol	Primary
54	1,3-Butadiene, 1-Butyne	Secondary
56	2-Propenal, Butene, 2-Methylpropene	Secondary
66	Cyclopentadiene	Secondary
67	Pyrrole	Secondary
74	3-Hydroxy propanal, Tetrahydrofuran	Primary
77	Fragment	Tertiary
78	Benzene	Tertiary
80	Pyrazine	Secondary
85	Methylpyrrolidine, Piperidine	Primary
86	Methylbutanal, 3-Methyl-2-butanone, Pentanone, 2,3-Butanedione	Primary
92	Toluene	Secondary
93	Aniline, Methylpyridine	Secondary
98	Furanmethanol, Methyl-2-pentenal, 5-Methyl-2(5 <i>H</i> )-furanone, 3-Methyl-2(5 <i>H</i> )-furanone, 1,3-Cyclopentanedione	Primary
103	Benzonitrile	Tertiary
104	Styrene, 3-Pyridinecarbonitrile	Secondary
105	Vinylpyridine	Secondary
112	Acetylcyclopentane, 2-Hydroxy-3-methyl-2-cyclopenten-1-one	Primary
118	Indane, Methyl styrene, Benzofuran	Secondary
119	Indoline, Aminostyrol, Methylvinylpyridin	Secondary
128	Naphthalene	Tertiary
129	Quinoline, Isoquinoline	Tertiary
130	Methylindene	Secondary
142	Methyl naphthalene	Secondary
152	Vanillin, 4-ethyl-2-methoxyphenol, 3-Methoxy-2-hydroxybenzaldehyde, Acenaphthylene	Tertiary
162	Nicotine, Anabasine	Primary

This group assignment makes it possible to draw conclusions on the formation and decomposition mechanisms of the detected species in smoke and provides an insight into the complex tobacco chemistry.

In this context the thermal behaviour of nicotine is of great interest since it is one of the target tobacco constituents for scientists and governmental regulations likewise. As reported in Chapter 1.4.2.7., Schmeltz and co-workers studied the thermal decomposition of nicotine in

nitrogen and found more than 38 pyrolysis and combustion products [145]. However, they performed pyrolysis experiments of the pure compound and at a temperature range between 600 °C and 900 °C. In contrast, the pyrolysis studies in this work were carried out with real tobacco samples. Furthermore, the temperature range spanned from 400 °C to 1000 °C. Therefore results of the present study can be used to determine whether pure nicotine behaves similarly to nicotine in tobacco. In addition to that, the thermal behaviour and fate of the pyrolysis products of nicotine is determined at the same time for a wide temperature range. Figure 24 accounts for the thermal decomposition of nicotine, specifically shown for Burley tobacco in nitrogen.

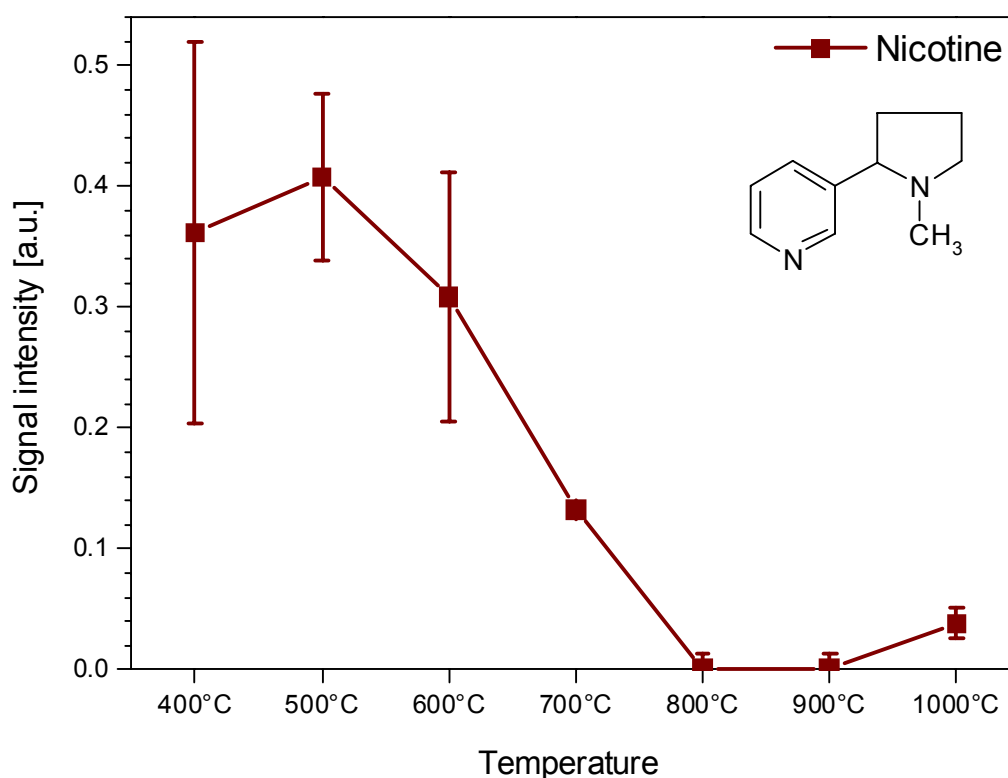


Figure 24: Thermal decomposition of nicotine in Burley tobacco in nitrogen in the temperature range from 400 °C to 1000 °C

Nicotine exhibits the typical behaviour of a primary compound. Yields at the lower temperatures are relatively high and decrease at more severe conditions until its complete decomposition at about 800 °C. Schmeltz et al. also reported that the most extensive degradation under their extreme pyrolysis conditions occurs above 600 °C but no indication is given about the temperature of total break-down. However, in practice, nicotine in a burning

cigarette is transferred into the cigarette smoke due to the elevated temperatures in the tobacco rod before the tobacco is actually burnt.

A wide range of possible pyrolysis products of nicotine could be detected which partially featured very different thermal behaviours. Schmeltz et al. [145] reported on simple pyridines, quinolines, aryl nitriles, and aromatic hydrocarbons, the two latter classes especially at high temperatures. The authors postulated extensive rupture of the pyrrolidine and, possibly, pyridine rings into small CH and CHN fragments, which then recombined, to form pyridine and quinoline structures and aromatic systems. Since tobacco is a highly complex matrix where many chemical reactions take place in parallel further origins for these smoke constituents cannot be excluded. Nevertheless, the high yield of nicotine in tobacco is supposed to contribute greatly to the detected signal intensities. Figures 25 A, B, and C show pyrroline (69  $m/z$ ; Fig. 25 A), myosmine (146  $m/z$ , Fig. 25 C), and 84  $m/z$  (Fig. 25 B). The latter compound always appeared in combination with nicotine which was also mentioned in [265] and is most likely a fragment formed when the pyridine and the methylpyrrolidine ring break apart homolytically. These three species appear at 400 °C already. Therefore they either distil out of unburnt tobacco or thermal formation occurs at rather low temperatures already. The formation maximum is between 500 °C and 700 °C and they do not play a great role at temperatures above 800 °C.

Fig. 25 A:

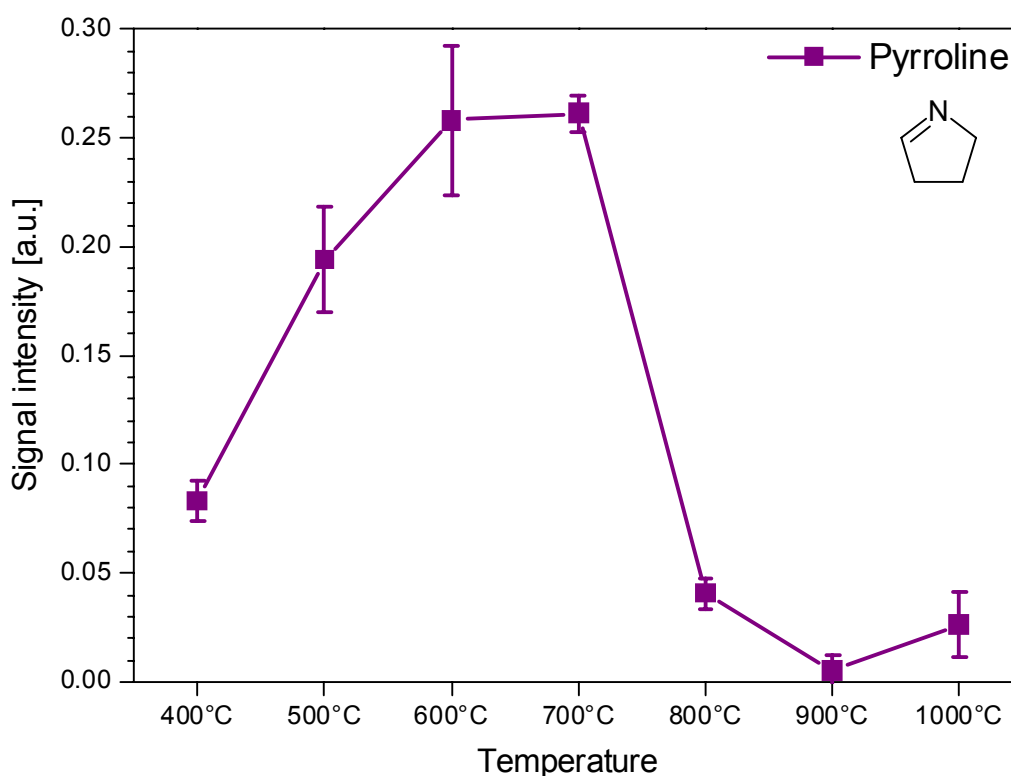


Fig. 25 B:

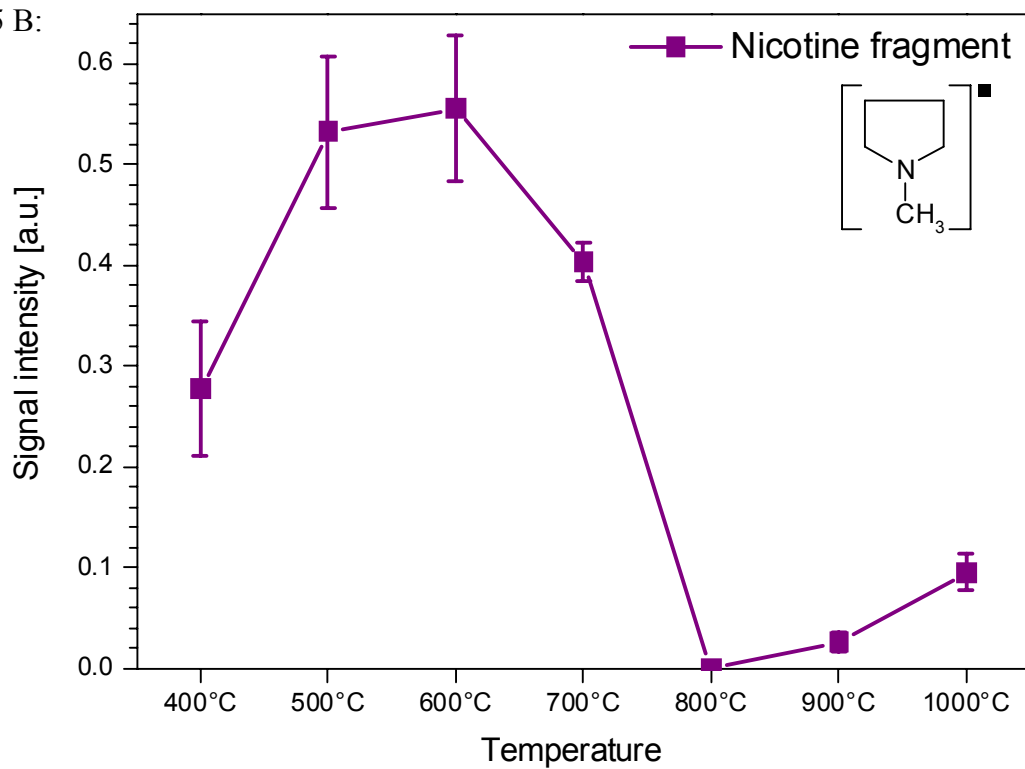


Fig. 25 C:

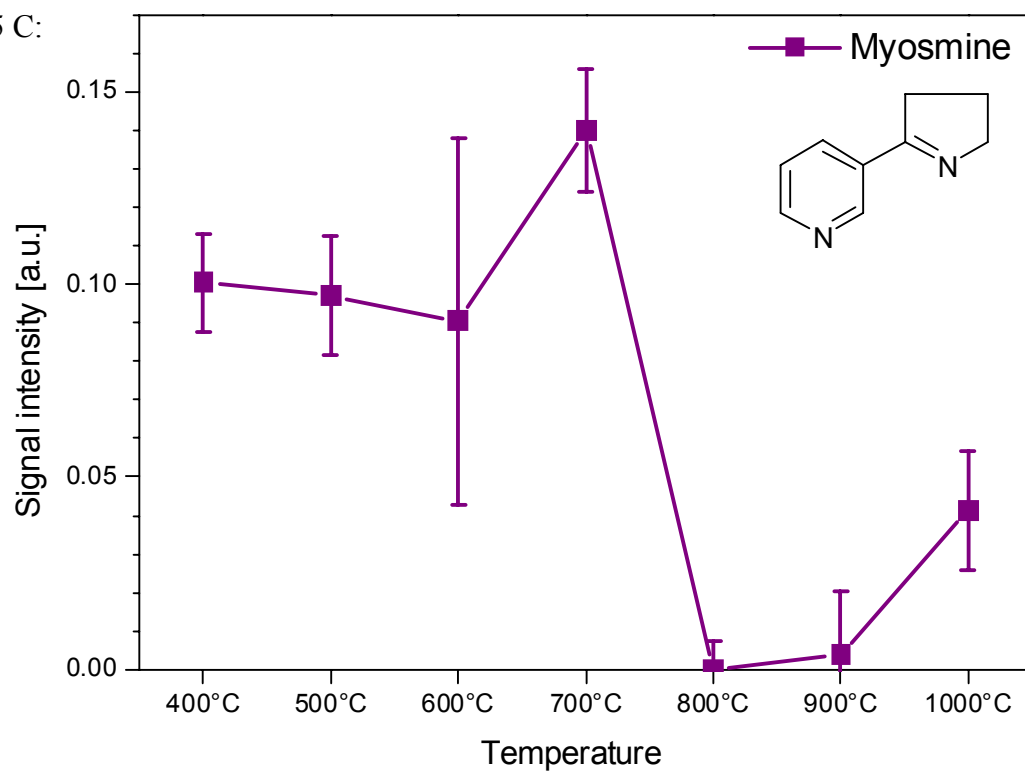


Figure 25 A, B, C: Thermal behaviour of the possible nicotine pyrolysis products pyrroline (69  $m/z$ , Fig. 25 A), a nicotine fragment (84  $m/z$ , Fig. 25 B), and myosmine (146  $m/z$ , Fig. 25 C) in Burley tobacco in nitrogen in the temperature range from 400 °C to 1000 °C

A second group of possible decomposition products of nicotine is mainly formed at higher temperatures. They appear in very small amounts only at the lowest temperature of 400 °C and their formation maximum is at approximately 800 °C. Therefore further decomposition of the first group of pyrolysis products could also contribute to this group of compounds. Examples of this type are given in Figures 26 A, B, C, and D.

Fig. 26 A:

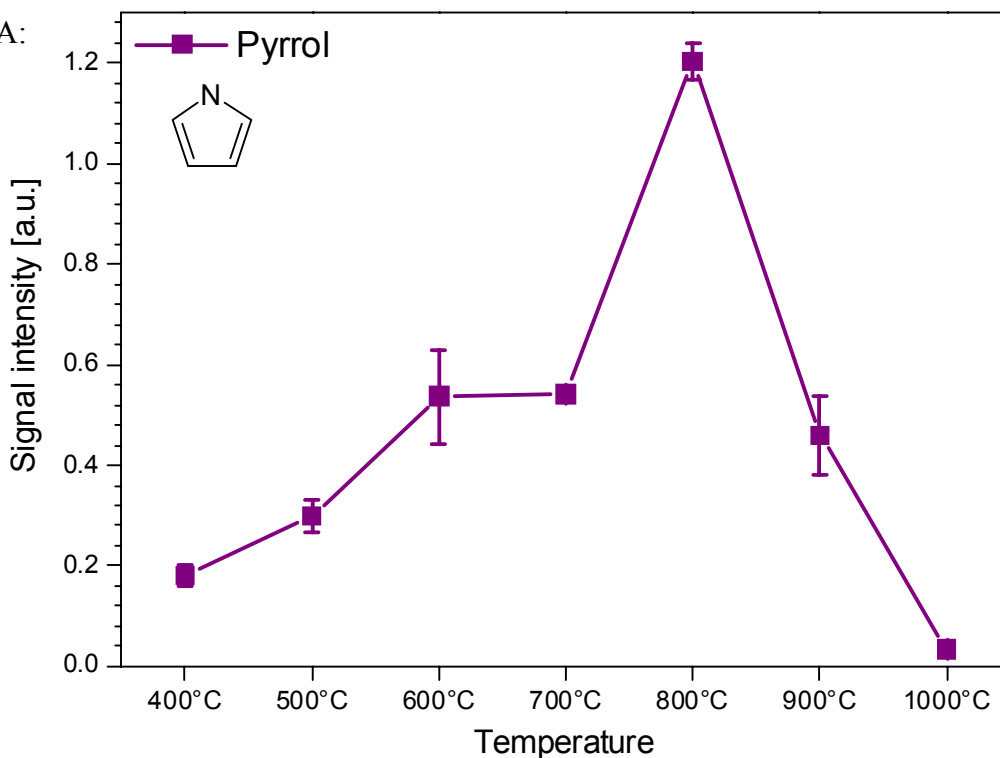
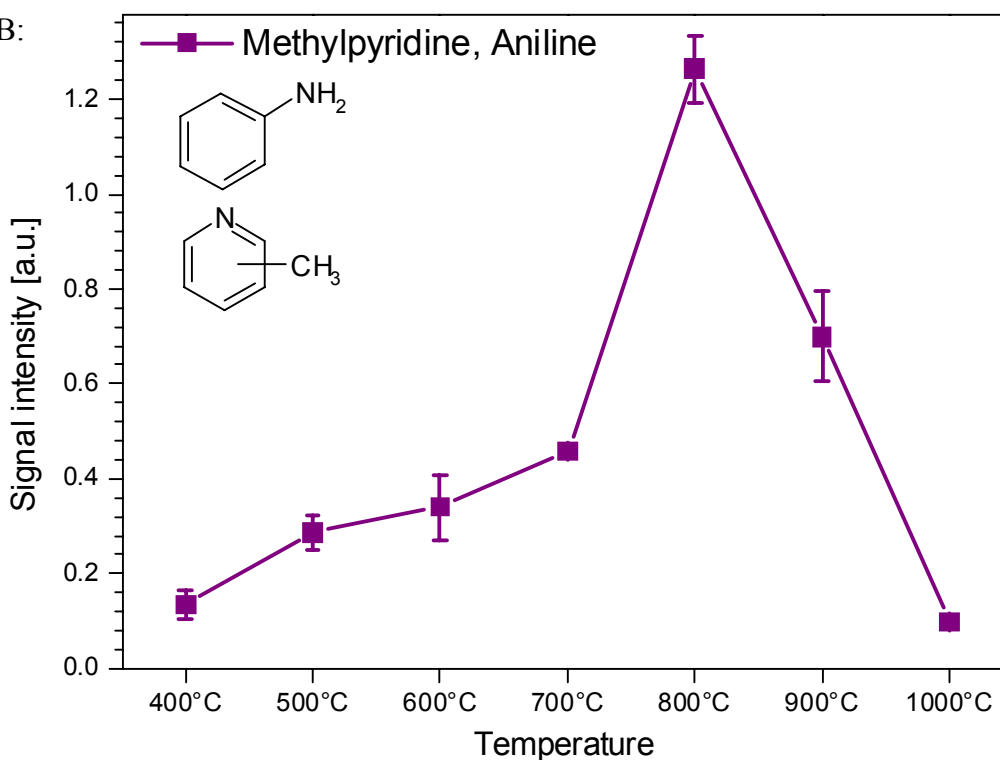
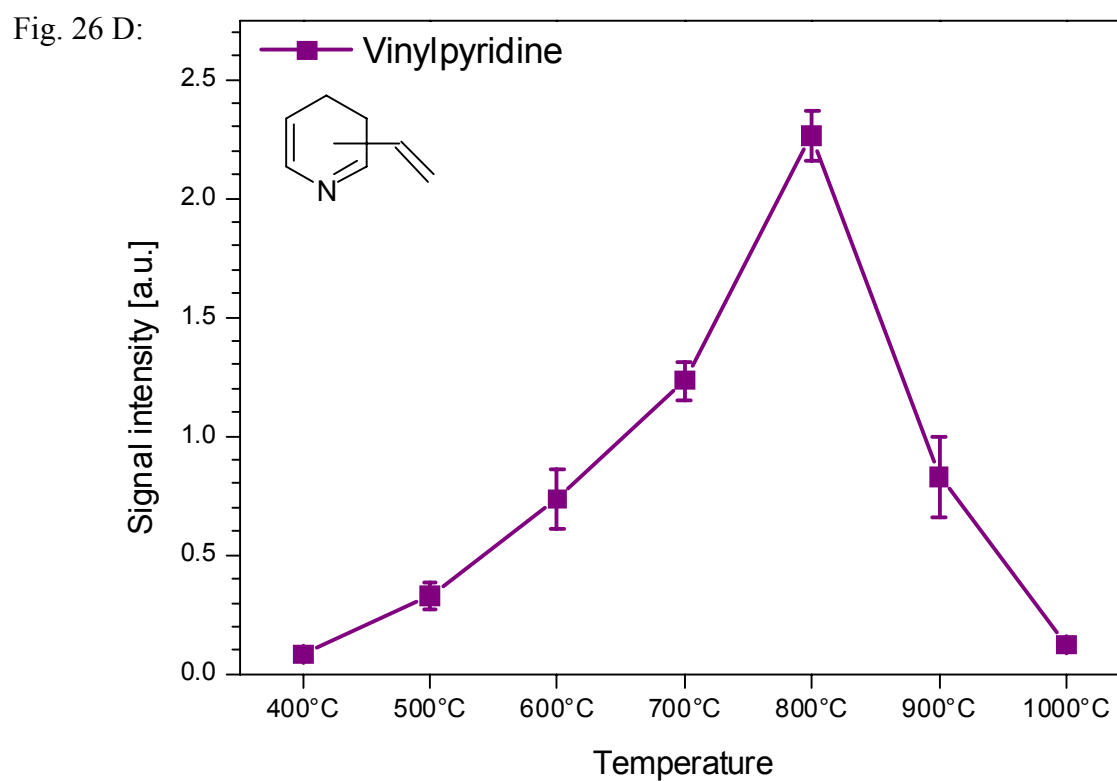
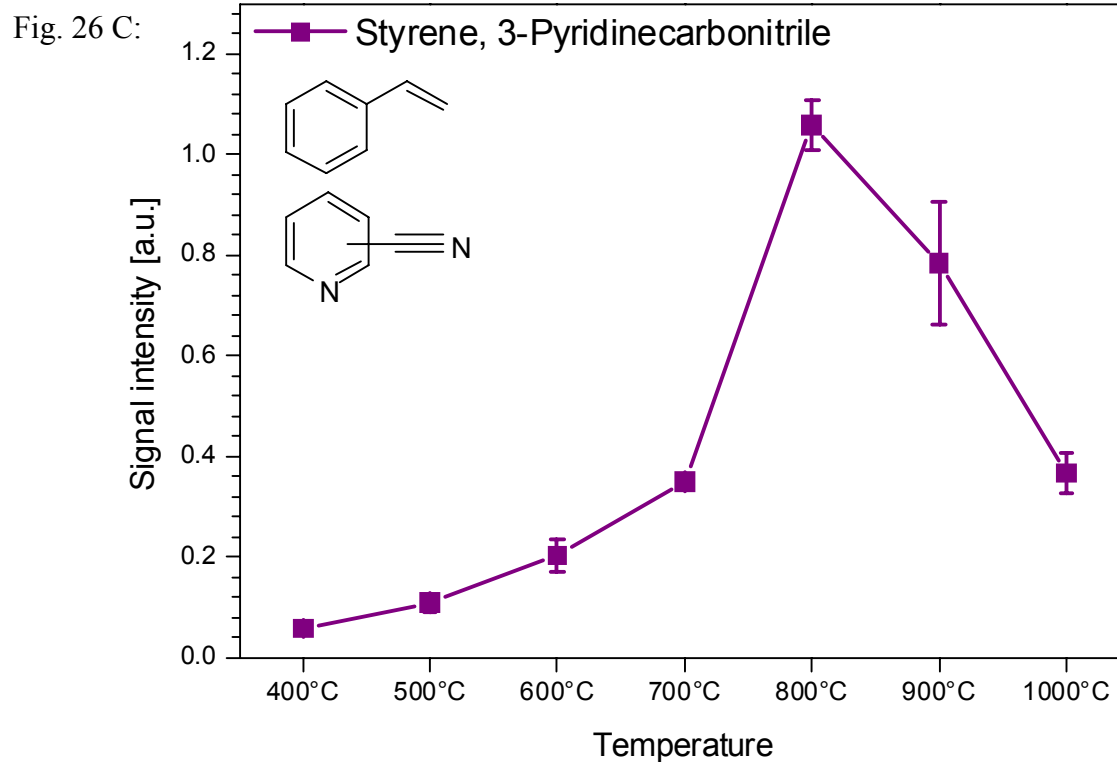


Fig. 26 B:





Figures 26 A, B, C, and D: Thermal behaviour of the possible nicotine pyrolysis products pyrrole (67  $m/z$ , Fig. 26 A), methyl pyridine/aniline (93  $m/z$ , Fig. 26 B), styrene/pyridinecarbonitrile (104  $m/z$ , Fig. 26 C), and vinylpyridine (105  $m/z$ , Fig. 26 D) in Burley tobacco in nitrogen in the temperature range from 400 °C to 1000 °C

However, both groups of compounds cannot be the final decomposition products of nicotine at very high temperatures since all species dramatically decline at 900 ° and 1000 °C. As mentioned earlier, only the most thermally stable compounds survive these severe conditions. Many of them only consist of aromatic skeletal structures without substitutes as indicated in Fig. 27 A, B, D, and E. Exceptions are benzonitrile (Fig. 27 C) and naphthalenecarbonitrile (Fig. 27 F).

Fig. 27 A:

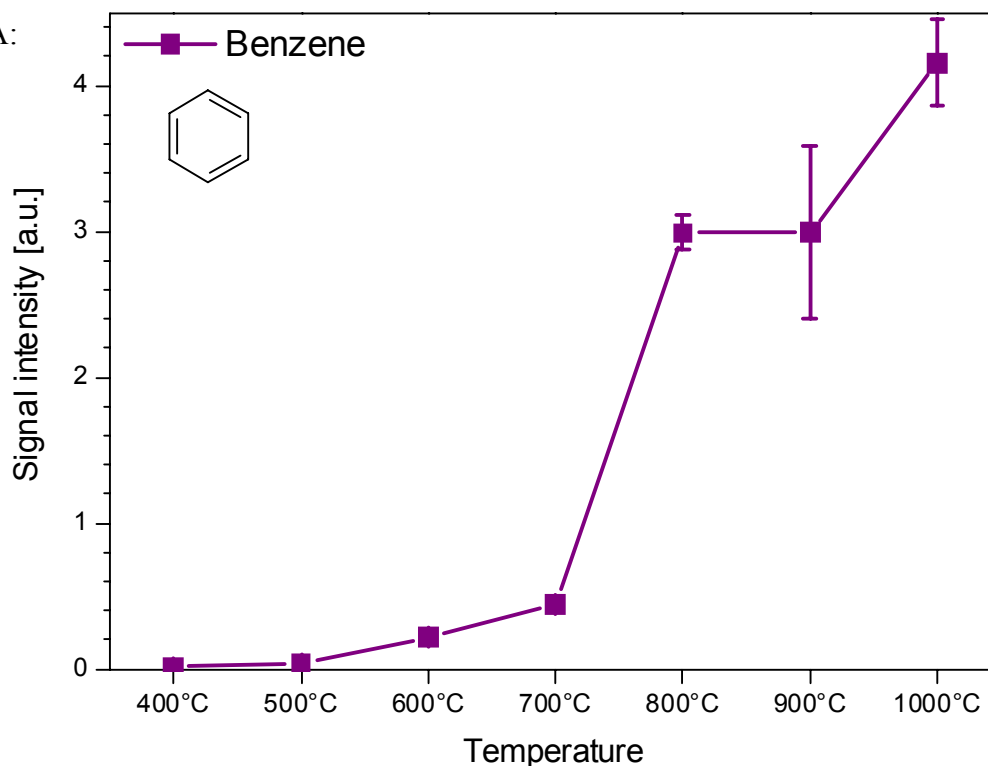


Fig. 27 B:

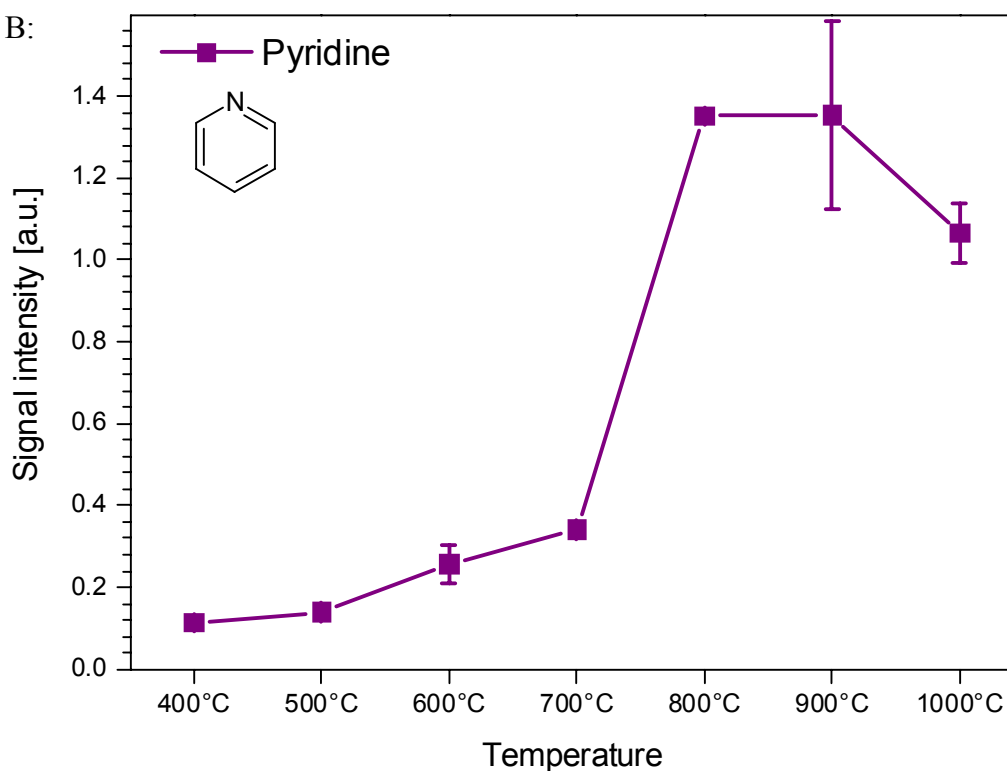


Fig. 27 C:

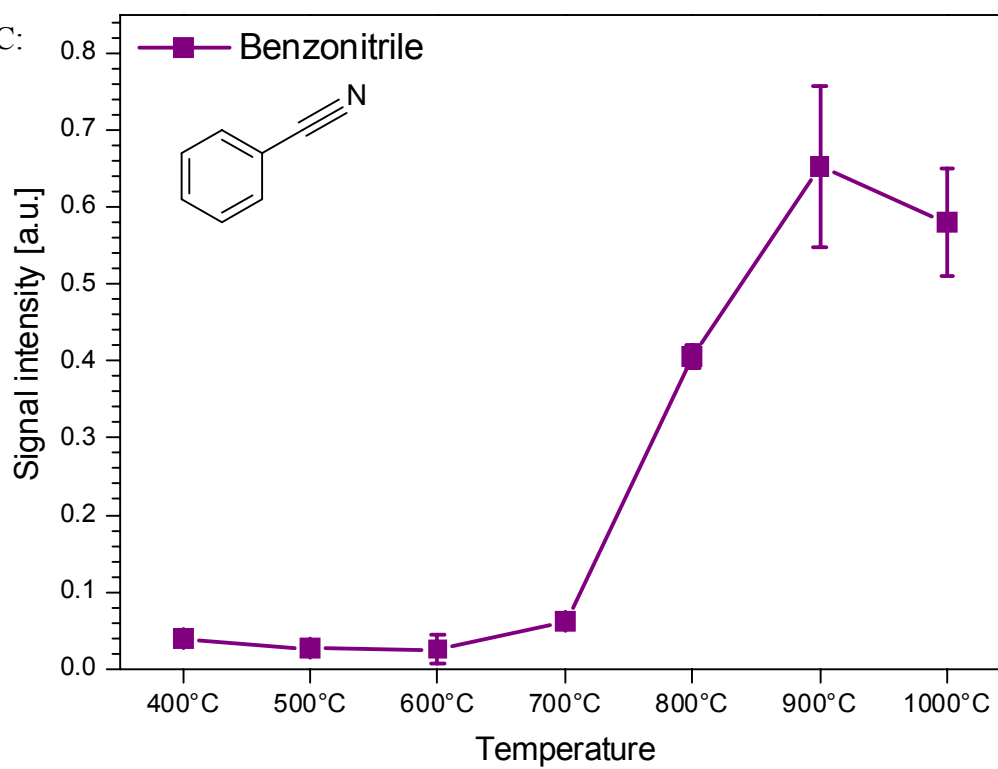


Fig. 27 D:

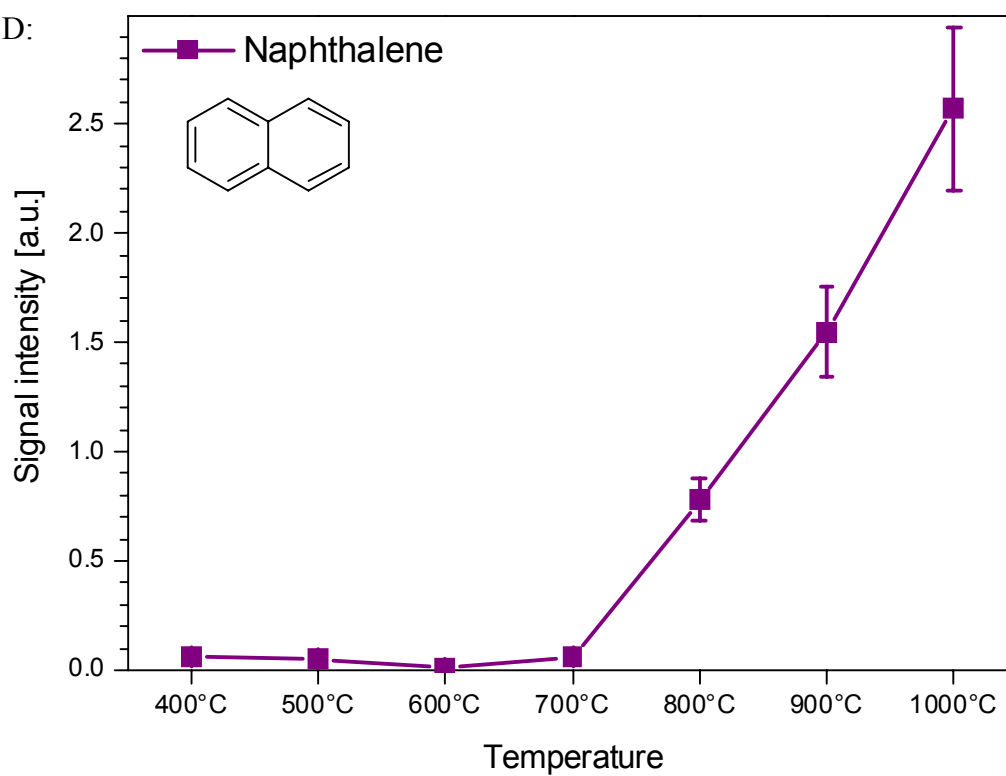


Fig. 27 E:

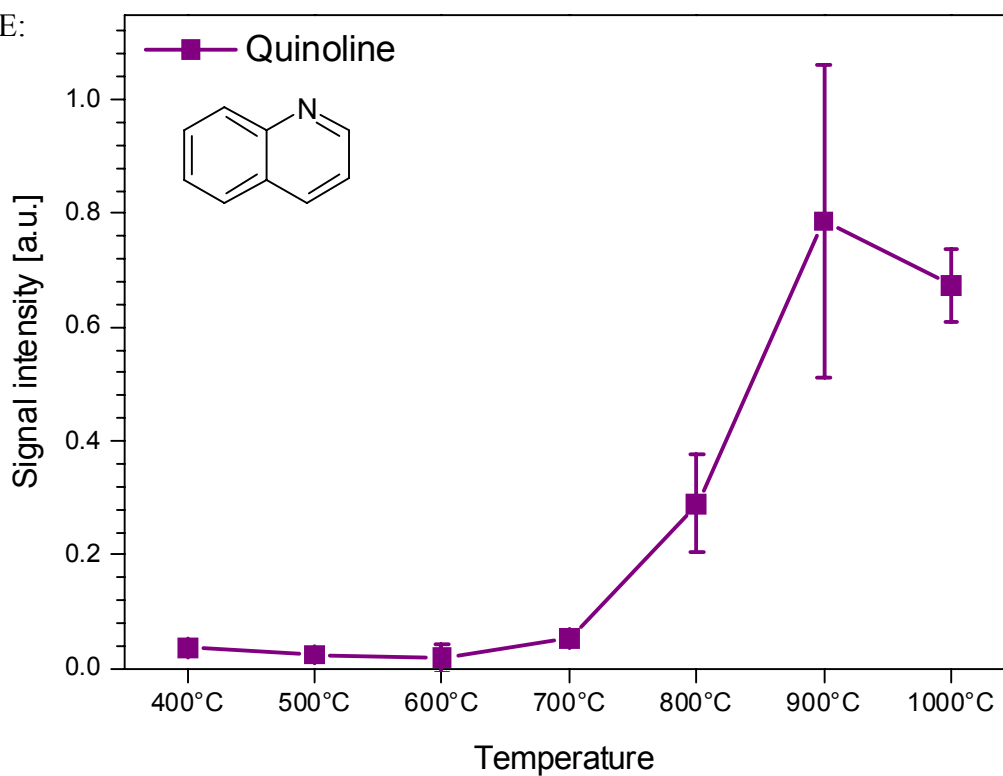
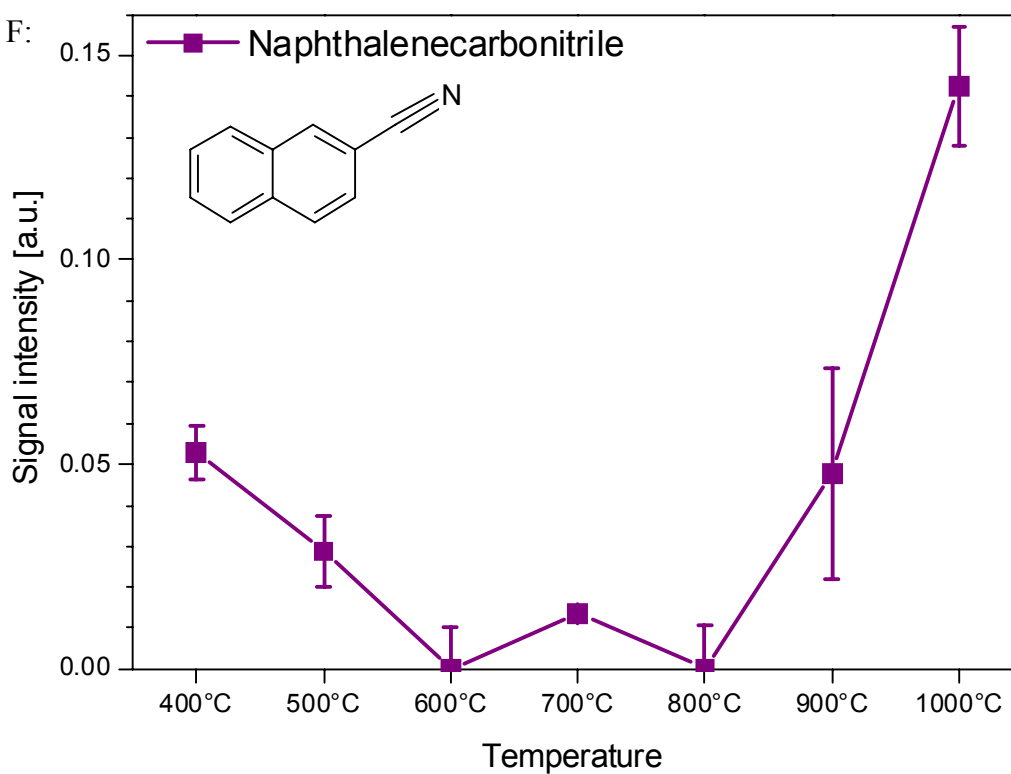


Fig. 27 F:



Figures 27 A, B, C, D, E, and F: Thermal behaviour of the most stable possible nicotine pyrolysis products benzene (78  $m/z$ , Fig. 27 A), pyridine (79  $m/z$ , Fig. 27 B), benzonitrile (103  $m/z$ , Fig. 27 C), naphthalene (128  $m/z$ , Fig. 27 D), quinoline (129  $m/z$ , Fig. 27 E), and naphthalenecarbonitrile (153  $m/z$ , Fig. 27 F) in Burley tobacco in nitrogen in the temperature range from 400 °C to 1000 °C

Only naphthalenecarbonitrile (Fig. 27 F) gives measurable signal intensities at low temperatures which vanish at about 600 °C. All species feature a great increase from 700 °C upward whereas benzene (Fig. 27 A), naphthalene (Fig. 27 D), and naphthalenecarbonitrile (Fig. 27 F) seem to be the most stable products.

In addition, indications regarding the fate and formation of sulphurous species have been found. Sulphur compounds have a strong impact on the flavour and aroma of tobacco, as is the case with food, such as garlic, horseradish or onion [55]. Playing an important role in the plant physiology, it is believed that sulphur is absorbed by the tobacco plant as sulphate ion and occurs in the plant as sulphates, sulphur containing proteins and esters of sulphuric acid [55]. A possible chemical pathway shows that methionine [55], an amino acid present in tobacco leaf, can easily be converted to methional. Subsequent  $\beta$ -elimination results in methanethiol, being known as a key flavour compound in coffee [179]. Figure 28 illustrates the signal intensities of H<sub>2</sub>S (34  $m/z$ ) and methanethiol (48  $m/z$ ) as a function of temperature for Burley tobacco in nitrogen.

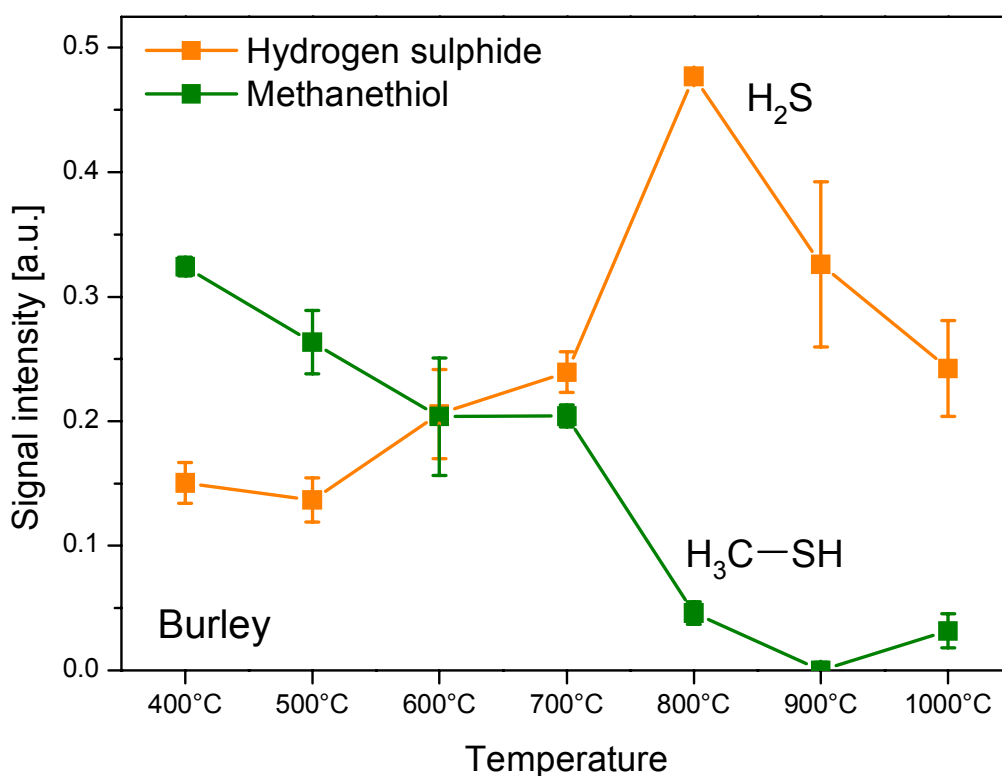


Figure 28: Thermal behaviour of H<sub>2</sub>S (34  $m/z$ ) and methanethiol (48  $m/z$ ) as a function of temperature for the pyrolysis of Burley tobacco in nitrogen in the temperature range from 400 °C to 1000 °C

Methanethiol (48  $m/z$ ) features the characteristic behaviour of a primary component. The signal intensity steadily decreases up to 900 °C where it decomposes completely. In contrast, H<sub>2</sub>S (34  $m/z$ ) has a maximum concentration at 800 °C and can be classified as a secondary component although it can also be detected at the lowest applied pyrolysis temperature of 400 °C. The opposite behaviour of both species up to the onset of decomposition of H<sub>2</sub>S at 800 °C leads one to assume a direct connection between the formation of H<sub>2</sub>S and the degradation of methanethiol.

### 3.4.3. Introduction to the three main tobacco types

Soil type and curing process strongly influence the character of the tobacco leaf, and therefore, play a key role in chemical composition of generated smoke and pyrolysis gas. Curing is the process for drying freshly harvested tobacco with partially or fully controlled temperature and moisture schedules. Table 14 and the following sub-chapter briefly characterise the investigated tobacco types.

Table 14: Growing, processing, and chemical properties of the tobacco types Virginia, Burley, and Oriental [13, 14, 269, 270, 275]

	<b>Virginia tobacco</b>	<b>Burley tobacco</b>	<b>Oriental tobacco</b>
Growing region	no preference	mainly USA	Eastern Mediterranean and Balkan regions
Soil type	sandy, infertile soils	heavier-textured, more fertile soils	poor and rocky soils
Fertilisation	little fertilisation	medium to strong fertilisation	no fertilisation
Curing process	flue-cured	air-cured	sun-cured
Curing duration	5 to 9 days	5 to 7 weeks	12 to 17 days
Total N as NH <sub>3</sub> *	2.0 %	4.0 %	2.7 %
Total volatile acids as acetic acid*	0.15 %	0.10 %	0.20 %
Reducing sugars as dextrose*	22.2 %	0.2 %	12.4 %

\* composition of moisture-free tobacco leaves after ageing; source [275]

### 3.4.3.1. Burley tobacco

Burley tobacco is a light air-cured tobacco mainly cultivated in the United States. It is usually grown on heavier-textured, more fertile soils and nitrogen-fertilisation using ammonium nitrate and urea is common. During the long curing process lasting several weeks chemical and microbiological reactions take place. In this regard Burley tobacco is cured by hanging in air with no additional heating. Carbohydrates are depleted to a great extent via metabolism of the plant cells. In the completing browning stage the leaves die and reactions cease resulting in cured leaves with relatively low sugar contents. Consequently, characteristic chemical components are nitrogen-containing species such as proteins, alkaloids, amino acids, and nitrates [270, 276]. Figure 29 illustrates an averaged sum spectrum including standard deviation of the pyrolysis of Burley tobacco in nitrogen at 800 °C.

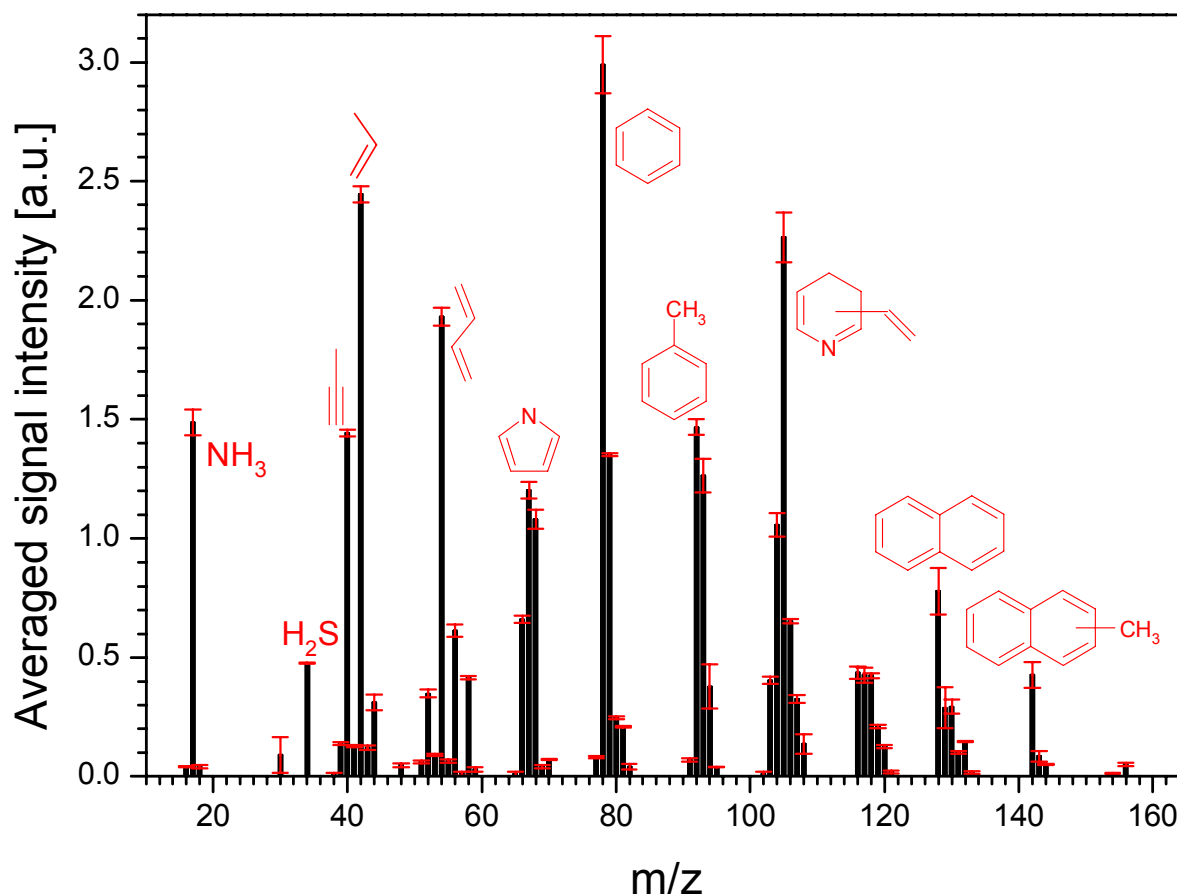


Figure 29: Averaged sum spectrum including standard deviation of the pyrolysis of Burley tobacco in nitrogen at 800 °C

### 3.4.3.2. Virginia tobacco

In turn Virginia is typically grown on infertile, sandy soils with low organic matter and nitrogen reserves leading to very light-bodied tobaccos. It is a flue-cured tobacco which means curing occurs in a barn with circulating heated air beginning at about 35 °C and ending at about 75 °C over a five to nine day period. During this process, degradation of the leaves' chlorophyll takes place and most carbohydrates are converted to simple sugars. At this so-called yellowing stage the reaction is stopped by killing the leaves' cells with drier and hotter air, which finally results in a smooth smoke character [13, 124, 276]. It is cultivated worldwide and primarily used in cigarettes. In this regard Virginia is the major constituent of cigarettes in many countries such as Britain, Canada and Australia. Figure 30 shows a typical sum spectrum of the pyrolysis of Virginia tobacco in nitrogen at 800 °C.

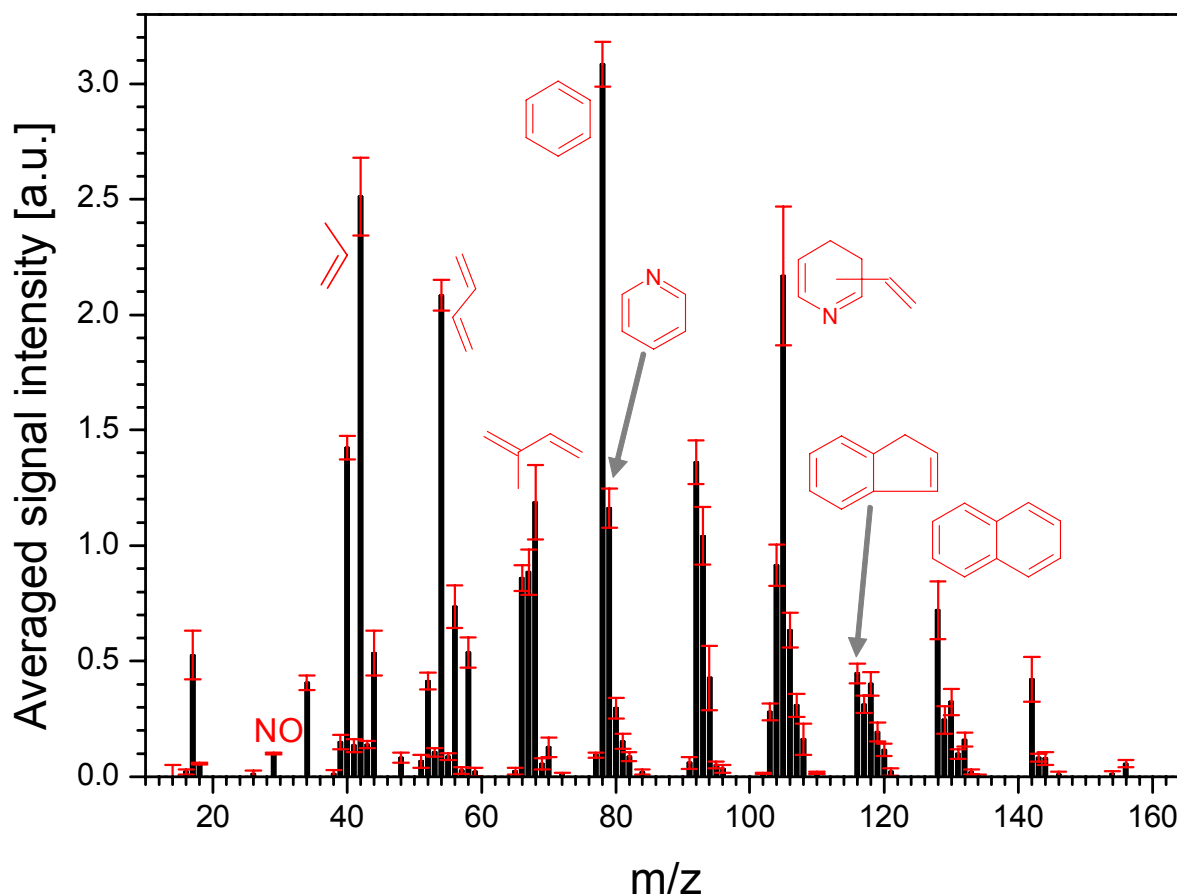


Figure 30: Averaged sum spectrum including standard deviation of the pyrolysis of Virginia tobacco in nitrogen at 800 °C

### 3.4.3.3. Oriental tobacco

Oriental tobacco resembles Virginia but is extensively cultivated in the eastern Mediterranean and Balkan regions where it often grows on rocky soils, which are low in nutrients. The plants do not have their top leaves removed during growing, leading to small, compact and highly aromatic leaves. Irrigation as well as fertilisation is not as conducive to tobacco quality as for other tobacco types. Curing takes place by hanging them directly in the sun for twelve to seventeen days. Oriental tobacco possesses significant amounts of sugars and lesser amounts of protein and amino acids. Sugar esters are believed to contribute to its distinctive flavour and aroma [269]. The averaged sum spectrum in Figure 31 gives the result for the pyrolysis of Oriental tobacco in nitrogen at 800 °C.

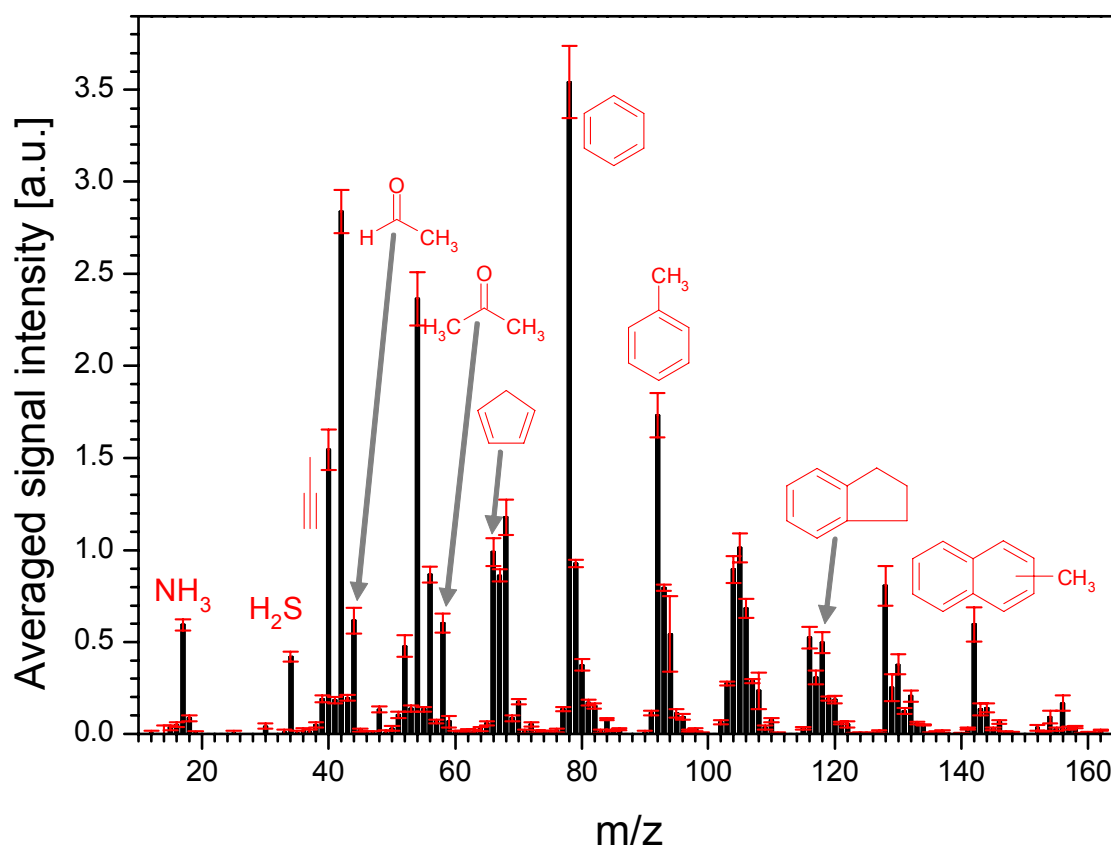


Figure 31: Averaged sum spectrum including standard deviation of the pyrolysis of Oriental tobacco in nitrogen at 800 °C

### 3.4.3.4. Discrimination of tobacco types by sum parameters

First differences of the three tobacco types can be determined by opposing single characteristic masses as shown in Figure 32 and 33. Figure 32 shows the content of nitrogenous substances by means of 17  $m/z$  ( $\text{NH}_3$ ) formed during pyrolysis at 800 °C in nitrogen and air. The columns represent averaged sum signals of the three replicates and are normalised to the highest occurring peak for easier comparison.

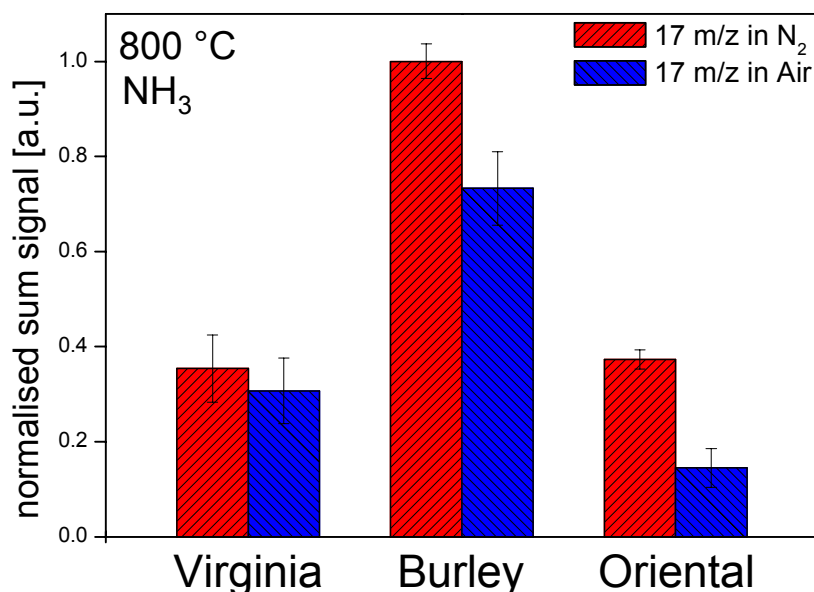


Figure 32: Comparison of the content of nitrogen-containing substances from pyrolysis of Virginia, Burley and Oriental tobacco at 800 °C in nitrogen and air by means of  $\text{NH}_3$  (17  $m/z$ ) formed

The ammonia content of the pyrolysis gases from Burley tobacco is more than twice as high as from Virginia and Oriental, whereas the amounts of ammonia from the latter two are about the same. This behaviour suggests a higher nitrogen-content of Burley tobacco. Oxidative pyrolysis conditions by application of air in the pyrolysis atmosphere results in partial decomposition of  $\text{NH}_3$  for all tobacco types.

In contrast to Burley, the pyrolysis products of Oriental and Virginia show an abundance of peaks assigned to carbohydrate-derived products. Figure 33 illustrates the different contents of 96  $m/z$ , which is most likely attributable to furfural and dimethylfuran, pyrolysed at 400 °C. These compounds are known to be decomposition products of cellulose and used as indicators for carbohydrates in tobacco smoke [265].

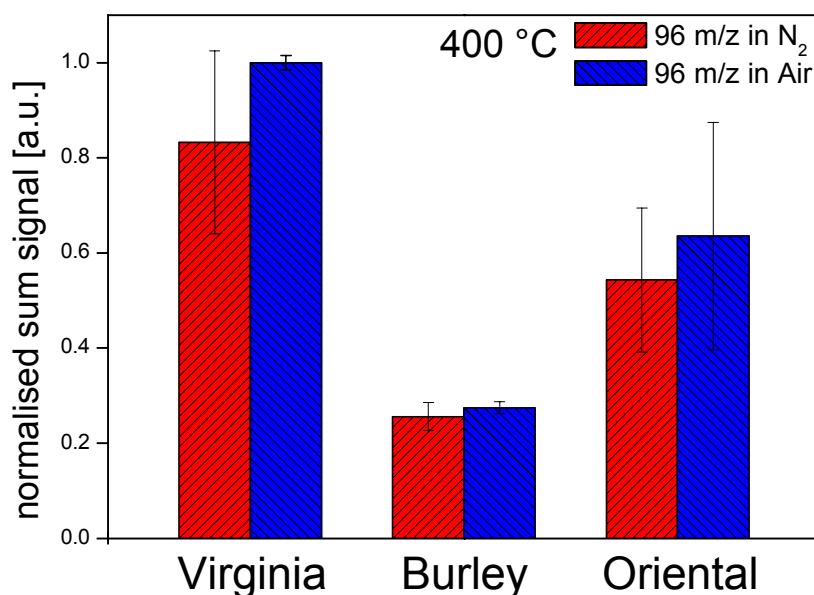


Figure 33: Comparison of carbohydrate content for Virginia, Burley, and Oriental tobacco pyrolysed at 400 °C in nitrogen and air by means of furfural/dimethylfuran (96  $m/z$ ) formed

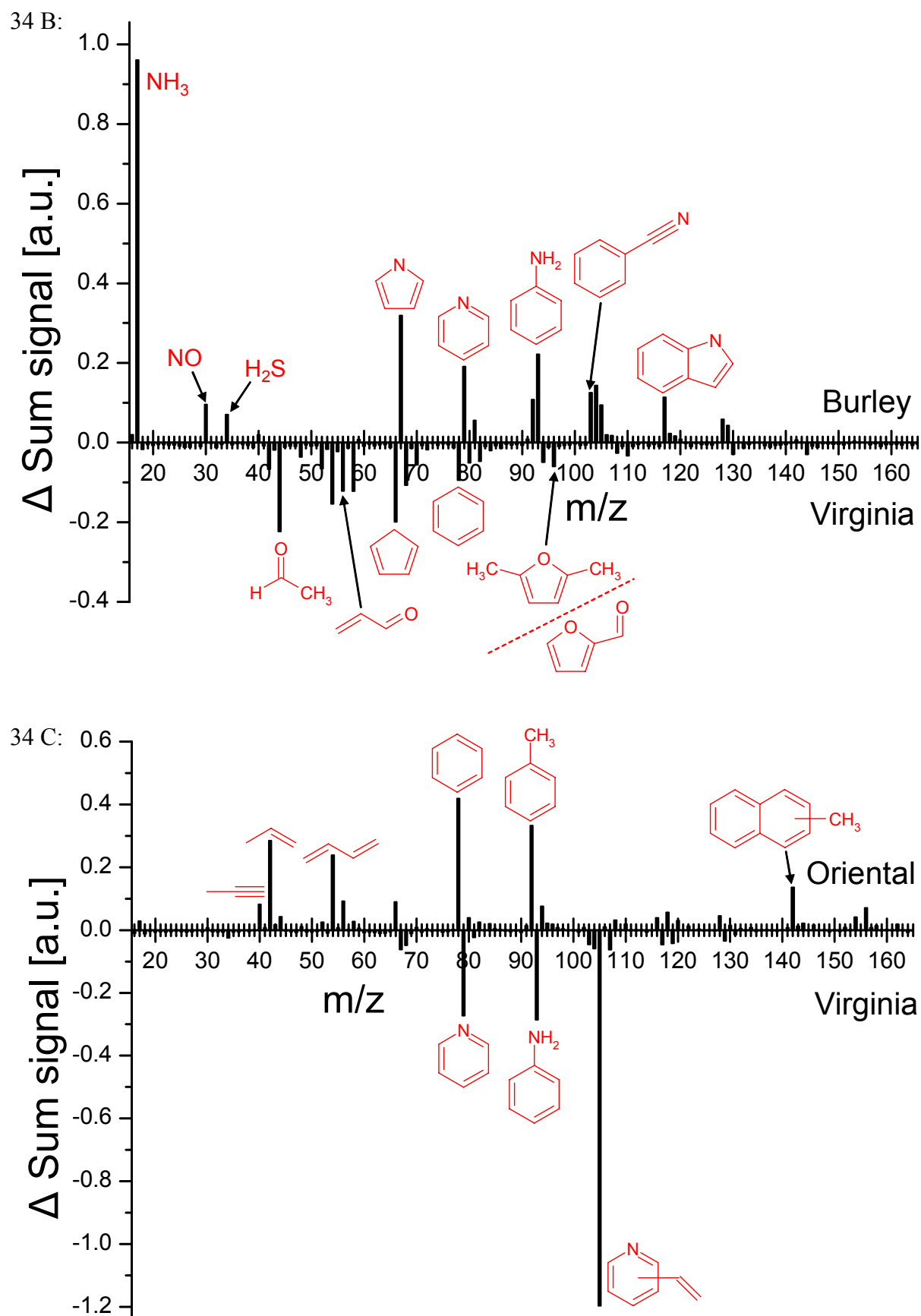
The amount of carbohydrates increases in the following order: Burley < Oriental < Virginia. The presence of oxygen in the pyrolysis atmosphere might enhance the decomposition reaction of carbohydrates, but the error margins do not allow further interpretations on that. However, the simple comparison of individual key compounds leads to the assumption that various compound classes, mainly carbohydrates and nitrogen-containing substances, yield specific signal intensities for the three different tobacco types. If this is the case the individual growing conditions and fertilisation procedures of the tobacco types should be the reason. Consequently, the behaviour of the three tobaccos was investigated in more detail.

#### 3.4.4. Discrimination of tobacco types by advanced statistical methods

In 1984 Meuzelaar claimed that the combined use of pyrolysis techniques, mass spectrometry and computerised data evaluation offers a promising approach for the investigation of highly complex organic matrices [239].

In the case of Py-SPI-TOFMS, the mass spectra have to be used for the characterisation and classification of different samples e.g. tobacco types. Differences between the tobacco samples can result in slightly different mass spectral information, which, however, might not





Figures 34 A, B, and C: Difference spectra between Burley and Oriental (Fig. 34 A), Burley and Virginia (Fig. 34 B) and Oriental and Virginia (Fig. 34 C) in nitrogen at 800 °C

The difference spectrum between Burley and Oriental tobacco (Fig. 34 A) illustrates that Burley exhibits higher signal intensities for e.g.  $m/z$  105, 17, 93, 79, 67, 104, 103, 117, 34, 30. These masses can almost entirely be assigned to nitrogen-containing compounds [55, 58, 114, 124, 245, 248, 249, 251, 265, 271]. In the final browning stage of Burley curing, reactions cease as the leaves die. Consequently, the characteristic chemical components are nitrogen-containing species such as proteins, alkaloids, amino acids, and nitrates. These compounds act as precursors of numerous tobacco smoke components such as ammonia, pyridines, amines, nitrosamines, pyrroles, pyrazines, indoles, nitriles, and hydrogen cyanide [270, 276]. As a result, concentrations of these compounds in the Burley pyrolysis gas are higher than in the Oriental and Virginia pyrolysis gases, which is also illustrated in Figure 34 B. Differences between Burley and Virginia are not as striking as between Burley and Oriental but are still outstanding. Again, Burley tobacco pyrolysis gas exhibits high amounts of nitrogenous species ( $m/z$  17, 67, 93, 79, 104, 103, 117, 30, 105, etc.) but is deficient in masses such as  $m/z$  44, 66, 54, 58, 56, 68, 78, 42, etc. compared to Virginia. Similar masses in slightly differing order of signal intensity characterise Oriental tobacco pyrolysis gas compared to Burley ( $m/z$  78, 54, 42, 66, 44, 92, 56, 58, 142, 94, etc.) and can mainly be identified as unsaturated hydrocarbons, some of them containing oxygen [55, 114, 124, 245, 248, 249, 251, 265, 271]. An explanation is that Oriental tobacco possesses significant amounts of sugars and lesser amounts of protein and amino acids resulting in typical masses for carbohydrate breakdown [124, 265, 269, 277]. In turn, when Virginia is compared to Burley, typical masses for carbohydrate decomposition prevail but if compared to Oriental nitrogenous species play a more important role demonstrated in Figure 34 C. As a result the pyrolysis gas compositions of Burley and Oriental are very characteristic and differ quite a lot. In contrast, Virginia tobacco features properties of both other types.

Tables 15 to 17 illustrate the prevailing twenty  $m/z$  of the difference spectra for each comparison and tobacco type assigned to the most likely compounds based on Table 12.

Table 15: Assignment of the twenty prevailing  $m/z$  of the difference spectrum Burley – Oriental

Ranking	$m/z$	Compound	Tobacco
1	105	Vinylpyridine	Burley
2	17	NH <sub>3</sub>	Burley
3	78	Benzene	Oriental
4	93	Aniline, Methylpyridine	Burley
5	79	Pyridine	Burley
6	54	1,3-Butadiene, 1-Butyne	Oriental
7	67	Pyrrole	Burley
8	42	Propene	Oriental
9	66	Cyclopentadiene	Oriental
10	44	Acetaldehyde	Oriental
11	92	Toluene	Oriental
12	56	2-Propenal, Butene, 2-Methylpropene	Oriental
13	104	Styrene, 3-Pyridinecarbonitrile	Burley
14	103	Benzonitrile	Burley
15	117	Indole	Burley
16	58	Acetone, Propanal	Oriental
17	142	Methyl naphthalene	Oriental
18	94	Phenol, 2-Vinylfuran	Oriental
19	34	H <sub>2</sub> S	Burley
20	52	1-Buten-3-yne,	Oriental

Table 16: Assignment of the twenty prevailing  $m/z$  of the difference spectrum Burley – Virginia

Ranking	$m/z$	Compound	Tobacco
1	17	NH <sub>3</sub>	Burley
2	67	Pyrrole	Burley
3	44	Acetaldehyde	Virginia
4	93	Aniline, Methylpyridine	Burley
5	66	Cyclopentadiene	Virginia
6	79	Pyridine	Burley
7	54	1,3-Butadiene, 1-Butyne	Virginia
8	104	Styrene, 3-Pyridinecarbonitrile	Burley
9	103	Benzonitrile	Burley
10	58	Acetone, Propanal	Virginia
11	56	2-Propenal, Butene, 2-Methylpropene	Virginia
12	117	Indole	Burley
13	92	Toluene	Burley
14	68	Furan, Isoprene, 1,3-Pentadiene, Cyclopentene	Virginia
15	30	NO	Burley
16	78	Benzene	Virginia
17	105	Vinylpyridine	Burley
18	34	H <sub>2</sub> S	Burley
19	42	Propene	Virginia
20	52	1-Buten-3-yne,	Virginia

Table 17: Assignment of the twenty prevailing  $m/z$  of the difference spectrum Oriental – Virginia

Ranking	$m/z$	Compound	Tobacco
1	105	Vinylpyridine	Virginia
2	78	Benzene	Oriental
3	92	Toluene	Oriental
4	93	Aniline, Methylpyridine	Virginia
5	42	Propene	Oriental
6	79	Pyridine	Virginia
7	54	1,3-Butadiene, 1-Butyne	Oriental
8	142	Methyl naphthalene	Oriental
9	56	2-Propenal, Butene, 2-Methylpropene	Oriental
10	66	Cyclopentadiene	Oriental
11	40	Propyne	Oriental
12	94	Phenol, 2-Vinylfuran	Oriental
13	156	Bipyridine, Dimethylnaphthalene	Oriental
14	107	Ethylpyridine, Methylbenzeneamine	Virginia
15	67	Pyrrole	Virginia
16	104	Styrene, 3-Pyridinecarbonitrile	Virginia
17	118	Indane, Methyl styrene, Benzofuran	Oriental
18	68	Furan, Isoprene, 1,3-Pentadiene, Cyclopentene	Virginia
19	117	Indole	Virginia
20	103	Benzonitrile	Virginia

Despite the valuable information obtained by this data analysis, the method entails some clear disadvantages. Firstly, averaged mass spectra were used for calculation but the corresponding standard deviations were not considered. According to

$$\mu_{ki} - \mu_{kj} = \mu_{kDiff} \quad [28]$$

and

$$\sigma_{kDiff} = \sqrt{\sigma_{ki}^2 + \sigma_{kj}^2} \quad [29]$$

standard deviations might reach relatively high values compared to the resulting difference values of the average signal intensities. Here  $\mu_{ki}$  and  $\mu_{kj}$  are the integrated mass signals in the average spectrum of compound k from tobacco types i and j,  $\mu_{kDiff}$  the corresponding difference value of compound k, and  $\sigma$  the respective standard deviations. By excluding these

affected masses the gained information can decrease tremendously. Furthermore, absolute values must be subtracted making a prior data normalisation to total ion signal impossible. This normalisation procedure eliminates possible sources of error such as incorrect sample weighing. Furthermore, only the direct comparison between two tobacco types is possible.

### 3.4.4.2. Fisher-Ratios

To find masses, which exhibit most characteristic features for discrimination between each pair and all three types of tobacco, a mathematically more reliable method was sought. Fisher suggested a criterion for selection of features in terms of their discriminative power in the case of a two-way classification problem [278]. Accordingly, the pair wise Fisher-Ratio (also called Fisher-Value (FV)) between any two classes is defined as the ratio of between-class scatter and within-class scatter. The best features in descending order of the Fisher-Ratios can then be selected for the classification task [279-284]. In addition, the Fisher criterion can be extended to multi-class problems enabling the simultaneous distinction between several groups [280, 285].

For the calculation of the Fisher-Ratios the mass spectra were normalised to total ion signal to eliminate influences on absolute mass signal values due to slightly changing experimental conditions (e.g. air flows, laser power etc.). The new variables obtained were calculated according to

$$y_k = \frac{x_k}{\sum x_k} \quad [30]$$

where  $x_k$  is the observed integrated ion signal in the average spectrum for compound k.

Fisher-Ratios were calculated for two-classes according to [285] as

$$F_{ijk} = \frac{(\mu_{ik} - \mu_{jk})^2}{(\sigma_{ik}^2 + \sigma_{jk}^2)}. \quad [31]$$

Here  $\mu_{ik}$  and  $\mu_{jk}$  denote the means for the  $k$ th compound in classes (tobacco types)  $i$  and  $j$ ,  $\sigma_{ik}^2$  and  $\sigma_{jk}^2$  are the corresponding variances, respectively. It can be seen that the Fisher-Ratio becomes largest when inter-class separation is high and inner-class variability is minimised.

After normalisation to total ion signal the pair wise Fisher-Ratios were calculated. Values obtained together with corresponding masses and most likely compounds based on Table 12 are illustrated in Tables 18 to 20 in descending order.

Table 18: The  $m/z$  featuring the 25 highest Fisher-Values for the discrimination between Burley and Oriental

Ranking	$m/z$	FV	Compounds
1	105	86.85	Vinylpyridine
2	103	52.58	Benzonitrile
3	93	48.07	Aniline, Methylpyridine
4	104	44.18	Styrene, 3-Pyridinecarbonitrile
5	17	36.79	NH <sub>3</sub>
6	106	30.59	Xylene, Ethylbenzene, Benzaldehyde
7	44	24.93	Acetaldehyde
8	107	23.35	Ethylpyridine, Methylbenzeneamine
9	66	15.53	Cyclopentadiene
10	43	13.86	Carbohydrate fragment: C <sub>3</sub> H <sub>7</sub> <sup>+</sup> , C <sub>2</sub> H <sub>3</sub> O <sup>+</sup>
11	81	12.79	Methyl pyrrole
12	42	9.16	Propene
13	79	9.03	Pyridine
14	59	8.47	2-Propanamine
15	94	8.33	Phenol, 2-Vinylfuran
16	78	8.25	Benzene
17	117	8.18	Indole
18	119	8.13	Indoline, Aminostyrol, Methylvinylpyridin
19	67	7.85	Pyrrole
20	58	7.17	Acetone, Propanal
21	80	6.49	Pyrazine
22	118	6.29	Indane, Methyl styrene, Benzofuran
23	86	5.70	Methylbutanal, 3-Methyl-2-butanone, Pentanone, 2,3-Butanedione
24	56	5.51	2-Propenal, Butene, 2-Methylpropene
25	52	4.97	1-Buten-3-yne,

Table 19: The  $m/z$  featuring the 25 highest Fisher-Values for the discrimination between Burley and Virginia

Ranking	$m/z$	FV	Compounds
1	17	51.11	NH <sub>3</sub>
2	59	14.84	2-Propanamine
3	103	12.39	Benzonitrile
4	96	10.12	Dimethylfuran, Furfural
5	117	8.48	Indole
6	44	7.79	Acetaldehyde
7	80	6.81	Pyrazine
8	116	6.53	Indene
9	30	4.08	NO
10	104	3.39	Styrene, 3-Pyridinecarbonitrile
11	136	2.81	Limonene, Methoxybenzaldehyde, 2-Ethyl-5-methylphenol
12	120	2.59	Methylethylbenzene, Trimethylbenzene
13	134	2.40	Isopropyltoluene
14	71	2.39	Pyrrolidine
15	93	2.31	Aniline, Methylpyridine
16	52	2.27	1-Buten-3-yne,
17	67	2.19	Pyrrole
18	66	2.09	Cyclopentadiene
19	110	1.66	Dihydroxybenzene, 2-Acetylfuran, Methylfurfural
20	86	1.60	Methylbutanal, 3-Methyl-2-butanone, Pentanone, 2,3-Butanedione
21	153	1.56	Naphthalenecarbonitrile
22	129	1.42	Quinoline, Isoquinoline
23	43	1.33	carbohydrate fragment: C <sub>3</sub> H <sub>7</sub> <sup>+</sup> , C <sub>2</sub> H <sub>3</sub> O <sup>+</sup>
24	146	1.13	Myosmine
25	58	1.11	Acetone, Propanal

Table 20: The  $m/z$  featuring the 25 highest Fisher-Values for the discrimination between Oriental and Virginia

Ranking	$m/z$	FV	Compounds
1	106	39.98	Xylene, Ethylbenzene, Benzaldehyde
2	79	32.43	Pyridine
3	105	23.41	Vinylpyridine
4	104	20.17	Styrene, 3-Pyridinecarbonitrile
5	93	15.02	Aniline, Methylpyridine
6	67	7.68	Pyrrole
7	81	5.88	Methyl pyrrole
8	103	5.74	Benzonitrile
9	107	5.36	Ethylpyridine, Methylbenzeneamine
10	43	4.08	Carbohydrate fragment: $C_3H_7^+$ , $C_2H_3O^+$
11	118	3.97	Indane, Methyl styrene, Benzofuran
12	77	3.57	Fragment
13	42	3.15	Propene
14	85	3.07	Methylpyrrolidine, Piperidine
15	142	2.43	Methyl naphthalene
16	108	2.20	Anisol, Dimethylpyridine, Methylphenol
17	119	2.12	Indoline, Aminostyrol, Methylvinylpyridin
18	94	2.07	Phenol, 2-Vinylfuran
19	84	1.78	Nicotine fragment, Cyclopentanone, Dimethylbutene, Hexene, 3-Methyl-3-buten-2-one
20	92	1.75	Toluene
21	154	1.54	Dimethoxyphenol, Vinylnaphthalene
22	78	1.42	Benzene
23	86	1.35	Methylbutanal, 3-Methyl-2-butanone, Pentanone, 2,3-Butanedione
24	17	1.24	$NH_3$
25	116	1.15	Indene

To a certain degree the pair wise Fisher-Ratios between two tobacco types lead to the same masses for distinction as the difference spectra already discussed in partially different order. Results of Fisher-Ratios and difference spectra were cross-checked by balancing the number of masses, which appeared in both rankings. Therefore it was determined how many of the ten highest ranked masses did not occur among the twenty highest ranked masses of the other method and vice versa. Regarding the comparison between Burley and Oriental, three of the top ten Fisher masses are not listed in the ranking of the corresponding difference spectrum ( $m/z$  106, 107, 43). In turn only one of the difference spectrum masses is absent in the list of twenty Fisher masses (54  $m/z$ ). Burley and Virginia yield a lower match as four of the Fisher masses ( $m/z$  59, 96, 80, 116) and two of the difference spectrum masses ( $m/z$  79, 54) do not

appear on the opposing table. For Oriental and Virginia tobacco, the balance is even worse as the table of Fisher-Ratios misses five of the top ten masses of the difference spectrum ( $m/z$  78, 92, 54, 56, 66) by four absences on the other list ( $m/z$  106, 67, 81, 43). As a conclusion, application of the Fisher criterion gains importance with more and more resembling classes.

The extension to three classes was calculated with

$$F_k = \frac{1}{J(J-1)} \frac{\sum_{i=1}^J \sum_{j=1}^J P_i P_j F_{ijk}}{\sum_{i=1}^J \sum_{j=1}^J P_i P_j} \quad ; i \neq j, \quad [32]$$

according to [285], where  $P_i$  and  $P_j$  are the a priori probabilities of the classes  $i$  and  $j$ , respectively, and  $J$  describes the total number of classes. Here, the test set was regarded as a fair representation and thus the probabilities as proportional to the number of performed measurements [285]. Table 21 shows the masses delivering the 25 highest Fisher-Values in descending order together with the assignment of the most likely compounds.

Table 21: The  $m/z$  featuring the 25 highest Fisher-Values for the discrimination between Burley, Oriental, and Virginia

Ranking	$m/z$	FV	Compounds
1	105	6.13	Vinylpyridine
2	17	4.95	NH <sub>3</sub>
3	103	3.93	Benzonitrile
4	106	3.93	Xylene, Ethylbenzene, Benzaldehyde
5	104	3.76	Styrene, 3-Pyridinecarbonitrile
6	93	3.63	Aniline, Methylpyridine
7	79	2.31	Pyridine
8	44	1.86	Acetaldehyde
9	107	1.61	Ethylpyridine, Methylbenzeneamine
10	59	1.32	2-Propanamine
11	81	1.08	Methyl pyrrole
12	43	1.07	Carbohydrate fragment: C <sub>3</sub> H <sub>7</sub> <sup>+</sup> , C <sub>2</sub> H <sub>3</sub> O <sup>+</sup>
13	66	1.02	Cyclopentadiene
14	67	0.98	Pyrrol
15	117	0.93	Indole
16	96	0.77	Dimethylfuran, Furfural
17	80	0.74	Pyrazine
18	42	0.71	Propene
19	94	0.62	Phenol, 2-Vinylfuran
20	119	0.59	Indoline, Aminostyrol, Methylvinylpyridin
21	78	0.58	Benzene
22	118	0.57	Indane, Methyl styrene, Benzofuran
23	86	0.48	Methylbutanal, 3-Methyl-2-butanone, Pentanone, 2,3-Butanedione
24	58	0.48	Acetone, Propanal
25	116	0.46	Indene

The ranking of the masses according to Fisher-Ratios for all three tobacco types (Table 21) is dominated by nitrogen-containing compounds. Seven out of ten masses with the greatest discriminative power can be clearly classified as nitrogenous species. The  $m/z$  exhibiting the highest Fisher-Values are 105  $m/z$ , 17  $m/z$ , 103  $m/z$ , 106  $m/z$ , 104  $m/z$ , 93  $m/z$ , and 79  $m/z$ .

### 3.4.4.3. Principal Component Analysis

In general, modern analysis techniques enable powerful and sophisticated investigations of all sorts of samples. At the same time the immense amount of data obtained often requires pruning datasets in order to focus on the most relevant features. In this way, chemometrics, the application of mathematical or statistical methods to scientific data, has gained great influence in modern analytical chemistry [286], which is expressed in the great number of publications and textbooks dealing with this topic, e.g. [287-293]. In this context Principal Component Analysis (PCA) is only one common method of choice. It basically seeks to reduce the dimensionality of a dataset consisting of a large number of interrelated variables, while retaining as much of the present variation as possible. This is achieved by transformation to a new set of variables, the Principal Components (PCs), which are uncorrelated and ordered so that the first few components contain most of the variation of the entire original data set. The PCA is based on the covariance matrix of the entire data set. The eigenvectors of the covariance matrix are the so-called loading vectors (which project the original data to the new space spanned by the Principal Components) and the respective eigenvalues represent the fraction of the variance explained by the Principal Component. Often a projection of the original data spanned by the first two PCs is sufficient. The outcome of PCA is mostly depicted by two two-dimensional plots, the loading-plot and the score-plot. The loading-plot visualises the influence of the original variables on the respective Principal Components, the scores are the projected data in the lower dimensional subspace defined by the PCs [294-296].

In respect of agricultural goods it is widely applied for classification or characterisation, such as beverages e.g. [179, 297-306], tobacco e.g. [246, 265, 266, 307], and foods e.g. [308-311].

The first step of processing the dataset was performed by normalisation to total ion signal and autoscaling. Autoscaling is often useful when variables span different ranges in order to make the variables of equal importance. It is carried out by mean centring the data i.e. subtracting the mean and subsequent variance scaling i.e. division by the standard deviation to make the data independent of scaling [291, 294, 295, 312]. Pre-selection of relevant masses was done by calculating the Fisher-Ratios as described in the previous section. Masses featuring the twenty-five highest Fisher-Ratios were incorporated into the PCA calculations. All the data pre-processing steps are summarised in the following diagram (Fig. 35).

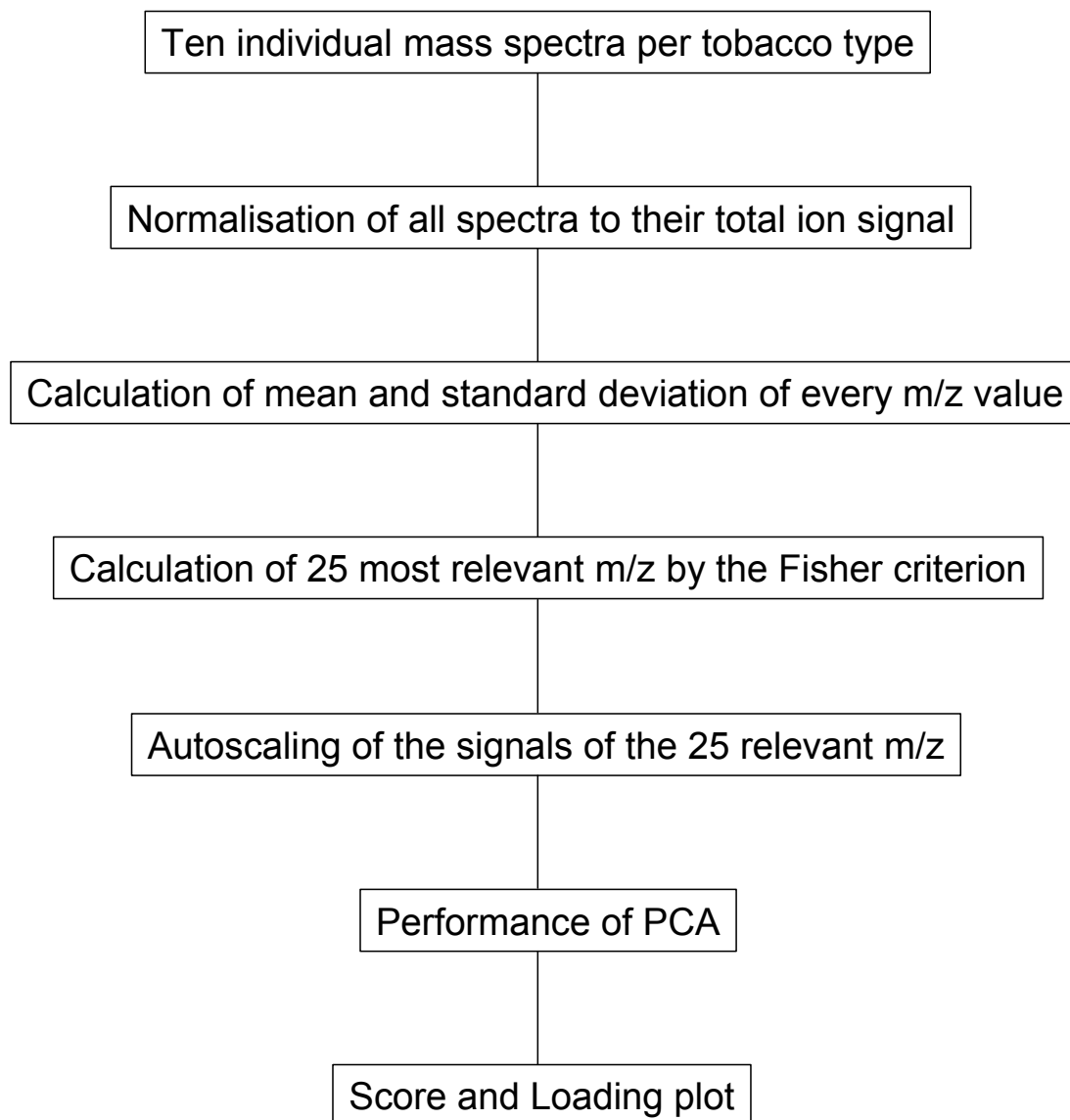
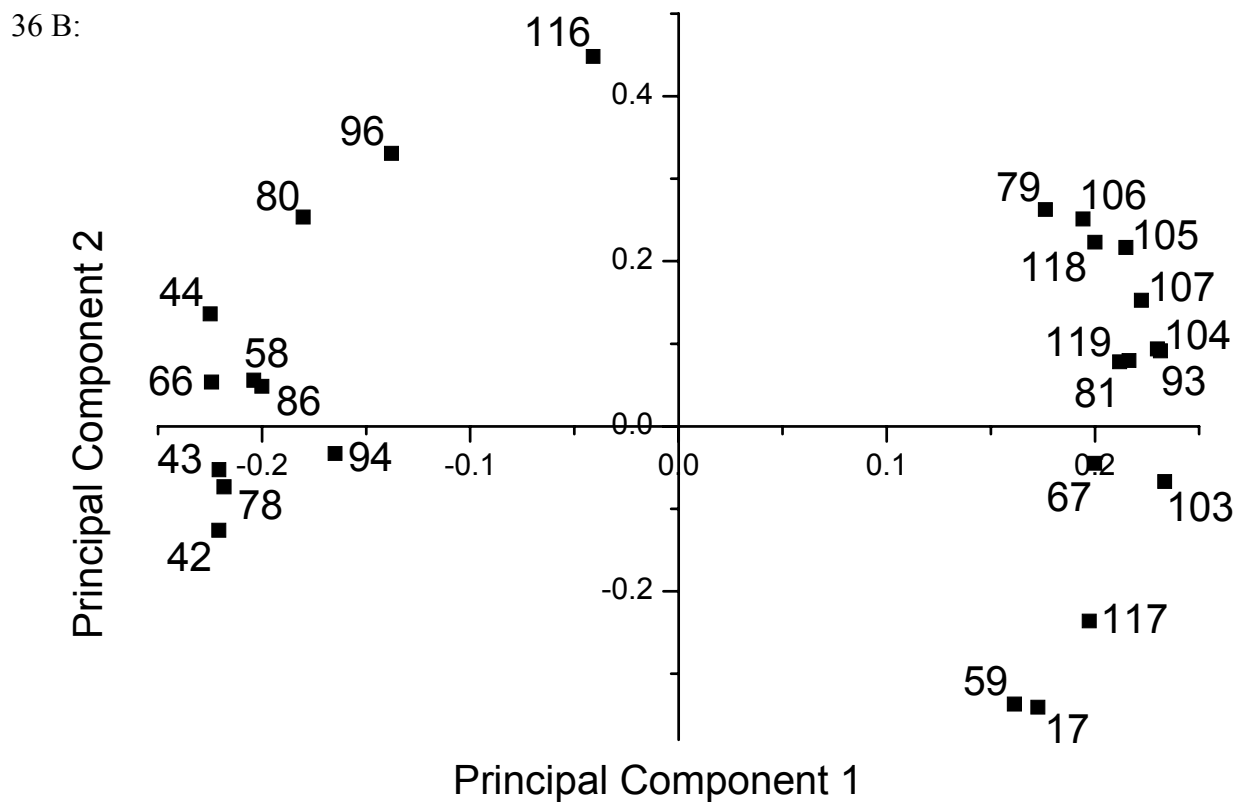
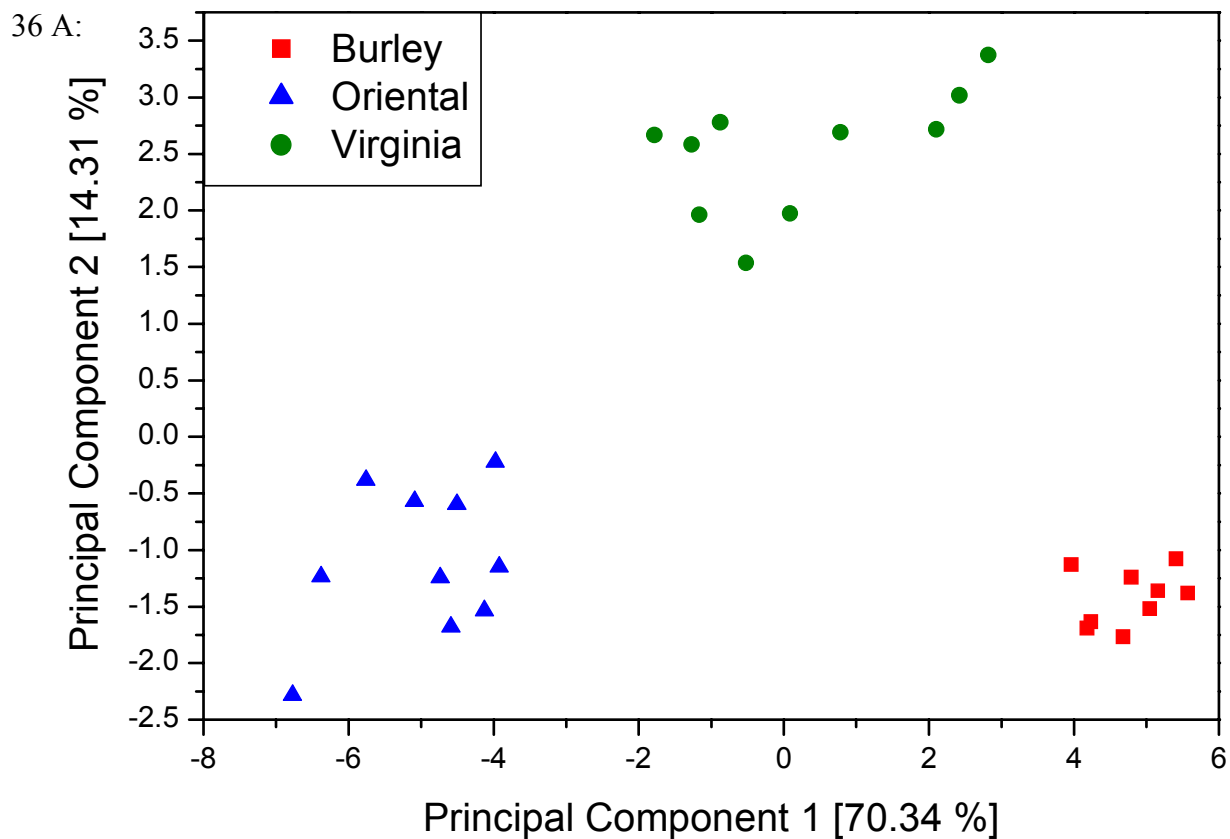


Figure 35: Flow chart of the data pre-processing steps prior to Principal Component Analysis

The score plot proves that a clear distinction between the three tobacco types can be achieved by Py-SPI-TOFMS which is illustrated in Figure 36 A.



Figures 36 A and B: Score (Fig. 36 A) and loading (Fig. 36 B) plots by using the  $m/z$  featuring the twenty five highest Fisher-Ratios for the Principal Component Analysis of the three tobacco types Burley, Oriental, and Virginia

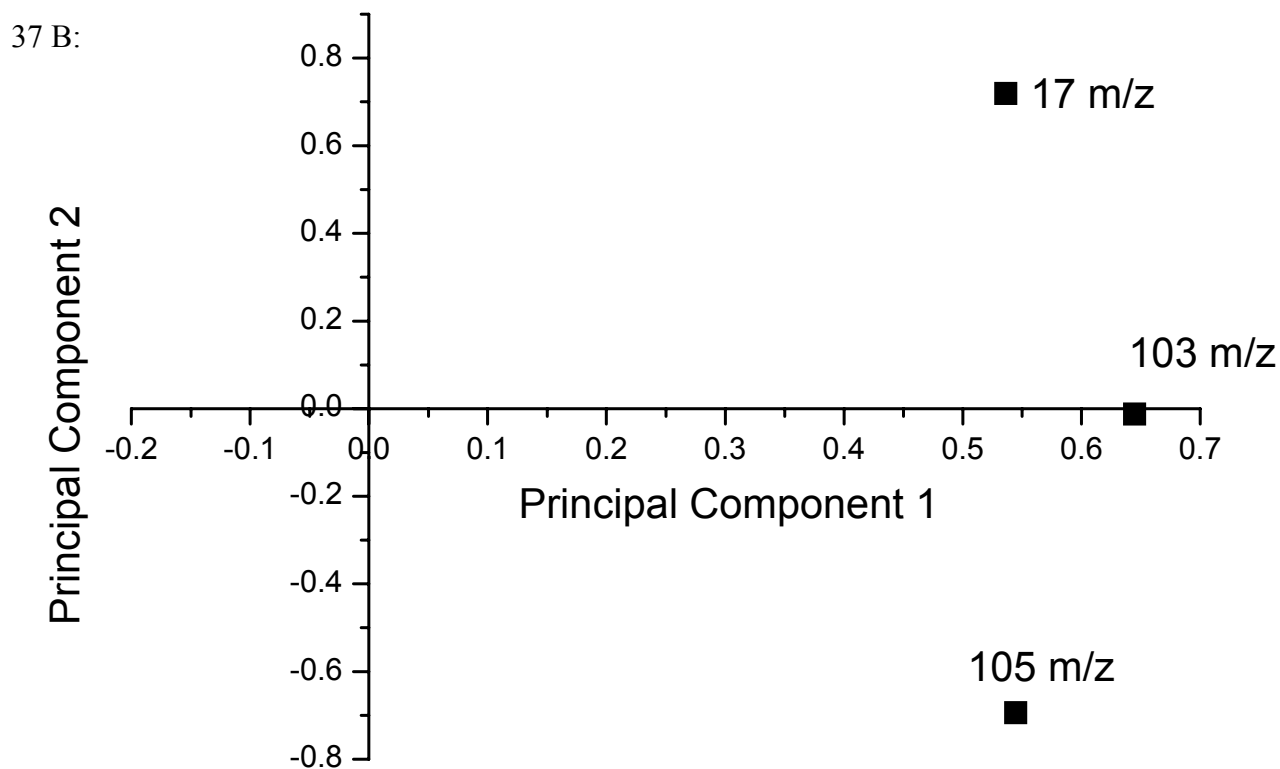
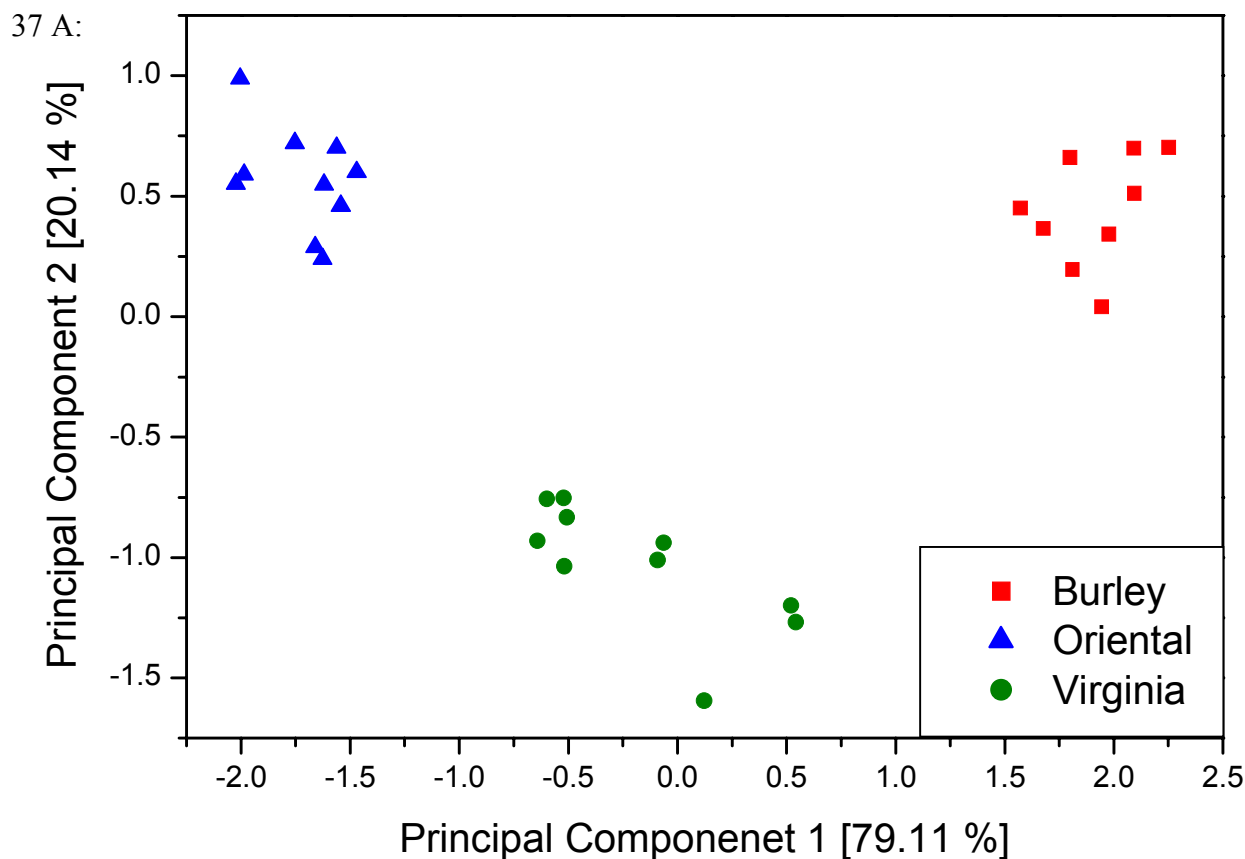
Burley and Oriental are clearly separated on the first PC (explaining 70.34% of the total variance), while Virginia is separated from the other two tobacco types along the second PC (14.31% of total variance). The loadings (Fig. 36 B) reveal the influence of the variables on the Principal Components and in conjunction with the scoreplot on each tobacco type. Consequently, all twenty five masses can be divided into two large groups either mainly influencing Oriental or Burley tobacco. The corresponding compounds are the same as discussed in the previous sections. Nitrogenous compounds typical for Burley have a strong influence on the first Principal Component towards positive values, whereas unsaturated carbohydrates show strong influence on negative values along the axis of the first PC. Regarding this, the first Principal Component mainly describes the differentiation between Burley and Oriental and is dominated by the appearance of nitrogen-containing species and carbohydrates. Therefore it is also related to cultivation conditions as explained beforehand. Virginia tobacco is affected solely on the second PC by components of both groups whereby some masses have got a greater impact (e.g.  $m/z$  116, 79, 96, 80, 106, 118, 105) than others (e.g.  $m/z$  59, 17, 117).

As a consequence PCA enables the discrimination of all three tobacco types and confirms the revelation that Virginia shows features of Burley and Oriental tobacco. This difficulty in classification of Virginia can also be seen in the small fraction of total variance explained by the second PC compared to PC1 (14.31% to 70.34%).

Most amazing was that a similar distinction of the classes can be achieved by only using the three masses exhibiting the highest Fisher-Ratios,  $m/z$  105 (vinylpyridine), 17 (ammonia), and 103 (benzotrile), which is demonstrated in Figures 37 A und B.

All three variables show a high impact towards positive values on PC1, whereas the second PC is influenced in opposite directions by ammonia and vinylpyridine. When compared to the difference spectra the resulting classification becomes understandable. Ammonia is only present in high concentrations in the pyrolysis gas of Burley. Vinylpyridine is abundant in Burley and Virginia, and benzotrile mainly appears in the pyrolysis spectra of Burley. This leads to the grouping of the samples in the scoreplot.

Using this information it would be possible to establish a simple and rapid method to distinguish between even unknown pure tobacco samples without any prior sample treatment, by only investigating the three compounds 105  $m/z$ , 17  $m/z$ , and 103  $m/z$ . In this context, applying an inexpensive quadrupole MS instead of the TOFMS would be sufficient.



Figures 37 A and B: Score (Figure 37 A) and loading (Fig. 37 B) plots by using the  $m/z$  featuring the three highest Fisher-Ratios for the Principal Component Analysis of the three tobacco types Burley, Oriental, and Virginia

### 3.5. Conclusion of the pyrolysis experiments

The coupling of SPI-TOFMS to the pyrolysis furnace enabled the comprehensive characterisation of many tobacco smoke constituents, regarding the influence of temperature and reaction gas composition. In this context, by spanning a temperature range between 400 °C and 1000 °C in steps of  $\Delta 100$  °C and applying two different gas compositions, pure nitrogen and synthetic air, the preferred formation conditions of many individual compounds could be identified as well as the overall change of the pattern was observed. Moreover, the classification of several substances in primary, secondary, and tertiary components was carried out. Furthermore, the thermal decomposition of nicotine in tobacco was investigated and compared to former studies dealing with the pyrolysis of pure nicotine. In this context several possible pyrolysis and combustion products of nicotine and, in turn, their fate and thermal behaviour was analysed. In addition, a correlation between formation and decomposition reactions of two sulphur-containing species was demonstrated. With respect to the three single tobacco types Virginia, Oriental, and Burley, differences in smoke composition were clearly illustrated by means of several data evaluation techniques. In this way the principle and possibility of discriminating these three tobacco types by focussing on selected key substances only was demonstrated, which could lead to commercial application in tobacco science regarding e.g. quality control, and, when utilized to other materials, to a wide range of applications in several related fields. In this context, the latest improvements of the ionisation technique are the development of electron-beam pumped rare-gas excimer VUV-lamp systems, which replace costly laser instruments [177, 178, 313]. Incorporating these enhancements, coupling of SPI-MS to commercially available pyrolyser devices including automated sampling systems, would lead to a wide applicable technique, whose operation requires a minimum of expenditure of time. In addition, future work needs to address the coupling of SPI-TOFMS to thermal analysis techniques. Taking advantage of the high time resolution, which was not the subject in this work, chemical reactions, phase transformations and structural changes of substances and materials could be analysed by monitoring the respective pattern of evolved organic species.

## 4. Puff-by-puff resolved measurements of cigarette smoke

The pyrolysis studies delivered a lot of valuable information regarding thermal behaviour of smoke constituents. The second experimental section deals with the investigation of real cigarettes by coupling the SPI-TOFMS to a smoking machine device for the first time. So far the great majority of cigarette smoke investigations have dealt with the analysis of the smoke of a whole cigarette. In this regard focus has been on the identification of smoke constituents and quantification of the most hazardous compounds. In contrast, puff-resolved or even time-resolved investigations, which would monitor the highly dynamic and constantly changing composition of the matrix smoke during the smoking cycle, are very rare, mainly due to the very difficult and challenging analytical task. In Chapter 4.1 a brief overview of previous studies is given reflecting the necessity for more sophisticated and comprehensive action in that field. In Chapter 4.2 the instrumental set-up of the SPI-TOFMS coupled to the smoking machine is described while in Chapter 4.3 the cigarettes used for the smoking experiments are thoroughly described. Chapter 4.4 deals with the processing and discussion of the results obtained. In that chapter a qualitative and quantitative puff-resolved characterisation and comparison of several research and commercial cigarette types is given on a puff-by-puff basis. In addition, problems and negative aspects of the machine-smoking regime are revealed when applied to puff-resolved measurements.

### 4.1. Introduction to smoking experiments

The first investigations on the analysis within single cigarette puffs were carried out by Vilcins [314] and Ceschini et al. [315]. Vilcins applied infrared spectroscopy to quantify ethylene and isoprene in the gas phase on a puff-by-puff basis. Cheschini et al. demonstrated the smoke's dynamic nature during the two second duration of a single puff by dividing the puff into three parts and analysing selected vapour phase constituents and total particulate matter in the respective thirds. Over the years several techniques have been applied for single puff or puff-by-puff characterisation. Fourier transform infrared spectroscopy (FTIR) based puff-by-puff measurements were reported by Parrish et al. [316] for the analysis of CO<sub>2</sub>, CO,

acetaldehyde, NO, hydrogen cyanide (HCN) and carbonyl sulphide (COS) as well as by Li et al [317] for formaldehyde. Moreover, quantum cascade infrared laser spectroscopy on single puffs was established by Parrish et al. [318] and applied to the investigation of formaldehyde [319] as well as NH<sub>3</sub>, ethylene and NO [171]. Recently, Baren et al. [170] published the simultaneous analysis of NH<sub>3</sub>, ethylene, NO, CO<sub>2</sub> and NO<sub>x</sub> (sum of NO and NO<sub>2</sub>) by using a quad quantum cascade laser spectrometer with dual gas cells. Furthermore, Plunkett et al. used a dual infrared tuneable diode laser system for the analysis of NH<sub>3</sub>, ethylene, formaldehyde and hydrazine in whole cigarette smoke [320, 321]. Thomas et al. [322] applied multiplex gas chromatography-mass spectrometry to monitor 25 puff-resolved components in smoke. However, the different puffs were not taken from the same cigarette. This was also the case for the set-up introduced by Wagner et al. [323] which aimed to collect the smoke in traps for further analysis. Crooks et al. developed a technique for determining intrapuff nicotine yield by using a rectangular filter travelling at a constant velocity of 5 cm/s behind the cigarette filter to collect the smoke condensate during puffing [324]. Recently, GC-MS has also been used by Li et al. [325] for quantitative studies on five polynuclear aromatic hydrocarbons in single puffs.

Limiting factors for most of these methods are either the low resolution times or the fact that only a few substances can be analysed simultaneously. Moreover, tobacco smoke is a highly dynamic matrix. Therefore, in order to gain analytical information of smoke components relevant for human smokers, it is important to investigate relatively fresh smoke (ca. one to two seconds old), rather than smoke that has aged over a few minutes [326]. In addition, the analysis technique must not interfere too much with the combustion and pyrolysis processes occurring in the cigarette. In this context, an inherent problem is the fact that besides the composition, the partition between the gas phase and particulate phase can also change continuously and is strongly influenced by time, temperature and dilution of smoke [14]. In practice, investigations of the effects of cigarette smoke constituents have generally concentrated on the particulate phase of smoke [74]. However, knowledge about the phase affiliation of smoke components is important because gas phase and particulate matter have very different deposition characteristics in the respiratory tract, be it oral, pharyngeal, bronchial, or alveolar. For most smokers the smoking process occurs in two steps. The first stage is a “mouth” phase, whereby smoke is drawn into the mouth without any evidence of inhalation. The second stage begins with a pause of variable duration, often associated with removing the cigarette from the mouth, which is followed by inhalation of smoke. Thus, high yields in gaseous constituents can result in a high uptake during the first (‘mouth’) phase

whereas particulate-related species are predominantly absorbed in the second (‘inhalation’) phase [327]. Animal inhalation tests have indicated that upper respiratory tract changes are specifically associated with the cigarettes’ vapour phase [74]. Particulate matter can penetrate deep into the respiratory tract and the regional deposition is influenced by several parameters e.g. the diameter of the inhaled particulate matter [81 and references in there ]. Pankow [328] argues that, in general, a given smoke constituent in inhaled smoke will be distributed between the aerosol particulate and vapour phase, and that there are four mechanisms by which a smoke constituent can deposit in the respiratory tract (see Figure 38):

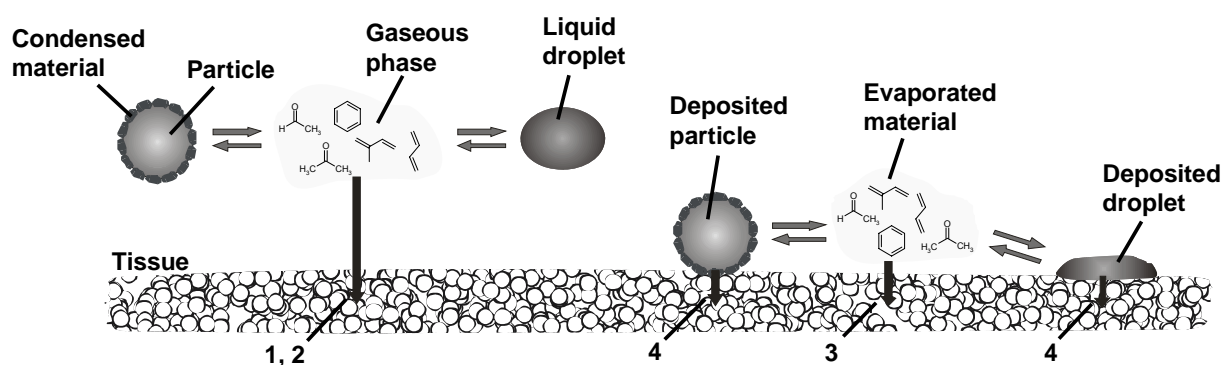


Figure 38: Four different uptake mechanisms of smoke constituents in the humans’ respiratory tract

- (1) direct deposition of compounds initially in the gas phase,
- (2) evaporation of the constituent out of the aerosol followed by gaseous deposition,
- (3) particle/droplet deposition, followed by evaporation of the constituent out of the deposited particle/droplet, followed by gaseous deposition,
- (4) aerosol deposition followed by diffusion/dissolution of the constituent into the respiratory tract tissue.

For high volatile compounds that reside almost exclusively in the gas phase, e.g.  $\text{CO}_2$ , only (1) will be important. For very low volatile substances (e.g. large PAHs), which tend to reside almost exclusively in the particulate phase, only (4) will be important. In contrast semivolatile components can be present in significant amounts in both phases and the phase affiliation can differ quite a lot. Therefore all mechanisms (1 to 4) can play a role [328].

Consequently, the ideal way for analysing tobacco smoke would be to analyse (i) simultaneously as (ii) many relevant compounds as possible, (iii) in both phases, (iv) on a real time basis. From the scientific point of view, the ideal analysis procedure is difficult to

achieve. The objective of the present study was to establish an instrumental set-up which best meets these requirements in order to analyse at trace levels several volatile and semivolatile compounds which are believed to cause health effects for human smokers. However, some compromises had to be accepted. Firstly, since fast gas phase measurements require modifications to the set-up due to the implementation of particulate matter precipitation techniques, the gas phase and the whole smoke phase were investigated in succession. Secondly, the approach of analysing whole smoke and vapour phase allows only indirectly drawing conclusions about the burden of organic matter in the particulate phase. Consequently, the focus of this study is on whole smoke and gas phase investigations. Main goal of the method is a fast and comprehensive analysis which interferes as little as possible with the complex smoke matrix.

## **4.2. Experimental set-up of smoking experiments**

The smoking machine and the SPI-TOFMS instrument were connected by the heated transfer line containing the deactivated capillary, similar to the experimental set-up described for the pyrolysis experiments. The experimental set-up is illustrated in Figure 39. The T-piece containing the capillary was placed orthogonally straight between the Cambridge filter holder, shown in Figure 40, and a smoking machine which was adjusted to perform ISO puffing conditions. The smoking machine used is a custom-made smoking machine based on a commercial Borgwaldt smoking machine. The main reason for the modifications was the fact that the former machine was insufficient for real-time measurements since the smoke was collected and mixed in a piston before being pumped to any analytical device. Since this work deals with puff-by-puff resolved measurements, the former smoking-machine would have been sufficient but it turned out that the custom-made smoking-machine was much more convenient than the commercial one. In this context, problematical was the fact that the original smoking machine caused much greater memory effects due to its higher dead volume. Therefore all measurements were performed by using the modified smoking machine. A detailed description of this smoking machine and its first application to sub-puff investigations of the smoking process can be found in [232] and will be thoroughly discussed in an upcoming dissertation [329]. During analysis a small portion of the smoke (flow: 8



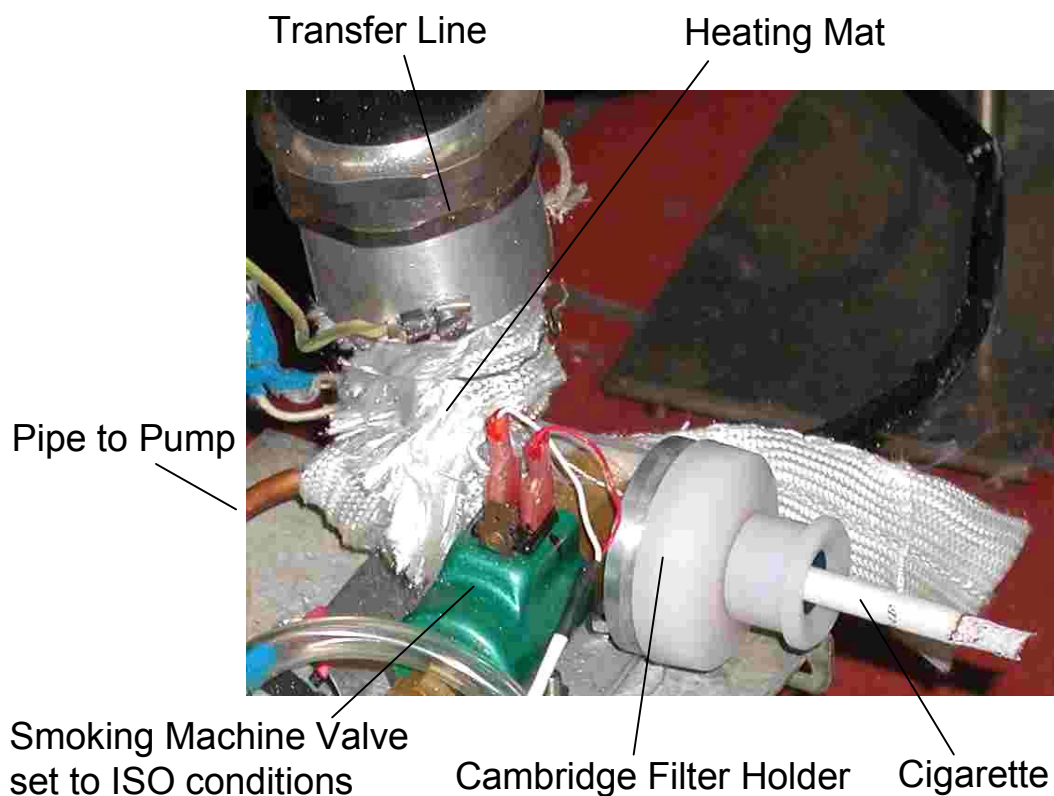


Figure 40: Photograph of the modified smoking-machine connected to the Cambridge filter holder and the transfer line

The cigarettes were lit with a Borgwaldt electric lighter and two series of cigarette mainstream measurements were carried out. The first series dealt only with the gas phase of cigarette smoke whereas in the second series whole cigarette smoke was analysed. Gas phase measurements were carried out by incorporating a Cambridge filter in the cigarette holder. For whole smoke measurements the Cambridge filter was removed. In this way, most volatile and semivolatile organic substances deposited on the particulate matter are evaporated by passing through the heated transfer line, and subsequently are also accessible to SPI-TOFMS. Similar to the pyrolysis experiments, three successive single laser shot mass spectra were averaged (time resolution 3.3 Hz) to improve signal stability.

### 4.3. Sample cigarettes

Concerning sample cigarettes, the main focus was on the 2R4F Kentucky Reference cigarette. The 2R4F, a widespread research cigarette, is available from the University of Kentucky, Kentucky Tobacco Research & Development Center (KTRDC) and replaces the former 1R4F research cigarette. The properties and smoke yields of the 2R4F and the 1R4F cigarettes have been thoroughly characterised in [330]. The 2R4F cigarette is manufactured under controlled conditions and its tobacco blend consists of four single tobacco types (Virginia, Burley, Maryland, and Oriental). Therefore it is a blended cigarette. Its percentage composition is illustrated in Table 22.

Table 22: Percentage composition of the University of Kentucky 2R4F research cigarette [330]

Constituent	%
Virginia tobacco	32.5
Burley tobacco	20.0
Maryland tobacco	1.06
Oriental tobacco	11.1
Reconstituted tobacco	27.2
Glycerol	2.80
Invert sugar	5.30

In addition to these four tobacco types, the 2R4F reference cigarette also contains reconstituted tobacco (27 %), added invert sugar (5.3 %) and the humectant glycerol (2.8 %) [330]. Reconstituted tobacco sheet is made from scraps of tobacco that has a size range unsuitable for cut tobacco filler. Therefore it was originally used in cigarette manufacture to lower costs [3]. It can also be treated to alter several tobacco properties such as taste, burn rate, and smoke composition [3, 331]. Glycerol is a natural ingredient of many plants, including tobacco. Around 1 to 3 % glycerol is also added to tobacco in some markets such as the USA, as a humectant, to aid tobacco processing and to improve the smoke taste of cigarettes [332, 333]. Invert sugar is a mixture of fructose and glucose and is added to blended cigarettes in the USA, for example, to keep the tobacco moist as it has a high affinity for water [333].

In order to account for the influence and the contribution of the four single tobacco types on the smoke composition of cigarette smoke, a further measurement series dealt with their detailed characterisation and the comparison to the 2R4F cigarette. Therefore, four different cigarette types consisting of only one type of tobacco each were manufactured under controlled conditions and investigated by using the same experimental set-up. Properties of the three tobacco types Virginia, Oriental, and Burley were described in detail in the pyrolysis section. In addition, Maryland is a relatively light bodied, mild, air-cured tobacco grown on the sandy coastal plains of Maryland, USA. Some blended cigarettes contain small amounts of Maryland tobacco [270]. Cigarette design parameters such as filter ventilation and paper permeability of all types were thoroughly characterised and did differ only slightly from those of the 2R4F cigarette. The design parameters of the four single tobacco cigarettes and the 2R4F cigarette are listed in Table 23.

Table 23: Design parameters of the four single tobacco cigarettes and the Kentucky 2R4F research cigarette

<b>Design parameter</b>	<b>Burley</b>	<b>Virginia</b>	<b>Oriental</b>	<b>Maryland</b>	<b>2R4F</b>
Filter type	Cellulose acetate				
Filter length [mm]	27	27	27	21	27
Filter ventilation [%]*	35	35	35	20	28
Cigarette paper permeability [cm min <sup>-1</sup> kPa <sup>-1</sup> ]	55	55	55	50	24
Tipping paper length [mm]	32	32	32	25	32
Cigarette length [mm]	83	83	84	83	84
Cigarette weight [mg]	786	827	985	690	1020
Tar [mg/cig]**	8.09	12.3	13.8	10.3	11.3
Number of puffs ***	6.0	8.3	11.0	5.0	8.7

\* Measured at an air flow of 17.5 ml/s

\*\* According to cigarette manufacturer; measured under ISO smoking conditions

\*\*\* Whole smoke measurements under ISO smoking conditions

A further measurement series dealt with the evaluation of two different approaches of reducing specific toxic smoke constituents. The first cigarette type is a so-called “light” cigarette (tar: 8 mg; nicotine: 0.8 mg; CO: 10 mg) in which ventilation of the cigarette by the use of porous paper and ventilation holes in the filter results in reduced generation of smoke constituents in the burning zone and dilution of the smoke and thereby a reduction of the

yield. The second cigarette type (tar: 10.0 mg; nicotine: 0.77 mg; CO: 9 mg) is based on a novel principle of combining two different approaches. Firstly, the tobacco had been treated by a newly developed technology which inhibits the formation of tobacco-specific nitrosamines [334]. Secondly, the cigarette filter consists of three sections: the tobacco rod is adjacent to the first section, which contains an ionic exchange resin, followed by a section that contains activated carbon, and thirdly by a cellulose acetate section. In contrast, most common cigarette filters in the western world are only made of cellulose acetate. This combination of three sections in the filter is designed to reduce the level of specific toxins in the smoke, in particular formaldehyde and other carbonyls as well as TSNAs. Both types, the 'light' cigarette and the novel cigarette type, referred to as 'new filter type cigarette' (NFT), are thoroughly characterised regarding smoke composition and also compared to the 2R4F research cigarette. Table 24 illustrates the cigarette parameters of both types unless known.

Table 24: Design parameters of the 'light' cigarette and the 'New Filter Technology' (NFT) cigarette

<b>Design parameter</b>	<b>'Light' cigarette</b>	<b>'NFT' cigarette</b>
Filter type	cellulose acetate	triple filter
Filter length [mm]	27	27
Tipping paper length [mm]	5	5
Cigarette length [mm]	83	83
Cigarette weight [mg]	850	960
Tar [mg/cig] *	8.0	10.0
Number of puffs **	8.0	6.0

\* According to cigarette manufacturer; measured under ISO smoking conditions

\*\* Whole smoke measurements under ISO smoking conditions

## **4.4. Results and discussion of smoking experiments**

The following chapter deals with the processing and interpretation of the cigarette smoking results. Firstly, it is demonstrated how the recorded data are converted into quantitative puff-resolved measurements. The results are used to characterise the cigarette smoking process in general. In addition to that, different tobacco type cigarettes as well as different cigarette designs are characterised and compared on a puff-by-puff basis with the main focus being on hazardous compounds. Moreover, drawbacks of the ISO smoking regime are discussed.

### **4.4.1. Spectra processing**

The recorded time-of-flight spectra were converted to mass spectra the same way as described for the pyrolysis experiments. For puff-by-puff evaluation, the time-resolved signal intensities of each individual smoking puff as well as the two corresponding cleaning puffs were summed and the cleaning puffs were added. Finally, the mean and standard deviation of the three replicates were calculated for every puff. The processing of the puff-resolved cigarette smoke measurements is demonstrated in Figure 41.

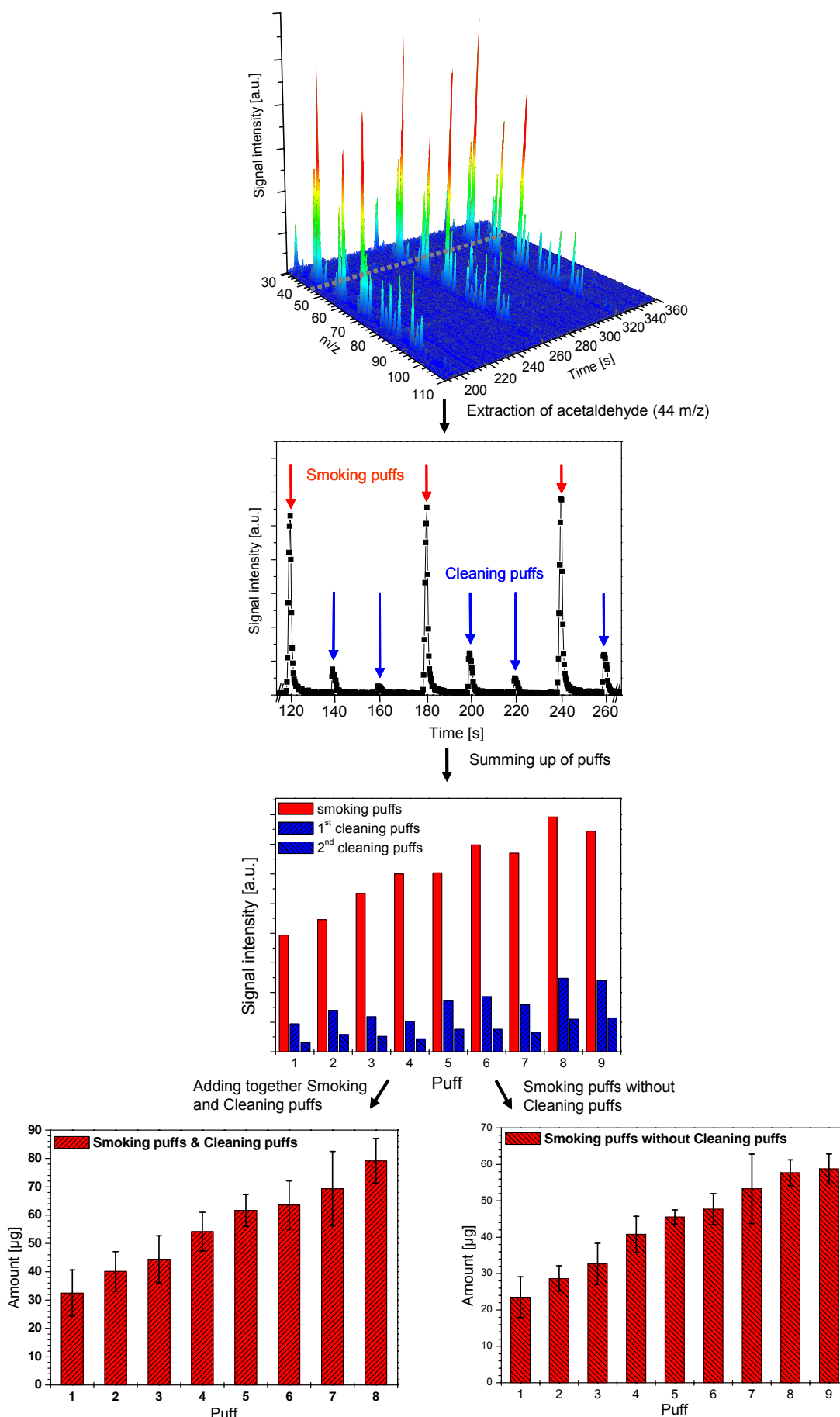
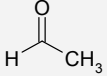
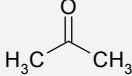


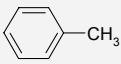
Figure 41: Processing of time-resolved mass spectra to quantified puff-by-puff resolved yields exemplarily shown for acetaldehyde

#### 4.4.2. Selection of hazardous target compounds for quantification

Quantification mainly focuses on a few constituents of special interest due to their harmful potential for the human smoker. These target compounds were chosen according to their accessibility by SPI-TOFMS as well as possible relevance for the human smoker and expected yield in tobacco smoke. The publications and reports [90, 94-96] introduced in Chapter 1.3 acted as a guideline. The substances studied quantitatively are nitric oxide, acetaldehyde, butadiene, acetone, isoprene, benzene, toluene, and the C2-benzene derivatives ethyl benzene and xylene. Table 25 illustrates the chemical structures of the nine hazardous target molecules, some important physical properties (vapour pressure ( $V_p$ ) and boiling point (Bp)) as well as toxicological data, such as the International Agency for Research on Cancer (IARC) categories, Occupational Safety and Health Administration (OSHA) permissible 8-hour time weighted average concentration ( $TWA_8$ ). The position in the three cancer potential rankings of smoke constituents are also illustrated. Moreover, yields for plain, non-filter cigarettes measured under ISO conditions are given.

Table 25: Chemical structures of the nine hazardous target molecules as well as some important physical and toxicological properties

Property	Nitric oxide	Acetaldehyde	Butadiene	Acetone	Isoprene
Chemical structure	NO				
CAS No.	10102-43-9	75-07-0	106-99-0	67-64-1	78-79-5
MW [g/mol]	30	44	54	58	68
Vp at 20 °C [kPa]	-	101	245	24	53.2
Bp [°C]	- 151.8	- 123	- 4	56	34
ISO yield per non-filter cigarette [µg] [3, 14]	100 – 600 (NO <sub>x</sub> )	400 - 1400	25 - 40	100 - 650	200 - 400
IARC class [335]	3	2B	2A	3	2B
OSHA TWA <sub>8</sub> [mg/m <sup>3</sup> ] [90, 335]	30	360	2.21	2400	n. e.
Fowles & Bates [95, 96]	n. e.	5	1	n. e.	n. e.
Vorhees [94]	n. e.	2	1	n. e.	n. e.
Rodgman & Green [90]	n. e.	5	1	n. e.	n. e.

Property	Benzene	Toluene	Ethyl benzene	Xylene
Chemical structure				
CAS No.	71-43-2	108-88-3	100-41-4	1330-20-7
MW [g/mol]	78	92	106	106
Vp at 20 °C [kPa]	10	2.9	0.9	0.9
Bp [°C]	80	111	136	138
ISO yield per non-filter cigarette [µg] [3, 14]	< 70	< 200	n. e.	n. e.
IARC class [335]	1	3	3	3
OSHA TWA <sub>8</sub> [mg/m <sup>3</sup> ] [90, 335]	3.19	754	434	434
Fowles & Bates [95, 96]	6	n. e.	n. e.	n. e.
Vorhees [94]	9	n. e.	n. e.	n. e.
Rodgman & Green [90]	16	n. e.	n. e.	n. e.

n. e.: none established

Nitric oxide (NO) causes inflammation of the lung [86]. NO is known to act as a nitrosation agent for tobacco alkaloids (e.g. nicotine) to form carcinogenic TSNAs in tobacco and smoke. Furthermore, NO<sub>2</sub> which is the oxidation product of NO, is believed to form small organic radicals via a steady state mechanism by addition to smoke constituents such as isoprene, butadiene, and acrolein [14, 155, 336-341].

Acetaldehyde is classed as a 2B carcinogen by IARC, i.e. possibly carcinogenic to humans based on sufficient evidence of carcinogenicity in experimental animals [143, 335, 342, 343]. The three cancer potential rankings list acetaldehyde on position two and five respectively [90, 94-96]. In this context Seeman et al. published a comprehensive review of the formation of acetaldehyde in mainstream cigarette smoke and its bioavailability in the smoker [271]. Bombick et al. 1997 indicated that a general reduction of carbonyls in the cigarette vapour phase reduces the cytotoxic activity of smoke [344]. Acetaldehyde is also responsible for respiratory health effects and eye irritation [95].

1,3-Butadiene is classed as 2A by IARC, i.e. probably carcinogenic to humans based on sufficient evidence of carcinogenicity from studies in humans, including epidemiological and mechanistic information, which show a causal relationship between occupational exposure and excess mortality from lymphatic and/or haematopoietic cancers [335, 345]. All three cancer risk calculations list 1,3-butadiene as the tobacco constituent with the highest cancer potential [90, 94-96]. Moreover, it is also believed to be responsible for reproductive and developmental effects [95].

Acetone causes irritations to eyes and respiratory tract [3].

Isoprene is classed as 2B by IARC, i.e. possibly a human carcinogen based on sufficient evidence of tumor formation at multiple organ sites in multiple species of experimental animals [346].

Benzene is known to be a human carcinogen due to sufficient evidence in humans. Case reports and case series have determined leukaemia in individuals exposed to benzene [335, 347]. Recently Lan et al. [348] described possible hematologic effects even below the U.S. occupational standard of one ppm benzene in air, particularly among susceptible subpopulations. It is ranked fifth, seventh, and 16<sup>th</sup> respectively in the cancer risk rankings [90, 94-96] and is also linked to reproductive and developmental effects [95].

Toluene does not have the carcinogenic potential of benzene but is classified as harmful to human health [349].

The C2-benzenes xylene (ortho-, meta-, and para-) and ethyl benzene feature low acute and chronic toxicity for humans. Ethyl benzene is stated as toxic to the central nervous system and

irritating to the mucous membranes and the eyes. There is no evidence concerning carcinogenic effects for any of the compounds [349]. According to Fowles and Bates [95], the toxicity of toluene, ethyl benzene and xylene play a more crucial role in sidestream cigarette smoke.

Finally, the IARC has classified tobacco smoking as a whole as known to be a human carcinogen. It has been assessed to cause cancer of the lung, urinary bladder, renal, pelvis, oral cavity, pharynx, larynx, esophagus, lip and pancreas in humans [335, 350].

Resolution of the TOFMS (1800  $m/z$  [351]) is such that separation between isobaric compounds is difficult. This is hardly a problem for most substances in the framework of this study since isobaric species of the selected target compounds are either not at all (IP above 10.49 eV) or only weakly (low  $\sigma_i$  at 10.49 eV) accessible by SPI, or their expected concentrations are lower than the standard deviations of the target compounds. Therefore, some quantitative information might be influenced by small amounts of isobaric species. In this context the main focus was on a fast and robust method that is simple to operate and, at the same time, delivers comprehensive information rather than a highly accurate but time-consuming technique, which is limited to a low number of observable compounds. However, since a separation of ethyl benzene and xylene is not possible, their yield is stated as the sum of both.

### 4.4.3. Characterisation of the 2R4F research cigarette

#### 4.4.3.1. Total yields of whole smoke and gas phase

For first evaluation of the composition of the gas phase and whole cigarette mainstream smoke, spectra from the smoking of a complete 2R4F research cigarette with and without a Cambridge filter pad were summed up (over all puffs) in order to compare the different signal patterns. The summed signal intensities of the gas phase and whole smoke are illustrated in Figure 42.

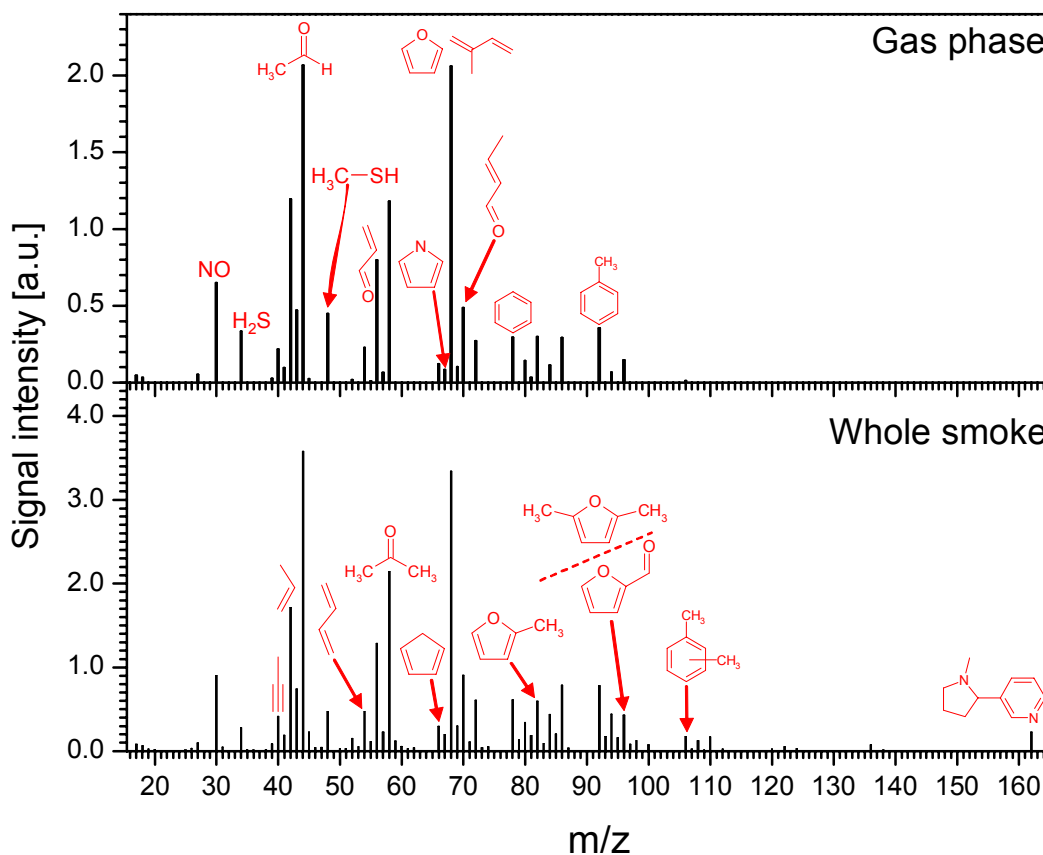
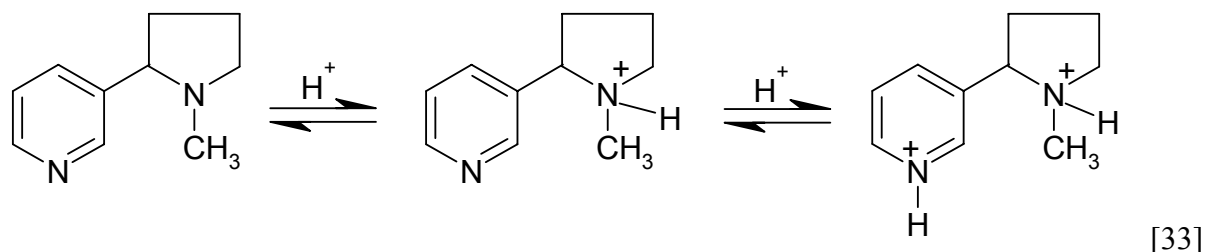


Figure 42: Comparison of gas phase and whole smoke by opposing two sum spectra of a completely smoked 2R4F cigarette

In general, signal intensities of almost all masses are higher for whole smoke compared to the vapour phase. In addition, whole smoke results in a greater variety of masses, especially in the mass region higher than 70  $m/z$ . The assignment of masses observed in cigarette smoke to the most likely compounds was given in Table 12 in Chapter 3.4.1. Most striking is the occurrence of nicotine (162  $m/z$ ) in whole smoke whereas in the cigarette vapour phase, nicotine is non-existent. This phenomenon can be explained by the fact that for a typical US

blended cigarette, the ‘smoke pH’ is in the range from 5.5 to 6.5 [317, 352]. Although applying the concept of pH to the dynamic aerosol mixture of smoke is not precise, the smoke will be acidic. Under such acidic conditions, dibasic nicotine is almost entirely protonated and will be bound ionically to the acids present.

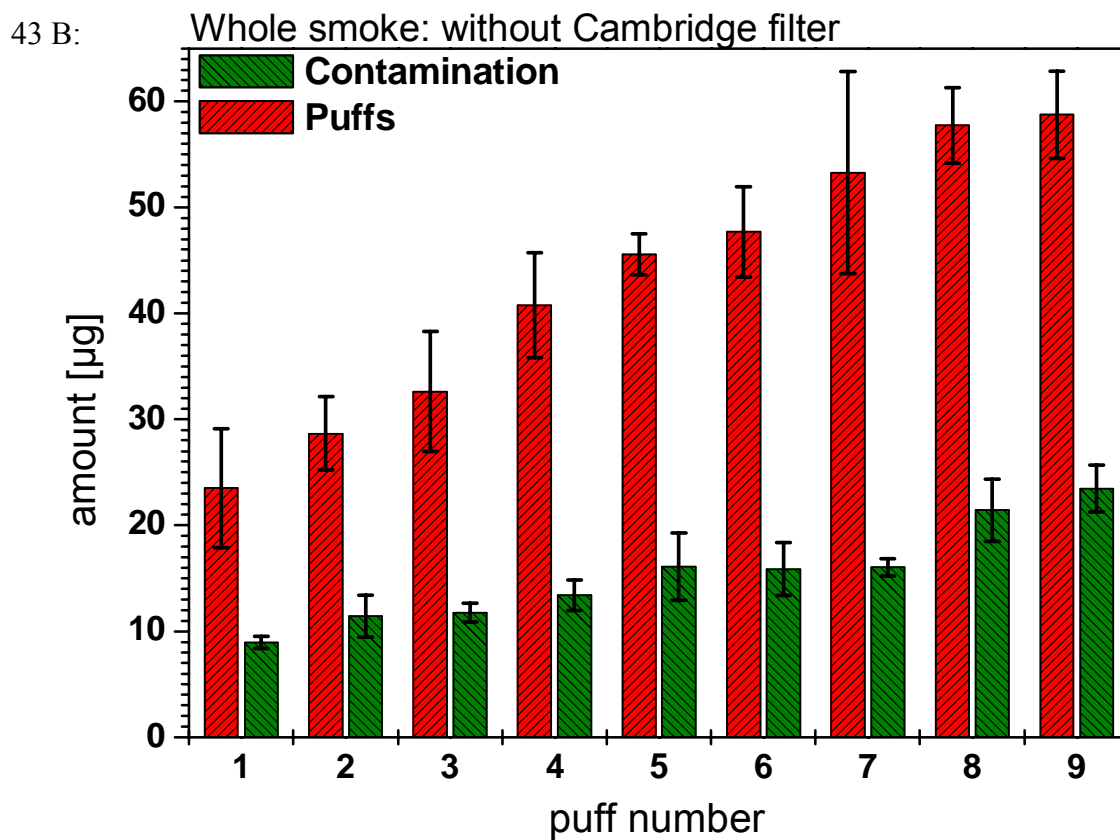
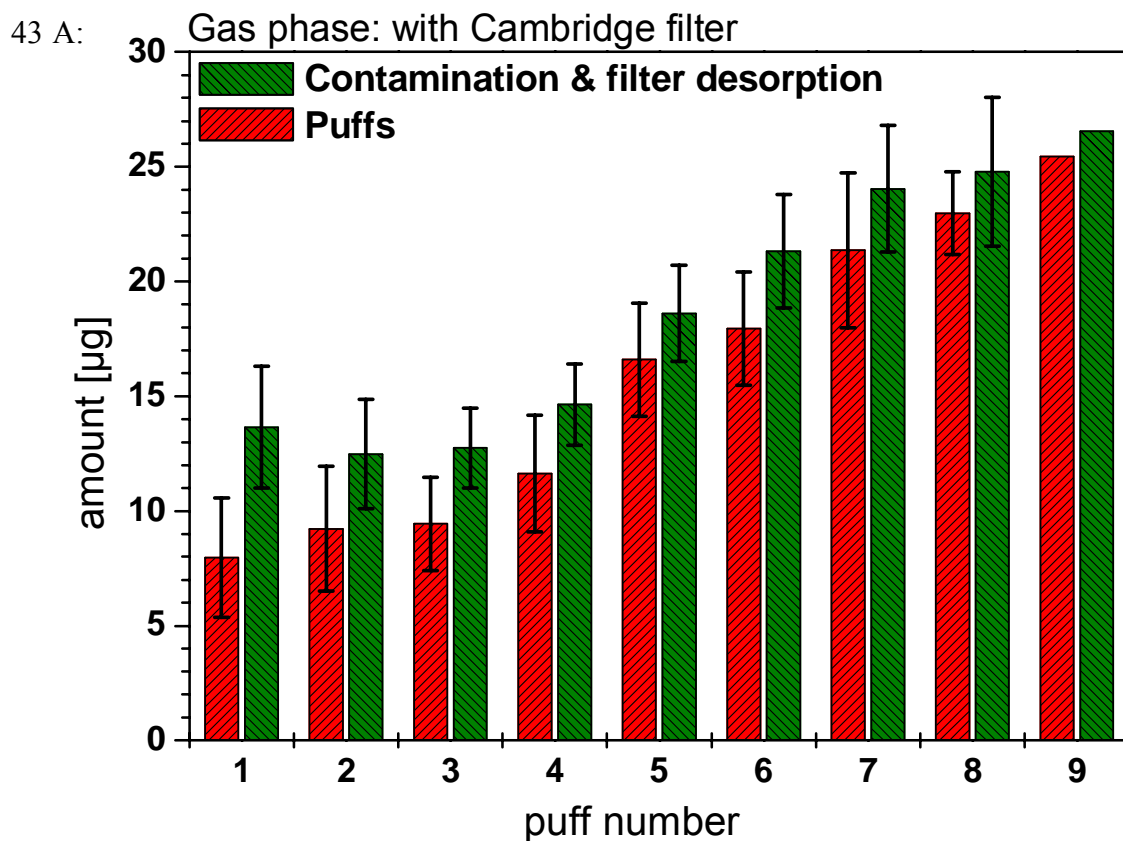


Equation 33: Protonation of nicotine

The resulting nicotine salts are found exclusively in the smoke aerosol particles and not in the gas phase [14, 353, 354].

#### 4.4.3.2. Drawbacks of the smoking regime

When contemplating puff-by-puff resolved smoking profiles for the first time it turned out that the smoking caused massive memory effects and contamination of the following puffs, and in addition, the effect was much greater for gas phase measurements. These effects were subsequently investigated by taking several cleaning puffs, with no cigarette present in between the actual cigarette smoking puffs, until the signals of the cleaning puffs declined to zero. In general, two cleaning puffs were necessary for this purpose. These signals were added together and compared to the smoking puffs. Figure 43 B shows the yields for acetaldehyde (44  $m/z$ ) in the successive unfiltered smoking puffs and subsequent cleaning puffs of a 2R4F research cigarette. To a first approximation, contamination and memory effects for each puff amounted for about one third of the corresponding smoking puff intensity. For whole smoke this will mostly depend on the type of smoking-machine used. However, the summed cleaning puffs of the gas phase measurements with a Cambridge filter pad present resulted in even higher signal intensities than for the smoking puff, especially for the earlier puffs (Fig. 43 A).



Figures 43 A and B: Successive smoking and cleaning puffs of the gas phase (Fig. 43 A) and whole smoke (Fig. 43 B) of the 2R4F cigarette, shown for acetaldehyde ( $44 m/z$ ).

This must be due mainly to desorption effects from the Cambridge filter. Apparently, none of the few previous studies dealing with puff-by-puff resolved measurements of cigarette mainstream smoke vapour phase mentioned similar observations. However, Parrish et al. [316] described the influence of several Cambridge filter parameters on smoke composition as well as trapping efficiencies for acetaldehyde and HCN. This desorption effect must also occur in total yield investigations from entire cigarettes but, since in this case signals of all puffs are summed up, are not as crucial as for single puff characterisation. Subsequently, the definition of “single puff” is problematical since it is not obvious if the subsequent contamination levels should be added to the yield of the previous puff. If this is not the case, thorough cleaning or filter changing after every puff will be required. Otherwise, this contamination level is added automatically to the subsequent smoking puff, which consequently affects this result. Therefore for single puff evaluation, two approaches are possible, which are visualised in Figure 44: either contemplation of the smoking puffs only without cleaning puffs (approach B’), or adding together smoking and corresponding (subsequent) cleaning puffs (approach A’). The former method results in a mismatch when all single puff yields are added together and compared to the conventional total yield measurements since it will result in smaller total amounts (approach B). The latter approach (A’) makes the results comparable to published data dealing with total amounts of various smoke compounds. Secondly, the levels of components in both the smoking puffs and the cleaning puffs are relevant to the human smoker. However, especially for gas phase analysis, some particulate matter held back by the filter might evaporate to the smoke stream of the following puffs and wrongly contributes to the gas phase. This source of error is also relevant for conventional total yield measurements. Regarding this work the puffs are defined as smoking puff plus subsequent cleaning puffs, mainly because both fractions affect the human smoker.

There was no evidence found that neither ISO nor any other institution dealing with the definition of standard smoking conditions is aware of these facts. One reason is probably the lower relevance for total yields. However, total yield investigations are also influenced but to a smaller extent. If smoke sampling is immediately stopped after the final smoking puff, the contamination and desorption yields of this final puff (here: 23  $\mu\text{g}$  and 26  $\mu\text{g}$  acetaldehyde for whole smoke and vapour phase respectively) remain in the smoking machine and/or filter. Therefore, under the ISO smoking standards the total cigarette amounts determined are missing these parts (approach C). As a consequence, approach A was used regarding total smoke analysis.

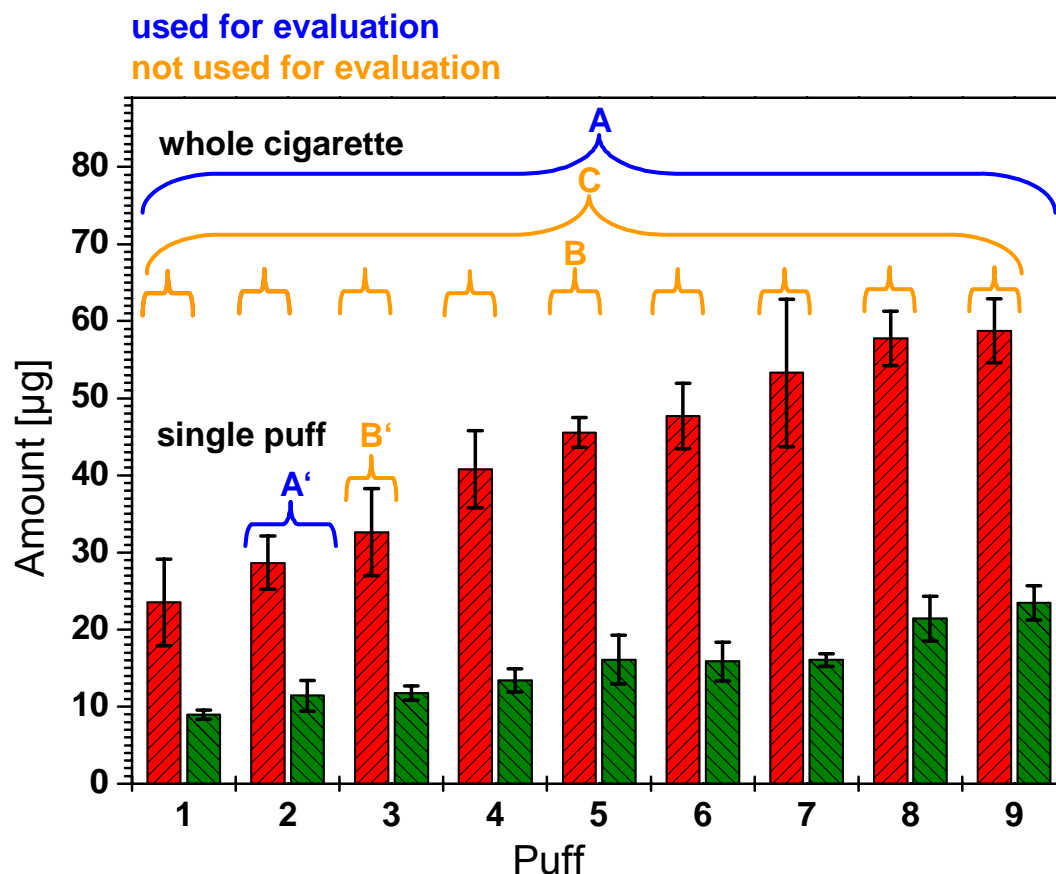


Figure 44: Illustration of the three different approaches (A, B, and C) for the definition of 'whole cigarette' and the two approaches for the definition of 'single puff' (A' and B')

Evaluation of the accuracy of the data obtained by comparison with other studies is difficult. Despite the standardisation of cigarette storage, smoke generation etc., results from different laboratories still differ and many reasons can be responsible for this well known fact [355]. However, Chen et al. [330] and Wagner et al. [323] recently published total yields of some smoke constituents of the 2R4F which are, overall, in good agreement with the values achieved in the present study. Purkis et al. [355] recently published a comprehensive comparison of many smoke constituents analysed by seven different laboratories. In their paper they described the tremendous variations in total yields' determined which varied e.g. for butadiene between 21.9 and 76.5 µg per cigarette for the same product. The comparison in the present study demonstrates that the approach of including the cleaning puffs leads to similar total amounts to those reported by Chen and Wagner. Without including the cleaning puffs the total yields would be lower. This procedure is probably unconsciously carried out the same way by many laboratories dealing with cigarette smoke analysis. Table 26 lists the species being quantitatively analysed in all three studies.

Table 26: Total yields of diverse smoke constituents of the 2R4F research cigarette analysed by three different research groups

Compound	This work	Chen et al. [330]	Wagner et al. [323]
<i>Whole Smoke</i>			
NO [ $\mu\text{g}/\text{cig}$ ]	$309.6 \pm 13.9$	223.41	-
Acetaldehyde [ $\mu\text{g}/\text{cig}$ ]	$527.1 \pm 26.7$	560.48; $583.74 \pm 13.18^*$	562
Butadiene [ $\mu\text{g}/\text{cig}$ ]	$38.5 \pm 2.2$	29.94	37.1
Acetone [ $\mu\text{g}/\text{cig}$ ]	$265.1 \pm 15.1$	264.74; $261.62 \pm 7.35^*$	248
Isoprene [ $\mu\text{g}/\text{cig}$ ]	$397.2 \pm 15.3$	297.68	391
Benzene [ $\mu\text{g}/\text{cig}$ ]	$48.2 \pm 3.6$	43.39	51.8
Toluene [ $\mu\text{g}/\text{cig}$ ]	$84.5 \pm 4.3$	64.91	88.0
<i>Gas Phase</i>			
Acetaldehyde [ $\mu\text{g}/\text{cig}$ ]	$310.7 \pm 17.6$	$396.78 \pm 71.02$	-
Acetone [ $\mu\text{g}/\text{cig}$ ]	$148.1 \pm 9.6$	$205.52 \pm 8.35$	-

\* Chen's publication contained two values for acetaldehyde and acetone because two different analytical techniques were used

#### 4.4.3.3. Puff-by-puff resolved characterisation of whole smoke and gas phase

Regarding inter-puff evaluation, smoking of the 2R4F cigarette resulted in puff numbers between eight and nine puffs. This is mainly due to slightly varying lighting behaviours of the cigarette and operator. The mean puff number out of three measurements was 8.7 for the whole smoke analysis and 8.3 for the vapour phase measurements. Consequently, in the following illustrations the standard deviation for the ninth puff of the gas phase is non-existent. On the one hand non-integer puff numbers appear curious but result from the strict compliance of the ISO conditions and the associated defined butt length. Moreover, it must be considered that the same puff, e.g. puff number five, of a cigarette reaching eight puffs and of a cigarette reaching nine puffs originates from a slightly different position/length of the tobacco rod. This can influence averaged puff yields and standard deviations and further complicates argumentation.

#### **4.4.3.4. Quantitative evaluation**

Figure 45 illustrates the puff profile of the quantitatively analysed substances in the smoke of the 2R4F cigarette for whole smoke and the gas phase. The cleaning puffs have been added to the corresponding preceding puffs as discussed earlier. The mean values including standard deviation are also listed in Table 27. The same yields for the smoking puffs only, i.e. without adding the cleaning puffs to the smoking puffs, are illustrated in Figure 46 for comparison. The corresponding list containing the total and puff-resolved yields can be found in the Appendix. However, for further evaluation it will be focussed on the approach of adding the cleaning puffs to the smoking puffs as discussed earlier.

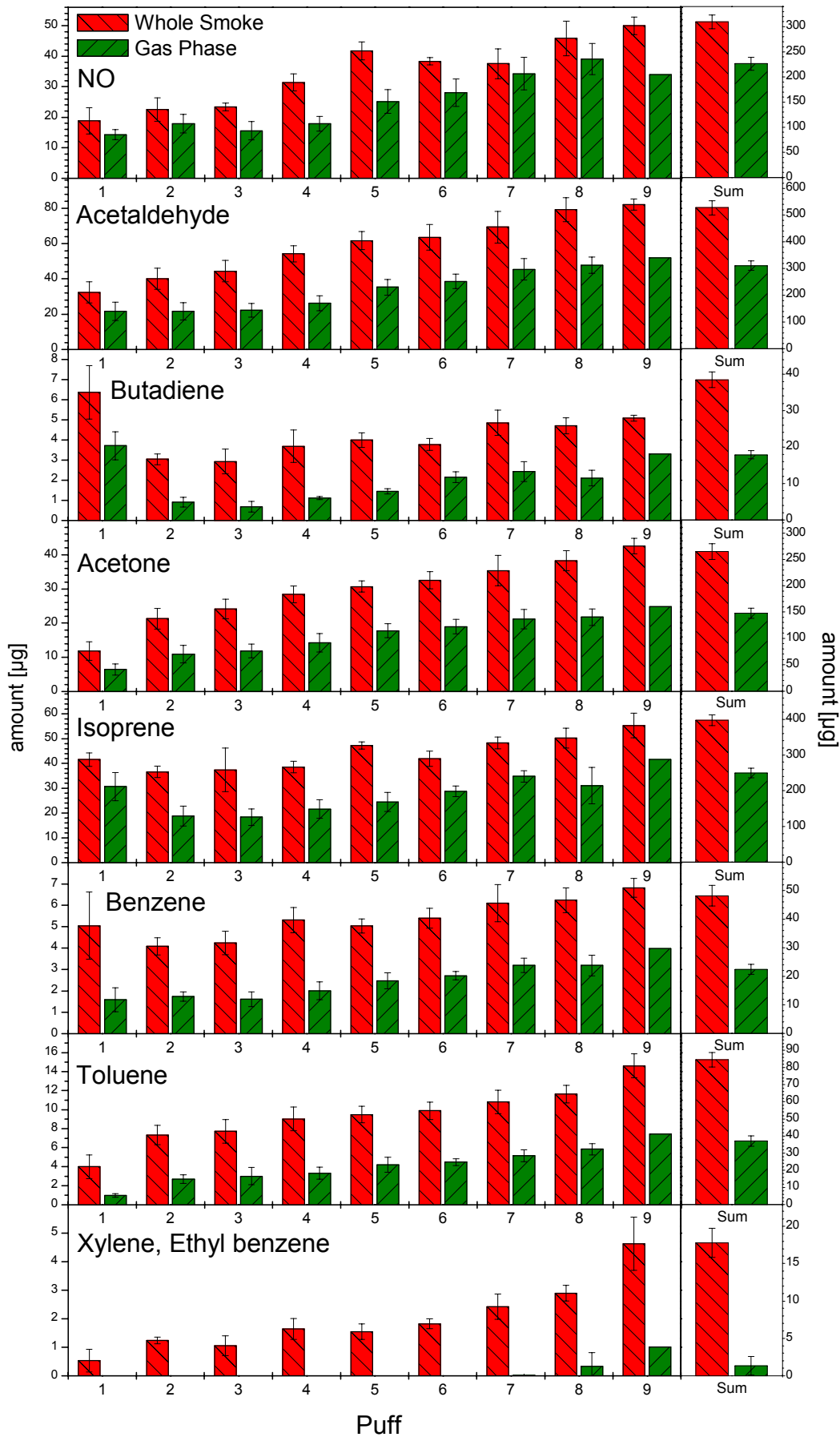


Figure 45: Quantitative, puff-by-puff resolved and total yields of hazardous substances analysed in the gas phase and whole smoke of the 2R4F research cigarette with cleaning puffs added to the smoking puffs

Tables 27 A and B: Averaged yield ( $\bar{m}$ ) and standard deviation (std) of the quantitative, puff-by-puff resolved compounds in  $\mu\text{g}$ , analysed in the gas phase (Table 27 B) and whole smoke (Table 27 A) of the 2R4F research cigarette by adding the cleaning puffs to the smoking puffs

## Whole smoke

Compound	Puff	1	2	3	4	5	6	7	8	9	$\Sigma$
NO	$\bar{m}$	18.9	22.5	23.4	31.4	41.7	38.3	37.6	45.9	50	309.6
	std	4.3	3.8	1.2	2.8	2.9	1.2	4.9	5.7	2.9	13.9
Acetaldehyde	$\bar{m}$	32.4	40.1	44.4	54.2	61.7	63.6	69.3	79.2	82.2	527.1
	std	6	6	6.1	4.6	5.1	7.4	9	6.8	3.2	26.7
Butadiene	$\bar{m}$	6.4	3	2.9	3.7	4	3.8	4.9	4.7	5.1	38.5
	std	1.3	0.3	0.6	0.8	0.4	0.3	0.6	0.4	0.1	2.2
Acetone	$\bar{m}$	11.9	21.3	24.1	28.4	30.7	32.5	35.3	38.3	42.5	265.1
	std	2.7	3	2.9	2.5	1.6	2.5	4.4	2.9	2.3	15.1
Isoprene	$\bar{m}$	41.6	36.6	37.4	38.6	47.2	41.9	48.3	50.2	55.3	397.2
	std	2.7	2.3	8.8	2.3	1.5	3.1	2.3	4	5	15.3
Benzene	$\bar{m}$	5	4.1	4.2	5.3	5	5.4	6.1	6.2	6.8	48.2
	std	1.6	0.4	0.5	0.6	0.3	0.5	0.9	0.6	0.4	3.6
Toluene	$\bar{m}$	4	7.3	7.7	9	9.5	9.9	10.8	11.6	14.6	84.5
	std	1.3	1	1.2	1.3	0.9	0.9	1.2	0.9	1.2	4.3
Xylene/Ethyl benzene	$\bar{m}$	0.5	1.2	1.1	1.6	1.6	1.8	2.4	2.9	4.6	17.8
	std	0.4	0.1	0.3	0.4	0.3	0.2	0.4	0.3	0.9	1.9

## Gas phase

Compound	Puff	1	2	3	4	5	6	7	8	9	$\Sigma$
NO	$\bar{m}$	14.3	17.9	15.6	17.9	25.1	28.1	34.3	39.1	34	226.2
	std	1.6	3	3	2.4	3.9	4.5	5.4	5.1	0	12.6
Acetaldehyde	$\bar{m}$	21.6	21.7	22.2	26.3	35.2	38.6	45.4	47.8	52	310.7
	std	5.2	4.9	3.9	4.3	4.5	4.2	6.1	4.7	0	17.6
Butadiene	$\bar{m}$	3.7	0.9	0.7	1.1	1.5	2.1	2.4	2.1	3.3	17.9
	std	0.7	0.2	0.3	0.1	0.1	0.3	0.5	0.4	0	1.1
Acetone	$\bar{m}$	6.5	10.9	11.9	14.3	17.8	19	21.2	21.8	24.9	148.1
	std	1.6	2.6	2	2.7	2.1	2.1	2.8	2.4	0	9.6
Isoprene	$\bar{m}$	30.7	18.8	18.4	21.6	24.5	28.8	34.8	31.1	41.5	250.2
	std	5.7	4	3.3	3.8	3.9	2.2	2.3	7.3	0	13.6
Benzene	$\bar{m}$	1.6	1.7	1.6	2	2.5	2.7	3.2	3.2	4	22.5
	std	0.6	0.2	0.3	0.4	0.4	0.2	0.3	0.5	0	1.7
Toluene	$\bar{m}$	1	2.7	3	3.3	4.2	4.5	5.2	5.8	7.4	37.1
	std	0.2	0.5	0.9	0.6	0.8	0.4	0.6	0.6	0	3.1
Xylene/Ethyl benzene	$\bar{m}$	0	0	0	0	0	0	0	0.3	1	1.3
	std	0	0	0	0	0	0	0	0.3	0	0.3

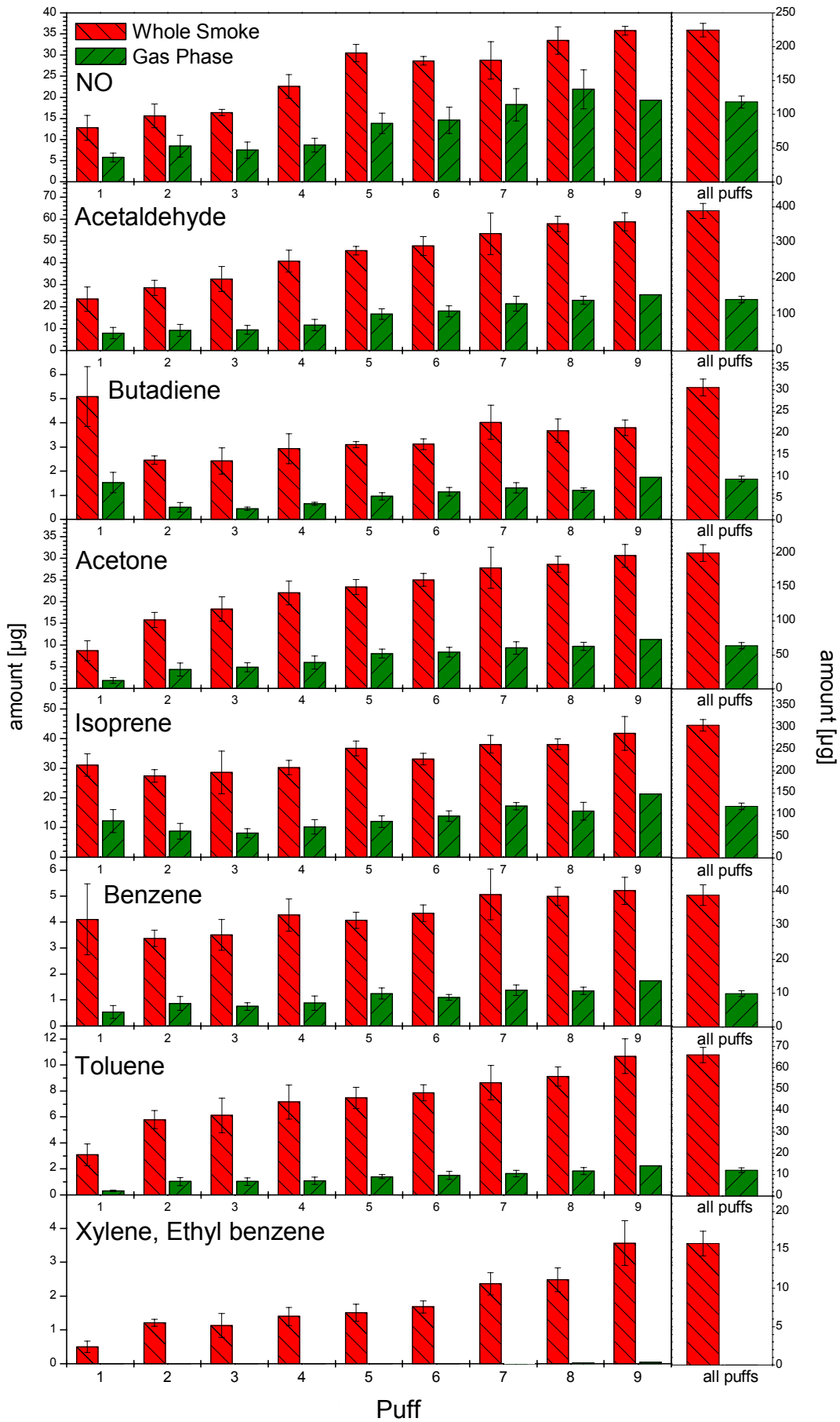


Figure 46: Quantitative, puff-by-puff resolved and total yields of hazardous substances analysed in the gas phase and whole smoke of the 2R4F research cigarette without cleaning puffs added to the smoking puffs

The presented results of NO reveal a further flaw of the Cambridge filter separation. NO is a small molecule and should be entirely in the gas phase of cigarette smoke. However, some NO seems to be trapped on the Cambridge pad since the yield is lower in the gas phase which indicates that the Cambridge pad is not an ideal filter for separating all the gas and particulate phase constituents of cigarette smoke. This effect is even more pronounced for the smoking puffs only which supports the trapping theory. The observed results for NO must reflect a reaction that removes NO, which is enhanced by the presence of the Cambridge pad. Although such an effect of the Cambridge pad has not been reported previously for NO, Williams [117] has observed recoveries of only 87-91% when NO was added to whole smoke using a non-dispersive infrared analytical technique together with a Cambridge filter pad. He postulated that NO was being lost by its reaction with other smoke constituents such as amines and alcohols to form nitrosamines and methyl nitrite respectively. Nitric oxide is known to oxidise within a few seconds in smoke to generate nitrogen dioxide, and the nitrogen dioxide subsequently reacts within a further few seconds with smoke constituents such as methyl alcohol, isoprene, butadiene and acrolein [337, 356]. The rate of oxidation of nitric oxide to nitrogen dioxide in mainstream smoke has been determined in several studies [117, 337, 338, 357]. The rate constant in smoke is almost a magnitude higher than for the pure gas phase oxidation, possibly due to catalysis of the reaction by free radicals present in smoke. In the present study the transit time of the smoke to the analyser will be greater in the presence of the Cambridge pad because of the tortuous path of the smoke through the filter pad. This allows more time for reaction of NO and will result in the measurement of lower quantities of NO when the Cambridge filter pad is present. It is experimentally convenient to use a Cambridge pad in smoke analysis but it does not give an absolute separation of the two phases. The materials collected on the pad are affected by a host of factors, including moisture content, temperature, flow rate and specific chemical interaction between aerosol constituents and the fibre glass. Different separation techniques, such as electrostatic precipitation, and jet impaction traps give different values for the vapour/aerosol composition [63].

The yields of most of the compounds present in cigarette smoke (whole smoke and gas phase) feature a continuous increase from puff to puff which can be clearly seen for e.g. NO, acetaldehyde, acetone, and toluene. This is due to a gradual reduction in tobacco length as the cigarette is consumed, which results in a decrease in filtration by the tobacco rod for products in the particulate phase of smoke, or a decrease in air dilution and outward gaseous diffusion for products in the gas phase [112, 358]. However, a second puff-by-puff behaviour was also observed in which the first puff exhibits the highest yield, followed by smaller yields in the

second puff and then the usual increase with puff number mentioned before. Species observed following this behaviour are mainly unsaturated hydrocarbons. Here (Fig. 45) butadiene and, less distinct, isoprene show this puff profile.

The reason for this behaviour must be related to the initial lighting of the cigarette before the first puff is taken. During lighting the tobacco is heated from ambient temperature, resulting in a much higher temperature increase and heating rate than is the case for the subsequent puffs, since the inter-puff smoulder temperature is around 600 °C to 700 °C. Thus, tobacco closest to the burning zone is preheated for all puffs except the first one.

This trend attracts special interest, especially regarding the highly toxic smoke constituents butadiene and isoprene, when assuming that human smokers inhale differently during the first puff. It is possible that many smokers inhale the first puff longer and deeper in order to light the cigarette properly. It is also possible that some human smokers don't inhale the first puff at all but keep to the "mouth" phase only. An interesting point though. Future smoking behaviour and retention studies could clarify this point.

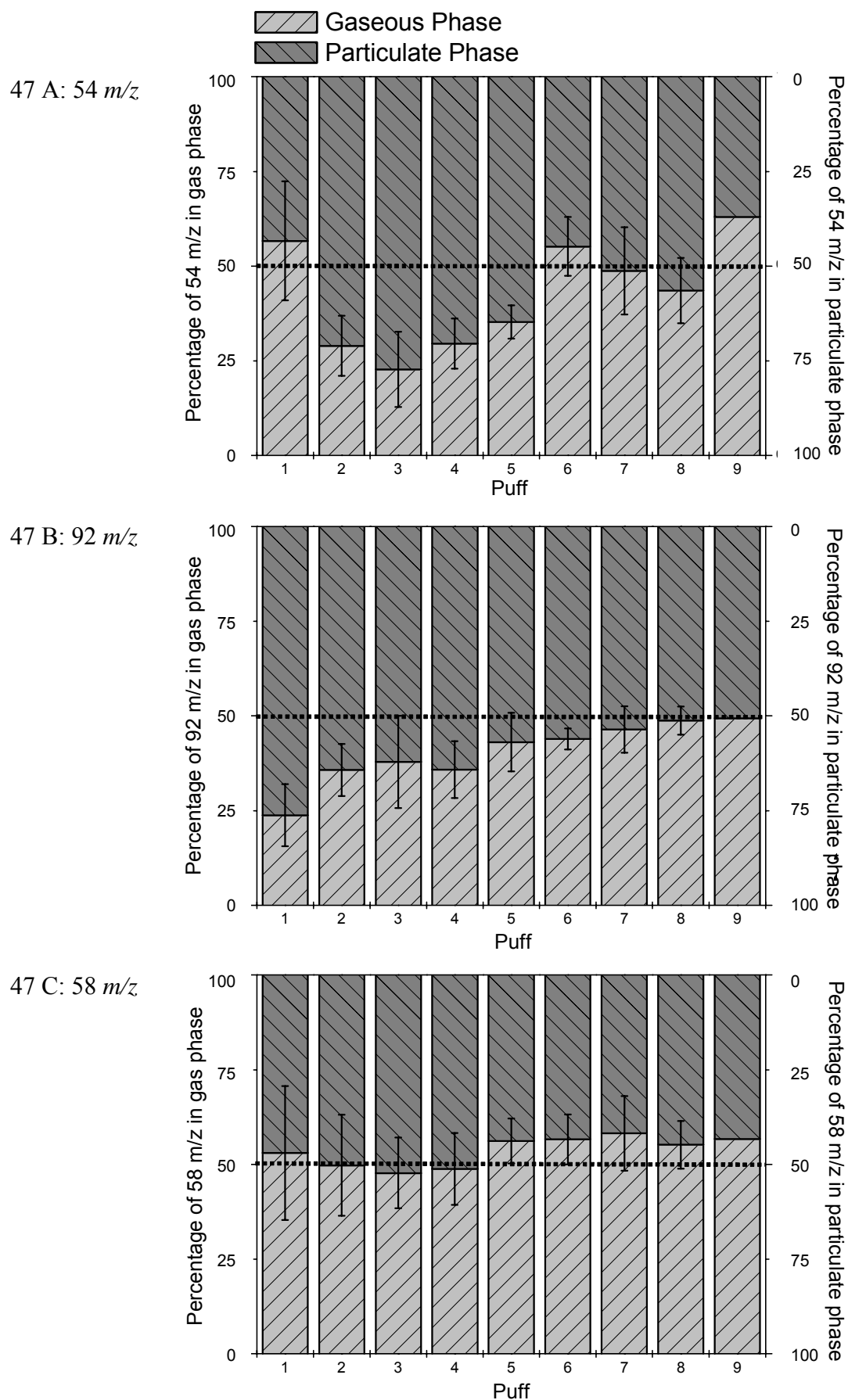
Similar high levels in the first puff have also been reported for formaldehyde and ethylene [170, 171, 314, 320] as well as benzo[a]pyrene [325, 359]. In doing so, formaldehyde and benzo[a]pyrene are considered as some of the most hazardous species in smoke. Therefore, formaldehyde seems to feature a unique smoking profile since it is the only oxygen-containing compound following this behaviour. All other species having high yields in the first puff are unsaturated or aromatic hydrocarbons. Vilcins [314] has reported that the manner of lighting a cigarette can sometimes cause the yields in the first puff to be higher or lower than expected. Li et al. [359] showed that the high levels of benzo[a]pyrene in the first puff were dependent on the method of lighting the cigarette. They showed that lighting the cigarette with a butane lighter (yellow flame) or match resulted in very high concentrations in the first puff whereas a torch lighter (blue flame) and electric lighter resulted in quite low levels of benzo[a]pyrene in the first puff. They deduced that the excess benzo[a]pyrene in the first puff with a yellow flame or match was from soot particles covered with polycyclic aromatic hydrocarbons, produced in the incomplete combustion of the yellow lighting flame. Furthermore, Parrish and Harward [319] compared butane lighters, electric lighters, and matches and did not find significant changes with respect to the high levels of formaldehyde in the first puff. In this work lighting was only performed by using an electric lighter.

When subtracting the gas phase from the whole smoke, conclusions can be drawn about the ratio of compounds in the vapour phase and the particulate phase for the experimental set-up

applied. Regarding the hazardous target compounds being focussed on in this study, three slightly different behaviours can be observed, as shown in Figures 47 A, B, and C.

Substances like acetone (Fig. 47 C) and, to a lesser extent, acetaldehyde, occur in both phases in equal amounts. Within the accuracy of measurement, no difference in phase affiliation can be observed between successive puffs. In contrast, toluene (Fig. 47 B) and benzene feature higher yields in the particulate phase in the first puff, and for the later puffs the ratio gradually shifts towards being balanced between both phases. The reasons for this behaviour are similar to the ones described earlier for the increasing yields with puff number. Reduction of cigarette length as the cigarette is smoked results in a smaller contact surface and residence time in the shorter tobacco rod and hence less condensation into aerosol particles. Less cooling of smoke in a shorter cigarette may also contribute to this. However, a decrease in dilution should support condensation, but apparently, plays a minor role for these substances. The same holds for the reduced filtration effect of the unburnt tobacco for particles. Again, compounds which featured high yields in the first puff, such as butadiene and isoprene, differ (Figure 47 A), since the fraction in the gas phase is higher for the first puff. In the second puff the ratio is shifted towards the particulate phase, followed by a rising of the gas phase fraction for the subsequent puffs. Consequently it seems as if the high yield in the first puff is predominantly caused by gaseous butadiene and isoprene. From the second puff onwards the typical behaviour can be observed again.

In general, by looking only at the smoking puffs without cleaning puffs the puff-by-puff partition looks similar for all compounds but is shifted towards the particulate phase (not shown here) because the cleaning puffs influence the vapour phase more strongly than the particulate phase.



Figures 47 A, B, and C: Puff-resolved ratios of the compounds butadiene (54  $m/z$ ; Fig. 47 A), toluene (92  $m/z$ ; Fig. 47 B), and acetone (58  $m/z$ ; 47 C) in the vapour phase and the particulate phase of the 2R4F cigarette

#### 4.4.3.5. Qualitative evaluation

The different characters of the first and second puff can also be examined by a difference spectrum in which the summed spectrum of the second puff is subtracted from the summed spectrum of the first puff, demonstrated for the 2R4F research cigarette in Figure 48.

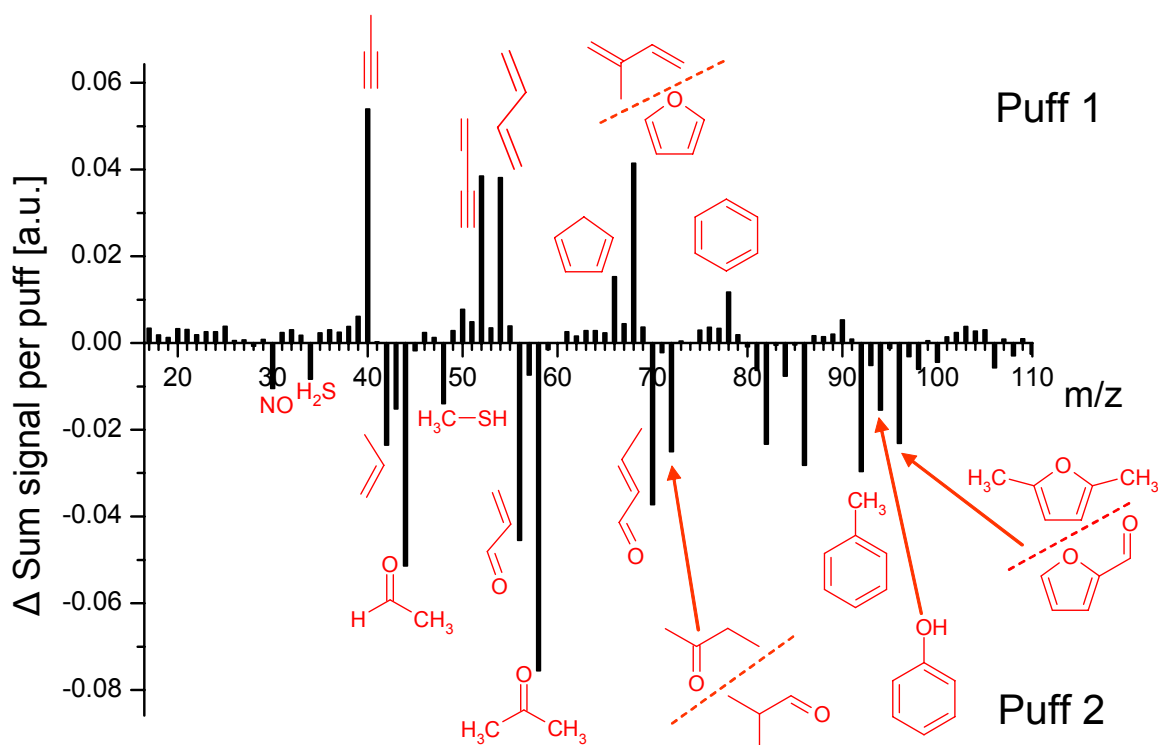


Figure 48: Difference spectrum of the first and second puff of the 2R4F research cigarette

In so doing, positive signal intensities account for higher amounts in the first puff and *vice versa*. The spectrum illustrates that the first puff is dominated by unsaturated species, mainly 40  $m/z$  (propyne), 52  $m/z$  (1-buten-3-yne), 54  $m/z$  (mainly butadiene), and 66  $m/z$  (cyclopentadiene). In contrast to this, the second puff is dominated by oxygen-containing species such as carbonyls, e.g. 44  $m/z$  (acetaldehyde), 56  $m/z$  (mainly acrolein), 58  $m/z$  (acetone), and 70  $m/z$  (mainly crotonaldehyde) as well as 94  $m/z$  (phenol), 30  $m/z$  (NO), and the sulphurous components 34  $m/z$  ( $H_2S$ ) and 48  $m/z$  (methanethiol). The only obvious exceptions are 92  $m/z$  (toluene) and 42  $m/z$  (propene).

The origin of mass 68  $m/z$  usually can be attributed to two isobaric compounds, isoprene and furan, both identified in cigarette smoke [55, 265]. Baker [14] and Hoffmann [3] reported that the yield of isoprene in plain non-filter cigarettes is approximately five to ten times higher than for furan. In Figure 48 it can be seen that 68  $m/z$  is much more abundant in the first puff.

Therefore it is assumed that the main proportion of 68  $m/z$  in fact originates from the unsaturated hydrocarbon isoprene, rather than the oxygen-containing furan. Variations in composition between other successive puffs (2  $\rightarrow$  3; 3  $\rightarrow$  4; etc.) could not be observed by this analytical method. Therefore the Fisher-Value and the PCA approach were applied. Calculating the pairwise (between two successive puffs) and the overall Fisher-Values (between all puffs) of the nine puffs of the 2R4F cigarette after normalisation to total ion signal led to the following results, which are illustrated for whole smoke in the Table 28. In this table the masses with the twenty-five highest Fisher-Values are listed in descending order.

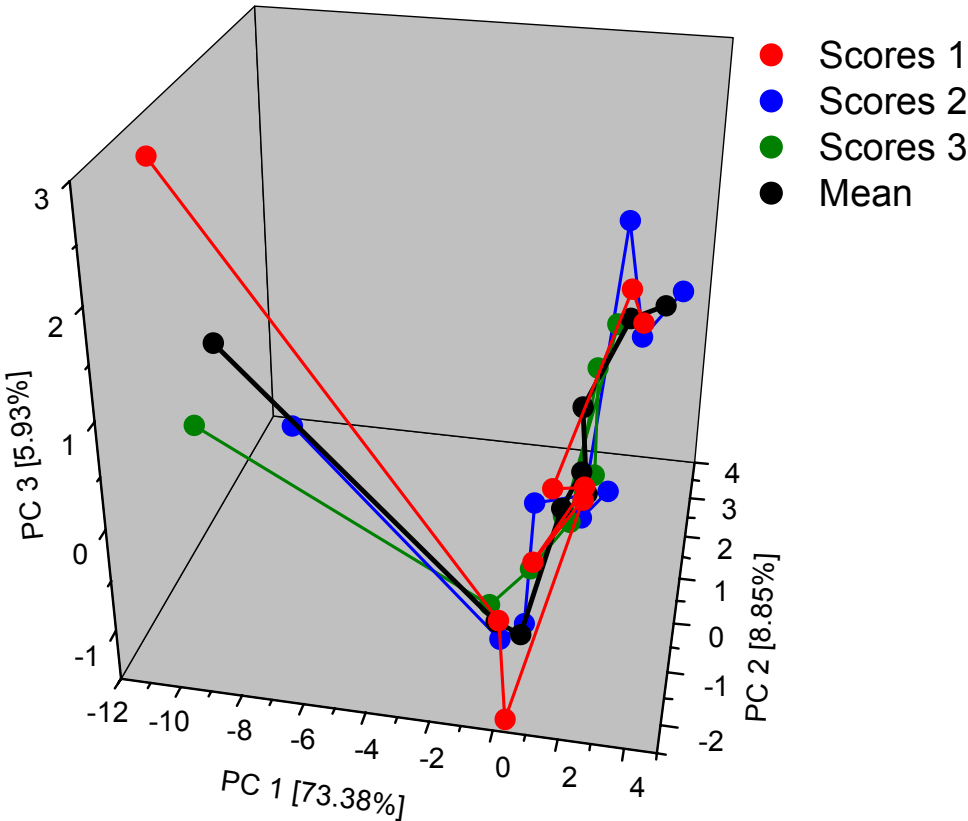
Table 28: Pairwise and overall Fisher-Values for the puff-resolved smoking of the 2R4F cigarette

	Puff 1 $\rightarrow$ 2		Puff 2 $\rightarrow$ 3		Puff 3 $\rightarrow$ 4		Puff 4 $\rightarrow$ 5		Puff 5 $\rightarrow$ 6	
	$m/z$	FV <sub>1<math>\rightarrow</math>2</sub>	$m/z$	FV <sub>2<math>\rightarrow</math>3</sub>	$m/z$	FV <sub>3<math>\rightarrow</math>4</sub>	$m/z$	FV <sub>4<math>\rightarrow</math>5</sub>	$m/z$	FV <sub>5<math>\rightarrow</math>6</sub>
1	58	2.108	58	0.094	30	0.294	68	1.09	68	1.199
2	70	1.766	44	0.067	44	0.235	30	0.682	30	0.227
3	40	1.719	86	0.043	58	0.099	44	0.221	69	0.036
4	54	1.409	54	0.015	56	0.033	78	0.051	58	0.032
5	56	1.374	40	0.014	86	0.028	69	0.025	96	0.018
6	52	1.213	103	0.014	78	0.027	67	0.023	40	0.014
7	82	0.958	70	0.013	42	0.023	96	0.022	67	0.012
8	92	0.926	105	0.013	43	0.02	48	0.015	162	0.011
9	96	0.891	72	0.013	142	0.014	58	0.011	93	0.011
10	72	0.741	106	0.011	82	0.012	138	0.011	124	0.011
11	68	0.673	138	0.011	148	0.01	82	0.011	98	0.01
12	86	0.65	43	0.008	118	0.01	128	0.009	54	0.01
13	48	0.357	130	0.008	48	0.01	98	0.008	136	0.009
14	66	0.34	116	0.006	92	0.008	120	0.007	82	0.009
15	94	0.265	118	0.006	102	0.008	163	0.007	79	0.008
16	44	0.225	115	0.006	72	0.007	17	0.006	120	0.006
17	34	0.159	48	0.005	67	0.006	40	0.006	146	0.006
18	43	0.158	119	0.005	39	0.006	132	0.005	128	0.006
19	78	0.138	52	0.005	112	0.005	105	0.005	138	0.004
20	106	0.11	165	0.005	17	0.005	50	0.005	72	0.004
21	50	0.088	135	0.005	136	0.005	34	0.005	86	0.004
22	39	0.079	132	0.004	50	0.005	119	0.005	117	0.003
23	93	0.065	117	0.004	134	0.004	70	0.005	70	0.003
24	30	0.056	126	0.004	139	0.004	79	0.005	154	0.003
25	146	0.049	78	0.004	94	0.004	42	0.004	78	0.002

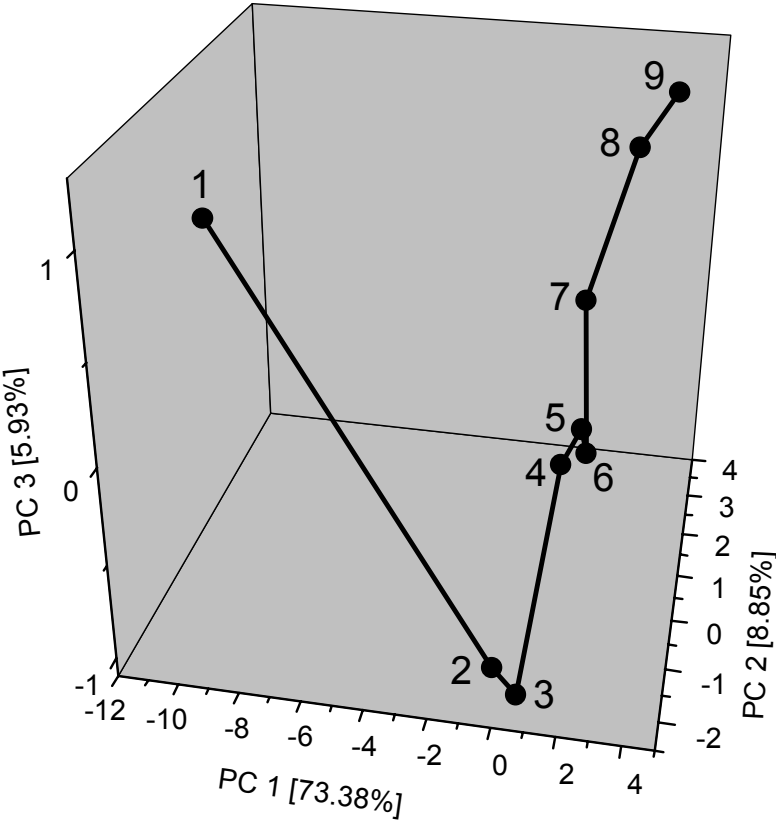
	Puff 6 → 7		Puff 7 → 8		Puff 8 → 9		Puff 1 → 9	
	<i>m/z</i>	FV <sub>6→7</sub>	<i>m/z</i>	FV <sub>7→8</sub>	<i>m/z</i>	FV <sub>8→9</sub>	<i>m/z</i>	FV <sub>1→9</sub>
1	68	0.125	30	0.236	42	0.19	58	0.028
2	30	0.099	44	0.18	92	0.178	44	0.024
3	54	0.075	48	0.055	106	0.147	30	0.014
4	40	0.064	92	0.043	82	0.135	56	0.011
5	106	0.039	34	0.038	68	0.075	70	0.01
6	42	0.02	42	0.032	70	0.068	86	0.008
7	66	0.019	58	0.028	96	0.065	40	0.008
8	78	0.015	54	0.022	86	0.06	92	0.006
9	52	0.014	130	0.018	94	0.06	54	0.006
10	84	0.011	52	0.017	44	0.051	52	0.006
11	104	0.011	40	0.016	56	0.05	68	0.006
12	67	0.011	118	0.016	84	0.041	82	0.006
13	162	0.01	117	0.015	66	0.031	72	0.005
14	86	0.009	128	0.015	58	0.029	96	0.005
15	122	0.008	142	0.012	93	0.016	48	0.003
16	70	0.008	94	0.012	74	0.008	43	0.002
17	94	0.008	112	0.011	69	0.008	42	0.002
18	79	0.008	67	0.01	67	0.008	94	0.002
19	44	0.008	56	0.009	105	0.008	34	0.002
20	116	0.008	136	0.009	48	0.007	106	0.002
21	56	0.007	119	0.007	119	0.006	66	0.001
22	153	0.006	162	0.006	103	0.005	50	0.0009
23	96	0.006	104	0.006	59	0.004	78	0.0008
24	82	0.005	103	0.006	17	0.003	93	0.0008
25	140	0.005	43	0.006	116	0.002	39	0.0007

As expected, the pair wise Fisher-Values between the first and the second puff reach the highest values, confirming the unique difference between both successive puffs. In so doing the same compounds stand out as were determined by the difference spectrum, mainly unsaturated hydrocarbons and carbonyl substances. For the later puffs only the first few masses attain reasonably high values. The rest are low or of no significance. Throughout all puffs the same known constituents play the most important role but, for instance, 30 *m/z* (NO) and 68 *m/z* (isoprene/furan) only gain importance from the third puff onward. The overall Fisher-Values show the substances for which it should be best to find out the differences and variations between all puffs in the smoking process. These 25 masses were used to perform a Principal Component Analysis. The three-dimensional illustrations of the first three Principal Components show that the nine puffs can be clearly separated (Fig. 49 A and B).

49 A:



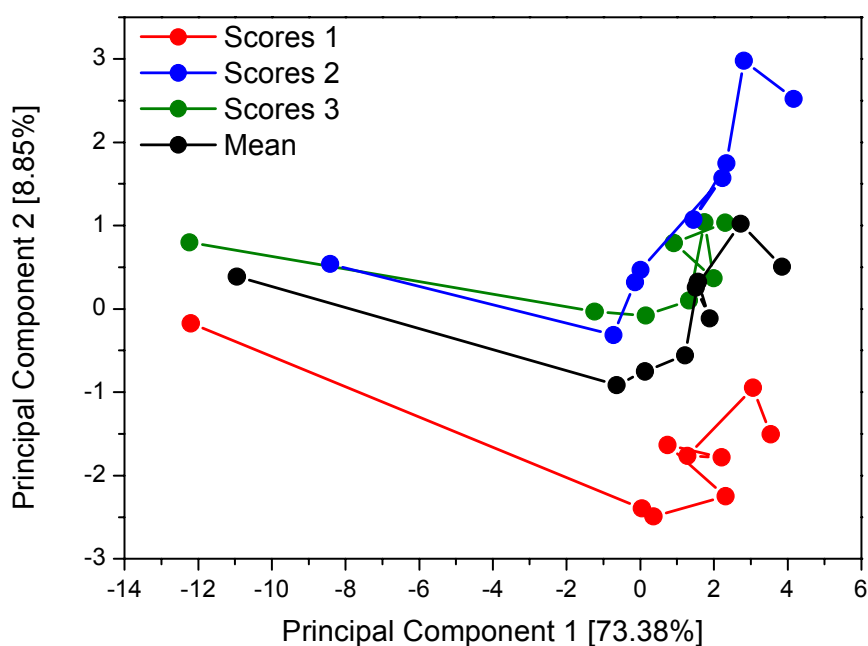
49 B:



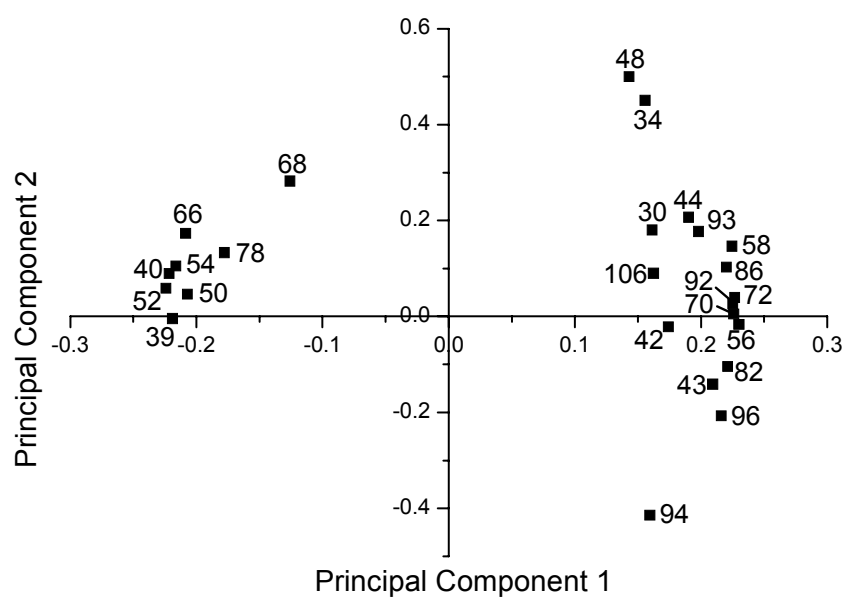
Figures 49 A and B: Fig. 49 A illustrates the score-plots of the three individual measurements and the mean of the scores. Fig. 49 B shows the mean only and the assigned puffs

The illustration on top (Fig. 49 A) includes the scores of the three individual measurements as well as the mean of the three individual scores. The one at the bottom (Fig. 49 B) contains the mean values and the puff numbers. Again, the first puff is unique and clearly separated from the other puffs. In addition, the following puffs are also separated and the puffs in the middle of the smoking process, from puff four to seven, seem to be similar. The loading plot describes the influence of the single masses on the separation of the puffs. Therefore the corresponding two-dimensional score-plots and loading-plots of the first and the second (Fig. 50 A and B), as well as the first and the third Principal Components are shown (Fig. 50 C and D).

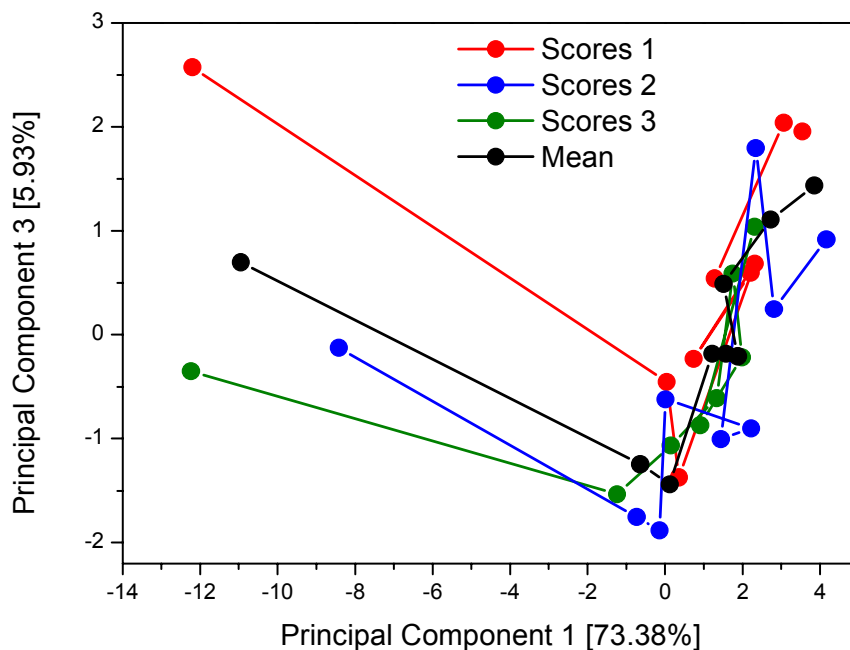
50 A:



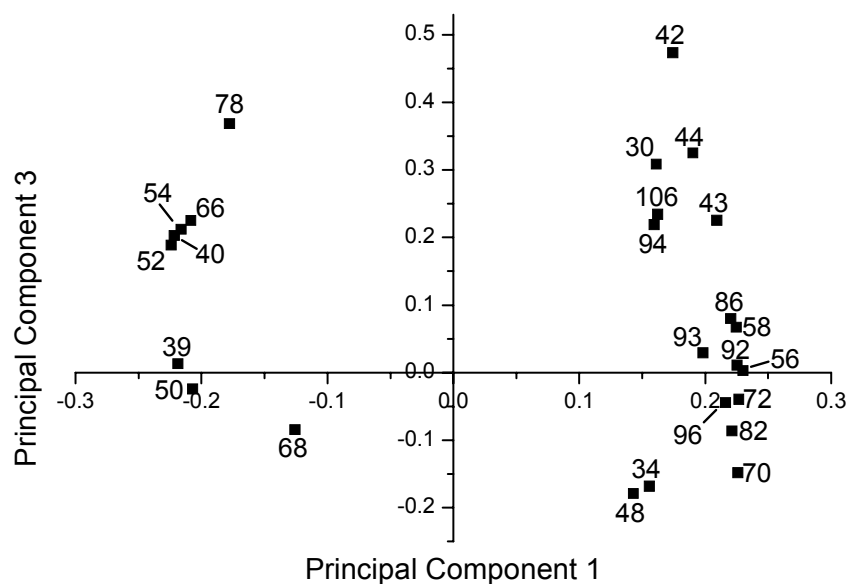
50 B:



50 C:



50 D:

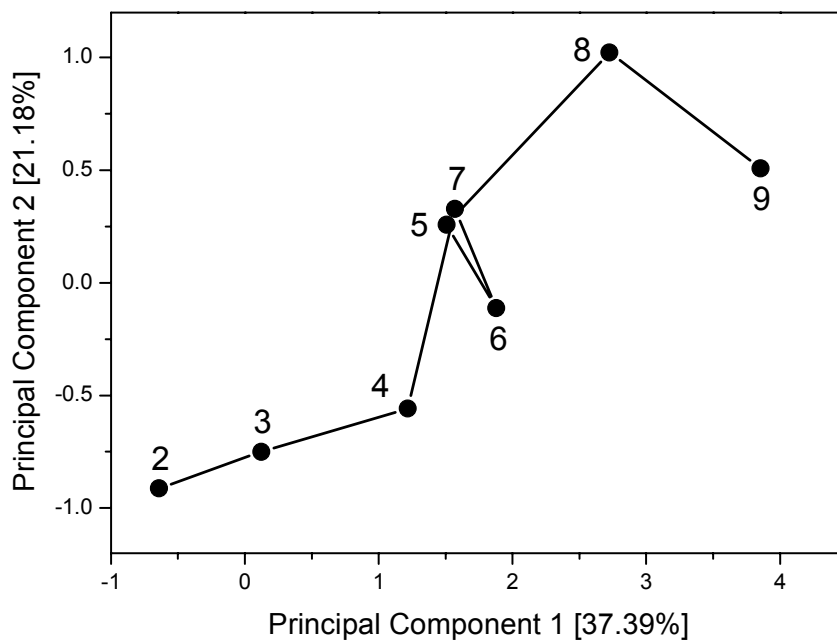


Figures 50 A to D: Score-plots and loading-plots of first and second (Fig. 50 A and B) and first and third (Fig. 50 C and D) principal components of the 25 Fisher-Values from the first to the ninth puff

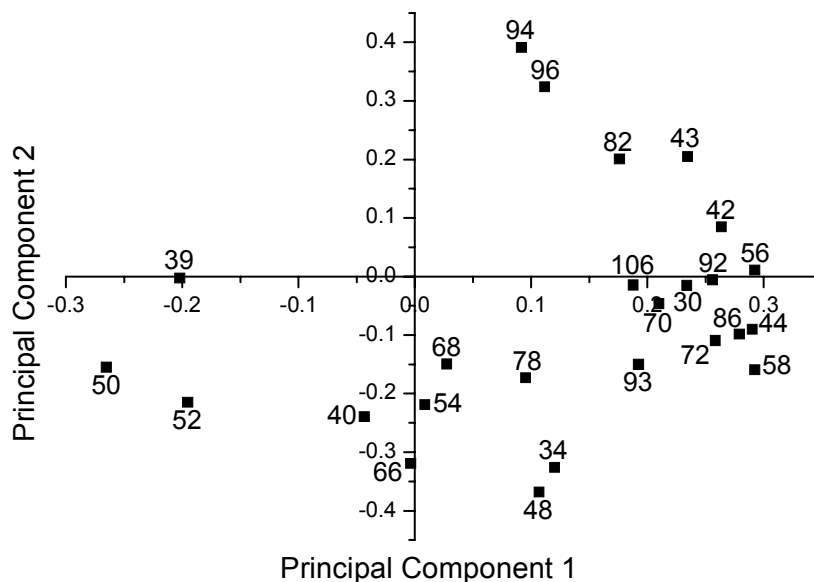
The results confirm the uniqueness of the first puff. The separation takes place on the first Principal Component (variance 73.38 %) whereas the separation of puffs two to nine occurs on the other two Principal Components but to a much smaller extent. The loading plots are dominated by the unsaturated compounds on the side of the first puff (left) and the oxygen-containing as well as some nitrogen-containing species on the right.  $\text{H}_2\text{S}$  (34  $m/z$ ) and methanethiol (48  $m/z$ ) also cluster together.

Apart from the extraordinary first puff, a small but ascertainable separation of puff two to puff nine could be observed. Therefore a further PCA was carried out whereby the first puff was excluded. In Figures 51 A to D the two-dimensional score-plots and loading-plots of the first three Principal Components containing the mean of the three measurements' scores are presented.

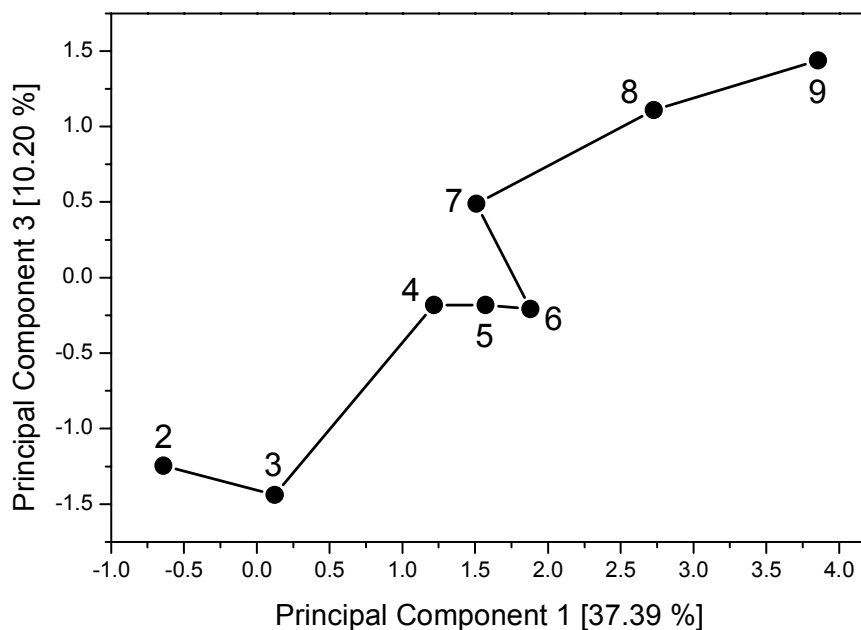
51 A:



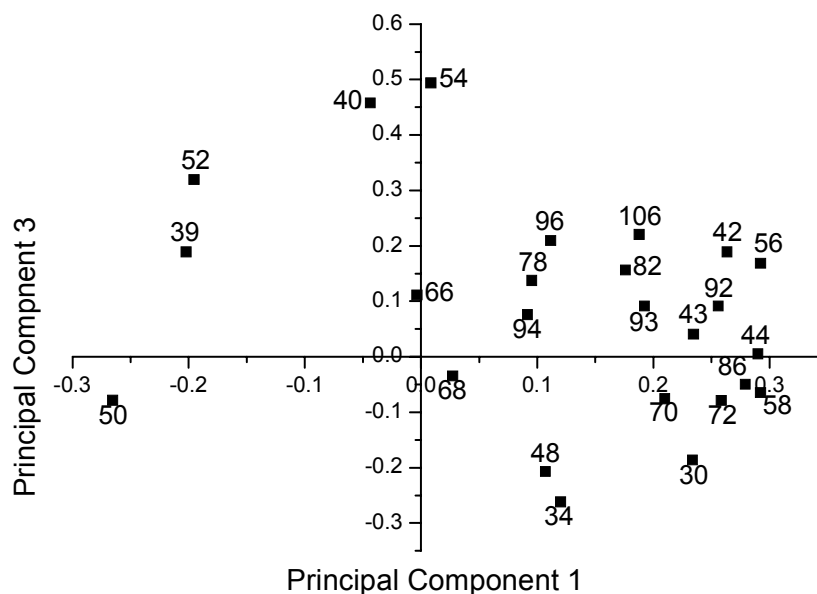
51 B:



51 C:



51 D:



Figures 51 A to D: Score-plots and loading-plots of first and second (Fig. 51 A and B) and first and third (Fig. 51 C and D) principal components of the 25 Fisher-Values from the second to the ninth puff

The quality of the separation is lower. However, the overall pattern of the smoke composition changes whereas the puffs in the middle are similar. Earlier puffs are stronger influenced by compounds which already influenced the first puff. For the later puffs the oxygen-containing substances apparently play a greater role. Sulphur compounds always cluster together but cannot be assigned to any specific puffs. Finally, it seems as if during the smoking cycle of a complete cigarette the influence of alkenes, alkynes etc. on the smoke composition weakens and, simultaneously, the influence of carbonyl compounds increases. However, single key

compounds which are related to specific puffs are not identified. This indicates that the overall change of the pattern is responsible for the observable trend.

#### **4.4.4. Different tobacco types compared to the 2R4F cigarette**

After characterising the smoking process in general by means of the 2R4F research cigarette the influence of individual tobacco types on the smoke composition was investigated. In so doing, the four single tobacco types Virginia, Oriental, Burley, and Maryland were investigated by using the same experimental set-up and calibration gases as for the analysis of the 2R4F research cigarette.

Smoking of the cigarettes resulted in varying puff numbers for each cigarette type. Maryland and Burley tobacco produced the lowest puff numbers out of three measurements, namely 5.0 and 6.0 puffs, whereas the Oriental tobacco cigarette gave 11.0 puffs and the Virginia tobacco cigarette resulted in 8.3 puffs, all for whole smoke. The following evaluation and discussion focuses on whole smoke measurements since the results of the gas phase measurements did not give any additional information. However, the total and the puff-by-puff resolved yields of the vapour phase measurements are illustrated in the Appendix.

Apart from the tobacco content, these five cigarette types have some small differences in design parameters such as filter ventilation and paper permeability, which were displayed in Table 23. These can cause small differences to the yields of smoke constituents. An approach to minimise effects caused by unequal total smoke formation in order to enable a comparison between these five cigarette types' total yields is to normalise the data to TPM or tar [271, 360]. This means that the signal intensity is divided by the TPM in order to make it independent of particulate matter yield, resulting in a dimensionless scaling for the quantitative values. In this context it is believed that the human smoker unconsciously controls the personal puff behaviour by means of the TPM uptake per puff because a high amount of TPM should be associated with high concentrations of stimulating substances in smoke but also with a harsher aroma [361]. Since this work deals with puff-resolved comparisons, the TPM values for every puff are required for normalisation. These data are not routinely determined. However, the results presented of the highly varying puff concentrations of many smoke constituents leads to the assumption that the TPM values of the individual puffs will differ as well. Therefore, gravimetric measurements of the TPM from the

single puffs of all cigarette types were carried out. In so doing the cigarettes were smoked in a conventional Borgwaldt smoking machine and every Cambridge pad was replaced and weighted after every puff by using an analytical balance (Sartorius AG, model R200D). Like in the smoke measurements, three replicates were performed. The puff resolved TPM yields including standard deviation of all four single tobacco type cigarettes and the 2R4F cigarette are illustrated in Figure 52 and are listed in the Appendix.

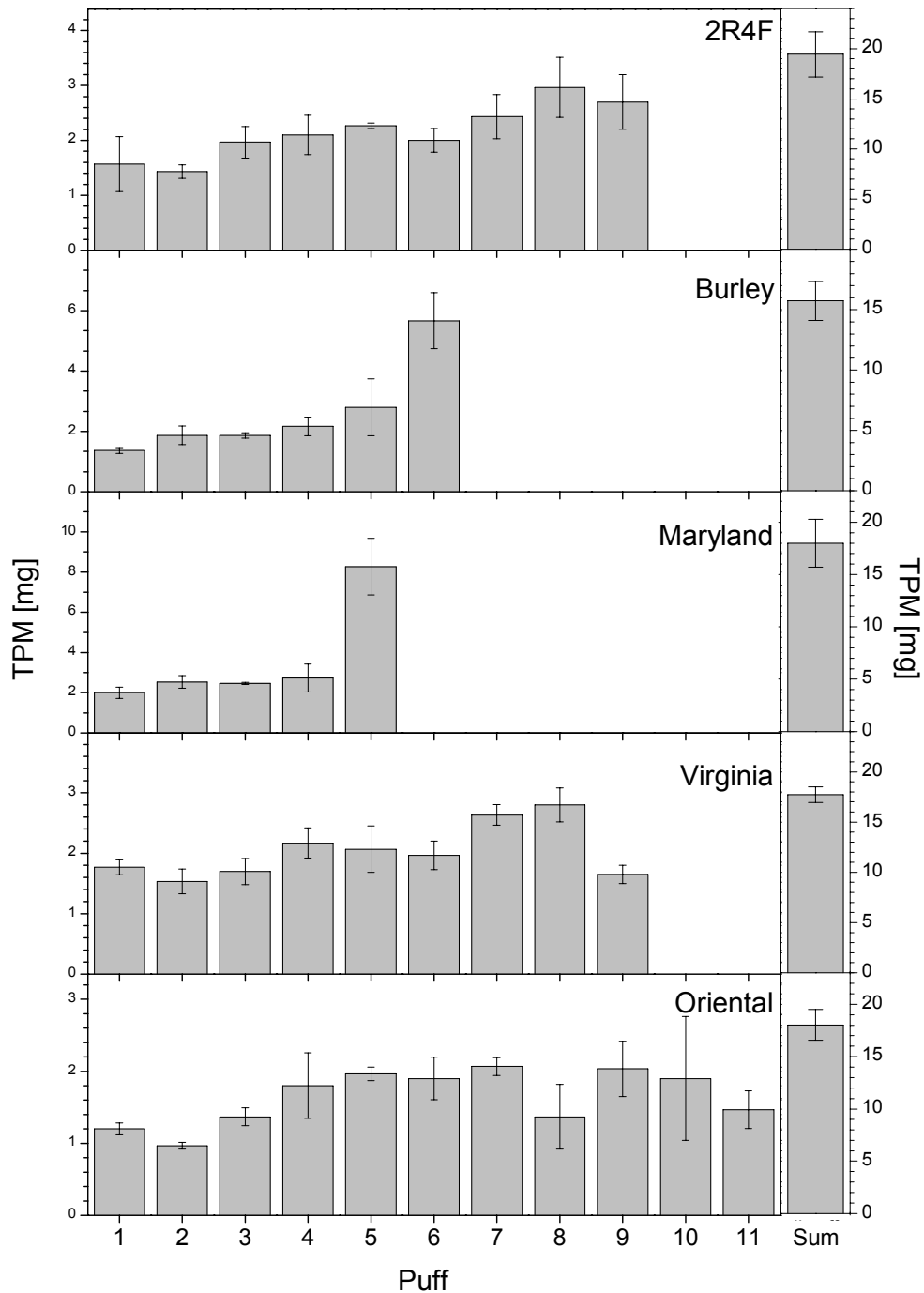
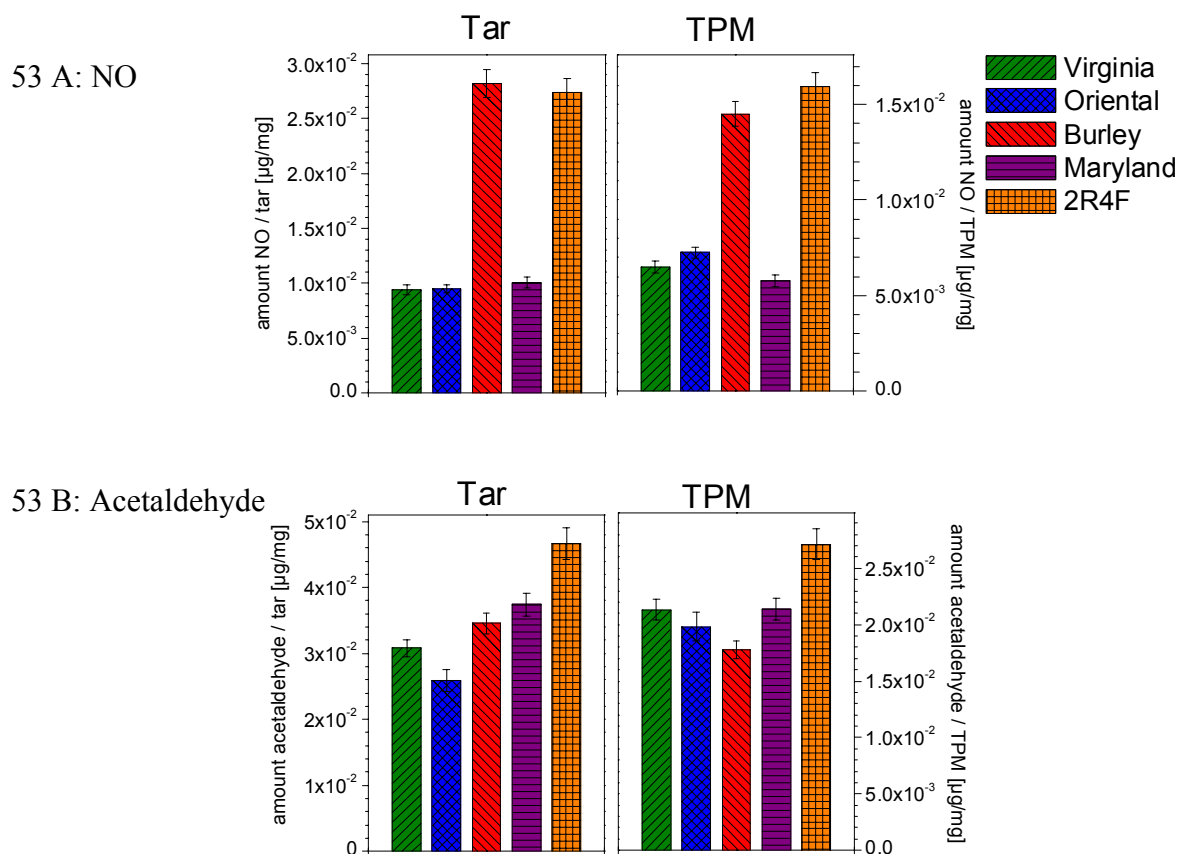


Figure 52: Puff-by-puff resolved TPM yields of the four single tobacco types Oriental, Burley, Maryland, and Virginia as well as the 2R4F research cigarette

Roughly speaking the total TPM is similar for the five different cigarettes but the individual puff profiles differ tremendously. The 2R4F cigarette features a slow increase in TPM from puff to puff similar to the Virginia and the Oriental tobacco. It also seems that the yield in the last puff decreases again for these three types, which is more pronounced for the Virginia. In contrast, Burley and Marland, the two air-cured tobaccos, first show a slight increase in TPM yield but the last puff is extraordinary high.

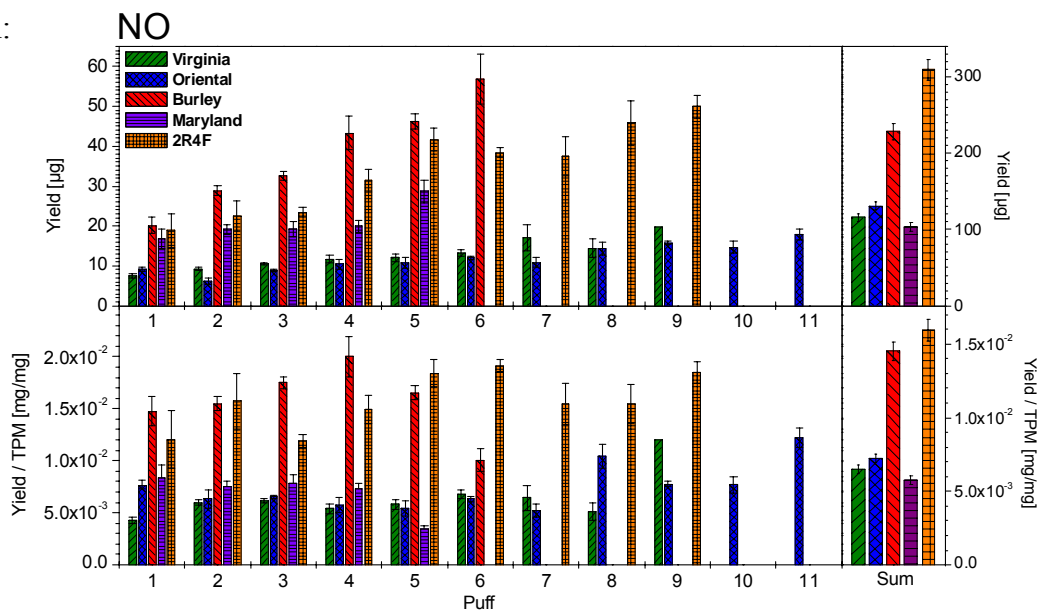
The set-up used is a simple approach but does not necessarily maintain strict ISO conditions. In contrast, particulate phase yields printed on cigarette packs, which are determined under ISO conditions by the cigarette manufacturers, refer to tar, i.e. TPM minus the water and nicotine content. On the other hand, the available equipment in the framework of this work does not enable the measurement of tar but TPM. Therefore normalisation of the total yields was carried out for both, the self-measured TPM values and the tar values reported by the cigarette manufacturer in order to compare both approaches and to evaluate if it is useful to continue with the self-measured TPM values. It turned out that the absolute figures of course differed due to the H<sub>2</sub>O and nicotine content, but the ratios of the different tobacco types towards each other were rather similar and revealed the same trends which is demonstrated for two examples, NO and acetaldehyde, in Figure 53 A and B.



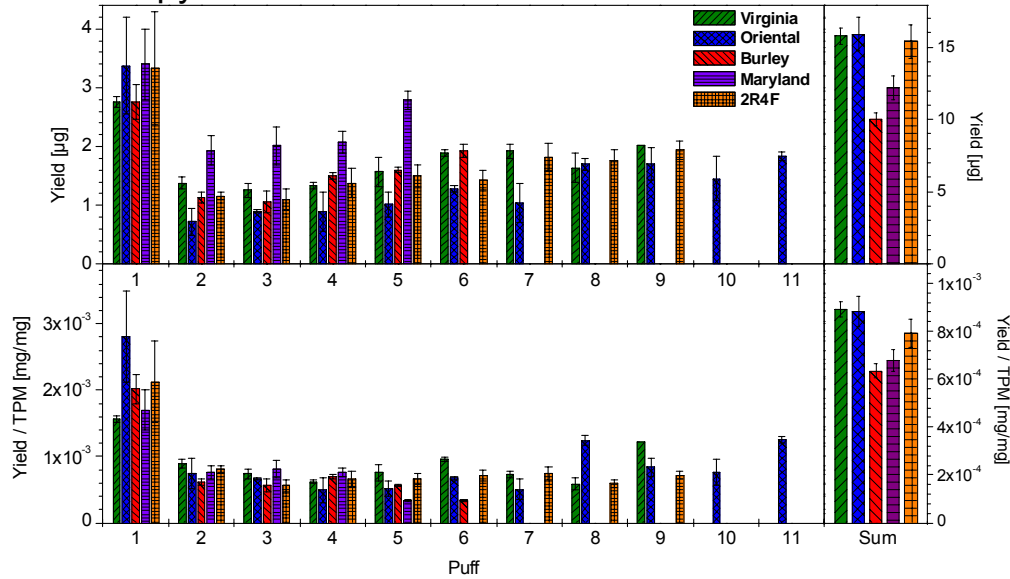
Figures 53 A and B: Comparison of two normalisation procedures shown for NO and acetaldehyde. On the left the total yields were divided by total tar and on the right by total TPM respectively

This proves that the simple approach of weighing is sufficient for the normalisation procedure, particularly because the weighing conditions were kept identical for all cigarette types and encouraged using the puff-resolved TPM yields for the puff-by-puff normalisation. Subsequently, the following characterisation and comparison of the four single tobacco types and the 2R4F cigarette are based on two approaches. On the one hand the absolute puff yields, delivered under ISO smoking conditions, are illustrated. On the other hand, these puff yields are normalised by means of the corresponding puff-resolved TPM mean values shown in Figure 53. Examination is done by considering all four illustrations, the quantified puff-resolved yields, the quantified total yields, the puff-resolved normalised yields, and the total normalised yields. Besides the hazardous substances which were quantified in the gas phase and whole smoke of the 2R4F, propyne and propene were incorporated in the quantification procedure due to their abnormal puff behaviour, mainly of the first and second puffs. Figures 54 A to J give the puff-by-puff resolved amounts of the quantitatively analysed compounds for each cigarette studied on top, and, normalised to puff-resolved TPM at the bottom. On the right hand side the total as well as normalised total yield of the substances are illustrated.

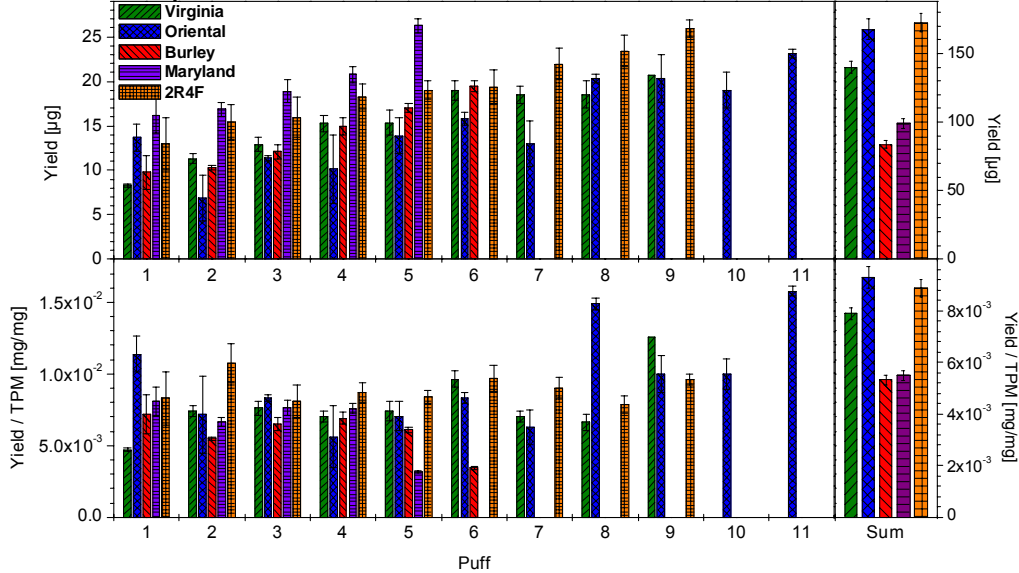
54 A:



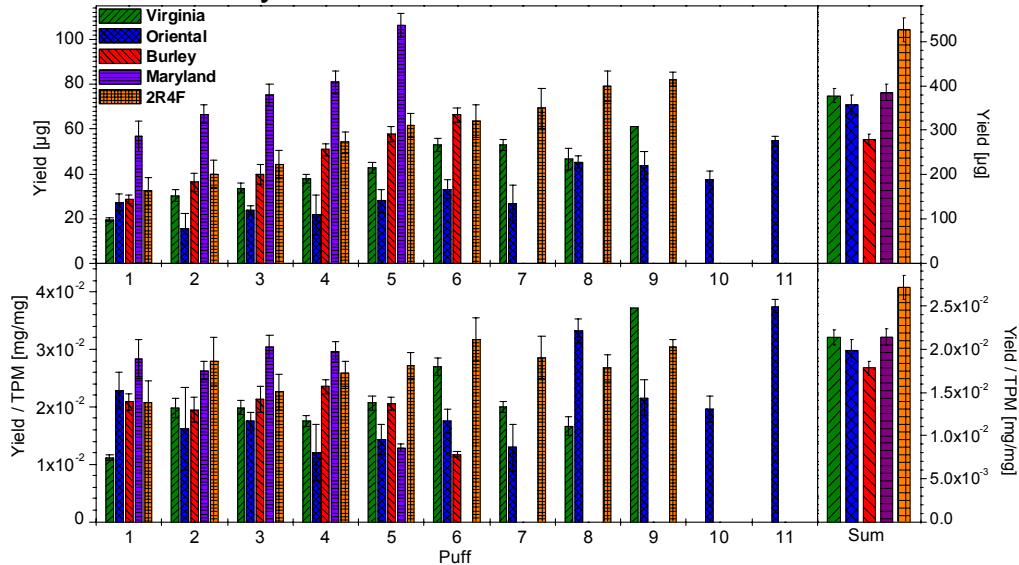
54 B: Propyne



54 C: Propene

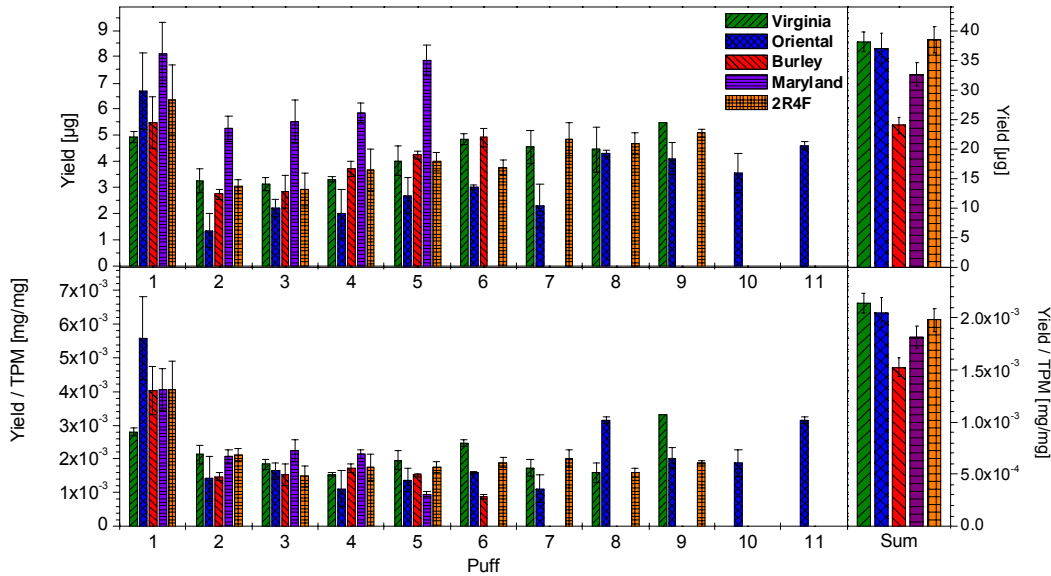


54 D: Acetaldehyde



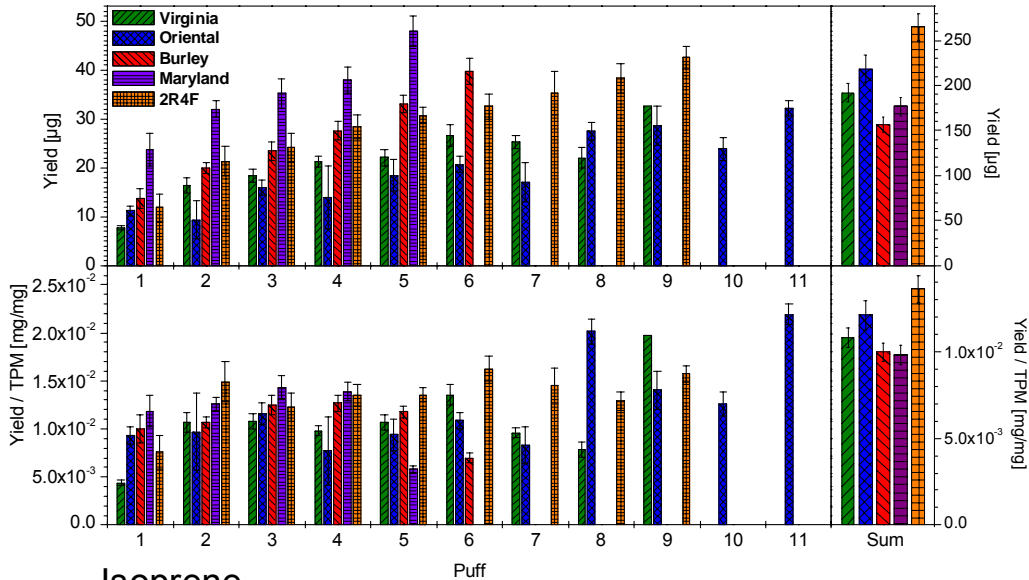
54 E:

Butadiene



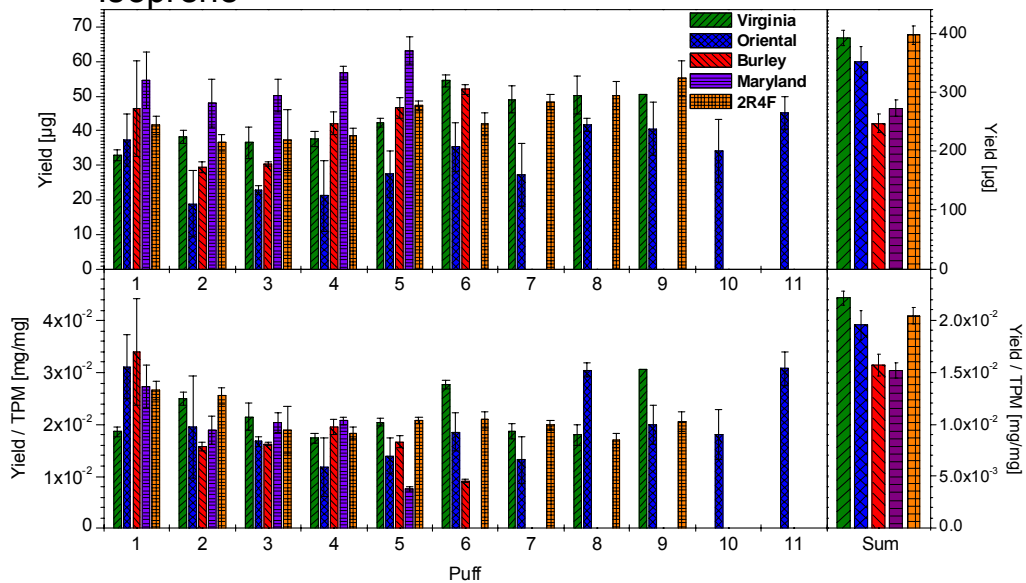
54 F:

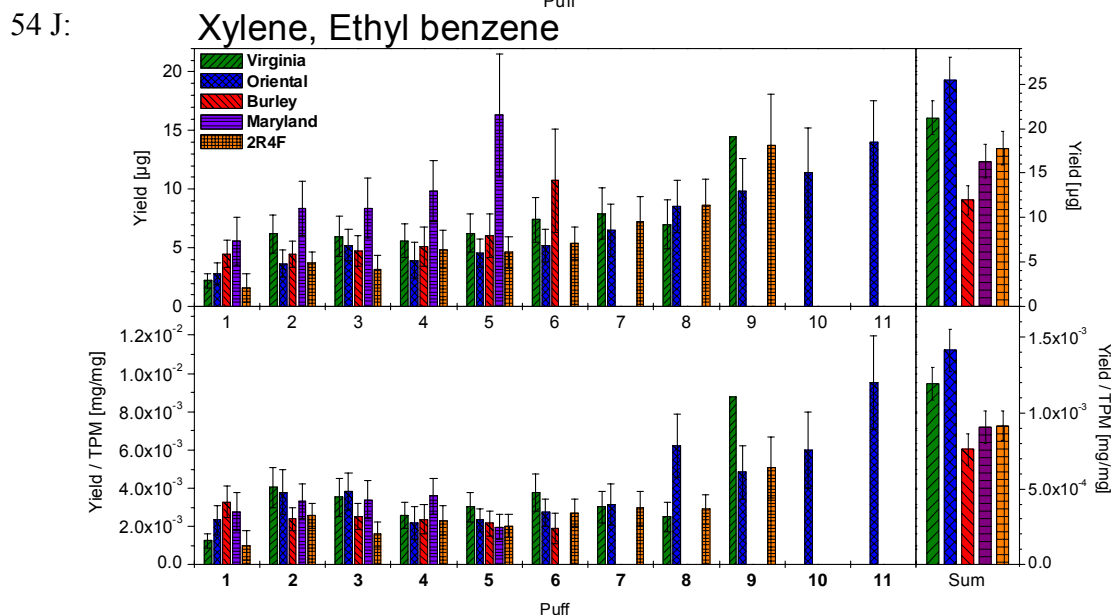
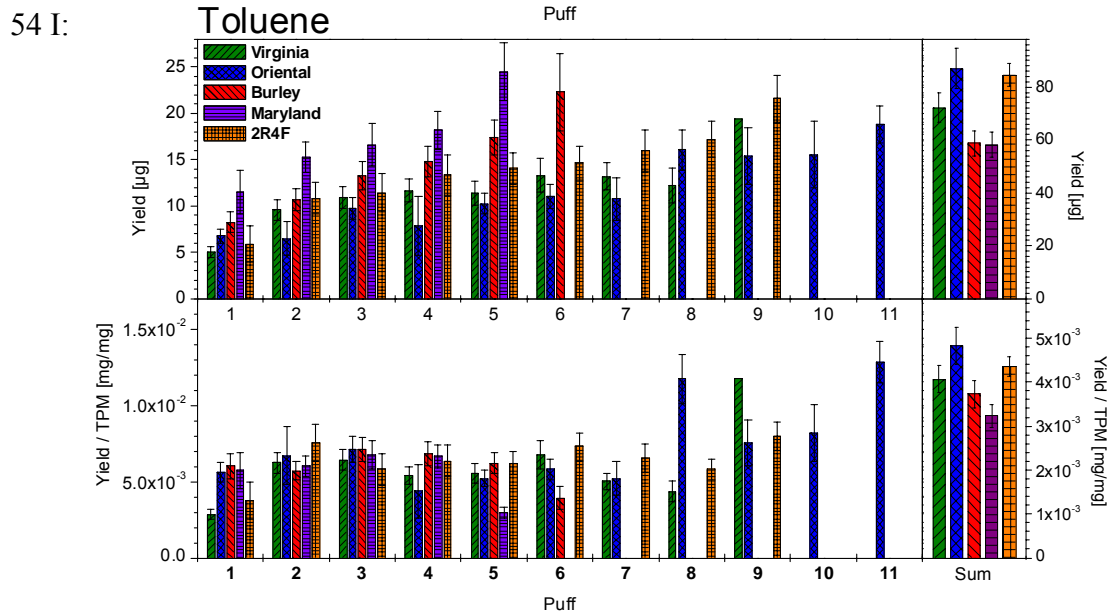
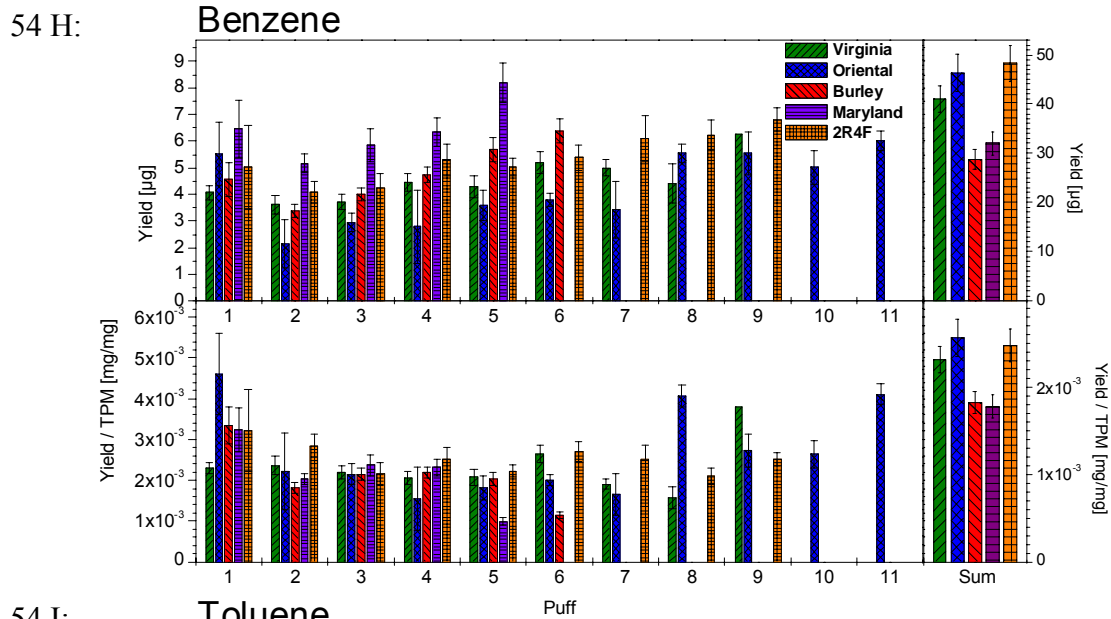
Acetone



54 G:

Isoprene





Figures 54 A to J: Quantitative puff-by-puff resolved and total absolute (top) and normalised (bottom) yields for each cigarette type

In general, all cigarette types feature the same puff behaviour for the different compounds. Apart from the quantitatively analysed substances, qualitative profiles including normalised puff resolved and total yields of a further 23 masses of interest can be found in the Appendix. As discussed in detail for the 2R4F research cigarette, mainly unsaturated compounds such as propyne, butadiene, and to a lower extent, isoprene and benzene are high in the first puff for all tobaccos. The normalised data show the same trend. By means of the example propyne it is good to see that after normalisation all tobaccos exhibit very similar puff intensities without increase from puff to puff, which is also the case for Maryland featuring the highest absolute puff yields. Normalisation even underlines the uniqueness of the first puff. Both air-cured tobaccos, Burley and Maryland are lower in the respective species. The other compounds increase gradually from the first to the last puff. Normalisation retards this rise. Similar general observations can be made for the qualitatively analysed masses in the Appendix. Moreover, Burley is high in nitrogen-containing substances as well as in sulphurous compounds. Unique to this tobacco is the occurrence of a third type of puff-by-puff behaviour for  $\text{NH}_3$  ( $17\ m/z$ ), which is expressed in an exponential increase in yield (Fig. 55).

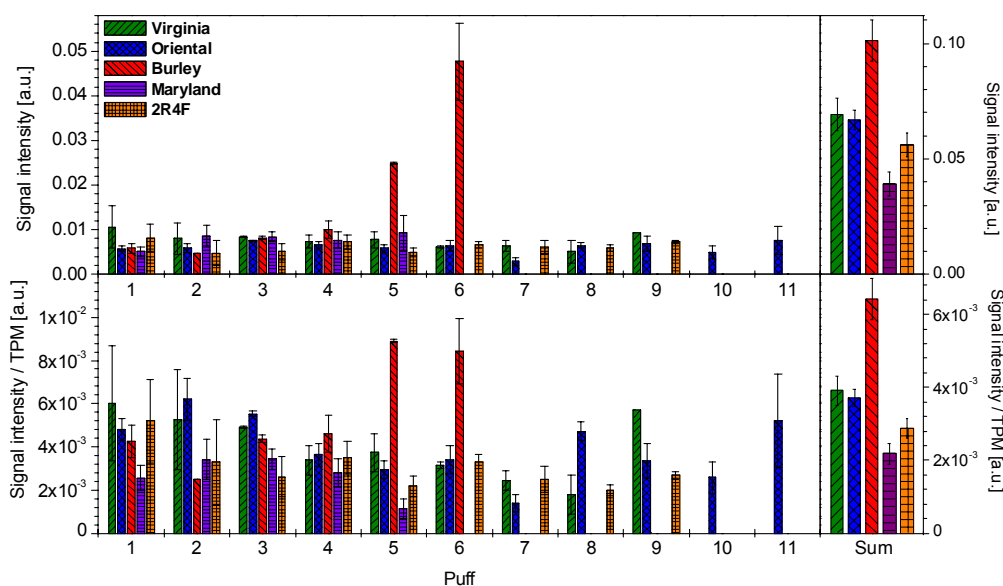
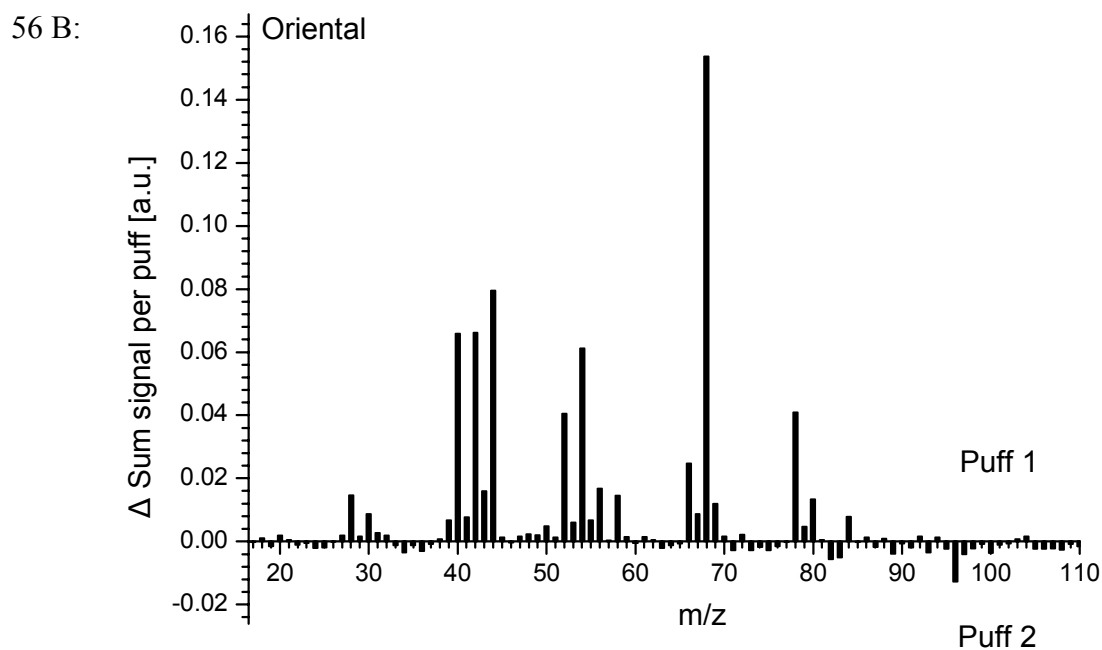
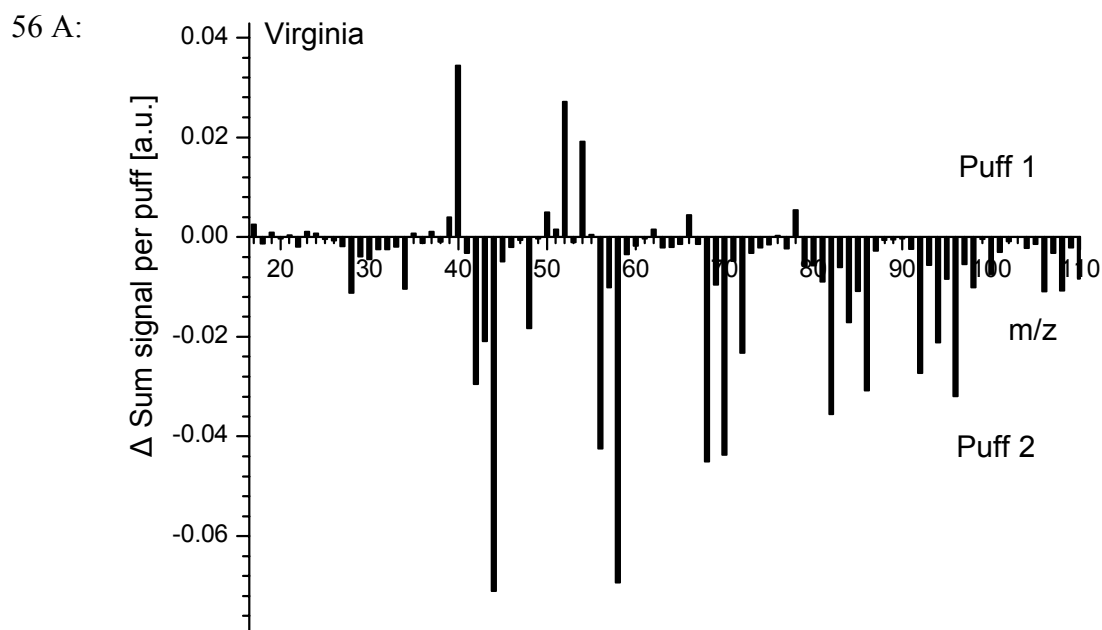
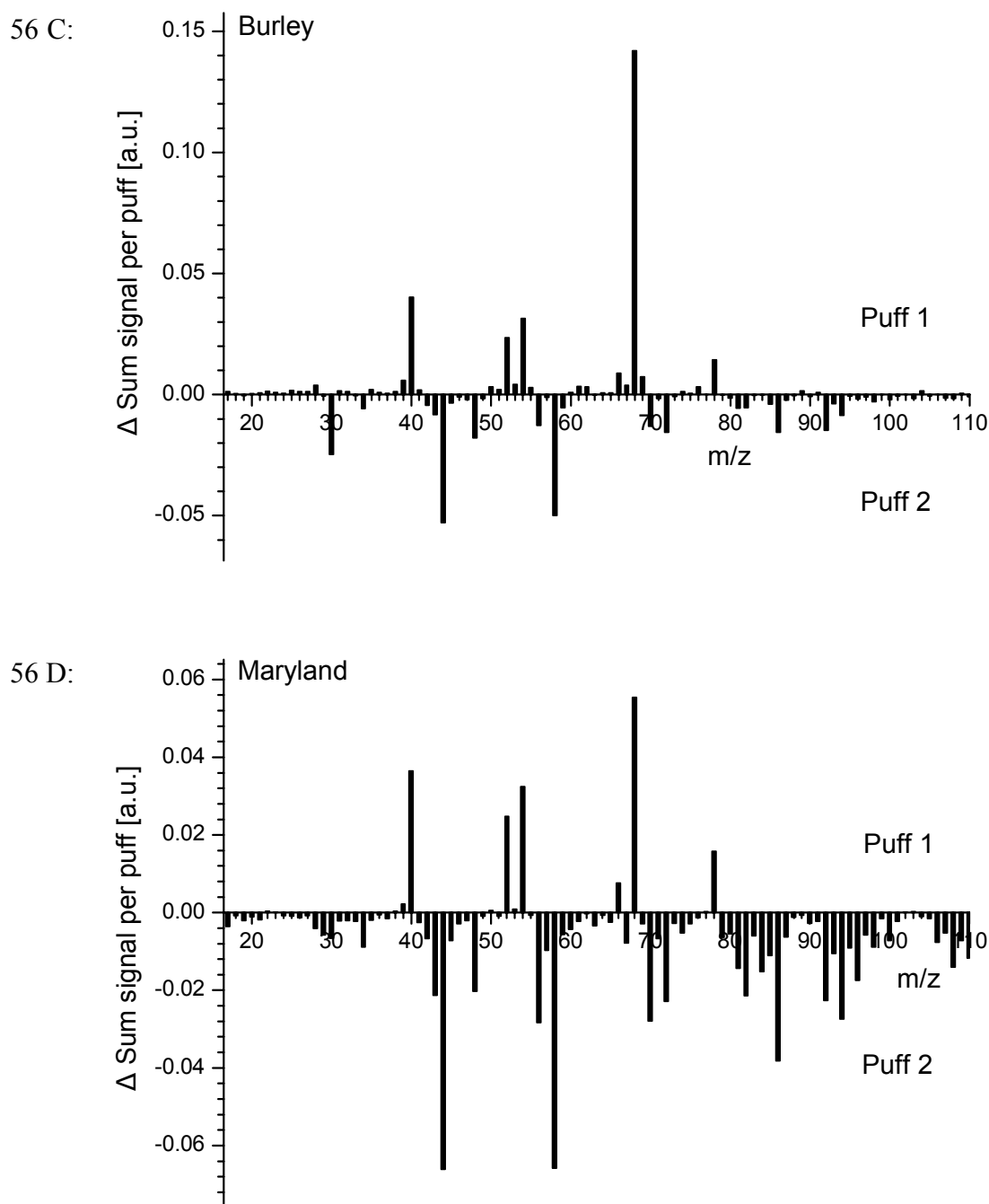


Figure 55: Qualitative puff-by-puff resolved and total absolute (top) and normalised (bottom) yields of  $\text{NH}_3$  ( $17\ m/z$ ) for each cigarette type

The  $\text{NH}_3$  profile looks very similar to its puff-resolved TPM profile which indicates a correlation. However, there is no observable connection for the similar TPM profile of Maryland tobacco since these  $\text{NH}_3$  yields are rather low. In turn, Virginia and Oriental tobacco feature elevated levels in many carbohydrate-derived hydrocarbons. Some of them

are also elevated in the 2R4F cigarette. Oriental tobacco also exhibits a unique puff-by-puff smoking pattern as almost all absolute yields are higher in the first puff. For those substances high in the first puff, this tobacco shows the greatest decline from puff one to puff two, e.g. observable for butadiene. This effect can also be illustrated by the difference spectra between the first and the second puff. They look similar for all analysed cigarettes, with slightly changing signal intensities, especially for Virginia which is lower in 68  $m/z$  (mainly isoprene), but it does not occur with the Oriental tobacco (Fig. 56 A to D).





Figures 56 A to D: Difference spectra between first and second puff for all four single tobacco types Virginia (Fig. 56 A), Oriental (Fig. 56 B), Burley (Fig. 56 C), and Maryland (Fig. 56 D)

The overall behaviour of Oriental tobacco can be explained by the nature of the tobacco. Oriental leaves are smaller and the resulting tobacco is very brittle with poor burning characteristics. Cigarettes consisting of Oriental tobacco almost always extinguish during the smoulder period between the puffs.

The cigarette types with the lowest puff numbers, Burley and Maryland, often exhibit higher absolute yields. After normalisation to particulate matter this effect is mostly equalised and

the tobaccos have similar values with only a few exceptions. One is the NO content of Burley and the 2R4F tobaccos. As expected, because of its high nitrogen content, Burley has the highest values and the amount rises steadily with puff number but the values for the 2R4F cigarette are surprising. The total yield of NO is even higher in the 2R4F than in Burley. The reason for this must be the high Burley content in the 2R4F blend (20 %) and possibly the reconstituted tobacco. However, NO is the only nitrogen-containing component where the 2R4F smoke has particularly high levels. In contrast, Burley exhibits elevated amounts for various masses. The exact composition and properties of the reconstituted tobacco used in the 2R4F cigarette is unknown. However, it is common that reconstituted tobacco exhibits high amounts of ribs and stems of the tobacco leaves. These parts of the tobacco plant are known to be often abundant in nitrate, which, in turn, can convert to NO when burnt [3, 118, 362]. Regarding acetaldehyde (44  $m/z$ ) Maryland tobacco gives the greatest rise with increasing puff number but the total yield as well as the normalised total yield in the 2R4F cigarette is higher. The same or similar effects occur for other masses such as 56  $m/z$  (mainly acrolein), 58  $m/z$  (acetone), 70  $m/z$  (mainly crotonaldehyde), 72  $m/z$ , and 86  $m/z$ , most of them being carbonyls. In principle differences in the tobaccos used for the 2R4F cigarette manufacture and the pure tobaccos are possible. Comparisons are complicated by the fact that even the same tobacco types can lead to changes in smoke composition due to varying conditions (e.g. growing region, year etc.) and treatments of the tobacco (e.g. plant cultivation, curing process etc.). But still, for some substances the higher yields in the 2R4F cigarette are remarkable. A possible source for the elevated levels of oxygen-containing components could be the added invert sugar. Regarding glycerol, pyrolysis experiments revealed that it transfers almost intact into the smoke i.e. it should hardly decompose in a burning cigarette [261]. All in all, smoking of the 2R4F cigarette results in higher amounts of several oxidation products compared to the single tobacco type cigarettes. Especially with regard to the influence of reconstituted tobacco, smoke formation remains uncertain and should be investigated in more detail since it is one of the main components of the blended tobacco composition of the 2R4F research cigarette.

#### **4.4.5. Different cigarette types compared to the 2R4F cigarette**

Besides the tobaccos used in cigarette manufacture, cigarette design greatly influences the smoke composition [142, 363-367]. Hence two commercially available cigarette types were

incorporated into the measurements. The two types are two different approaches of reducing toxic smoke constituents, which were introduced in Chapter 4.3. The “light” cigarette in which ventilation of the cigarette by the use of porous paper and ventilation holes in the filter results in reduced generation of smoke constituents in the burning zone and dilution of the smoke and thereby a reduction of the yield [110].

The ‘new filter type cigarette’ (NFT) is based on the novel principle of combining two different approaches. Firstly, the tobacco had been treated by a newly developed technology which inhibits the formation of tobacco-specific nitrosamines [334]. Secondly, the cigarette filter consists of three sections: the tobacco rod is adjacent to the first section, which contains an ionic exchange resin, followed by a section that contains activated carbon, and thirdly by a cellulose acetate section.

These two cigarette types were investigated in the same way as the different tobacco type cigarettes: gas phase and whole smoke analysis whereby quantitative measurements were performed for the same substances. Normalisation was carried out by considering puff-by-puff resolved and total TPM. TPM values were obtained by the same method as described for the different tobacco types and are illustrated in Figure 57 and the actual yields are given in the Appendix.

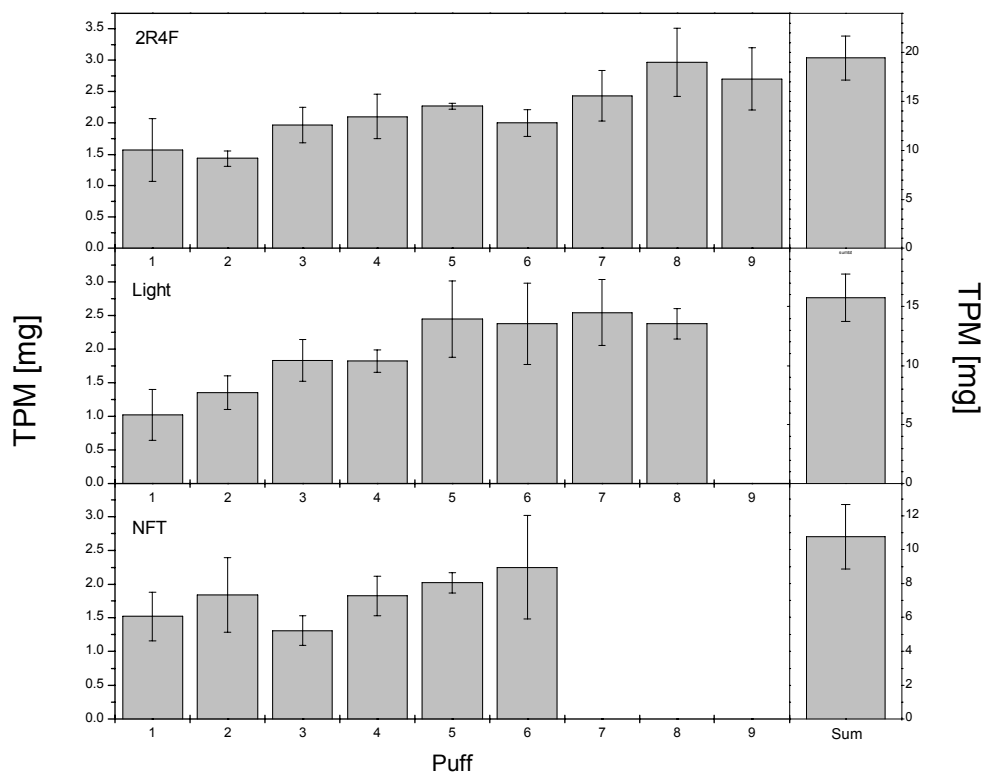
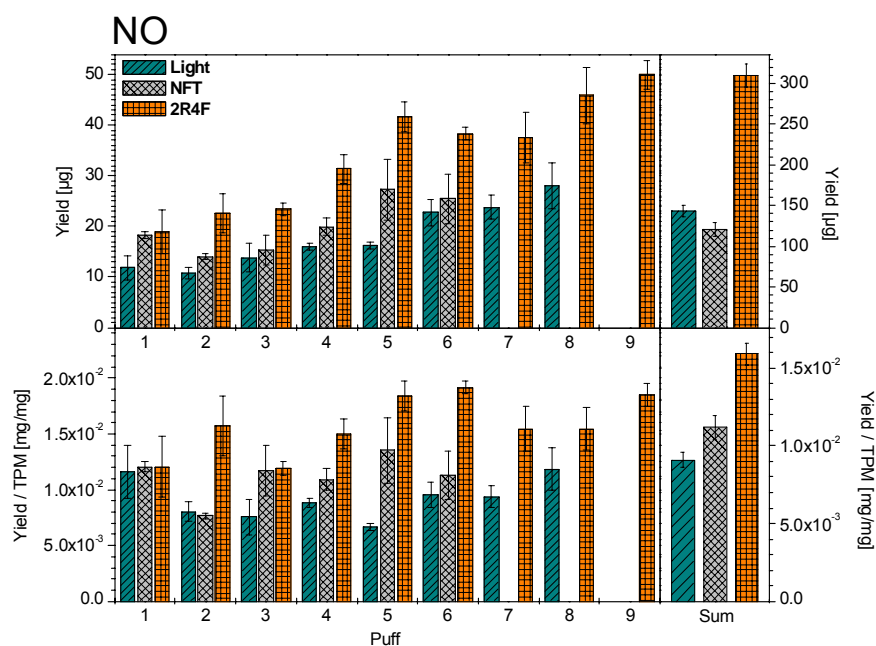


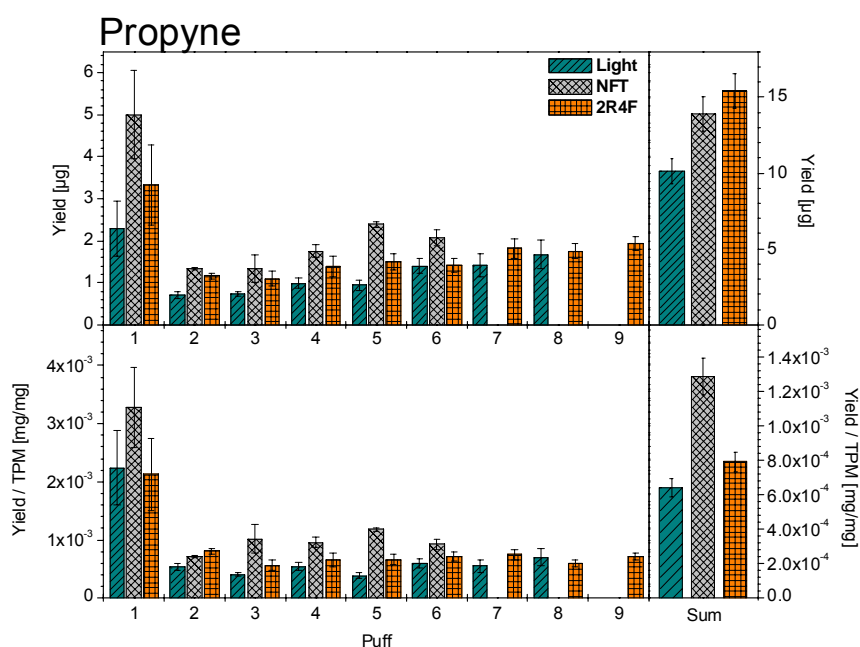
Figure 57: Puff-by-puff resolved and total TPM yields of the two cigarette types ‘light’ and ‘NFT’ as well as the 2R4F

The comparison with the 2R4F is only demonstrated for whole smoke because vapour phase does not provide any additional information. However, the puff-by-puff yields for both, inclusive and exclusive cleaning puffs, are listed in the Appendix. Figures 58 A to J illustrate the puff-by-puff resolved and the total amounts of the quantitatively analysed compounds for the two cigarette types and the 2R4F cigarette.

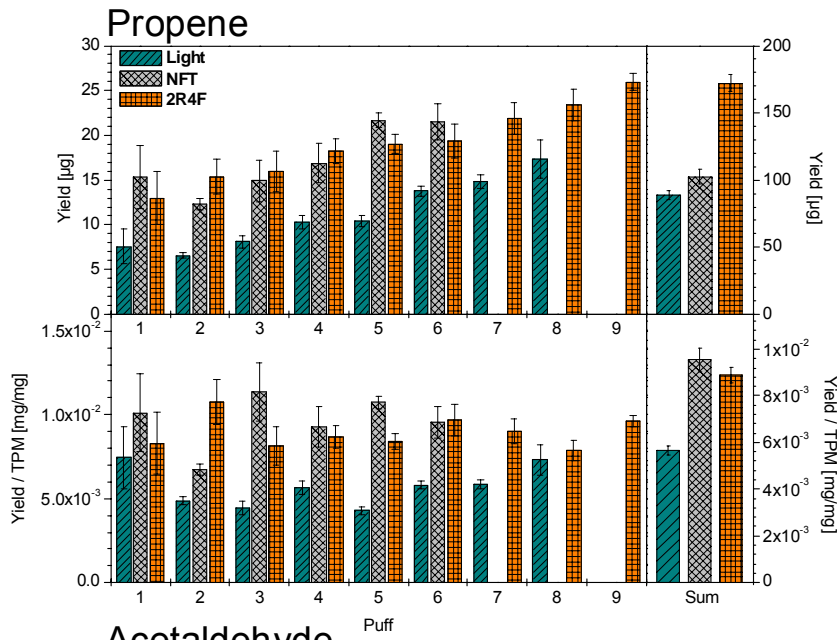
58 A:



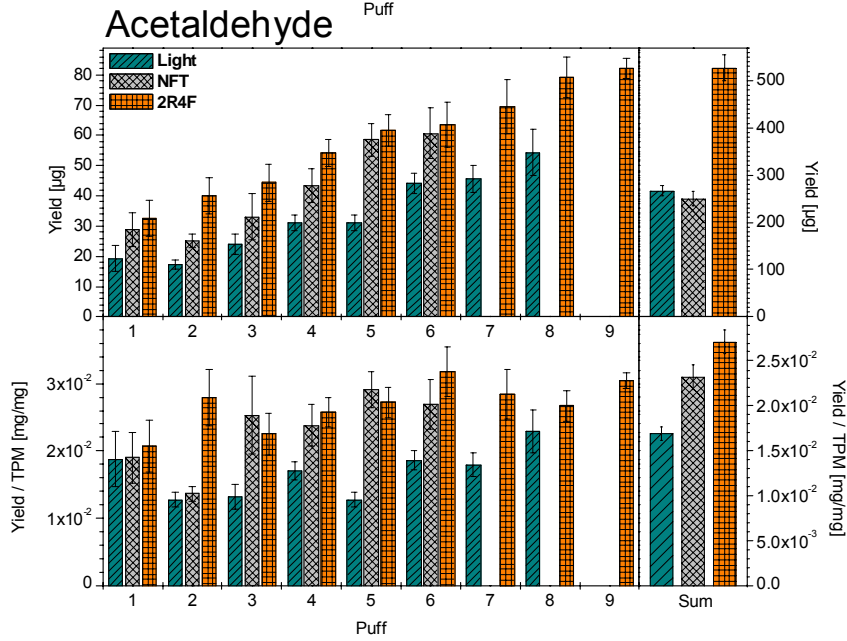
58 B:



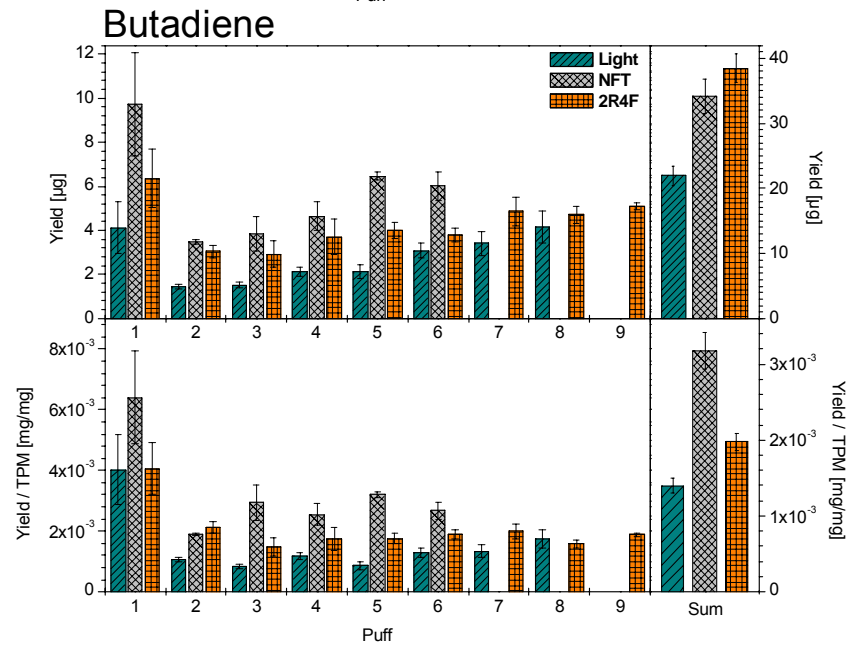
58 C:



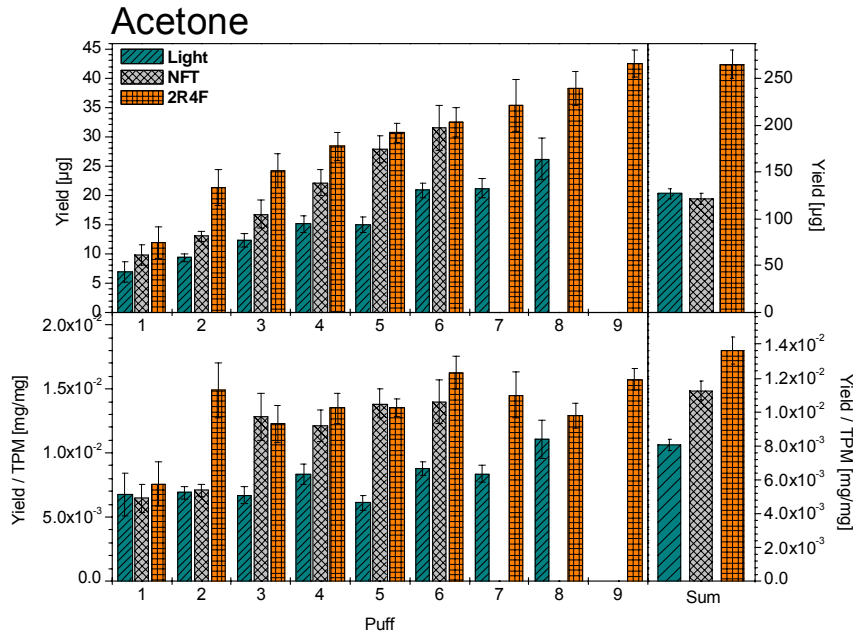
58 D:



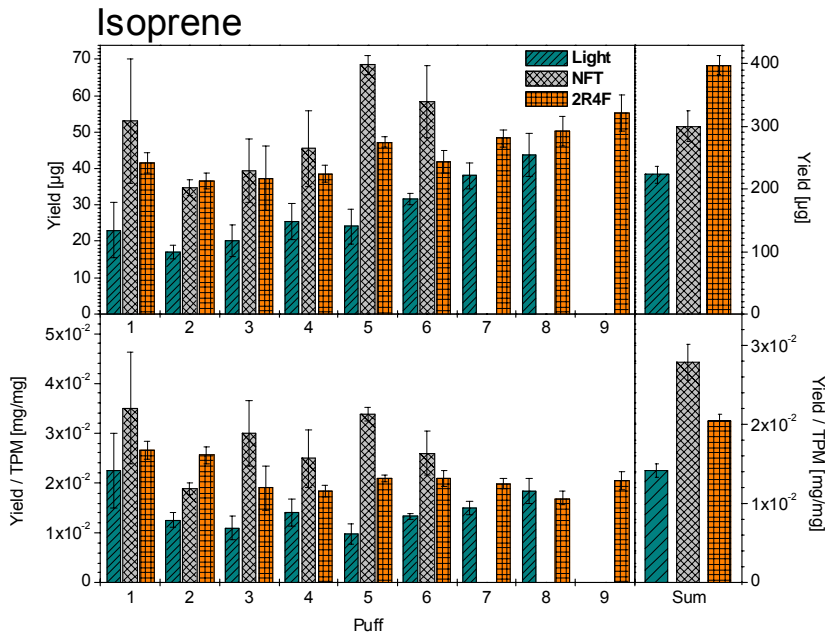
58 E:



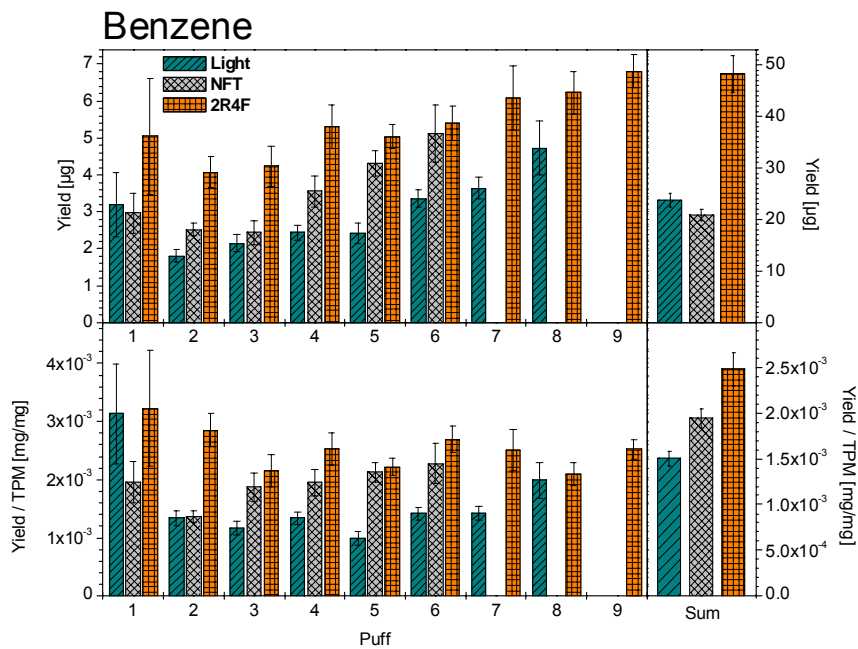
58 F:



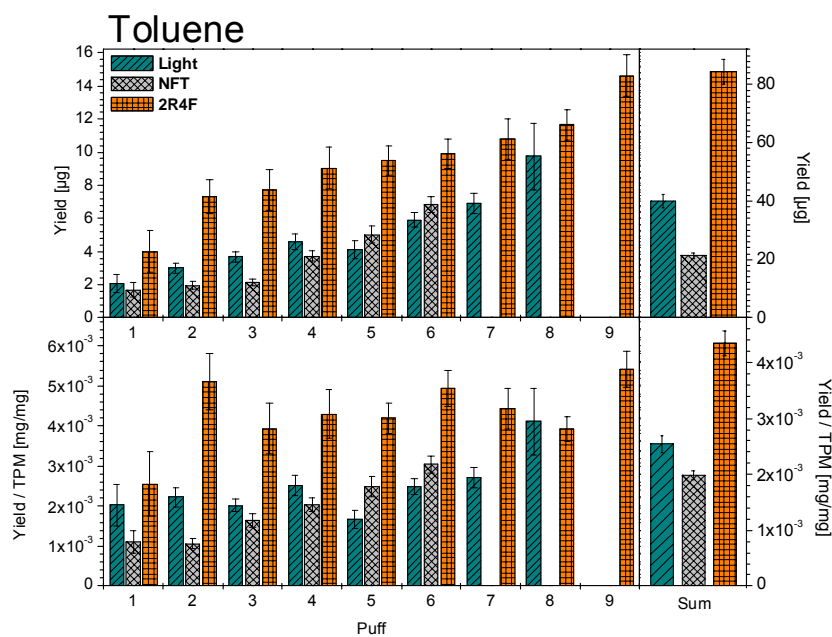
58 G:



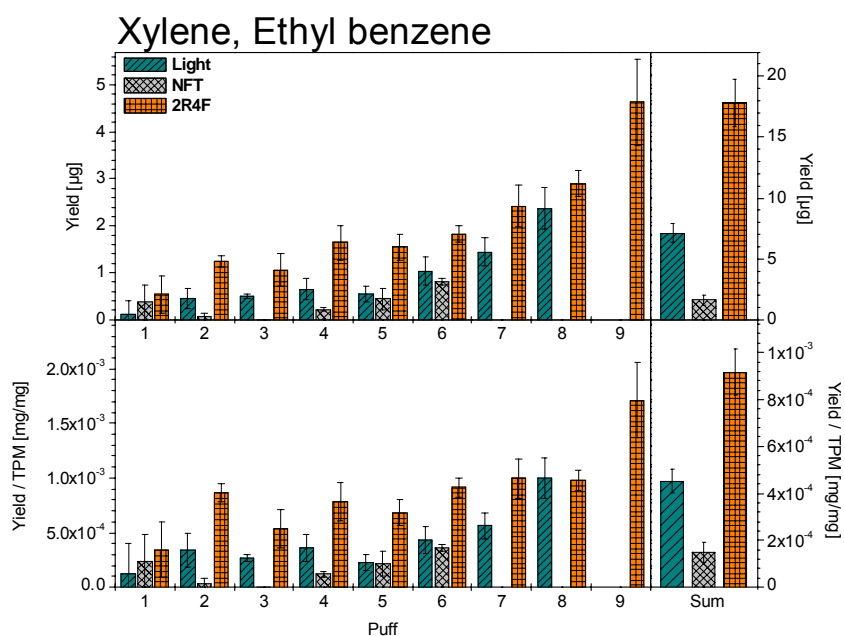
58 H:



58 I:



58 J:



Figures 58 A to J: Quantitative puff-by-puff resolved and total absolute (top) and normalised (bottom) yields for the three cigarette types

As mentioned before the 2R4F yielded 8.7 puffs on average whereas the investigated ‘light’ cigarette was finished after 8.0 puffs and the NFT cigarette after 6.0 puffs. Under these circumstances it is not surprising that the 2R4F reaches the highest values for all observed compounds when measuring the total yield as well as TPM. Because of the lowest puff number the NFT should feature the lowest amounts which is only the case for NO, toluene, xylene/ethyl benzene, and total TPM. Regarding acetaldehyde, acetone, and benzene the total yields are about the same as for the light cigarette whereas the latter one exhibits the lowest

yield of butadiene and isoprene. The fact of varying puff numbers of different cigarettes emphasises the necessity of puff-resolved measurements for objective comparisons.

By looking at the puff-resolved measurements it can be seen that the NFT and the 'light' cigarette also follow the usual puff behaviours. Interestingly, the NFT cigarette delivers rather high amounts of butadiene, isoprene, and propyne as well as 52  $m/z$ , and 66  $m/z$  all of them being unsaturated hydrocarbons. In Chapter 4.4.3 it was demonstrated that some of these substances are abundant in the gas phase. Consequently, it seems as if the triple filter either lacks efficient filtering of these vapour phase constituents or their formation is generally higher. Regarding benzene and its derivatives, yields for the NFT cigarette are lower the higher the degree of substitution (benzene  $\rightarrow$  toluene  $\rightarrow$  xylene/(ethyl benzene)). When compared to the light cigarette, the NFT exhibits higher or about the same puff yields for benzene and slightly lower or roughly the same for toluene. In contrast for ethyl benzene/xylene, puff concentrations are lower, which indicates improved filtration of substituted aromatic species. This assumption is corroborated by the rather similar levels of benzene and toluene in the NFT. In general, the amounts of toluene are higher than for benzene [14], which is also the case for the light and the 2R4F cigarette here. Reduction of NO in the NFT cigarette compared to the 2R4F can be explained by the newly developed tobacco treating process, which aims to reduce the levels of tobacco-specific nitrosamines. NO is known to act as the nitrosation agent of tobacco alkaloids to form TSNAs. However, the level of the NO reduction, as well as that for acetaldehyde and acetone, is in the range of the light cigarette. Finally, under the adjusted smoking conditions the principle of ventilation leads in general to the lowest yield of target compounds in smoke. The newly developed filter system in combination with the adjusted tobacco treatment also reduces amounts of most observed compounds but some hazardous substances, mainly isoprene and butadiene, feature higher yields.

#### **4.5. Conclusion of the smoking experiments**

Application of the SPI-TOFMS to the analysis of cigarette smoke enabled the comprehensive characterisation of the smoking process (gas phase and whole smoke) to be made on a puff-by-puff basis. In so doing, the very unique chemical composition of the first cigarette puff was discovered and described. In addition, evidence was found for a continuous change of the smoke composition from the second to the last cigarette puff. Besides the qualitative information of a wide range of substances, puff-resolved quantification of nine health-related smoke constituents was carried out, demonstrating the varying hazardous burden of each single puff for the human smoker. These observed effects are only visible when puff-resolved analysis techniques are applied and not by the more common determination of total yields of cigarette smoke. In this context, drawbacks and limitations of the existing standardised smoking regime were discovered, first and foremost when applied to puff-by-puff analysis. Furthermore, the influence of different tobacco types on the smoke composition was investigated by comparing the 2R4F research cigarette to several pure tobacco cigarettes. Evidence was found for the influence of reconstituted tobacco on smoke formation. Finally, the 2R4F cigarette was compared to two different cigarette types which both aim to reduce several smoke toxins. Both developments were characterised and the benefits and disadvantages were discussed.

## 5. Conclusion and Outlook

This thesis describes the application of single photon ionisation (SPI) time-of-flight mass spectrometry (TOFMS) for the investigation of cigarette smoke and tobacco pyrolysis gases. SPI is a soft photoionisation technique i.e. ionisation takes place without any or only little fragmentation of the original molecule. In contrast, most conventional ionisation methods, such as electron impact (EI) ionisation, cause fragmentation of the target molecules. In this case identification of compounds is carried out by addressing specific fragment patterns. However, this technique is not convenient for the analysis of highly complex samples containing hundreds of different compounds such as tobacco smoke. Tobacco smoke is known to be a very dynamic matrix containing thousands of compounds, which are separated between two phases, the gas phase and the particulate phase. Therefore, superpositions of mother ions and fragments take place which make the identification of individual species difficult or even impossible.

In the framework of this work, VUV photons featuring a wavelength of 118 nm were used for ionisation of the target molecules. As a consequence, all species having an ionisation potential below 10.49 eV are addressable, which incorporates a wide range of organic compounds such as hydrocarbons, carbonylic, aromatic as well as heterocyclic compounds etc. VUV photons are generated by directing the third harmonic of a pulsed Nd:YAG laser through a rare gas cell filled with xenon. Due to a non-linear polarisation effect in the isotropic gas medium, VUV light is formed. The repetition rate of the laser system used is 10 Hz.

SPI is combined with a time-of-flight mass spectrometer. In TOFMS all ionised molecules can be detected simultaneously and on a real time basis since one spectrum only requires ca. 30  $\mu$ s. Due to the soft ionisation of the tobacco smoke constituents the resulting spectrum only contains mother ion peaks, which can be therefore identified rather easily. This enables the monitoring of all substances with the repetition rate of the VUV generation being the time-limiting factor.

After characterisation of the instrument used, a calibration scheme was developed which enables the simultaneous calibration of many different species by only calibrating one compound of choice. The scheme is based on the fact that every compound has individual photoionisation properties but the ratio of the photoionisation cross sections for different compounds is constant for a fixed wavelength, here 118 nm. Therefore, once this ratio is

determined for a compound of choice, here benzene, this ratio can be used for all future quantifications by applying calibration gases of the same concentration.

The experimental part of this thesis is divided into two sub-sections. In the first section the SPI-TOFMS is coupled to a pyrolysis furnace in order to perform tobacco pyrolysis experiments. This enables the comprehensive characterisation of tobacco smoke constituents regarding the influence of temperature and reaction gas composition. These conditions can be deliberately adjusted in order to investigate their influence on the chemical composition of the tobacco smoke. In so doing, seven different temperatures were applied between 400 °C and 1000 °C in steps of  $\Delta 100$  °C as well as two different gas compositions, pure nitrogen and synthetic air. Thereby the thermal behaviour of many smoke constituents was observed. This points to correlations between formation and decomposition reactions and enabled the classification of several substances according to their thermal behaviour. In this context, primary pyrolysis compounds are originally present in tobacco and decay with increasing temperature until they completely vanish. Secondary pyrolysis components are originally not present in tobacco or only appear in low concentrations. However, their amounts rise with increasing temperature until a maximum is reached. Above this threshold their yields decrease again because formation is lowered or thermal decomposition prevails. In contrast, the yields of tertiary pyrolysis components steadily rise with temperature, reaching the formation maximum at the highest temperature applied. Nicotine, one of the target constituents of tobacco smoke because of its concentration and toxicity, was clearly identified as a primary compound. Its thermal behaviour reveals that the majority of nicotine in cigarette smoke is transferred into the smoke by evaporation before the tobacco is actually burnt because total decomposition takes place at temperatures which are far below the temperatures inside the burning zone. In addition, several combustion and pyrolysis products of nicotine could be identified which, in turn, feature different thermal behaviours. In addition, a correlation between the formation of hydrogen sulphide and decomposition of methanionol, two sulphur-containing species, was demonstrated. Besides the general characterisation of the thermal behaviour of tobacco, the pyrolysis experiments were extended to the investigation of the three main single tobacco types Virginia, Oriental, and Burley used in cigarettes world-wide. Each of the single tobacco types was characterised and differences to the other two tobacco types were determined. Part of this analysis was the determination of characteristic key substances for each tobacco type. Most of these differences could be identified as originating with varying cultivation and processing properties of the tobaccos. Moreover, a method for the fast discrimination between these three tobacco types was developed, which is based on

evaluation of the SPI-TOFMS results by statistical analytical methods. In principle, only three key substances were required for a successful discrimination of the tobacco types. Therefore, for this purpose, an inexpensive quadrupole mass spectrometer would be sufficient. Furthermore, the pyrolysis furnace could be replaced by a commercially available pyrolyser device including an automated sampling system. The latest improvements of the ionisation technique are the development of electron-beam pumped rare-gas excimer VUV-lamp systems, which replace costly laser instruments. Incorporating all these enhancements could lead to a commercial application of Py-SPI-TOFMS in tobacco science regarding e.g. quality control and possibly to a wide range of applications in several related fields, whose operation requires a minimum of expenditure of time. With respect to scientific applications, future work needs to address the coupling of SPI-TOFMS to thermal analysis techniques. Taking advantage of the high time resolution, which was not the subject of this work, phase transformations, chemical reactions, and structural changes of substances and materials could be analysed by monitoring the respective pattern of evolved organic compounds.

The second experimental part dealt with the coupling of SPI-TOFMS to a cigarette smoking device for the first time. The purpose of this work was the qualitative and quantitative investigation of a wide range of tobacco smoke constituents on a puff-by-puff basis, with the focus on biologically active species. In this context, analysis of the cigarette's smoke gas phase and of whole smoke i.e. gas phase and particulate phase, was carried out. Separation of the particles from the gas phase was achieved by utilising a quartz fibre filter, which is commonly used in tobacco science. The machine smoking conditions defined by several institutions were applied to a puff-resolved characterisation of the cigarette smoking process. By this means, several flaws of the existing smoking regime were discovered, which affect the results. To minimise these drawbacks a modified smoking machine was applied and some new basic definitions were introduced. By utilising these definitions a comprehensive characterisation of the cigarette smoking process in general was carried out. Regarding quantification, nine target compounds were selected which are believed to be relevant to tobacco smoke-related health effects in humans and which are addressable by SPI-TOFMS. In doing so, it was shown that most of the tobacco smoke constituents increase in yield with puff number. The main reasons for this behaviour are the decreasing length of the tobacco rod, which results in a decrease in dilution of smoke because less ambient air is entering the cigarette through the cigarette paper. Moreover, many substances present in the smoke recondense on the tobacco rod between the burning zone and cigarette filter. As a consequence, the unburnt tobacco is enriched with a variety of compounds and the subsequent smoking puffs lead to higher

concentrations of these substances in smoke. However, it could be demonstrated for the first time that several smoke constituents follow a unique puff behaviour since their concentrations are the highest in the first puff. In general it can be stated that mainly unsaturated hydrocarbons follow this behaviour. The main reason for the high amounts in the first puff must be the quite different combustion and pyrolysis conditions occurring during the first puff when the cigarette is lit compared to later puffs where the cigarette is burning and the tobacco had been exposed to elevated temperatures already. The former described conditions seem to favour the formation of unsaturated hydrocarbons. Therefore, butadiene, which is believed to be the smoke constituent with the highest cancer potential and which is one of the nine quantified target compounds in this study, also follows this unique behaviour. This might be highly important when the findings are applied to the human smoker. Moreover, evidence was found for a continuous change of the smoke composition from the second to the last cigarette puff. In addition, the investigation of the cigarette's smoke gas phase as well as whole smoke enabled conclusions to be drawn indirectly about the burden of several smoke constituents in the particulate phase. Knowledge on the phase affiliations of smoke compounds during the smoking process is important since the uptake mechanisms in the human respiratory tract are very different for gas and particulate phase smoke constituents. By this means it was demonstrated that the puff-resolved gas phase to particulate phase ratio of several semivolatile compounds varies. Several substances are predominantly present in the particulate phase during the first puffs and this ratio changes towards the gas phase with rising puff number. Other compounds exhibit a similar phase affiliation for all puffs. In contrast high yields in the first puff, as described for butadiene, are accompanied with high fractions in the gas phase. After a general characterisation of the cigarette smoking process, the experiments were extended to four single tobacco type cigarettes and two different cigarette types, which both aim to reduce specific harmful smoke constituents. The four single tobacco type cigarettes were analysed and compared to a common blend research cigarette containing all four of these tobaccos as well as further constituents, mainly glycerol, reconstituted tobacco, and inverted sugar. In so doing, the influence of the single tobacco types on cigarette smoke formation of the blend cigarette was demonstrated, which is especially the case for Burley tobacco. Evidence was also found for the influence of reconstituted tobacco and invert sugar on smoke composition. The two cigarette types developed to reduce specific toxicants in smoke featured different results. The type which is mainly based on a higher extent of dilution of smoke, a so-called 'light' cigarette, produced lower concentrations for most substances. The second type, which was specifically designed to reduce tobacco-specific

nitrosamines and formaldehyde in smoke, contains a specially treated tobacco as well as a newly developed cigarette filter system consisting of three adjacent different filter parts. This cigarette showed lower concentrations for some compounds especially benzene and its derivatives. However, some toxicants feature elevated levels compared to the blend research cigarette e.g. butadiene and isoprene.

In conclusion, the coupling of the SPI-TOFMS to a smoking machine has proven to be a sophisticated and powerful approach for the investigation and characterisation of the cigarette smoking process. In the framework of this study, new results and findings were achieved which give insight into the highly complex processes taking place when tobacco burns. Many of the observed effects were solely detectable because the technique used enabled a puff-resolved analysis of the smoking process, which proves the necessity for further action in this field. It was demonstrated that the technique is also well-suited to quickly compare different cigarette types, e.g. new developments and to account for the resulting smoke composition. On the basis of this study several further projects are planned in the field of tobacco smoke analysis. Future work will focus on the on-line monitoring of the cigarette smoking process. Thereby the high time-resolution of up to 10 Hz will be applied since this work only dealt with inter-puff comparisons. The aim is to better understand the sub-puff behaviour of the cigarette smoking process to unravel formation mechanisms and correlations between different smoke constituents. Moreover, the instrument will be coupled to particle analyser devices in order to simultaneously examine several particle properties, such as particle nature, number, size distribution, and surface area to find possible correlations. These measurements will also incorporate a second photoionisation technique, the resonance-enhanced multiphoton ionisation because this technique is highly sensitive for polycyclic aromatic hydrocarbons which will then play a greater role. By this means, the characterisation of several cigarette parameters, e.g. new filter types will be possible. In this context it is planned to develop a micro-sampling probe which, inserted into the tobacco rod, enables sampling directly from the burning zone and its surroundings. A further experiment will deal with the investigation of sidestream smoke, which greatly contributes to the formation of environmental tobacco smoke. ETS is of public interest since all people, regardless if smoker or non-smoker, are affected and because it is known that the concentrations of several smoke constituents are even higher in sidestream smoke than in mainstream smoke. This experiment will also include both photoionisation techniques, SPI and REMPI. One of the greatest achievements within this study was the finding of the unique puff behaviour of the first puff. This fact will be further investigated by applying other analytical techniques. In so doing, GC×GC TOFMS

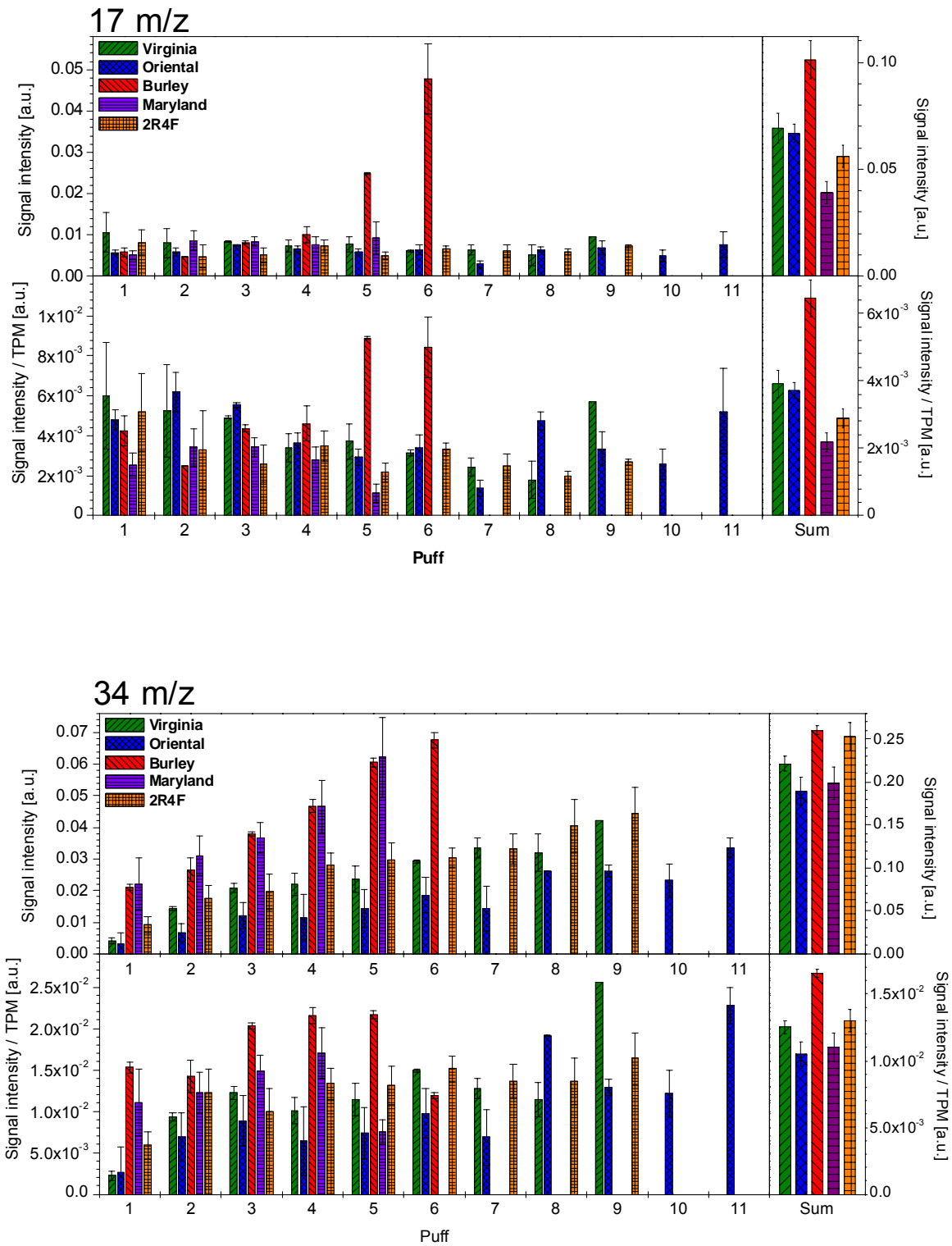
and thermodesorption–SPI-TOFMS will concentrate on puff-resolved particulate phase investigations in order to find species in the smoke’s particulate matter featuring a similar behaviour.

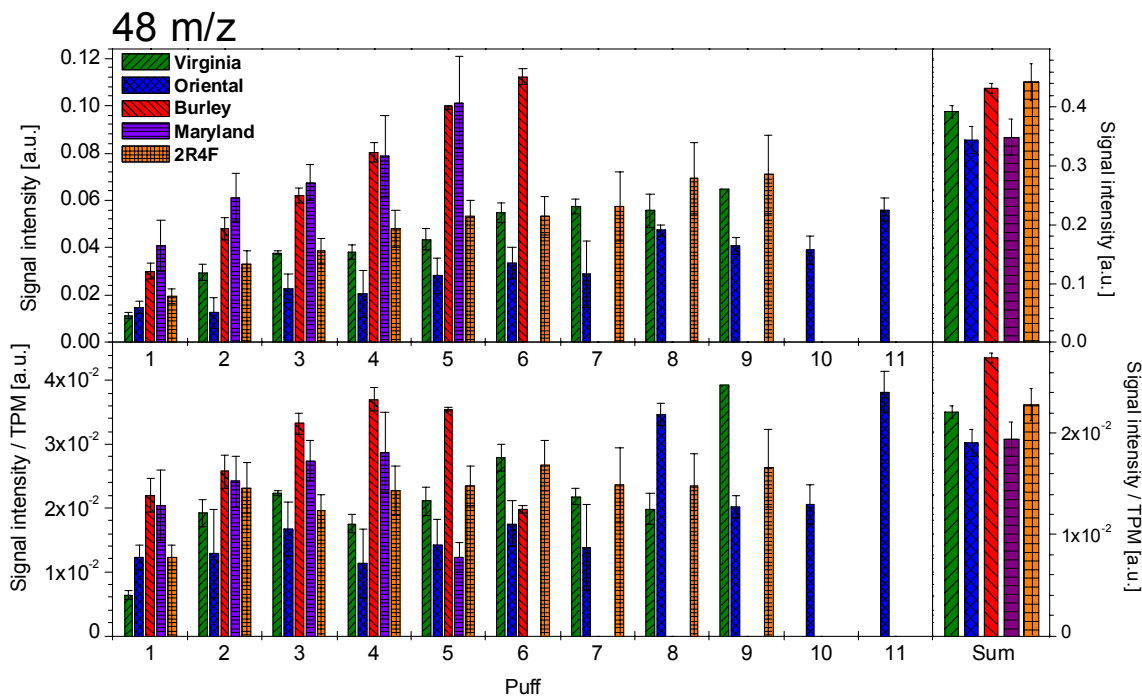
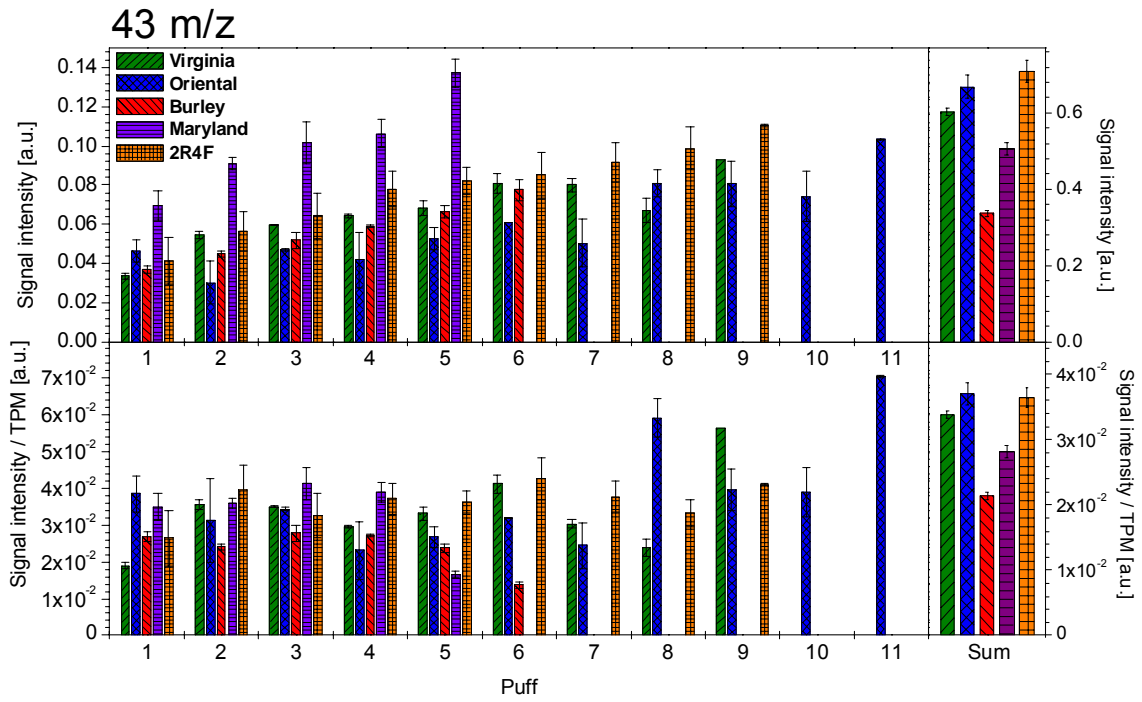
All these experiments use a smoking-machine for smoke generation. However, human smoking behaviour might differ from the smoking conditions used in the smoking machine. Therefore, in order to examine the influence of the human puff behaviour and to determine the retention of hazardous smoke constituents in human smokers, another project just started, funded by the Institute for Science and Health, USA. In the framework of this project, SPI/REMPI-TOFMS is coupled to a flow box which measures the stream of smoke inhalation and exhalation of voluntary test smokers. In this way the real impact of all sorts of cigarette design parameters, compensation, and personal smoking habits of the carefully recruited test smokers will be evaluated. The results might give new insights on the health effects of human smokers.

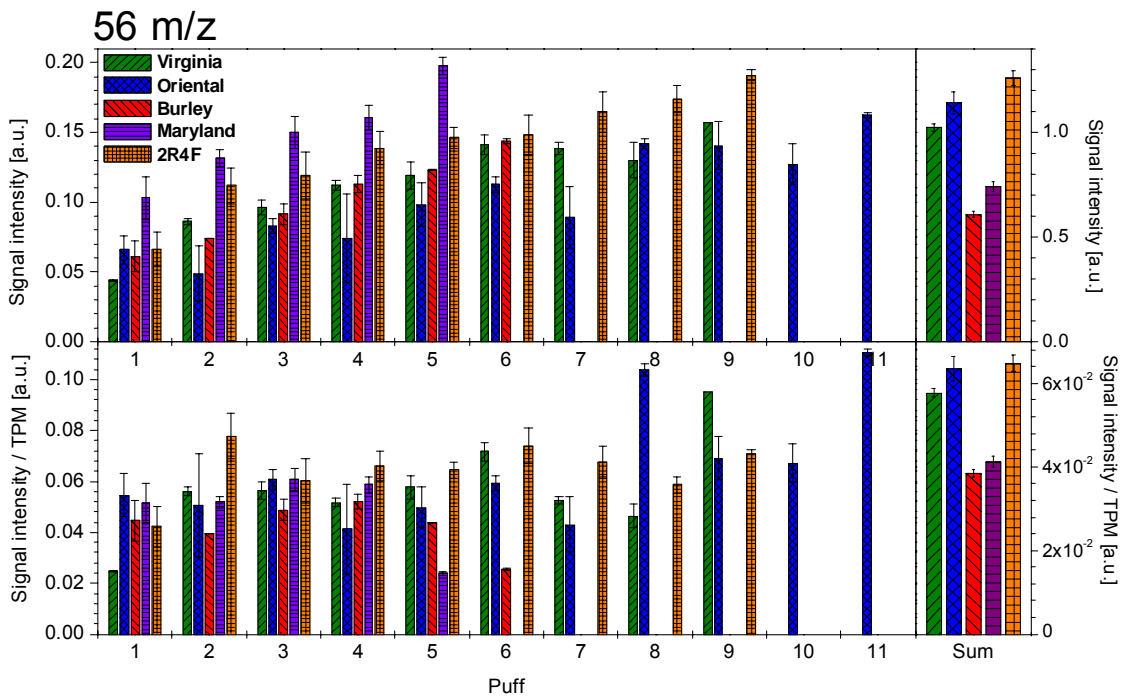
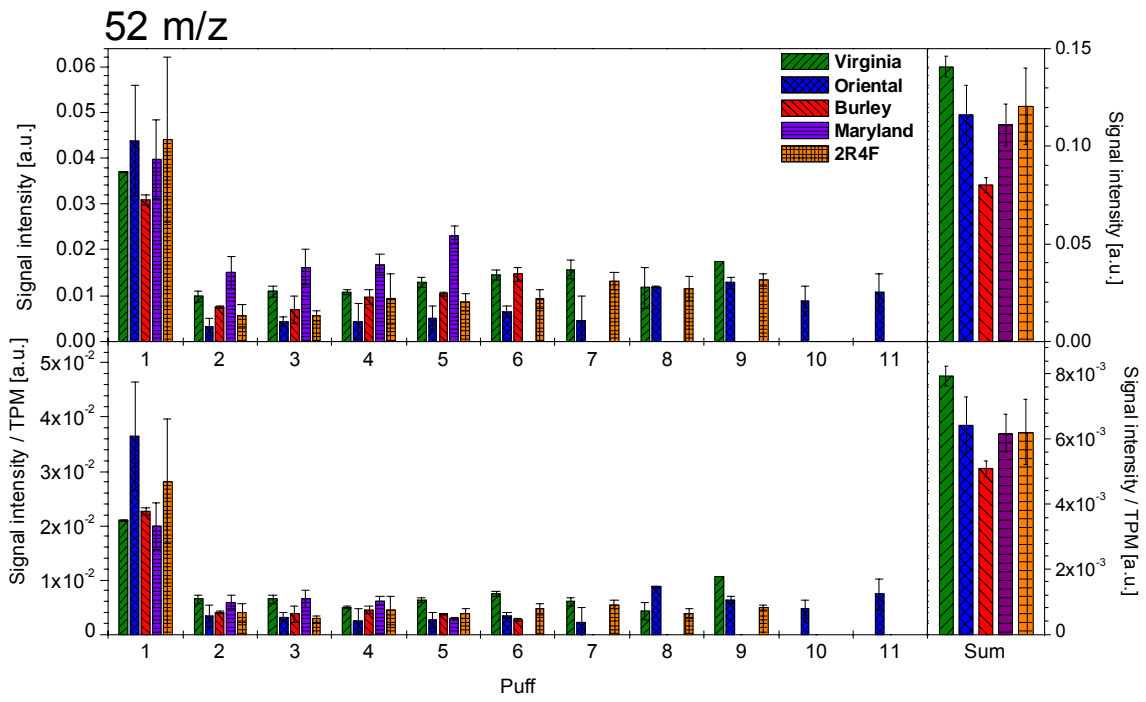
## 6. Appendix

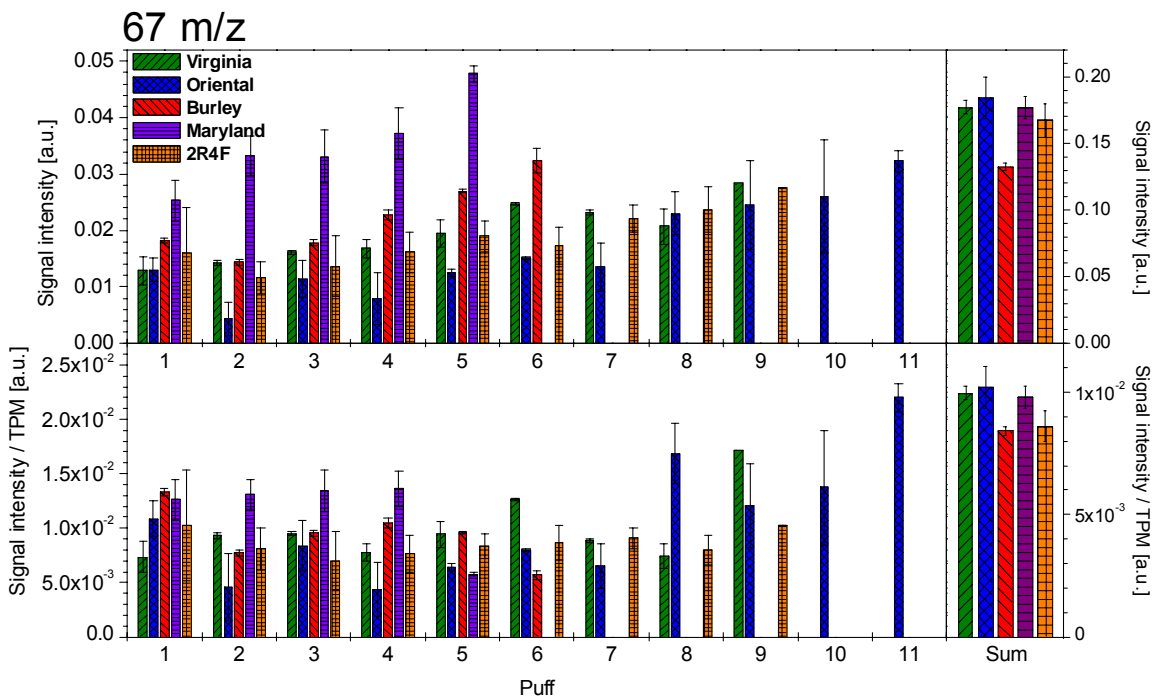
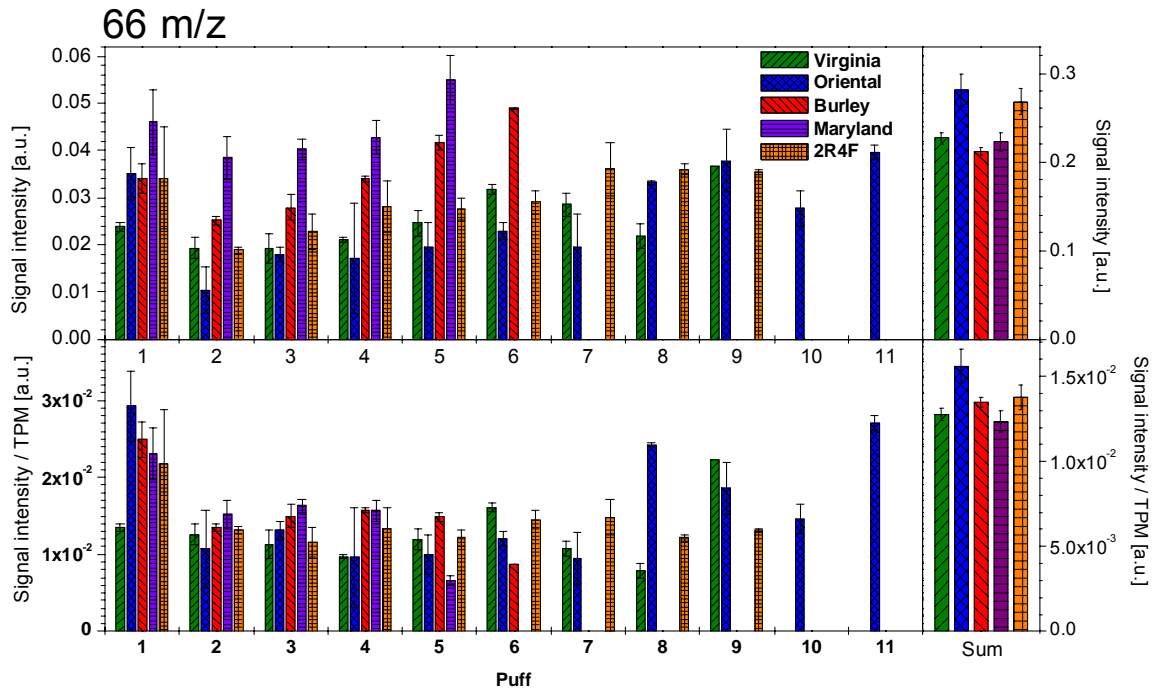
### 6.1. Figures

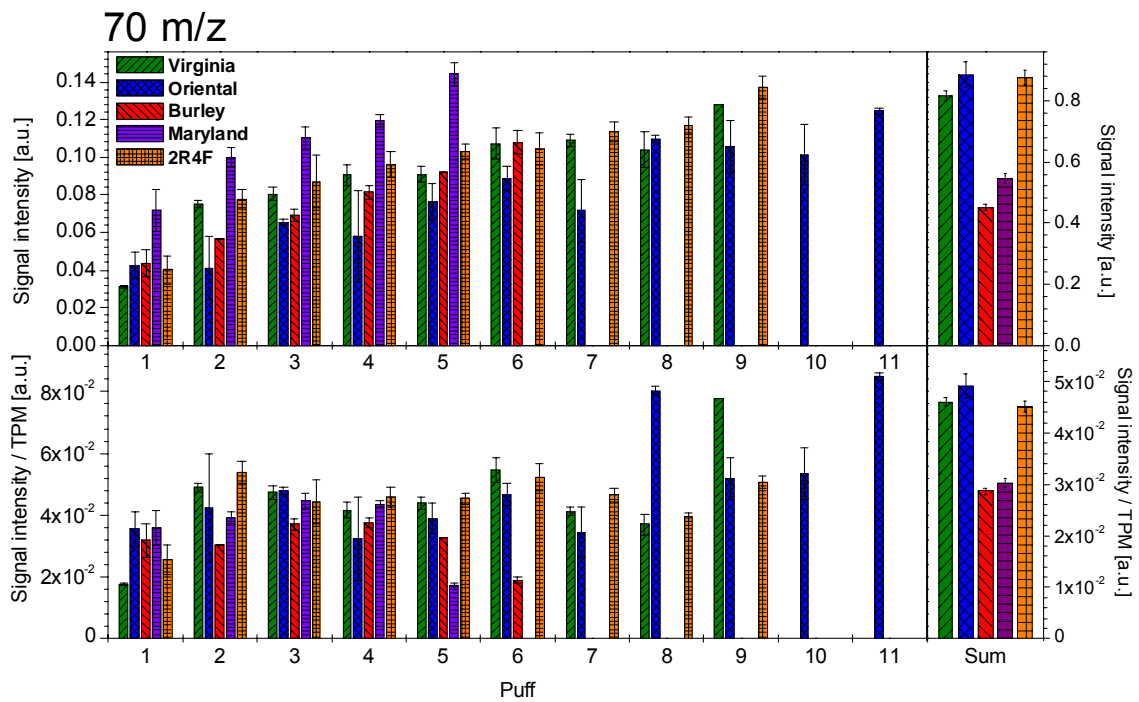
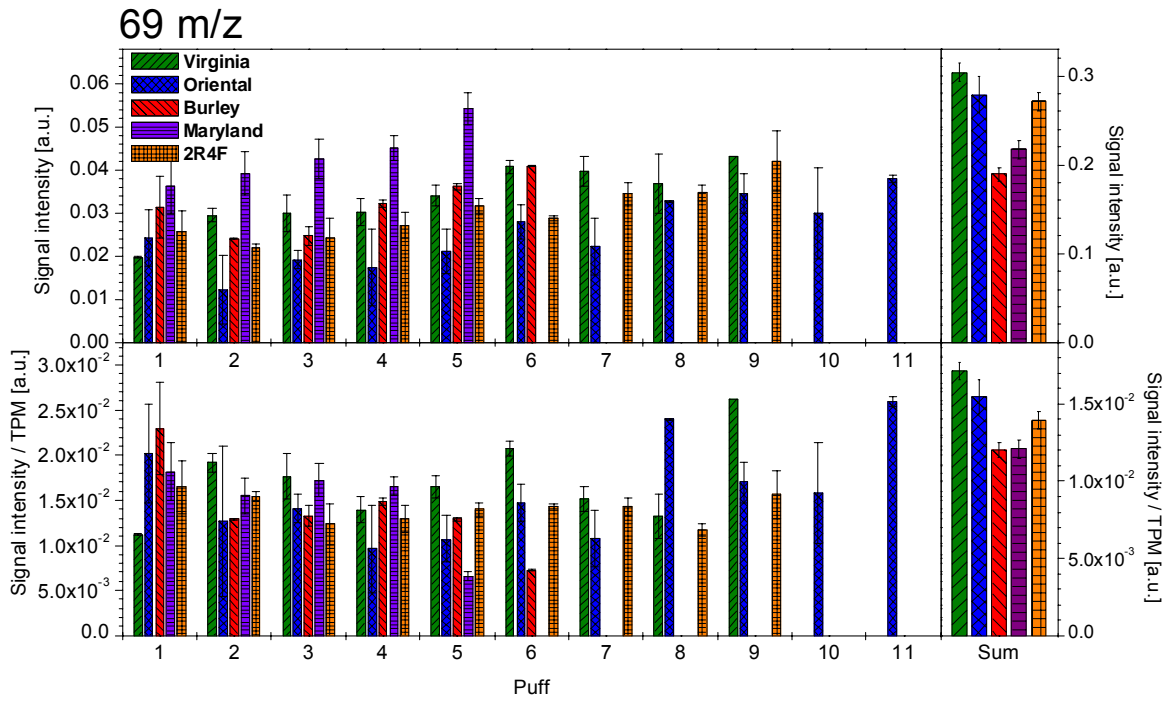
#### 6.1.1. Different tobacco types compared to the 2R4F cigarette

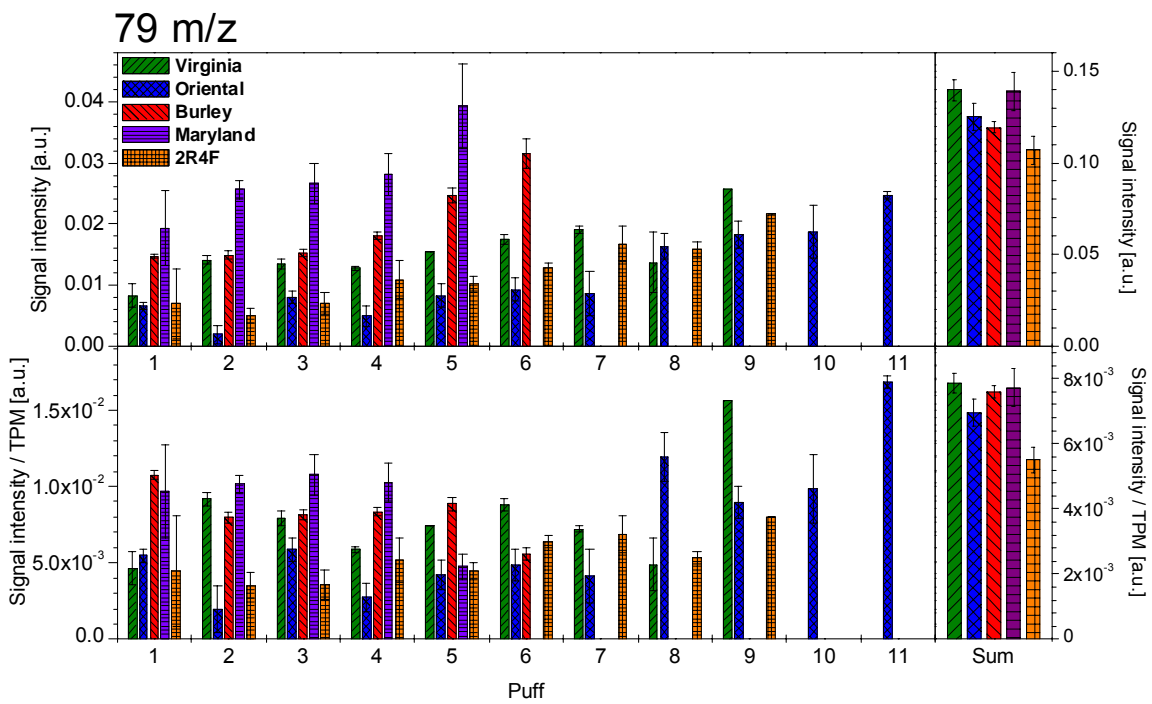
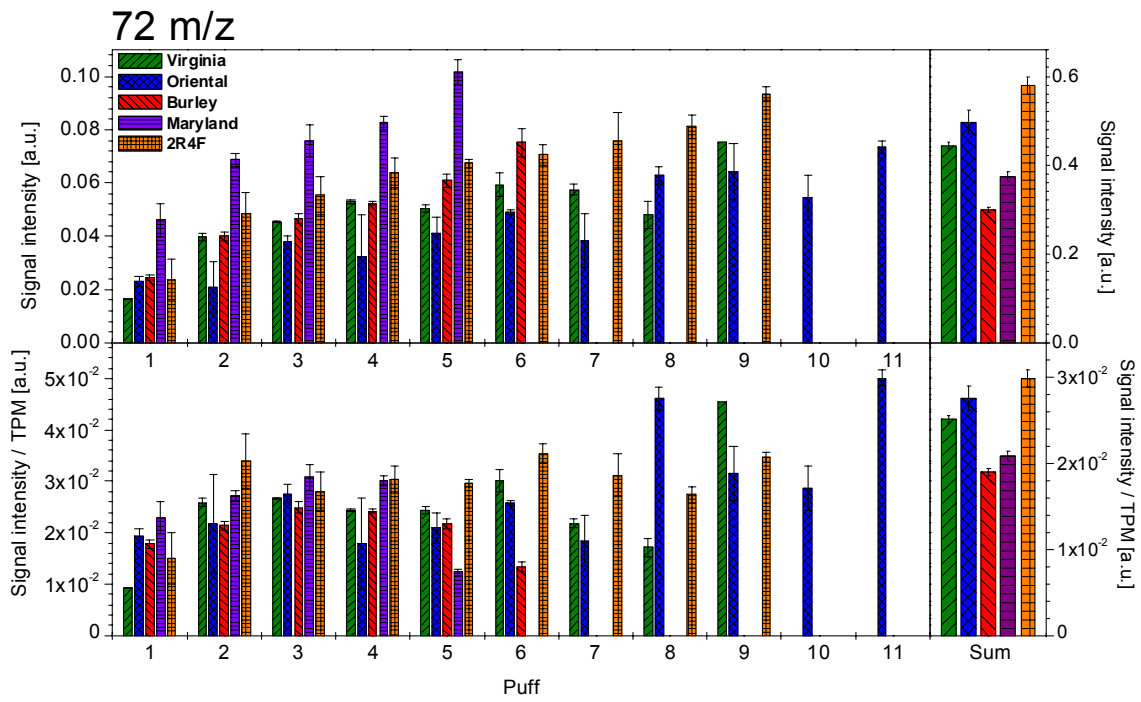


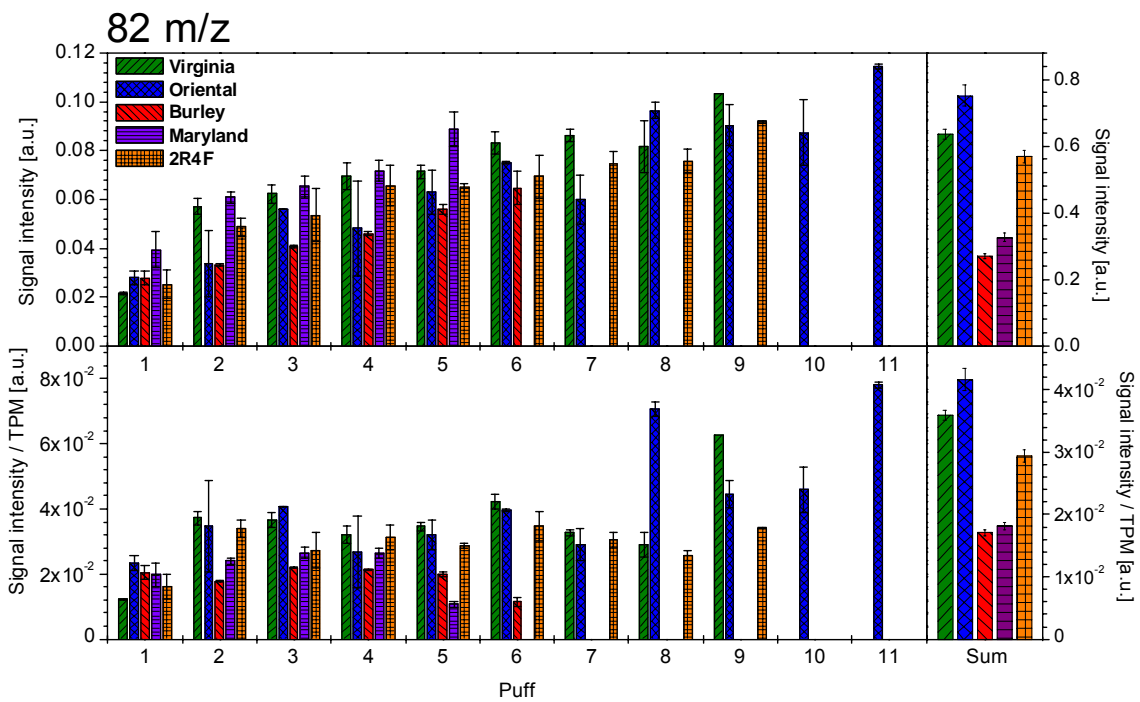
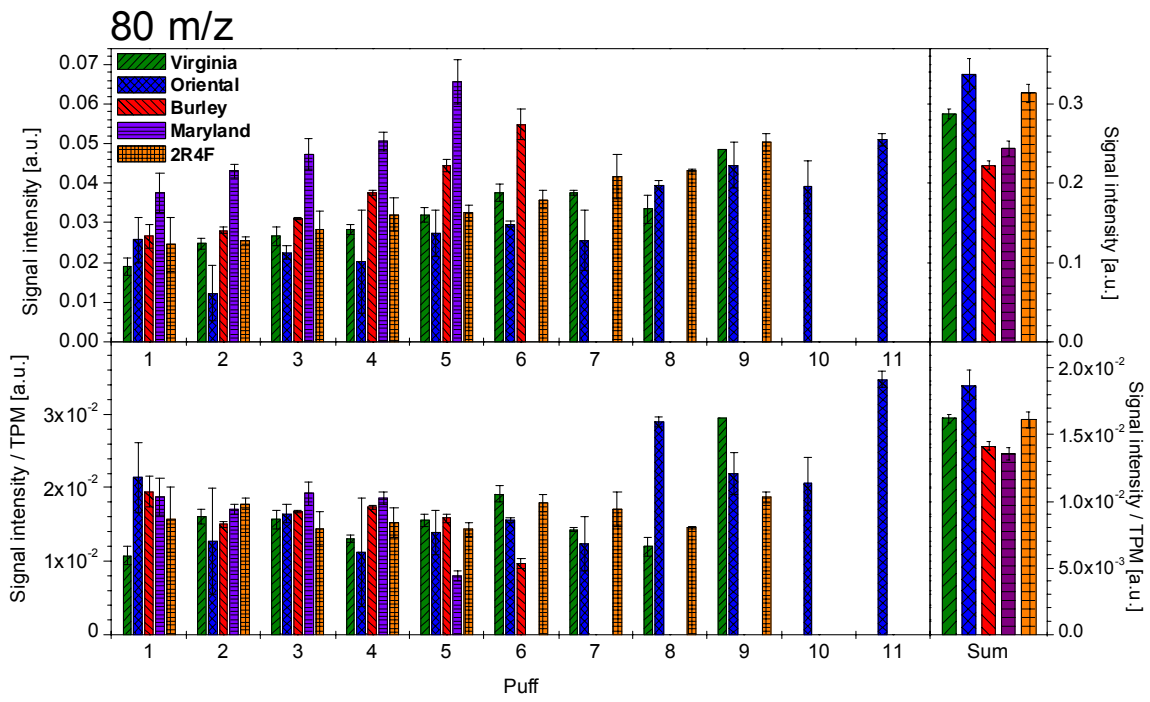


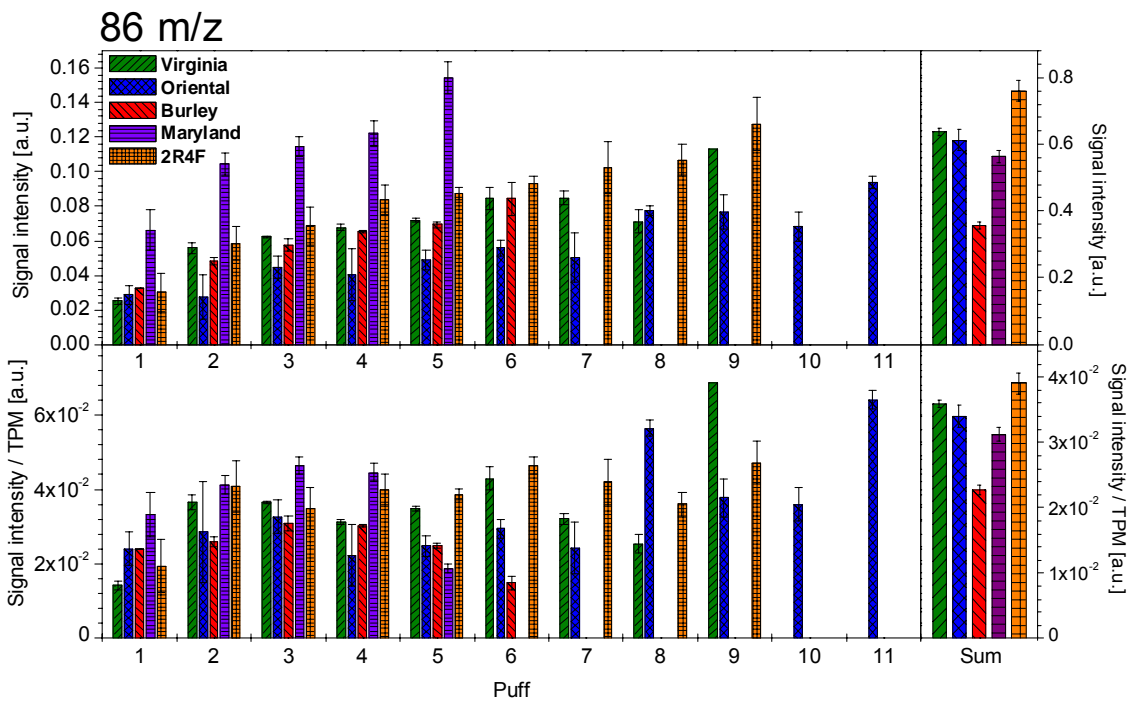
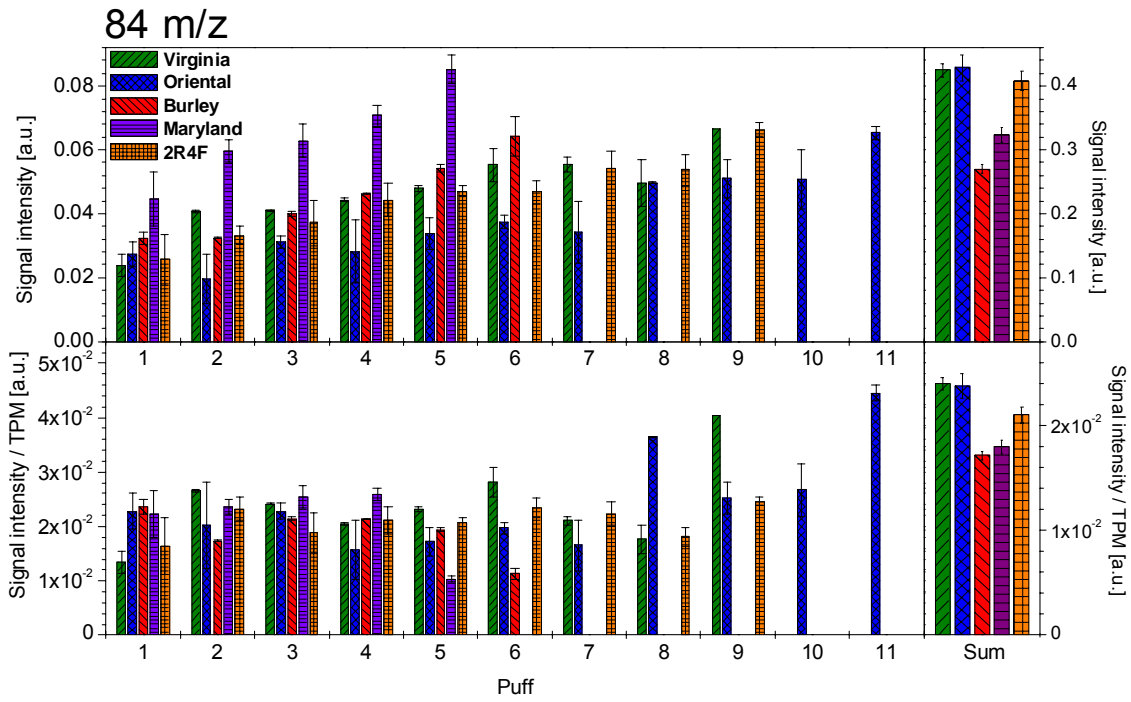


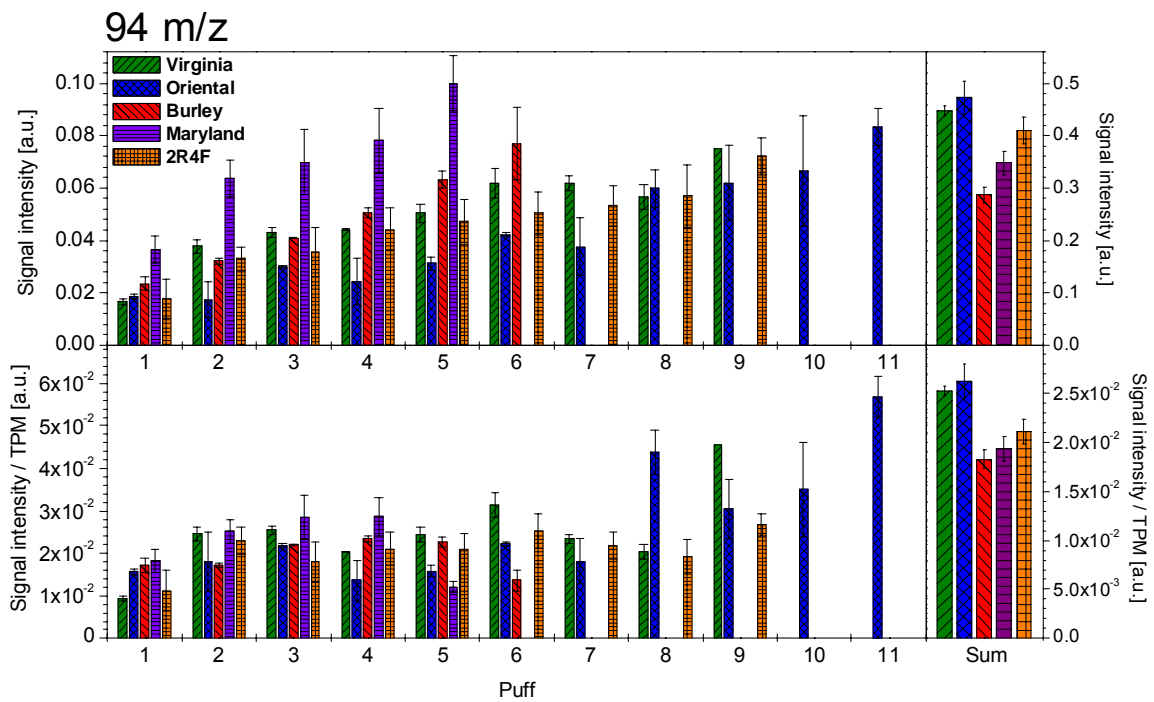
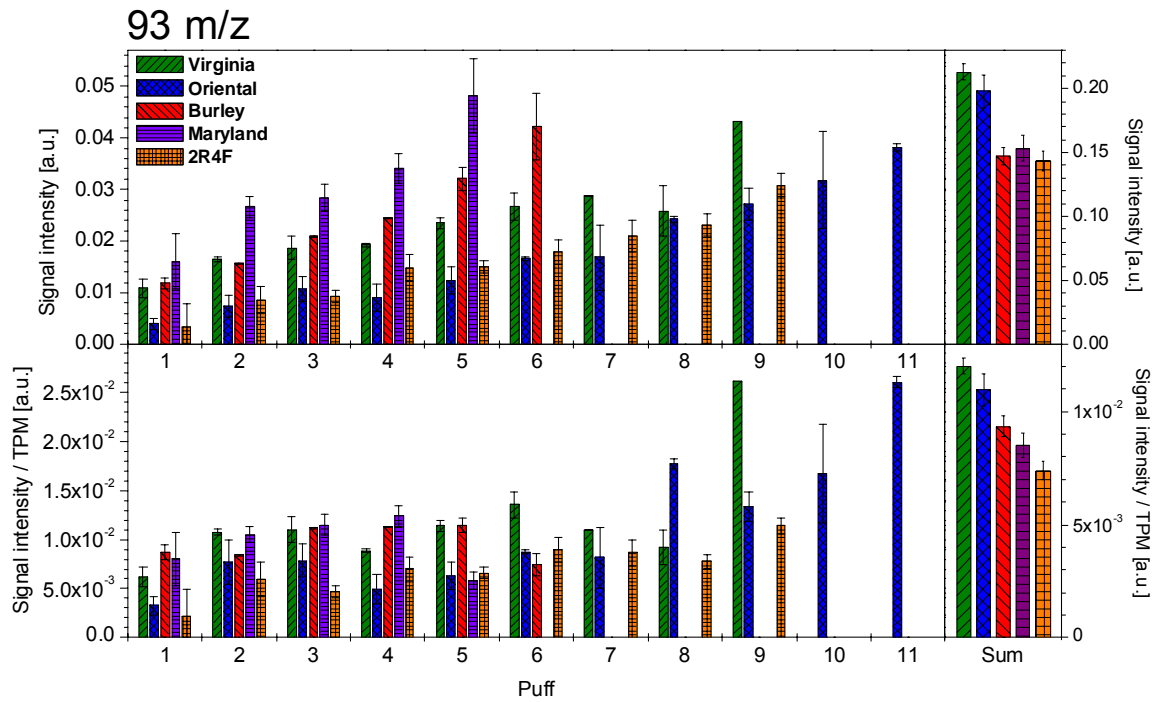


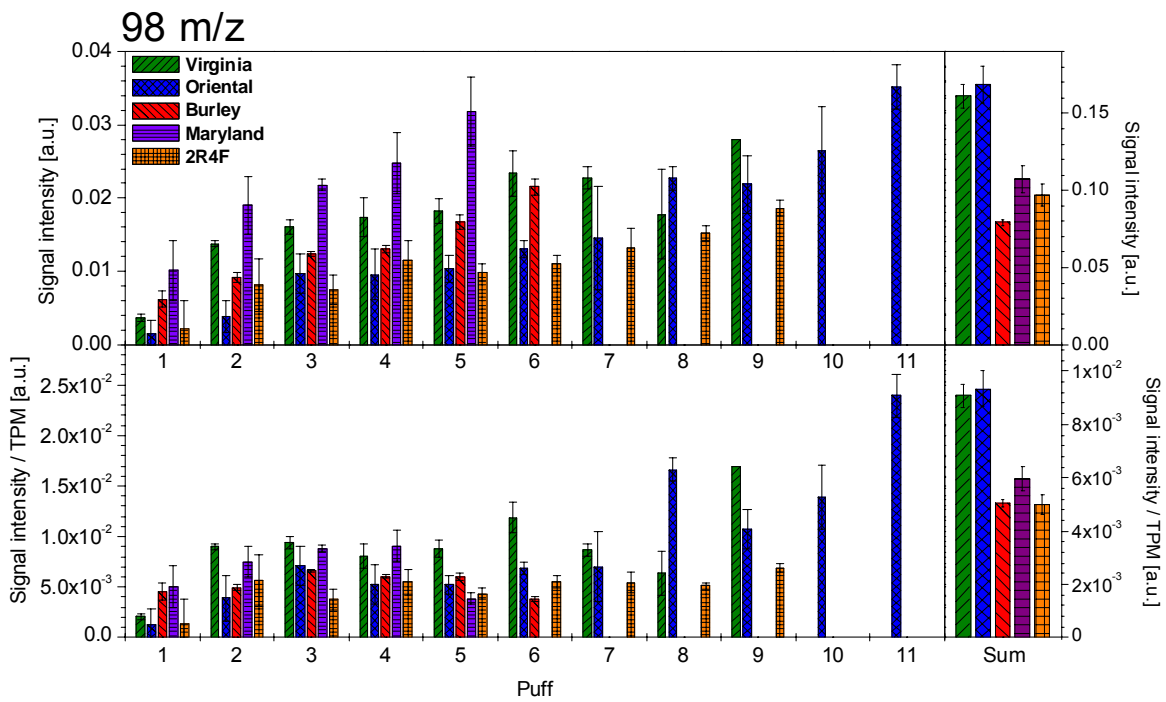
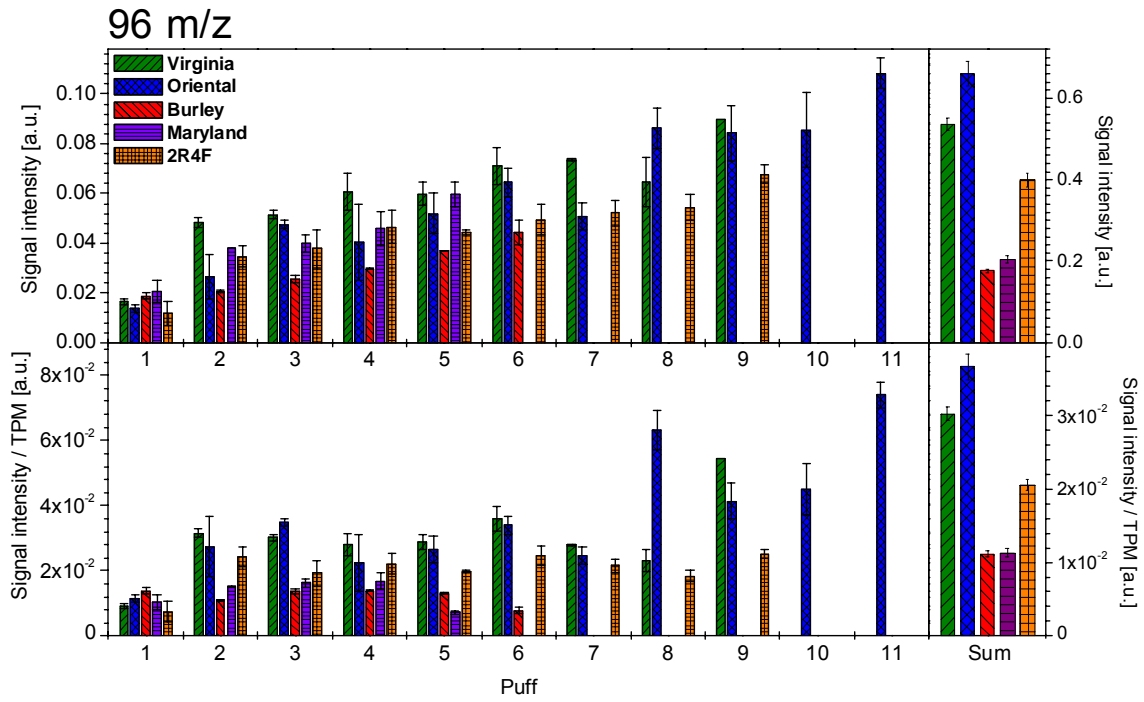


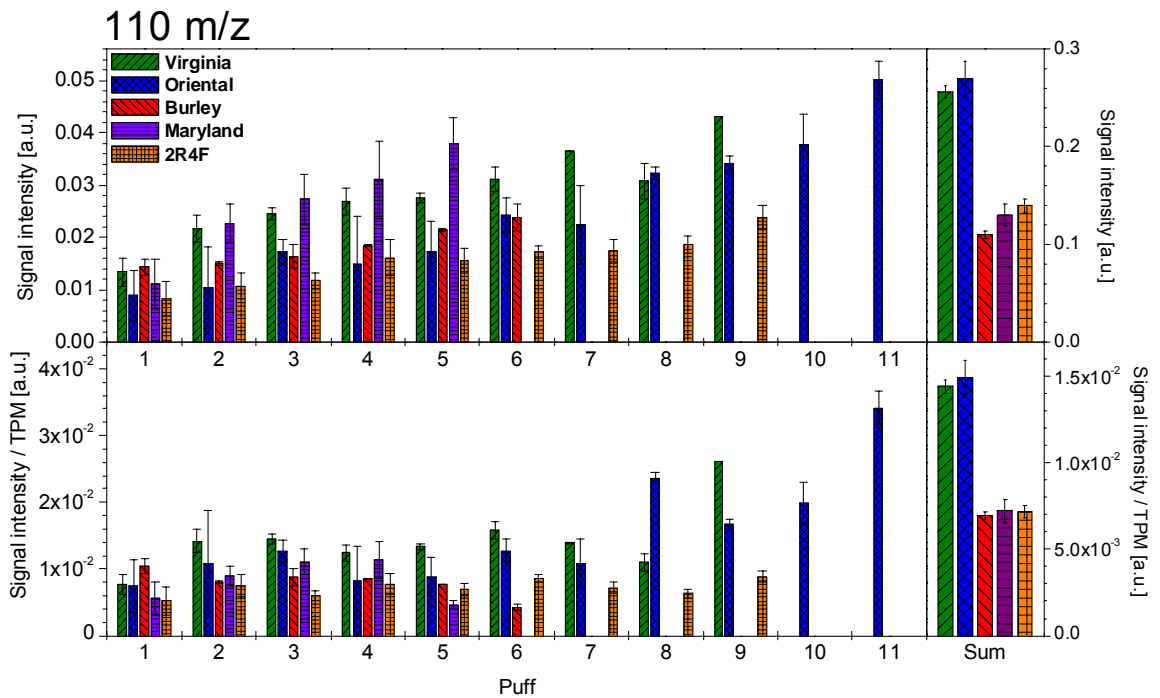
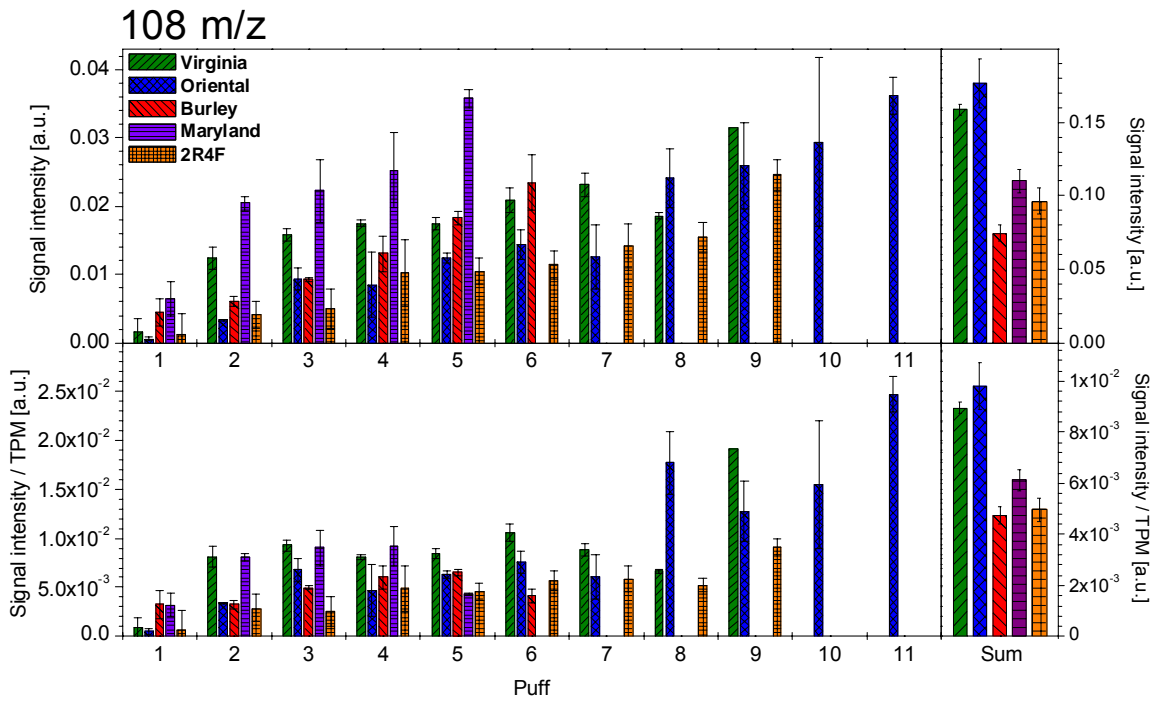


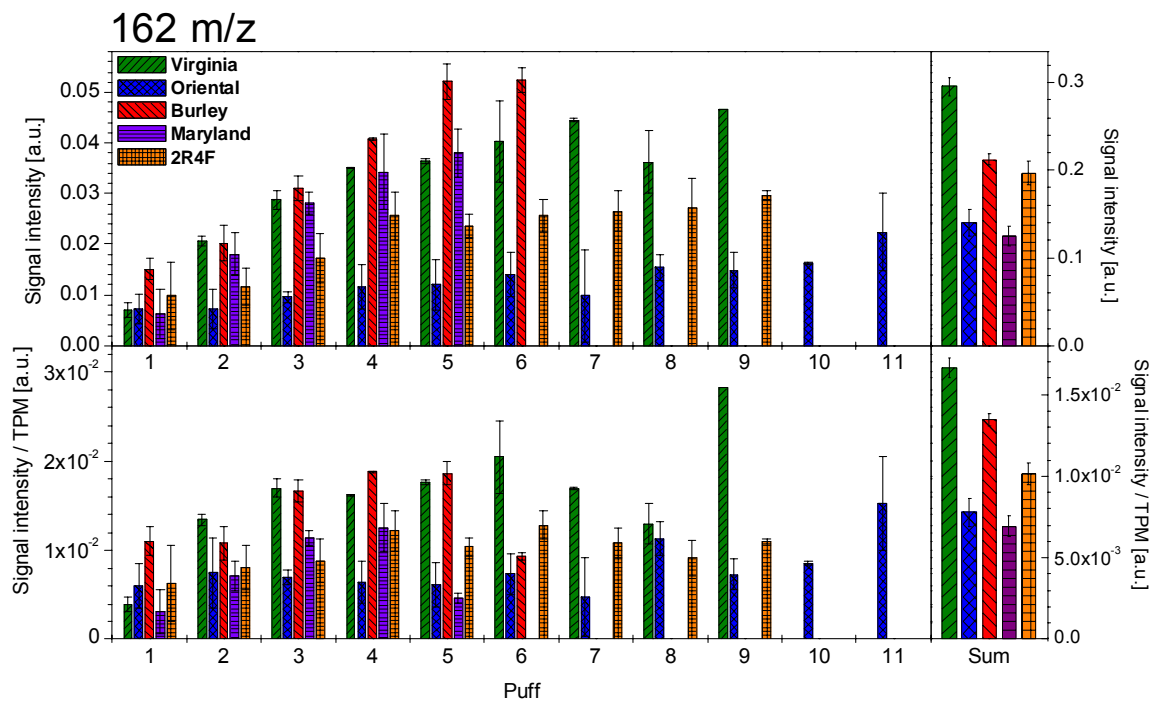




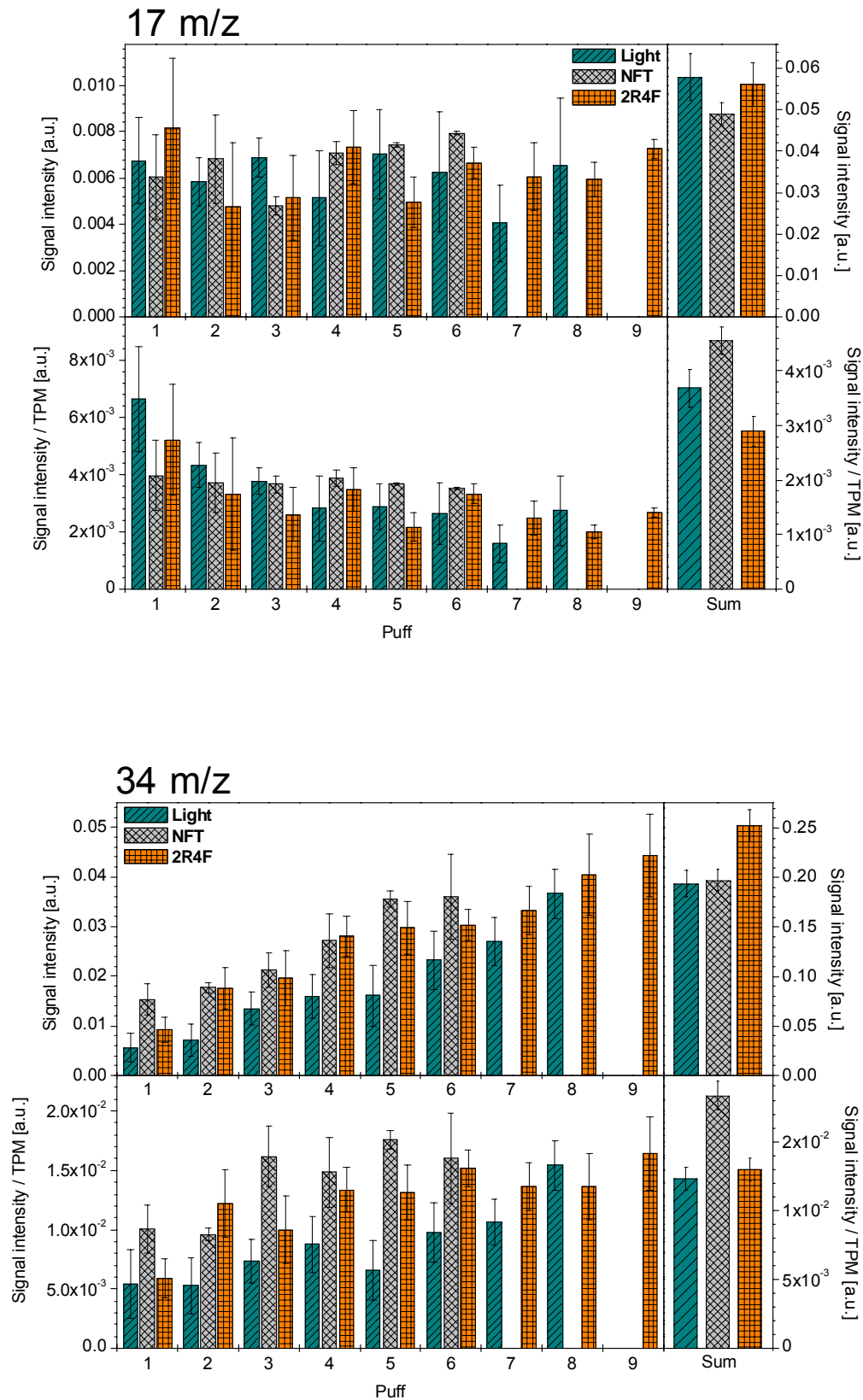


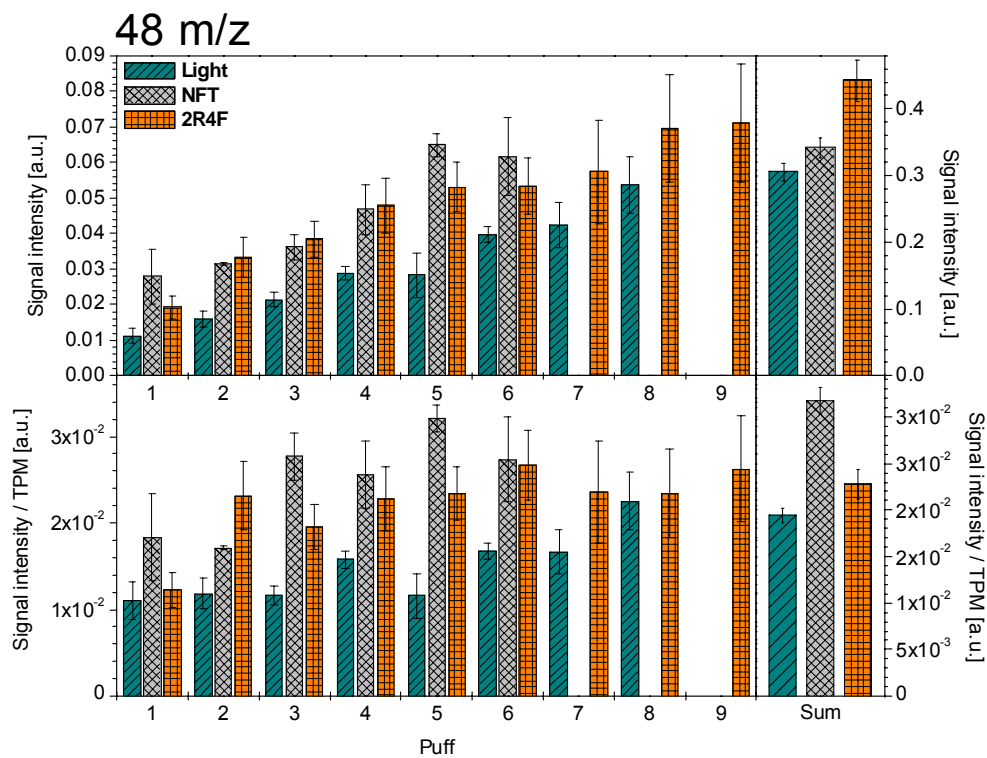
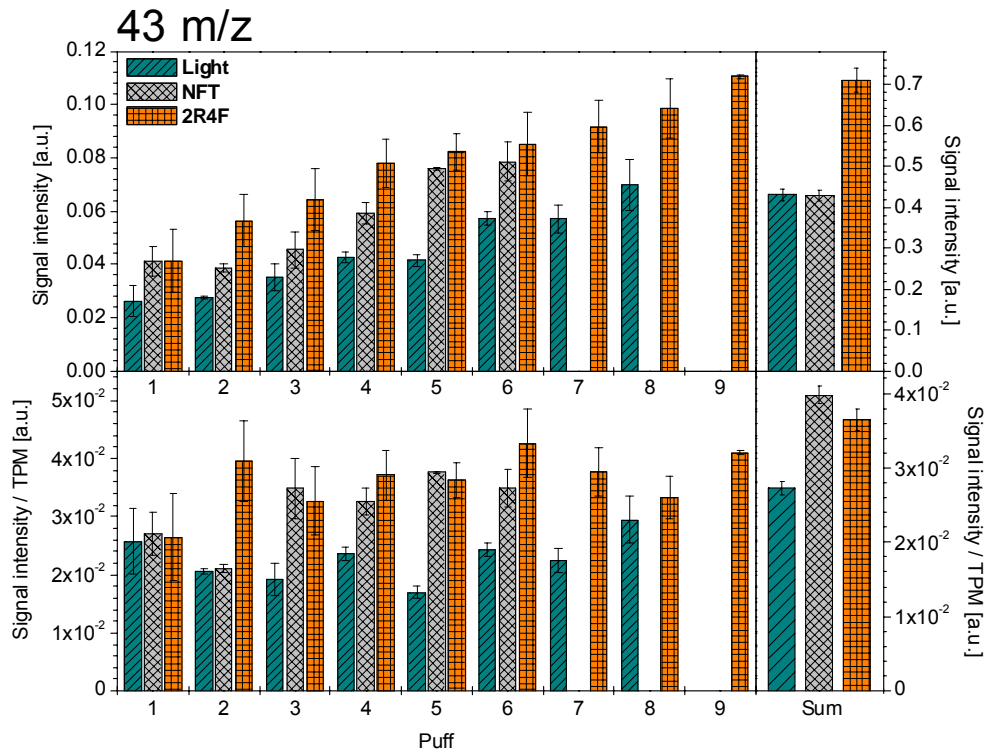


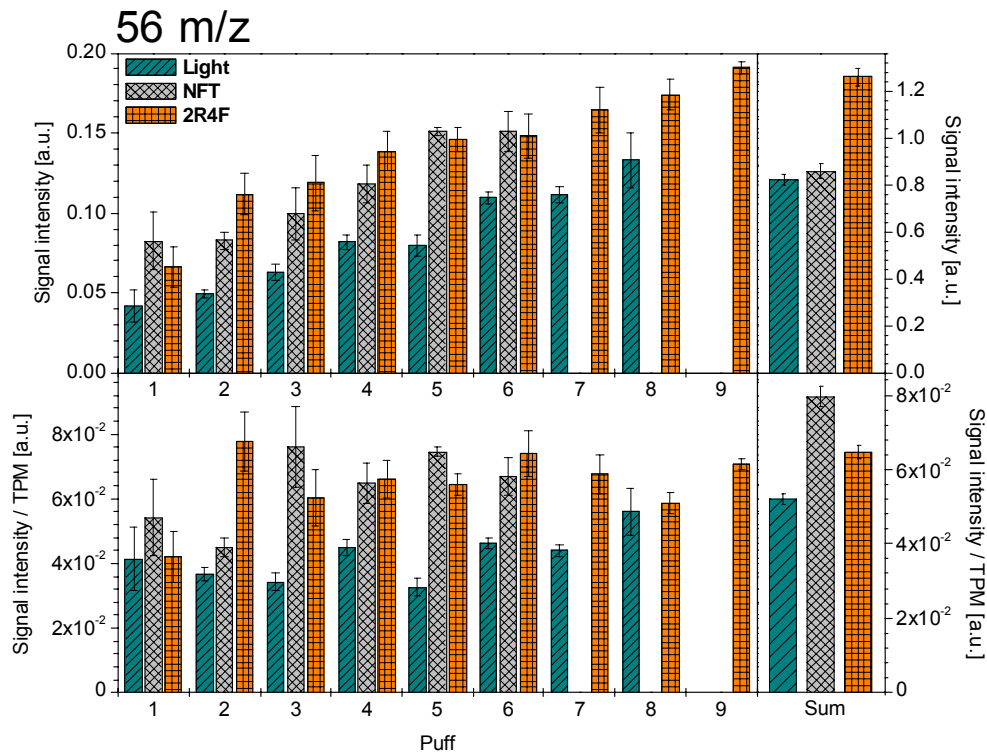
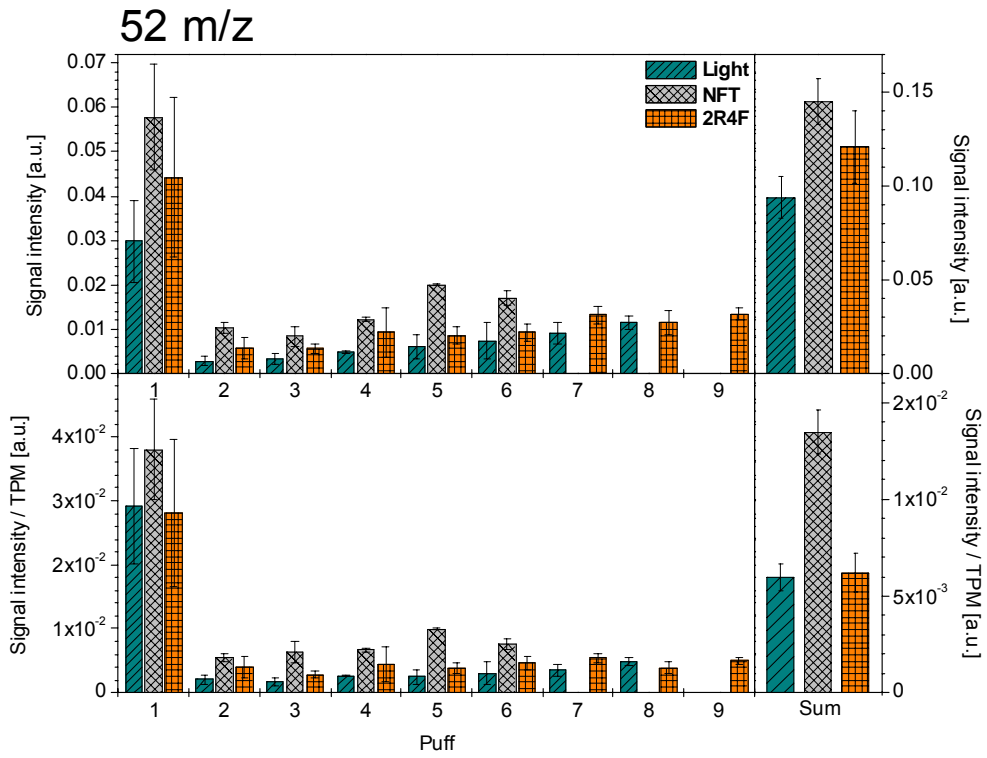




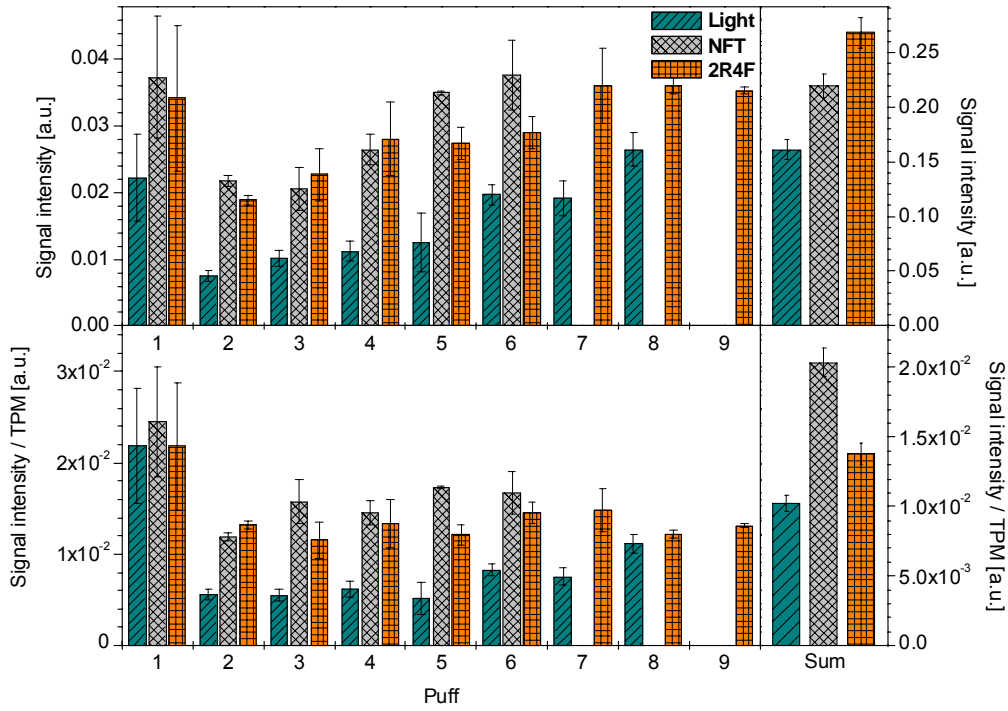
## 6.1.2. Different cigarette types compared to the 2R4F cigarette



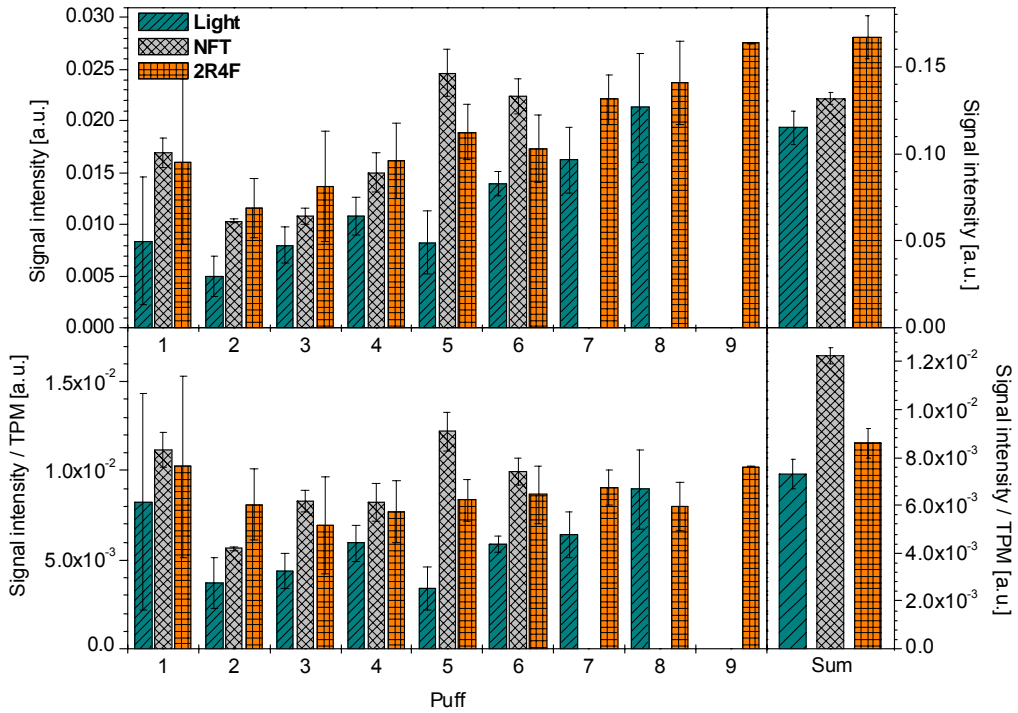


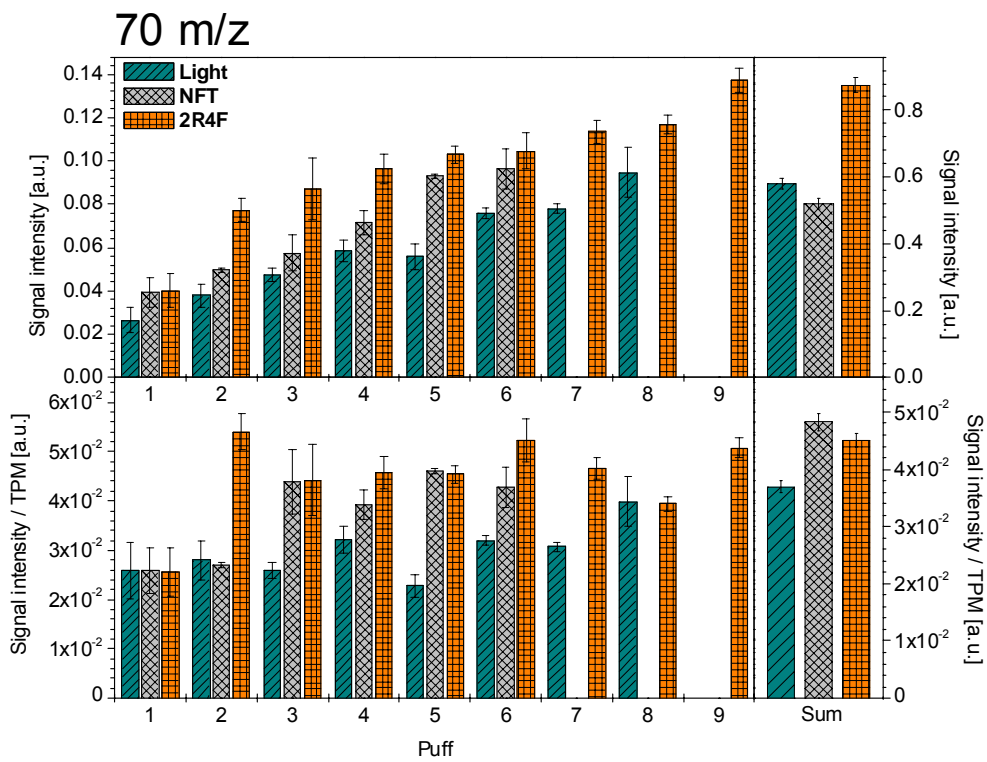
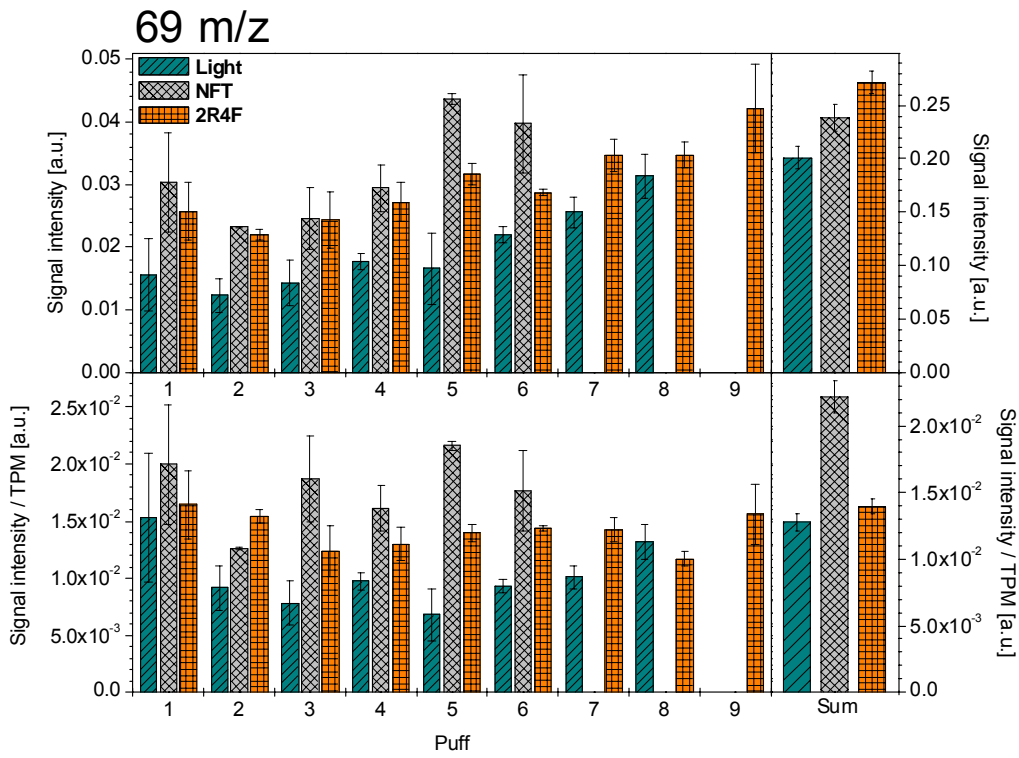


### 66 m/z

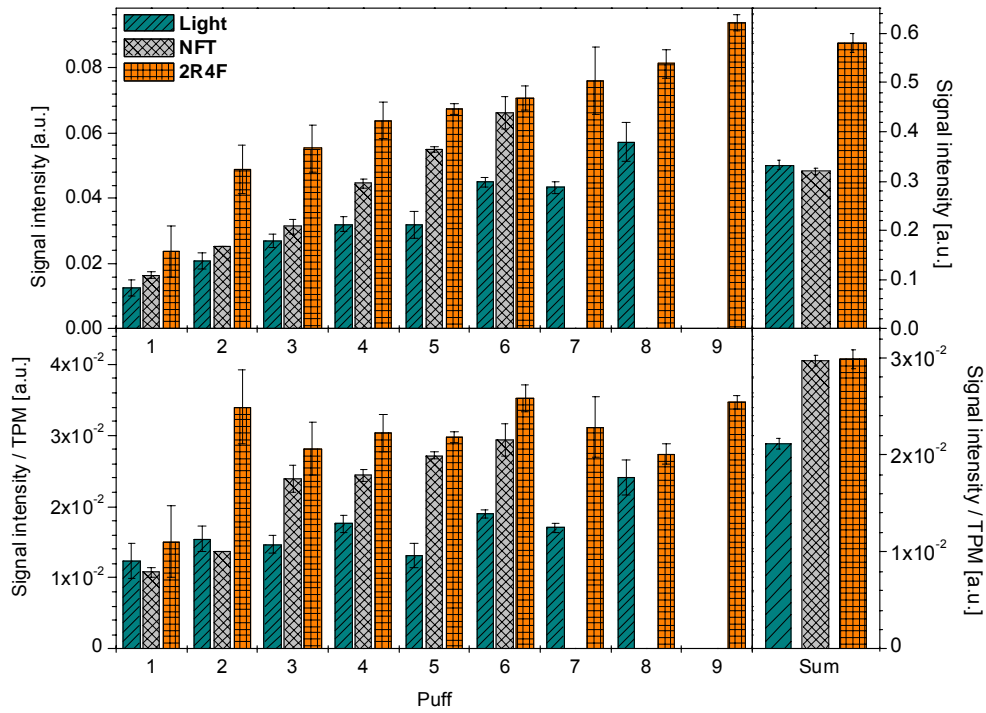


### 67 m/z

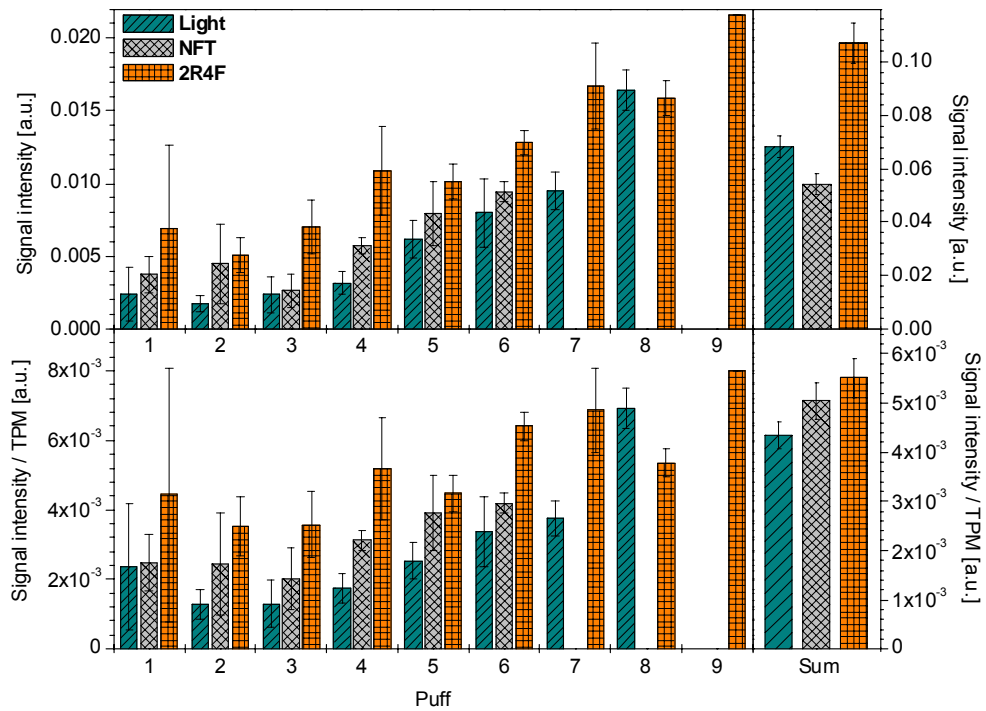


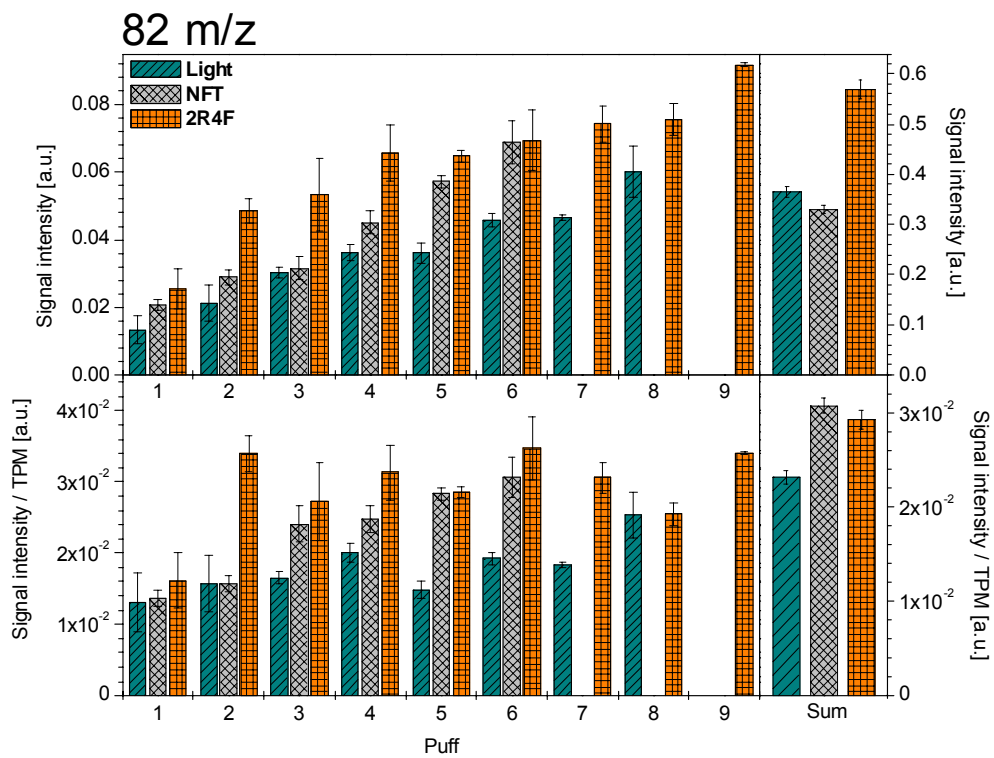
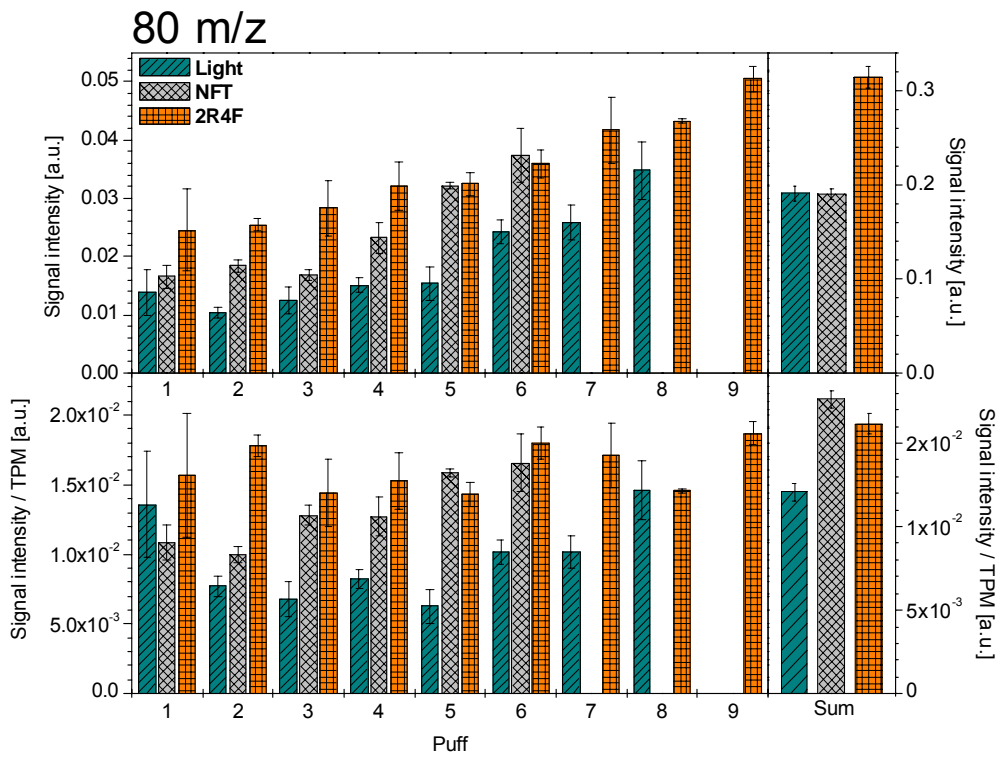


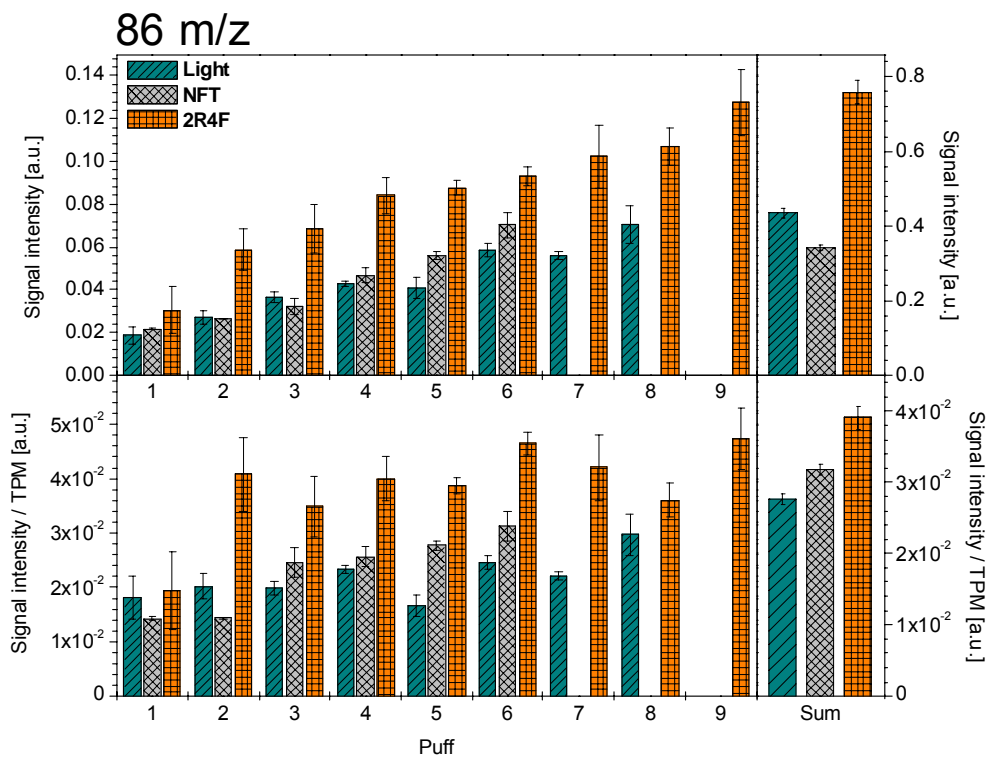
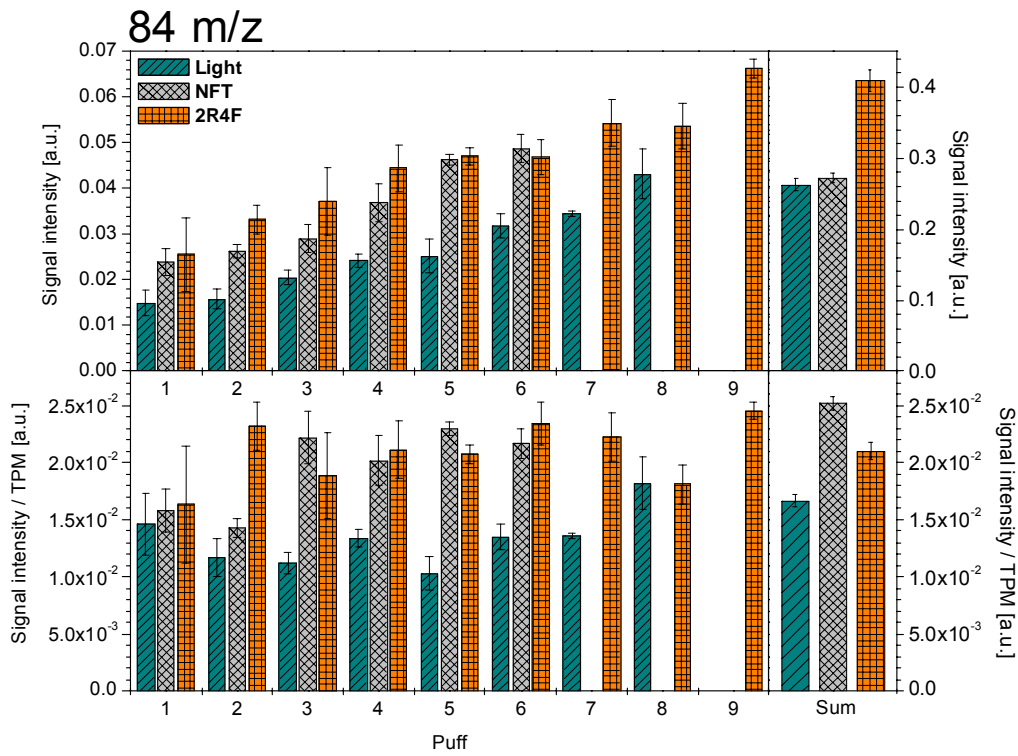
### 72 m/z

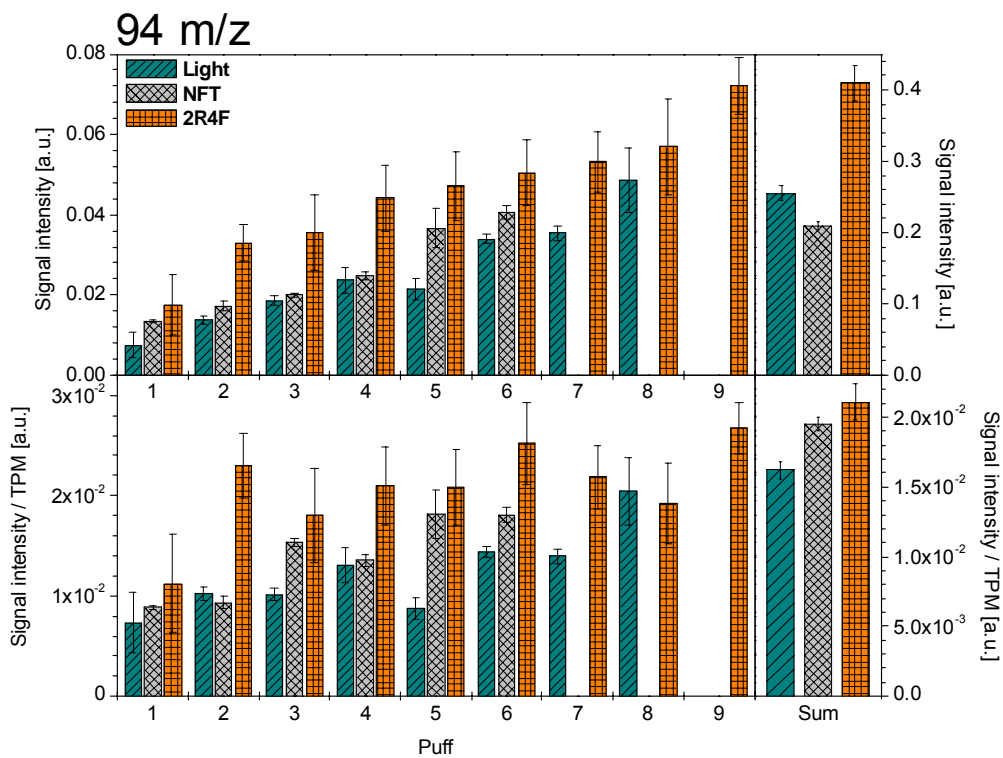
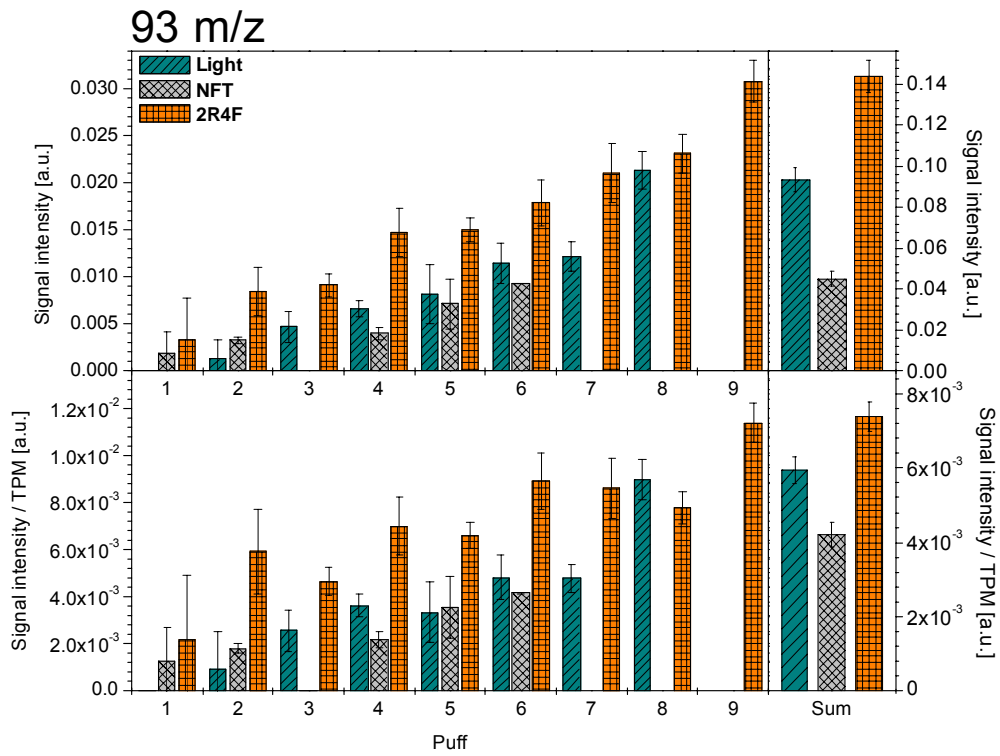


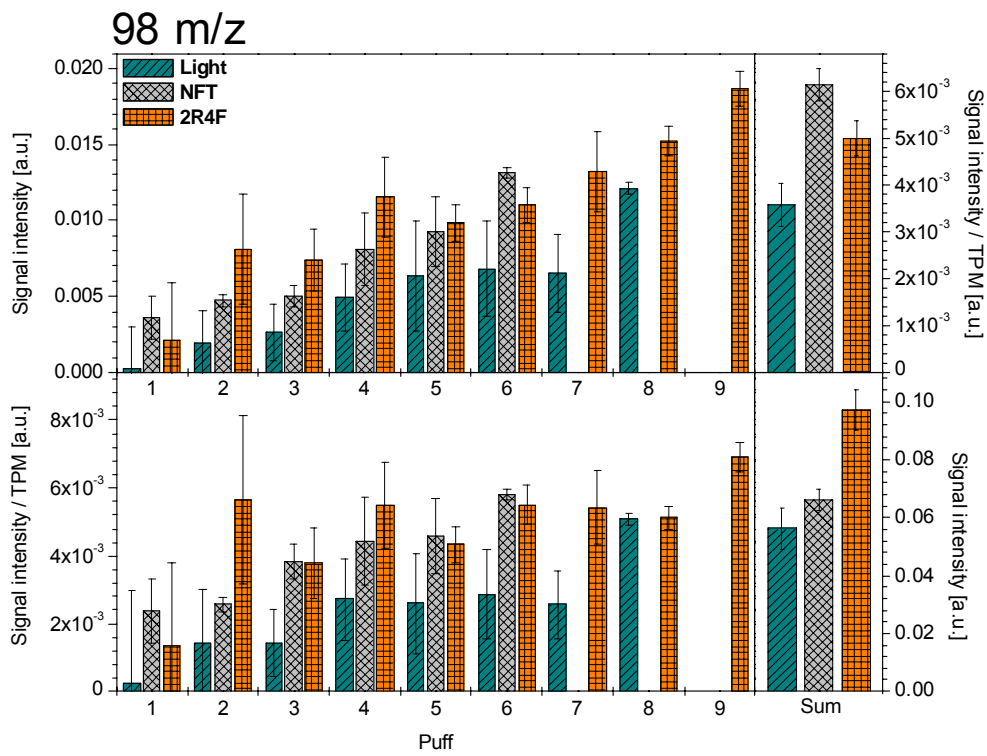
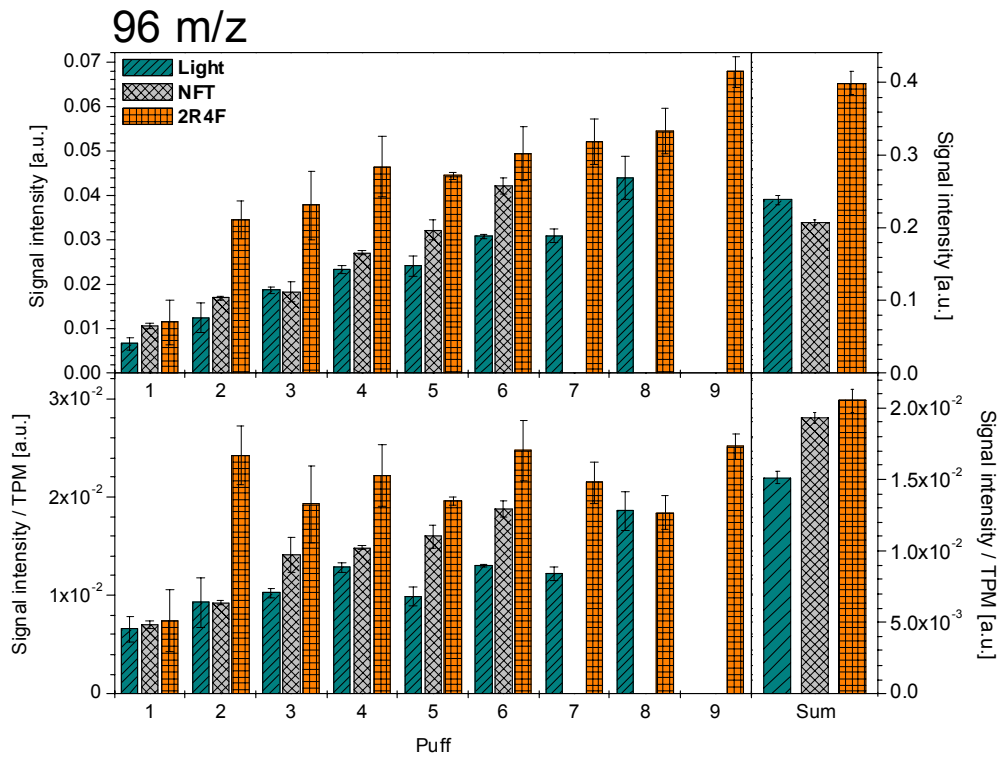
### 79 m/z



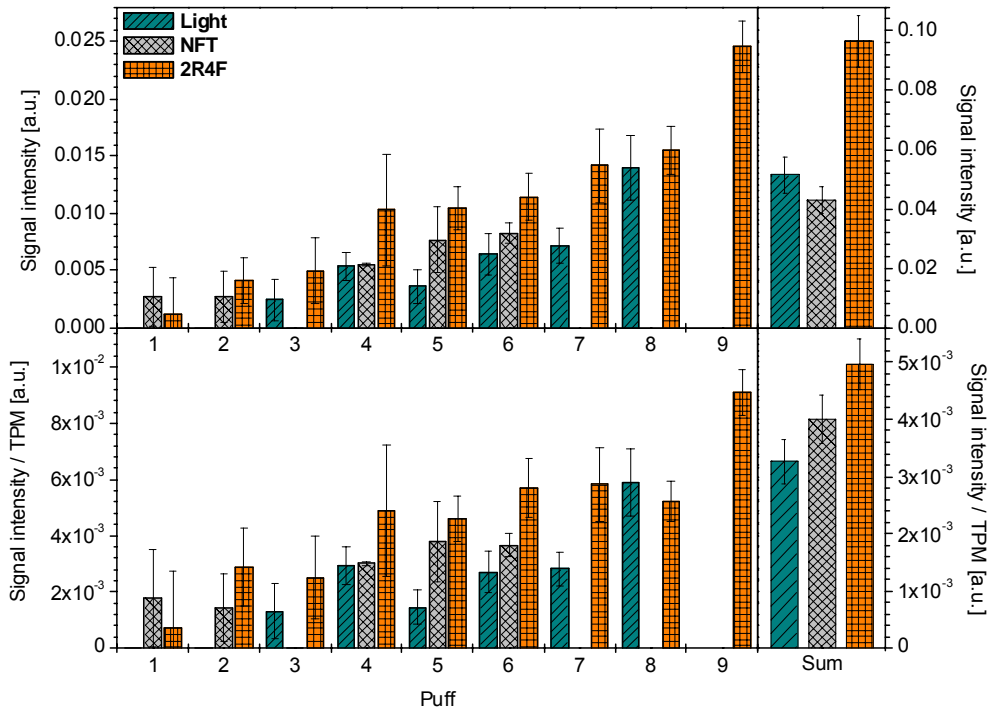




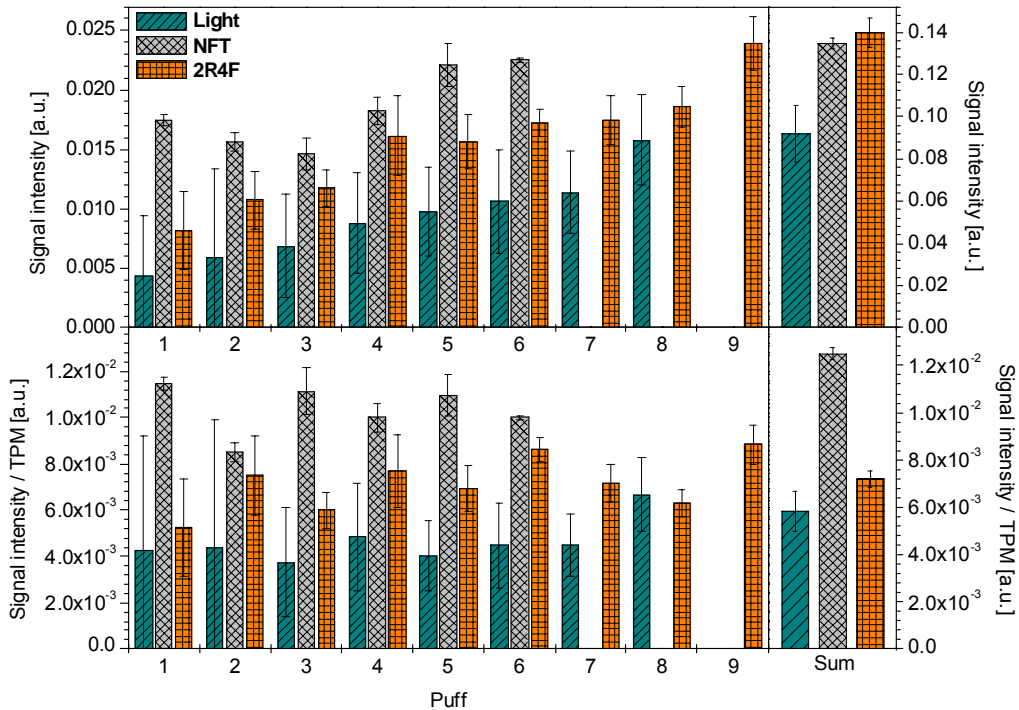


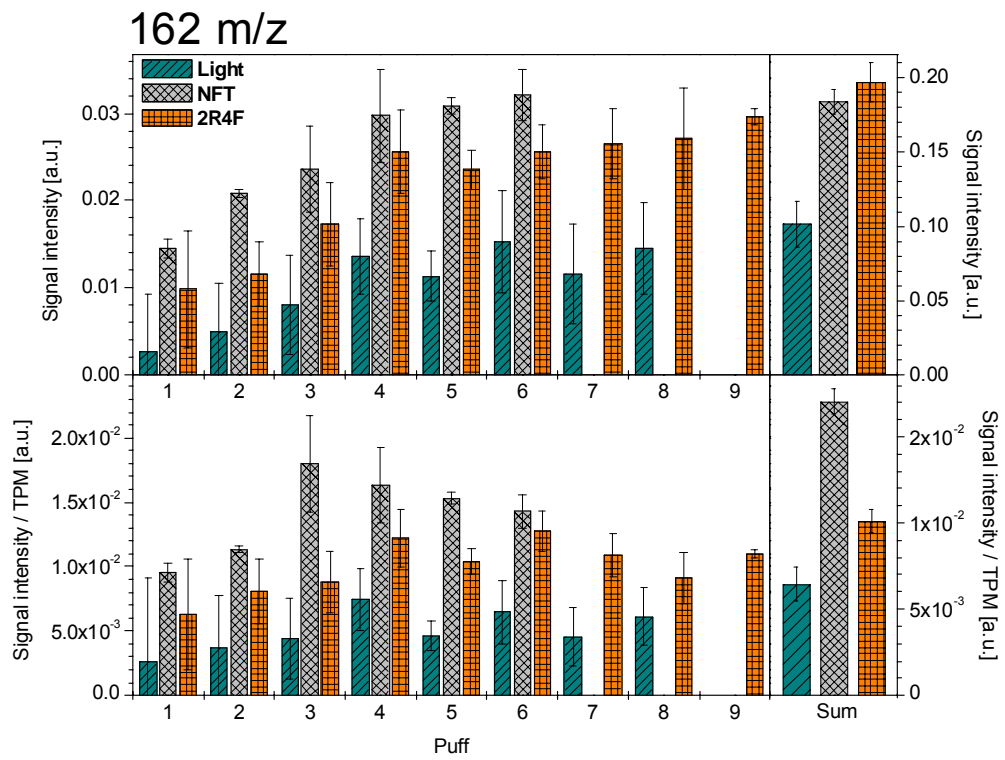


### 108 m/z



### 110 m/z





## 6.2. Tables

### 6.2.1. Cleaning puffs added to smoking puffs

Averaged yields ( $\bar{m}$ ) and standard deviations (std) of the quantitative, puff-by-puff resolved compounds in  $\mu\text{g}$ , analysed in the gas phase and whole smoke by adding the cleaning puffs to the smoking puffs

#### 2R4F: Whole smoke (8.7 puffs)

Compound	Puff	1	2	3	4	5	6	7	8	9	$\Sigma$
NO	$\bar{m}$	18.9	22.5	23.4	31.4	41.7	38.3	37.6	45.9	50	309.6
	std	4.3	3.8	1.2	2.8	2.9	1.2	4.9	5.7	2.9	13.9
Propyne	$\bar{m}$	3.3	1.2	1.1	1.4	1.5	1.4	1.8	1.8	1.9	15.4
	std	1	0.1	0.2	0.2	0.2	0.2	0.2	0.2	0.2	1.2
Propene	$\bar{m}$	13	15.4	16	18.2	19	19.4	21.9	23.4	25.9	172.3
	std	2.9	1.9	2.2	1.4	1.1	1.8	1.8	1.8	0.9	6.6
Acetaldehyde	$\bar{m}$	32.4	40.1	44.4	54.2	61.7	63.6	69.3	79.2	82.2	527.1
	std	6	6	6.1	4.6	5.1	7.4	9	6.8	3.2	26.7
Butadiene	$\bar{m}$	6.4	3	2.9	3.7	4	3.8	4.9	4.7	5.1	38.5
	std	1.3	0.3	0.6	0.8	0.4	0.3	0.6	0.4	0.1	2.2
Acetone	$\bar{m}$	11.9	21.3	24.1	28.4	30.7	32.5	35.3	38.3	42.5	265.1
	std	2.7	3	2.9	2.5	1.6	2.5	4.4	2.9	2.3	15.1
Isoprene	$\bar{m}$	41.6	36.6	37.4	38.6	47.2	41.9	48.3	50.2	55.3	397.2
	std	2.7	2.3	8.8	2.3	1.5	3.1	2.3	4	5	15.3
Benzene	$\bar{m}$	5	4.1	4.2	5.3	5	5.4	6.1	6.2	6.8	48.2
	std	1.6	0.4	0.5	0.6	0.3	0.5	0.9	0.6	0.4	3.6
Toluene	$\bar{m}$	4	7.3	7.7	9	9.5	9.9	10.8	11.6	14.6	84.5
	std	1.3	1	1.2	1.3	0.9	0.9	1.2	0.9	1.2	4.3
Xylene/Ethyl benzene	$\bar{m}$	0.5	1.2	1.1	1.6	1.6	1.8	2.4	2.9	4.6	17.8
	std	0.4	0.1	0.3	0.4	0.3	0.2	0.4	0.3	0.9	1.9

#### 2R4F: Gas phase (8.3 puffs)

Compound	Puff	1	2	3	4	5	6	7	8	9	$\Sigma$
NO	$\bar{m}$	14.3	17.9	15.6	17.9	25.1	28.1	34.3	39.1	34	226.2
	std	1.6	3	3	2.4	3.9	4.5	5.4	5.1	0	12.6
Propyne	$\bar{m}$	1.7	0.4	0.3	0.5	0.6	1	1	0.9	1.4	15.4
	std	0.3	0.1	0.2	0.1	0.1	0.1	0.2	0.1	0	1.2
Propene	$\bar{m}$	10.5	9.3	9.6	11.3	13.6	14.5	16.7	16.6	20.4	172.3
	std	1.8	1.2	1.4	2	1.2	0.9	0.9	1.9	0	6.6
Acetaldehyde	$\bar{m}$	21.6	21.7	22.2	26.3	35.2	38.6	45.4	47.8	52	310.7
	std	5.2	4.9	3.9	4.3	4.5	4.2	6.1	4.7	0	17.6
Butadiene	$\bar{m}$	3.7	0.9	0.7	1.1	1.5	2.1	2.4	2.1	3.3	17.9
	std	0.7	0.2	0.3	0.1	0.1	0.3	0.5	0.4	0	1.1
Acetone	$\bar{m}$	6.5	10.9	11.9	14.3	17.8	19	21.2	21.8	24.9	148.1
	std	1.6	2.6	2	2.7	2.1	2.1	2.8	2.4	0	9.6
Isoprene	$\bar{m}$	30.7	18.8	18.4	21.6	24.5	28.8	34.8	31.1	41.5	250.2
	std	5.7	4	3.3	3.8	3.9	2.2	2.3	7.3	0	13.7
Benzene	$\bar{m}$	1.6	1.7	1.6	2	2.5	2.7	3.2	3.2	4	22.5
	std	0.6	0.2	0.3	0.4	0.4	0.2	0.3	0.5	0	1.7
Toluene	$\bar{m}$	1	2.7	3	3.3	4.2	4.5	5.2	5.8	7.4	37.1
	std	0.2	0.5	0.9	0.6	0.8	0.4	0.6	0.6	0	3.1
Xylene/Ethyl benzene	$\bar{m}$	0	0	0	0	0	0	0	0.3	1	1.3
	std	0	0	0	0	0	0	0	0.3	0	0.3

## Burley: Whole smoke (6.0 puffs)

Compound	Puff	1	2	3	4	5	6	$\Sigma$
NO	$\bar{m}$	20.2	28.9	32.7	43.4	46.3	56.9	228.3
	std	1.9	1.3	1.1	4.2	1.9	6.3	10.3
Propyne	$\bar{m}$	2.8	1.1	1.1	1.5	1.6	1.9	10.0
	std	0.3	0.1	0.2	0.1	0	0.1	0.5
Propene	$\bar{m}$	9.8	10.3	12.1	14.9	17	19.5	83.7
	std	1.9	0.2	0.8	0.9	0.5	0.6	2.9
Acetaldehyde	$\bar{m}$	28.5	36.4	39.8	50.9	57.6	66.5	279.7
	std	2	4	4.4	2.7	3.3	3.1	12.7
Butadiene	$\bar{m}$	5.5	2.8	2.8	3.7	4.2	4.9	24.0
	std	1	0.2	0.6	0.3	0.1	0.4	1.4
Acetone	$\bar{m}$	13.6	19.9	23.4	27.5	33	39.6	157.1
	std	2	1.1	1.9	1.9	1.7	2.7	8.5
Isoprene	$\bar{m}$	46.4	29.4	30.4	42.2	46.7	51.9	247.0
	std	13.9	1.6	0.8	3.3	3	1.4	15.7
Benzene	$\bar{m}$	4.6	3.4	4	4.7	5.7	6.4	28.8
	std	0.6	0.2	0.3	0.3	0.5	0.5	1.9
Toluene	$\bar{m}$	5.6	7.2	9	10	11.8	15.1	58.6
	std	0.6	0.5	0.7	0.8	0.9	2.5	4.9
Xylene/Ethyl benzene	$\bar{m}$	1.5	1.5	1.6	1.7	2	3.6	12.0
	std	0.1	0.1	0.2	0.4	0.4	1.2	1.6

## Burley: Gas phase (6.0 puffs)

Compound	Puff	1	2	3	4	5	6	$\Sigma$
NO	$\bar{m}$	20.4	17.5	22	34.2	38.6	45.8	178.5
	std	2.1	1	3	4.9	9.4	9.4	15.5
Propyne	$\bar{m}$	1.6	0.4	0.5	0.7	0.8	1.1	5
	std	0.4	0.1	0.3	0.3	0.3	0.2	0.7
Propene	$\bar{m}$	10.1	6.5	9	10.6	12.4	14.5	63
	std	1.3	0.3	1	1.5	2.8	3.1	4.9
Acetaldehyde	$\bar{m}$	27.2	18.2	24.1	30.6	35.8	45.7	181.6
	std	3.2	2.1	3.2	2.6	8.5	10.9	16.2
Butadiene	$\bar{m}$	4	0.7	1.1	1.4	1.9	2.2	11.3
	std	1	0.3	0.8	0.7	1.2	0.9	2.1
Acetone	$\bar{m}$	11.9	11.3	14.8	17.9	20.2	23.7	99.8
	std	2	0.9	2.2	2.3	5.2	5.9	9.8
Isoprene	$\bar{m}$	34.2	17.7	22.5	27.8	30.7	34.6	167.4
	std	6.1	0.8	3.2	3.5	6.7	8.2	13.7
Benzene	$\bar{m}$	2.7	1.5	1.9	2.3	2.5	3.6	14.5
	std	0.7	0.2	0.6	0.7	1.1	1.2	2.1
Toluene	$\bar{m}$	3.9	3.6	4.2	4.6	5.5	8	29.8
	std	0.8	0.6	0.9	0.8	1.5	1.8	3.4
Xylene/Ethyl benzene	$\bar{m}$	0	0	0	0	0	0.9	0.9
	std	0	0	0	0	0	0.6	0.6



## Oriental: Whole smoke (11.0 puffs)

Compound	Puff	1	2	3	4	5	6	7	8	9	10	11	Σ
NO	$\bar{m}$	9.2	6.1	8.9	10.4	10.8	12	10.8	14.3	15.8	14.6	17.9	131.0
	std	0.5	0.9	0.3	1.3	1.5	0.5	1.2	1.6	0.5	1.5	1.3	5.2
Propyne	$\bar{m}$	3.4	0.7	0.9	0.9	1	1.3	1	1.7	1.7	1.5	1.8	15.9
	std	0.8	0.2	0	0.3	0.2	0.1	0.3	0.1	0.3	0.4	0.1	1.2
Propene	$\bar{m}$	13.7	6.9	11.4	10.1	13.9	15.8	13	20.3	20.3	19	23.1	167.7
	std	1.5	2.6	0.3	3.9	2.1	0.7	2.5	0.5	2.7	2	0.5	7.7
Acetaldehyde	$\bar{m}$	27.5	15.7	23.9	21.7	28	33.3	26.7	45.3	43.8	37.2	54.7	357.7
	std	3.7	6.9	2.1	9	5.2	3.9	8.4	2.8	6.4	4.2	2.2	22.4
Butadiene	$\bar{m}$	6.7	1.4	2.2	2	2.7	3	2.3	4.3	4.1	3.6	4.6	36.9
	std	1.5	0.6	0.3	0.9	0.7	0.1	0.8	0.1	0.6	0.8	0.1	2.6
Acetone	$\bar{m}$	11.2	9.4	15.9	13.9	18.5	20.7	17.1	27.5	28.6	23.9	32.2	218.7
	std	1.1	3.9	1.6	6.4	3.2	1.6	4	1.7	4	2.3	1.6	14.9
Isoprene	$\bar{m}$	37.3	18.9	22.9	21.2	27.4	35.3	27.3	41.7	40.6	34.2	45.1	351.9
	std	7.4	9.5	1.3	10.2	6.8	7	9.2	1.8	7.7	9.2	4.8	25.8
Benzene	$\bar{m}$	5.5	2.1	2.9	2.8	3.6	3.8	3.4	5.6	5.5	5	6	46.4
	std	1.2	0.9	0.3	1.4	0.6	0.2	1.1	0.4	0.8	0.6	0.4	3.8
Toluene	$\bar{m}$	4.6	4.4	6.6	5.3	6.9	7.5	7.3	10.9	10.4	10.5	12.7	87.1
	std	0.4	1.2	0.6	2.1	0.5	0.6	1.4	1.2	1.9	2.3	0.9	7.5
Xylene/Ethyl benzene	$\bar{m}$	0.9	1.2	1.8	1.3	1.5	1.7	2.2	2.9	3.3	3.8	4.7	25.5
	std	0.2	0.2	0.2	0.4	0.1	0.2	0.5	0.3	0.5	0.9	0.4	2.5

## Oriental: Gas phase (10.0 puffs)

Compound	Puff	1	2	3	4	5	6	7	8	9	10	Σ
NO	$\bar{m}$	5.7	5.6	6	5.8	5.8	7.7	8	8.8	11.7	14	79.1
	std	1.5	1.4	1.3	0.3	1.9	0.4	0.8	1.2	1.4	2.6	5.1
Propyne	$\bar{m}$	2.4	0.4	0.2	0.4	0.4	0.6	0.6	0.9	1.1	1.3	8.3
	std	0.7	0.3	0.1	0	0.2	0.1	0.1	0.1	0.1	0.4	0.9
Propene	$\bar{m}$	13	7.9	7.2	9.3	9.8	11.8	13.9	15	18.2	19.8	125.8
	std	2	1.2	0.9	0.6	1.4	0.9	1.5	3.2	4	6	9
Acetaldehyde	$\bar{m}$	20.5	15	11.7	16.3	17.8	23.5	25.8	29.3	34.7	37.3	231.8
	std	3.3	3.1	1.4	1.3	3	3.2	2.4	6	9.2	8.2	17.5
Butadiene	$\bar{m}$	5.1	1	0.6	1	0.9	1.6	1.8	2	2.8	3.1	19.9
	std	1.6	0.7	0.3	0.1	0.6	0.2	0.4	0.8	0.5	1.4	2.6
Acetone	$\bar{m}$	7.9	10.2	8.9	11.6	11.5	14.8	16.5	18.5	21.1	21.6	142.5
	std	1.9	2.1	1.5	0.7	2.4	1.3	1.5	5.2	7.1	6.2	13.5
Isoprene	$\bar{m}$	29.6	16.4	12.7	16.9	19.6	21.3	23.9	25.7	31.5	33.8	231.4
	std	8.6	3.8	1.6	1.6	4.6	2.7	4.4	4.4	6.8	11.5	19.2
Benzene	$\bar{m}$	3.3	1.8	1.2	1.7	1.5	2	2.4	2.7	3.5	3.7	23.9
	std	1.8	0.7	0.5	0.3	0.7	0.2	0.5	1.1	1.4	1.5	3.5
Toluene	$\bar{m}$	2.8	3.8	3.2	3.5	3.1	3.8	4.9	5.6	7.1	8.2	46.2
	std	1.3	1	0.9	0.3	1.1	0.3	0.8	1.5	2.4	2.5	5.4
Xylene/Ethyl benzene	$\bar{m}$	0	0	0	0	0	0	0.5	0.7	1.2	2.3	4.1
	std	0	0	0	0	0	0	0.3	0.8	1.1	1.4	2.4

## Maryland: Whole smoke (5.0 puffs)

Compound	Puff	1	2	3	4	5	$\Sigma$
NO	$\bar{m}$	16.8	19.1	19.3	19.9	28.7	103.8
	std	2.4	1.3	2	1.4	2.8	5.4
Propyne	$\bar{m}$	3.4	1.9	2	2.1	2.8	12.2
	std	0.6	0.3	0.3	0.2	0.2	0.8
Propene	$\bar{m}$	16.1	16.8	18.9	20.8	26.3	98.9
	std	1.9	0.8	1.3	0.9	0.8	3.4
Acetaldehyde	$\bar{m}$	56.7	66.5	75.1	80.8	106.2	385.4
	std	6.8	4.2	4.8	5	5.4	17.7
Butadiene	$\bar{m}$	8.1	5.3	5.5	5.8	7.9	32.6
	std	1.2	0.5	0.8	0.4	0.6	1.9
Acetone	$\bar{m}$	23.7	31.9	35.2	38	48	176.8
	std	3.3	1.7	3.1	2.7	3.1	10.1
Isoprene	$\bar{m}$	54.7	48	50.1	56.8	63.2	272.9
	std	8.2	6.9	4.6	2	3.8	13.8
Benzene	$\bar{m}$	6.5	5.2	5.9	6.3	8.2	32.0
	std	1.1	0.4	0.6	0.6	0.7	2.4
Toluene	$\bar{m}$	7.8	10.3	11.2	12.3	16.6	58.2
	std	1.5	0.8	1.3	1	1.7	4.7
Xylene/Ethyl benzene	$\bar{m}$	1.9	2.8	2.8	3.3	5.5	16.3
	std	0.5	0.4	0.5	0.3	1.2	1.9

## Maryland: Gas phase (5.0 puffs)

Compound	Puff	1	2	3	4	5	$\Sigma$
NO	$\bar{m}$	9.8	7.7	11.5	16.8	16.1	62
	std	2	1.2	1.3	2.4	3.1	5
Propyne	$\bar{m}$	2.5	0.6	0.6	1.2	1.4	6.3
	std	0.4	0.3	0.1	0.1	0.3	0.6
Propene	$\bar{m}$	13.1	10.9	13	16.7	19.5	73.2
	std	2.1	2.3	1.4	2.4	3.5	5.7
Acetaldehyde	$\bar{m}$	40.7	36.5	46.2	60.7	69.3	253.4
	std	5.4	7.6	6.8	6.1	12.4	20
Butadiene	$\bar{m}$	6.1	1.8	1.9	3.3	3.9	16.9
	std	1.1	1	0.5	0.6	1.3	2.2
Acetone	$\bar{m}$	16.4	19.3	22.2	28.4	31.6	117.9
	std	2.8	4.8	3.8	4.1	6.7	11.6
Isoprene	$\bar{m}$	39.5	26.9	27.9	39.9	44.4	178.6
	std	5	7.3	4.3	4.8	8	14.1
Benzene	$\bar{m}$	4.1	2.7	3	3.7	4.4	18
	std	1.3	1.1	0.6	1.1	1.2	2.6
Toluene	$\bar{m}$	4.1	4.7	5.5	7.3	9.4	31.1
	std	1.5	1.5	1.2	1.9	2.3	4.3
Xylene/Ethyl benzene	$\bar{m}$	0	0	0	0.6	1.3	2
	std	0	0	0	0.4	0.7	1.1



## 'NFT' cigarette: Whole smoke (6.0 puffs)

Compound	Puff	1	2	3	4	5	6	$\Sigma$
NO	$\bar{m}$	18.3	14.1	15.3	19.9	27.3	25.5	120.4
	std	0.7	0.5	2.9	1.8	6	4.9	8.5
Propyne	$\bar{m}$	5	1.3	1.3	1.7	2.4	2.1	13.9
	std	1	0	0.3	0.1	0.1	0.2	1.1
Propene	$\bar{m}$	15.4	12.4	14.9	16.9	21.7	21.5	102.7
	std	3.5	0.6	2.3	2.2	0.8	2	5.3
Acetaldehyde	$\bar{m}$	28.9	25.1	33.1	43.4	58.6	60.7	249.8
	std	5.7	2.1	7.6	5.7	5.4	8.4	15.0
Butadiene	$\bar{m}$	9.7	3.5	3.9	4.6	6.5	6	34.2
	std	2.3	0.1	0.8	0.7	0.2	0.6	2.6
Acetone	$\bar{m}$	9.8	13	16.8	22.1	27.9	31.5	121.2
	std	1.7	0.9	2.4	2.2	2.3	3.9	5.9
Isoprene	$\bar{m}$	53.2	34.8	39.3	45.5	68.5	58.4	299.5
	std	17.1	2.2	8.7	10.5	2.7	9.9	24.2
Benzene	$\bar{m}$	3	2.5	2.4	3.6	4.3	5.1	20.9
	std	0.5	0.2	0.3	0.4	0.3	0.8	1.1
Toluene	$\bar{m}$	1.7	1.9	2.2	3.7	5	6.8	21.4
	std	0.4	0.2	0.2	0.3	0.5	0.5	0.9
Xylene/Ethyl benzene	$\bar{m}$	0	0	0	0.2	0.4	0.8	1.6
	std	0	0	0	0	0.2	0.1	0.5

## 'NFT' cigarette: Gas phase (6.0 puffs)

Compound	Puff	1	2	3	4	5	6	$\Sigma$
NO	$\bar{m}$	10.7	12.2	13.7	18.9	18.2	21.4	95.2
	std	1.8	3	0.9	1.7	2.9	1.5	5.8
Propyne	$\bar{m}$	2.8	0.7	0.7	1	1	1.3	7.5
	std	0.3	0.1	0.2	0.1	0.1	0.2	0.4
Propene	$\bar{m}$	12.7	11.5	14.6	15.7	15.7	17.8	88
	std	1.6	1.5	1.7	1.4	1.8	1.9	4.4
Acetaldehyde	$\bar{m}$	15.8	15.2	21.8	27.1	29.3	35.6	144.8
	std	1.6	0.8	1.2	3.8	4.7	3.7	9
Butadiene	$\bar{m}$	6.1	1.9	2.3	2.7	2.5	3.2	18.6
	std	0.6	0.1	0.2	0.3	0.3	0.6	1.1
Acetone	$\bar{m}$	3	6.8	10.3	13.3	14.9	17.2	65.5
	std	0.2	0.9	0.7	1.8	2.8	2.7	5.3
Isoprene	$\bar{m}$	29.1	24.4	30.6	32.4	36	34.7	187.2
	std	2.2	4.5	4.3	4.5	4.5	5.7	11.5
Benzene	$\bar{m}$	0	0.3	0.6	1.2	1.5	2.1	5.4
	std	0.1	0.3	0.1	0.1	0.3	0.4	0.7
Toluene	$\bar{m}$	0	0	0	0	0.6	1.3	1.9
	std	0	0	0	0	0.3	0.3	0.7
Xylene/Ethyl benzene	$\bar{m}$	0	0	0	0	0	0	0
	std	0	0	0	0	0	0	0



## Burley: Whole smoke (6.0 puffs)

Compound	Puff	1	2	3	4	5	6	Σ
NO	$\bar{m}$	13.9	20.7	24.3	32.6	36.1	44.3	171.9
	std	2.5	1	0.8	4.1	1.2	2.8	7.5
Propyne	$\bar{m}$	2.1	0.8	0.8	1.1	1.3	1.5	7.6
	std	0.4	0.1	0.1	0.1	0.1	0.1	0.5
Propene	$\bar{m}$	7.5	7.9	9.6	11.5	13.9	15.9	66.3
	std	2.2	0.2	0.5	0.9	0.9	0.9	3
Acetaldehyde	$\bar{m}$	20.7	26.9	30.5	38.3	45.8	52.6	214.9
	std	3.8	2.8	2.7	2.4	1.8	2.9	10.1
Butadiene	$\bar{m}$	4.5	2.2	2.2	3	3.6	4.1	19.5
	std	1.3	0.2	0.4	0.4	0.3	0.1	1.5
Acetone	$\bar{m}$	10.2	15.2	18.3	21.2	26.8	31.9	123.6
	std	2.6	0.8	1.2	1.5	1.6	4.3	7.9
Isoprene	$\bar{m}$	37	22.9	24.1	32.2	38.5	42.5	197.3
	std	15	1	0.7	2.8	4	3.8	16.8
Benzene	$\bar{m}$	3.7	2.8	3.3	3.8	4.9	5.5	24
	std	0.9	0.2	0.2	0.3	0.3	0.7	1.9
Toluene	$\bar{m}$	4.4	5.7	7.1	7.7	9.6	12.3	46.8
	std	0.8	0.4	0.5	0.6	0.8	3	4.5
Xylene/Ethyl benzene	$\bar{m}$	1.4	1.2	1.4	1.5	1.9	3.3	10.7
	std	0.2	0.2	0.1	0.1	0.2	1.1	1.4

## Burley: Gas phase (6.0 puffs)

Compound	Puff	1	2	3	4	5	6	Σ
NO	$\bar{m}$	11	8.5	11.9	18.7	21.7	26.7	98.6
	std	1.9	1.4	0.9	2.5	5	5.4	8.6
Propyne	$\bar{m}$	0.9	0.2	0.3	0.3	0.4	0.6	2.6
	std	0.1	0	0.1	0.1	0.1	0.1	0.3
Propene	$\bar{m}$	5.5	3.4	4.8	5.8	6.9	8.3	34.6
	std	0.7	0.4	0.4	0.6	1.4	1.8	2.7
Acetaldehyde	$\bar{m}$	13.2	8.5	11.6	14.6	18.1	23.2	89.3
	std	1.7	1.5	1.3	0.7	4.4	5.5	8.2
Butadiene	$\bar{m}$	2.3	0.5	0.7	0.9	1.1	1.4	6.9
	std	0.4	0	0.3	0.3	0.5	0.5	0.9
Acetone	$\bar{m}$	5	5.1	6.9	8.3	9.8	11.1	46.2
	std	1.2	0.7	1	1.2	2.8	3.3	5.2
Isoprene	$\bar{m}$	17.8	8.9	11.4	13.9	16.1	19.2	87.3
	std	3	0.9	1.5	1.4	3.2	4.2	6.8
Benzene	$\bar{m}$	1.3	0.8	0.9	1.1	1.2	1.6	6.9
	std	0.4	0.1	0.2	0.3	0.5	0.7	1.1
Toluene	$\bar{m}$	1.6	1.4	1.5	1.5	1.8	2.5	10.4
	std	0.6	0.1	0.3	0.3	0.7	0.9	1.5
Xylene/Ethyl benzene	$\bar{m}$	0	0	0	0	0	0	0
	std	0	0	0	0	0	0	0



## Oriental: Whole smoke (11.0 puffs)

Compound	Puff	1	2	3	4	5	6	7	8	9	10	11	$\Sigma$
NO	$\bar{m}$	5	3.7	5	6.5	6.8	8	7.4	10.2	10.9	10	13.2	86.6
	std	0.5	0.2	0.2	0.8	1	0.3	1.1	0.9	0.4	1.7	0.8	3.7
Propyne	$\bar{m}$	2.4	0.5	0.6	0.7	0.8	0.9	0.9	1.3	1.2	1.1	1.5	11.9
	std	0.7	0.2	0	0.3	0.1	0	0.3	0.1	0.2	0.4	0	1
Propene	$\bar{m}$	10.7	5.4	8.6	7.6	10.9	12.4	10.9	16.7	15.6	15.1	19.1	133.1
	std	1.2	1.9	0.4	3.3	1.2	0.3	2.4	0.5	2.2	2.9	0.6	6.7
Acetaldehyde	$\bar{m}$	18.6	11.4	17.3	15.7	20.9	25.1	21.8	35.6	32.1	28.7	43.7	270.8
	std	2.9	4.8	1.8	7	3.5	2.1	7.3	2.5	5	5.6	2.1	17.9
Butadiene	$\bar{m}$	4.8	1.3	1.6	1.7	2.3	2.5	2.2	3.7	3.3	2.9	3.9	30.2
	std	1.3	0.5	0.2	0.7	0.5	0.1	0.7	0.1	0.5	0.8	0.2	2.2
Acetone	$\bar{m}$	7.6	7.1	11.8	10.5	14.2	16.1	14.1	22.2	21.4	18.9	26.3	170.3
	std	0.9	2.9	1.4	5	2.3	0.9	3.7	1.5	3.2	3.2	1.5	12
Isoprene	$\bar{m}$	25.9	14.4	17.4	15.9	21.3	27.3	22.8	33.8	30.8	27.5	37	274.1
	std	5.8	7.1	1.5	8.2	4.8	4.6	8.2	1.4	5.9	9.1	4.9	21.2
Benzene	$\bar{m}$	4.2	1.8	2.4	2.2	3	3.1	3	4.8	4.5	4.3	5.1	38.4
	std	1.1	0.7	0.3	1.1	0.4	0.2	0.9	0.3	0.6	0.9	0.4	3.2
Toluene	$\bar{m}$	3.6	3.6	5.1	4.2	5.6	6	6.2	9.3	8.3	8.8	10.8	71.5
	std	0.4	1.1	0.5	1.7	0.4	0.6	1.3	1.1	1.5	2.4	0.9	6.4
Xylene/Ethyl benzene	$\bar{m}$	0.9	1.2	1.6	1.3	1.5	1.7	2.2	2.6	2.9	3.5	4.1	23.8
	std	0.2	0.2	0.1	0.4	0.2	0.2	0.4	0.3	0.5	1.1	0.4	2.4

## Oriental: Gas phase (10.0 puffs)

Compound	Puff	1	2	3	4	5	6	7	8	9	10	$\Sigma$
NO	$\bar{m}$	2.3	2.7	2.6	2.9	3.1	3.8	4.1	4.7	6.8	7.9	40.9
	std	0.6	0.4	0.5	0.2	0.8	0.3	0.5	0.5	0.8	0	2.2
Propyne	$\bar{m}$	1.2	0.2	0.1	0.2	0.2	0.3	0.3	0.4	0.6	0.7	4.3
	std	0.4	0.1	0.1	0	0.1	0.1	0	0.1	0.1	0	0.5
Propene	$\bar{m}$	8.8	4	3.4	4.7	4.7	6.1	6.9	7.3	10	10.9	66.8
	std	1.3	0.4	0.4	0.4	0.8	0.6	0.4	1.6	2.3	0	4.5
Acetaldehyde	$\bar{m}$	9.2	6.8	5.5	7.9	8.1	11.4	12	13.6	17.3	19	110.7
	std	1.4	1.2	0.5	0.8	1.6	1.9	0.7	2.9	4.5	0	8.3
Butadiene	$\bar{m}$	2.5	0.6	0.4	0.7	0.6	0.9	0.9	1	1.6	1.7	10.9
	std	0.8	0.2	0.1	0.1	0.2	0.1	0.1	0.3	0.3	0	1.2
Acetone	$\bar{m}$	3.1	4.6	4	5.4	5.1	6.8	7.2	8	10.1	10.6	65
	std	0.5	0.7	0.5	0.4	1.1	0.7	0.4	2.4	3.5	0	6.1
Isoprene	$\bar{m}$	14.1	7.6	6.1	8.3	9.2	10.5	11.2	11.9	16.7	18	113.5
	std	4.1	1.5	0.5	0.8	1.9	0.7	1.2	1.8	3.5	0	8.8
Benzene	$\bar{m}$	1.6	1	0.6	1	0.7	0.9	1.1	1.2	1.8	1.8	11.7
	std	0.9	0.2	0.2	0.1	0.3	0.1	0.1	0.5	0.7	0	1.6
Toluene	$\bar{m}$	1.1	1.6	1.3	1.4	1.1	1.4	1.6	1.9	2.7	3.4	17.5
	std	0.5	0.4	0.3	0.2	0.4	0.1	0.2	0.7	1.1	0	2.2
Xylene/Ethyl benzene	$\bar{m}$	0	0	0	0	0	0	0.2	0.3	0.5	0.8	1.6
	std	0	0	0	0	0	0	0.1	0.3	0.4	0	0.9

## Maryland: Whole smoke (5.0 puffs)

Compound	Puff	1	2	3	4	5	$\Sigma$
NO	$\bar{m}$	10.5	12.8	13.1	13.5	20.5	70.4
	std	2.4	0.7	1.7	1.7	3.1	5
Propyne	$\bar{m}$	2.6	1.4	1.5	1.6	2	9.1
	std	0.6	0.2	0.3	0.2	0.2	0.8
Propene	$\bar{m}$	12.3	13.1	14.6	16.2	20.1	76.4
	std	2.1	0.7	1.1	0.7	1.7	3.4
Acetaldehyde	$\bar{m}$	40.9	51.1	56.6	61.4	79.1	289.1
	std	7.4	3.7	4.2	4.5	7.4	16.1
Butadiene	$\bar{m}$	6.2	4.1	4.4	4.6	6.1	25.5
	std	1.4	0.4	0.8	0.5	0.8	2
Acetone	$\bar{m}$	17.2	24.9	27	29.2	36.1	134.3
	std	3.5	2	2.5	2.5	4.4	9.1
Isoprene	$\bar{m}$	41.4	37.7	38.6	44	47.7	209.4
	std	9	5.1	5.1	2.7	1.6	12.7
Benzene	$\bar{m}$	5.2	4.2	4.7	5.2	6.5	25.7
	std	1.1	0.3	0.5	0.5	0.8	2.1
Toluene	$\bar{m}$	5.9	8.3	8.9	9.9	12.9	45.7
	std	1.5	0.6	1.1	0.8	1.8	4
Xylene/Ethyl benzene	$\bar{m}$	1.4	2.3	2.4	2.6	4.2	12.9
	std	0.7	0.2	0.5	0.3	1	1.7

## Maryland: Gas phase (5.0 puffs)

Compound	Puff	1	2	3	4	5	$\Sigma$
NO	$\bar{m}$	4.5	3.9	6.1	9.2	9.5	33.2
	std	1	0.4	0.9	1.2	2	2.9
Propyne	$\bar{m}$	1.3	0.3	0.3	0.6	0.8	3.3
	std	0.3	0.2	0	0.1	0.1	0.4
Propene	$\bar{m}$	7.1	5.6	6.9	9.6	11.2	40.4
	std	1.3	1.3	0.8	1.3	2	3.2
Acetaldehyde	$\bar{m}$	18.1	17.3	22.2	31.2	35.9	124.7
	std	3.1	3.5	4.4	3.7	5.9	10.4
Butadiene	$\bar{m}$	3.2	1	1.2	1.9	2.3	9.4
	std	0.7	0.4	0.2	0.3	0.6	1.1
Acetone	$\bar{m}$	6.3	8.8	10.3	14.1	15.7	55.2
	std	1.3	2.2	2.1	2.2	3.2	5.6
Isoprene	$\bar{m}$	18.9	14.1	14.4	20.9	23.9	92.1
	std	2.5	4.3	2.4	2.9	4.6	8
Benzene	$\bar{m}$	2	1.3	1.6	1.9	2.3	9.1
	std	0.8	0.5	0.3	0.5	0.6	1.3
Toluene	$\bar{m}$	1.6	1.9	2.1	2.7	3.3	11.6
	std	0.6	0.6	0.5	0.8	0.9	1.8
Xylene/Ethyl benzene	$\bar{m}$	0	0	0	0.1	0.4	0.5
	std	0	0	0	0.1	0.3	0.3



## 'NFT' cigarette: Whole smoke (6.0 puffs)

Compound	Puff	1	2	3	4	5	6	$\Sigma$
NO	$\bar{m}$	11.9	9.3	10.7	14.4	19.8	17.8	103.7
	std	1	0.7	2.4	1.7	5.5	4	8
Propyne	$\bar{m}$	3.8	1	1	1.3	1.8	1.5	12.4
	std	1.1	0	0.2	0.1	0.1	0.2	1.2
Propene	$\bar{m}$	11.3	9.7	12	13.9	17.1	16.8	100.3
	std	3.1	0.5	2.1	2.1	1.1	1.7	5.2
Acetaldehyde	$\bar{m}$	20.1	18.5	24.8	34.1	44.3	44.3	237.2
	std	5	1.6	6.6	5.5	5.6	6.2	15.6
Butadiene	$\bar{m}$	7.3	2.8	3.1	3.9	5.2	4.8	32.5
	std	2.2	0.1	0.6	0.7	0.3	0.5	2.6
Acetone	$\bar{m}$	6.8	9.8	13.1	17.7	21.5	23.7	120.3
	std	1.5	0.6	2.4	2.2	2.4	2.9	7.7
Isoprene	$\bar{m}$	37.9	27.1	30.5	36.9	52.3	44.2	280.5
	std	13.8	1.7	7.7	9	3.4	7.1	20.9
Benzene	$\bar{m}$	2.2	2.1	2.2	2.9	3.6	4.1	22.1
	std	0.6	0.1	0.3	0.4	0.4	0.5	1.7
Toluene	$\bar{m}$	1.4	1.4	1.9	3.2	4.1	5.5	25.9
	std	0.2	0.1	0.1	0.2	0.3	0.4	1.9
Xylene/Ethyl benzene	$\bar{m}$	0.4	0.2	0.1	0.3	0.5	0.8	4.2
	std	0.1	0.1	0.1	0	0.2	0.1	0.5

## 'NFT' cigarette: Gas phase (6.0 puffs)

Compound	Puff	1	2	3	4	5	6	$\Sigma$
NO	$\bar{m}$	4.7	6.4	7.5	10.2	10	12.5	51.4
	std	1	1	0.6	1.4	1.9	1.2	3.4
Propyne	$\bar{m}$	1.3	0.3	0.4	0.5	0.5	0.7	3.7
	std	0.1	0	0	0.1	0.1	0.1	0.2
Propene	$\bar{m}$	6	6.2	8.1	8.8	8.9	10.3	48.2
	std	0.7	1.2	1.1	1	1	1.7	2.9
Acetaldehyde	$\bar{m}$	6.4	6.5	9.8	12.7	13.8	16.9	66.2
	std	0.7	0.7	0.6	1.9	2	2.4	4.5
Butadiene	$\bar{m}$	2.7	1	1.2	1.4	1.3	1.7	9.4
	std	0.3	0.1	0.1	0.1	0.2	0.3	0.5
Acetone	$\bar{m}$	1	3.1	5.1	6.7	7.4	8.5	31.9
	std	0.1	0.5	0.4	0.9	1.3	1.4	2.6
Isoprene	$\bar{m}$	11	11.9	14.8	15.9	17.7	17.6	88.9
	std	0.4	2.7	2.2	2.8	2.1	3.5	6.4
Benzene	$\bar{m}$	0	0.2	0.5	0.8	0.8	1.1	3.3
	std	0	0.1	0.1	0.1	0.1	0.2	0.3
Toluene	$\bar{m}$	0	0	0	0	0.3	0.4	0.7
	std	0	0	0	0	0.1	0.1	0.2
Xylene/Ethyl benzene	$\bar{m}$	0	0	0	0	0	0	0
	std	0	0	0	0	0	0	0

## 7. References

1. World Health Organization - Regional Office for Europe; 2005; *Tobacco control database*; <http://data.euro.who.int/tobacco/>
2. Spiegel online; 2005; *Italienisches Rauchverbot - Grappa ohne Glimmstengel*; <http://www.spiegel.de/reise/aktuell/0,1518,335709,00.html>
3. D. Hoffmann and I. Hoffmann; 2001; *The changing cigarette: Chemical studies and bioassays*; Monograph 13: Risks associated with smoking cigarettes with low tar machine-measured yields of tar and nicotine; Rockville, Maryland, U.S.; Chapter 5; 159 - 185
4. GSF aktuell, Pressemitteilungen 2004; Presse- und Öffentlichkeitsarbeit; *Todesfälle und Milliardengrab Zigarettenschmerz: Volkswirtschaftliche Kosten des Rauchens*; Neuherberg; GSF - Research Center for Environment and Health
5. U. John and M. Hanke; 2003; *Tobacco- and alcohol-attributable mortality and years of potential life lost in Germany*; European Journal of Public Health; 13; 275 - 277
6. R. Welte, H.-J. König and R. Leidl; 2000; *The costs of health damage and productivity losses attributable to cigarette smoking in Germany*; European Journal of Public Health; 10; 31 - 38
7. C. E. Bartecchi, T. D. MacKenzie and R. W. Schrier; 1994; *The human costs of tobacco use (first of two parts)*; New England Journal of Medicine; 330; 13; 907 - 912
8. T. D. MacKenzie, C. E. Bartecchi and R. W. Schrier; 1994; *The human costs of tobacco use (second of two parts)*; New England Journal of Medicine; 330; 14; 975 - 980
9. Contrapress media GmbH; 2005; *Steuereinnahmen aus Tabak sinken*; <http://www.taz.de/pt/2005/08/27/a0135.nf/textdruck>; die tageszeitung taz
10. K. Strobel; 2005; *Tabakwerbeverbot: Fallbeil aus Brüssel*; ZDF - Zweites Deutsches Fernsehen; <http://www.zdf.de/ZDFde/inhalt/25/0,1872,2343641,00.html>

11. Commission of the European Communities; 2003; *Tobacco regime. Extended Impact Assessment*;  
[http://europa.eu.int/comm/agriculture/publi/reports/tobacco/fullrep\\_en.pdf](http://europa.eu.int/comm/agriculture/publi/reports/tobacco/fullrep_en.pdf)
12. ASPECT Consortium; 2004; *Chapter 2 - The economics of tobacco and tobacco control in the European Union*; Tobacco or health in the European Union - past, present and future; Luxembourg
13. G. F. Peedin; 1999; *5 A. Flue-cured tobacco*; L. D. Davis and M. T. Nielsen; Tobacco - Production, Chemistry, and Technology; Oxford, U.K.; Blackwell Science; 104 - 142
14. R. R. Baker; 1999; *Smoke Chemistry*; L. D. Davis and M. T. Nielsen; Tobacco: Production, Chemistry, and Technology; Oxford, U. K.; Blackwell Science; 398 - 439
15. K. E. Kingsborough; 1825; *Antiquities of Mexico. Comparing facsimilies of ancient Mexican paintings*; London; 1831 - 1849
16. T. C. Tso; 1990; *Production, physiology and biochemistry of the tobacco plant*; Beltsville, Maryland; Ideals Inc.; p. 753
17. J. Leavey; 1998; *A history of tobacco*; <http://www.forces.org/writers/james/files/history.htm>
18. D. Hoffmann and I. Hoffmann; 1998; *Chemistry and toxicology*; D. Burns, K. M. Cummings and D. Hoffmann; Cigars: Health effects and trends, smoking and tobacco control monograph No. 9; Bethesda; US Department of Health and Human Services, National Institutes of Health, National Cancer Institute; NIH Publication No. 98-4302; 55 - 104
19. G. Borio; 1997; *The history of tobacco. Part I*; <http://www.historian.org/bysubject/tobacco1.htm>
20. H. P. Jeffers and K. Gordon; 1996; *The good cigar*; New York; Lyons and Burford Publishers
21. G. Borio; 1997; *The history of tobacco. Part II*; <http://www.historian.org/bysubject/tobacco2.htm>

22. V. R. Randall; 1999; *History of tobacco*; <http://academic.udayton.edu/health/syllabi/tobacco/history.htm>; Boston University Medical Center
23. RJ Reynolds; *Tobacco Risk Awareness Timeline*; <http://www.rjrt.com/smoking/aware/Timeline.aspx>
24. R. N. Proctor; 2004; *Tobacco and health*; <http://www.psljournal.com/archives/papers/tobacco2.cfm>; The journal of philosophy, science and law
25. J. Cortyl; 1897; *Du cancer des fumeurs*; Paris; Henri Jouve
26. R. N. Proctor and H. Collins; 1996; *Cancer wars: how politics shapes what we know and don't know about cancer*; Harpercollins
27. H. L. Lombard and C. R. Doering; 1928; *Cancer studies in Massachusetts*; New England Journal of Medicine; 198; 481 - 487
28. H. Rottmann; 1898; *Über primäre Lungencarcinome*; University of Würzburg
29. I. Adler; 1912; *Primary malignant growths of the lungs and bronchi*; London; Longmans
30. F. Lickint; 1929; *Tabak und Tabakrauch als ätiologischer Faktor des Carcinoms*; Zeitschrift für Krebsforschung; 30; 349 - 365
31. F. H. Müller; 1939; *Abuse of the tobacco and carcinoma of lung*; Journal of the American Medical Association; 113; p. 1372
32. F. H. Müller; 1939; *Tabakmissbrauch und Lungencarcinom*; Zeitschrift für Krebsforschung; 49; 57 - 85
33. R. Pearl; 1938; *Tobacco smoking and longevity*; Science; 87; 216 - 217
34. A. Ochsner and M. DeBakey; 1939; *Primary pulmonary malignancy*; Surgery, Gynecology and Obstetrics; 68; 435 - 451
35. A. Ochsner and M. DeBakey; 1947; *Primary cancer of the lung*; Journal of the American Medical Association; 135; 6; 321 - 327

36. E. J. Grace; 1944; *Tobacco smoking and cancer of the lung*; American Journal of Surgery; 60; 361 - 364
37. F. E. Tylecote; 1927; *Cancer of the lung*; Lancet; 2; 256 - 257
38. R. Doll and A. B. Hill; 1950; *Smoking and carcinoma of the lung*; British Medical Journal; 2; 739 - 748
39. E. L. Wynder and E. A. Graham; 1950; *Tobacco smoking as a possible etiologic factor in bronchiogenic carcinoma*; Journal of the American Medical Association; 143; 4; 329 - 335
40. E. L. Wynder, F. R. Lemon and I. J. Bross; 1959; *Cancer and coronary artery disease among seventh-day adventists*; Cancer; 12; 1016 - 1028
41. E. L. Wynder, I. J. Bross, J. Cornfield and W. E. O'Donnell; 1956; *Lung cancer in women*; New England Journal of Medicine; 255; 24; 1111 - 1121
42. E. L. Wynder; 1954; *Tobacco as a cause of lung cancer*; The Pennsylvania Medical Journal; 57; 11; 1073 - 1083
43. A. Ochsner, P. T. DeCamp, M. E. DeBakey and C. J. Ray; 1952; *Bronchogenic carcinoma*; Journal of the American Medical Association; 148; 9; 691 - 697
44. A. Ochsner; 1953; *Carcinoma of the lung*; Chicago Medical Society Bulletin; 138 - 142
45. R. Doll and A. B. Hill; 1954; *The mortality of doctors in relation to their smoking habits*; British Medical Journal; 1457 - 1455
46. R. Doll and A. B. Hill; 1956; *Lung cancer and other causes of death in relation to smoking*; British Medical Journal; 1071 - 1081
47. A. B. Hill and R. Doll; 1956; *Lung cancer and tobacco*; British Medical Journal; 1160 - 1163
48. E. L. Wynder, E. A. Graham and A. B. Croninger; 1953; *Experimental production of carcinoma with cigarette tar*; Cancer Research; 13; 855 - 864

49. E. L. Wynder, E. A. Graham and A. B. Croninger; 1955; *Experimental production of carcinoma with cigarette tar. II. Tests with different mouse strains*; Cancer Research; 15; 445 - 448
50. E. L. Wynder, P. Kopf and H. Ziegler; 1957; *A study of tobacco carcinogenesis. II. Dose - response studies*; Cancer; 10; 1193 - 1200
51. R. L. Cooper, A. J. Lindsey and R. E. Waller; 1954; *The presence of 3,4-benzopyrene in cigarette smoke*; Chemistry and Industry; 46; p. 1418
52. W. Dontenwill, H. J. Chevalier, H.-P. Harke, U. Lafrenz, G. Reckzeh and B. Schneider; 1973; *Investigations on the effects of chronic cigarette smoke inhalation in Syrian golden hamsters*; Journal of the National Cancer Institute; 51; 6; 1781 - 1832
53. P. Bernfeld, F. Homberger and A. B. Russfield; 1974; *Strain differences in the response of inbred Syrian hamsters to cigarette smoke inhalation*; Journal of the National Cancer Institute; 53; 4; 1141 - 1157
54. R. A. W. Johnstone and J. R. Plimmer; 1959; *The chemical constituents of tobacco and tobacco smoke*; Chemical Reviews; 59; 885 - 936
55. R. L. Stedman; 1968; *The chemical composition of tobacco and tobacco smoke*; Chemical Reviews; 68; 153 - 207
56. D. L. Roberts; 1988; *Natural tobacco flavour*; Recent Advances in Tobacco Science; 14; 49 - 81
57. C. R. Green and A. Rodgman; 1996; *The Tobacco Chemists' Research Conference: a half century forum for advances in analytical methodology of tobacco and its products*; Recent Advances in Tobacco Science; 22; 131 - 304
58. E. L. Wynder and D. Hoffmann; 1967; *Tobacco and tobacco smoke. Studies in experimental carcinogenesis*; New York; Academic press; p. 730
59. M. Z. DeBardleben, J. E. Wickham and W. F. Kuhn; 1991; *The determination of tar and nicotine in cigarette smoke from an historical perspective*; Recent Advances in Tobacco Science; 17; 115 - 148

60. R. R. Baker; 2002; *The Development and Significance of Standards for Smoking-Machine Methodology*; Beiträge zur Tabakforschung International; 20; 1; 23 - 41
61. 1997; *Smoking machines*; Beiträge zur Tabakforschung International; 17; 3; 99 - 100
62. M. F. Borgerding; 1997; *The FTC method in 1997 - what alternative smoking condition(s) does the future hold?*; Recent Advances in Tobacco Science; 23; 75 - 151
63. M. F. Dube and C. R. Green; 1982; *Methods of collection of smoke for analytical purposes*; Recent Advances in Tobacco Science; 8; 42 - 102
64. W. B. J. Wartman, E. C. Cogbill and E. S. Harlow; 1959; *Determination of particulate matter in concentrated aerosols. Application to analysis of cigarette smoke*; Analytical Chemistry; 31; 1705 - 1709
65. R. E. Thornton; 1978; *Smoking behaviour, physiological and psychological influences*; London; Churchill Livingstone; p. 405
66. A. R. Guyatt, A. J. T. Kirkham, A. G. Baldry, M. Dixon and G. Cumming; 1988; *How does puffing behaviour alter during the smoking of a single cigarette?*; Pharmacology Biochemistry & Behaviour; 33; 189 - 195
67. G. C. Kabat; 2003; *Fifty years' experience of reduced-tar cigarettes: What do we know about their health effects?*; Inhalation Toxicology; 15; 1059 - 1102
68. M. V. Djordjevic, D. Hoffmann and I. Hoffmann; 1997; *Nicotine regulates smoking patterns*; Preventive Medicine; 26; 435 - 440
69. R. R. Baker and L. S. Lewis; 2001; *A review of the incidence and consequences of cigarette filter vent blocking among smokers*; Beiträge zur Tabakforschung International; 19; 4; 209 - 228
70. G. Scherer; 1999; *Smoking behaviour and compensation: a review of the literature*; Psychopharmacology; 145; 1 - 20
71. J. Dallüge, L. L. P. van Stee, X. Xu, J. Williams, J. Beens, R. J. J. Vreuls and U. A. T. Brinkman; 2002; *Unravelling the composition of very complex samples by comprehensive gas chromatography coupled to time-of-flight mass spectrometry: Cigarette Smoke*; Journal of Chromatography A; 974; 169 - 184

72. W. Welthagen, S. Mitschke, T. Adam, T. Streibel and R. Zimmermann; 2005; *Puff-by-puff resolved tobacco smoke particulates analyzed by comprehensive two-dimensional gas chromatography time-of-flight mass spectrometry (GCxGC-TOFMS)*; CORESTA Congress; Coresta Joint Study Groups Meeting 2005; Smoke Science & Product Technology; Stratford-upon-Avon, U.K.
73. H. Wakeham; 1971; *Recent trends in tobacco and tobacco smoke research*; I. Schmeltz; 162<sup>nd</sup> National Meeting of the American Chemical Society; Washington DC; NY: Plenum Press; 1 - 20; Proceedings of the symposium on the chemical composition of tobacco and tobacco smoke
74. C. L. Gaworski, M. M. Dozier, S. R. Eldridge, R. Morrissey, N. Rajendran and J. M. Gerhart; 1998; *Cigarette smoke vapor-phase effects on the rat upper respiratory tract*; Inhalation Toxicology; 10; 857 - 873
75. V. Norman; 1977; *An overview of the vapor phase, semivolatile and nonvolatile components of cigarette smoke*; Recent Advances in Tobacco Science; 3; 28 - 58
76. S. Bondurant, P. Shetty, R. Wallace and K. Stratton; 2001; *Tobacco smoke and toxicology. Chapter 10*; S. Bondurant, P. Shetty, R. Wallace and K. Stratton; Clearing the smoke; Washington D.C.; National Academy Press; 238 - 308
77. B. J. Ingebrethsen; 1986; *Aerosol studies of cigarette smoke*; Recent Advances in Tobacco Science; 12; 54 - 142
78. W. Stöber; 1982; *Generation, size distribution and composition of tobacco smoke aerosols*; Recent Advances in Tobacco Science; 8; 3 - 41
79. D. D. McRae; 1990; *The physical and chemical nature of tobacco smoke*; Recent Advances in Tobacco Science; 16; 233 - 323
80. C. H. Keith; 1982; *Particle Size Studies on Tobacco Smoke*; Beiträge zur Tabakforschung International; 11; 3; 123 - 131
81. D. M. Bernstein; 2004; *A review of the influence of particle size, puff volume, and inhalation pattern on the deposition of cigarette smoke particles in the respiratory tract*; Inhalation Toxicology; 16; 675 - 689

82. G. A. Ferron; 1977; *The size of soluble aerosol particles as a function of the humidity of the air: application to the human respiratory tract*; Journal of Aerosol Science; 8; 251 - 267
83. D. Hoffmann and S. S. Hecht; 1990; *Advances in tobacco carcinogenesis*; C. S. Cooper and P. L. Grover; Chemical carcinogenesis and mutagenesis I; London; Springer-Verlag; 307 - 364
84. D. Hoffmann and I. Hoffmann; 1997; *The changing cigarette: 1950 - 1995*; Journal of Toxicological and Environmental Health; 50; 307 - 364
85. D. Hoffmann and I. Hoffmann; 1998; *Letters to the Editor: Tobacco Smoke Components*; Beiträge zur Tabakforschung International; 18; 1; 49 - 52
86. D. Hoffmann, I. Hoffmann and K. El-Bayoumy; 2001; *The less harmful cigarette: A controversial issue. A tribute to Ernst L. Wynder*; Chemical Research in Toxicology; 14; 7; 767 - 790
87. C. J. Smith, T. A. Perfetti, M. A. Rumpel, A. Rodgman and D. J. Doolittle; 2001; *"IARC group 2B carcinogens" reported in cigarette mainstream smoke*; Food and Chemical Toxicology; 39; 183 - 205
88. C. J. Smith, T. A. Perfetti, M. A. Rumpel, A. Rodgman and D. J. Doolittle; 2000; *"IARC group 2A carcinogens" reported in cigarette mainstream smoke*; Food and Chemical Toxicology; 38; 371 - 383
89. C. J. Smith, S. D. Livingston and D. J. Doolittle; 1997; *An international literature survey of "IARC group I carcinogens" reported in mainstream cigarette smoke*; Food and Chemical Toxicology; 35; 1107 - 1130
90. A. Rodgman and C. R. Green; 2003; *Toxic chemicals in cigarette mainstream smoke - hazards and hoopla*; Beiträge zur Tabakforschung International; 20; 8; 481 - 545
91. C. K. Lee, C. W. Fulp, D. W. Bombick and D. J. Doolittle; 1996; *Inhibition of mutagenicity of N-nitrosamines by tobacco smoke and its constituents*; Mutation Research; 367; 83 - 92
92. A. Rodgman; 2003; *The Composition of Cigarette Smoke: Problems with Lists of Tumorigens*; Beiträge zur Tabakforschung International; 20; 6; 402 - 437

93. M. Ball, O. Pöpke and A. Lis; 1990; *Polychlordibenzodioxine und Polychlordibenzofurane in Cigarettenrauch*; Beiträge zur Tabakforschung International; 14; 6; 393 - 402
94. D. J. Vorhees, W. Heiger-Bernays and M. D. McClean; 1997; *Human health risk associated with cigarette smoke: The link between smoke constituents and additives*; Chelmsford; Menzie-Cura & Associates
95. J. Fowles and M. Bates; 2000; *The chemical constituents in cigarettes and cigarette smoke: Priorities for harm reduction, A report to the New Zealand Ministry of Health*; Pirirua; Kenepuru Science Centre; 1 - 67
96. J. Fowles and E. Dybing; 2003; *Application of toxicological risk assessment principles to the chemical constituents of cigarette smoke*; Tobacco Control; 12; 424 - 430
97. *ROEMPP Chemie-Lexikon*; 1995; J. Falbe and M. Regitz; Stuttgart; Thieme; 9<sup>th</sup> edition
98. K. D. Brunemann and D. Hoffmann; 1982; *Pyrolytic origins of major gas phase constituents of cigarette smoke*; Recent Advances in Tobacco Science; 8; 103 - 140
99. R. R. Baker; 1975; *Temperature variation within a cigarette combustion coal during the smoking cycle*; High Temperature Science; 7; 236 - 247
100. R. R. Baker and K. D. Kilburn; 1973; *The distribution of gases within the combustion coal of a cigarette*; Beiträge zur Tabakforschung International; 7; 2; 79 - 87
101. R. R. Baker; 1981; *Variation of the Gas Formation Regions within a Cigarette Combustion Coal during the Smoking Cycle*; Beiträge zur Tabakforschung International; 11; 1; 1 - 17
102. K. Gulan; 1966; *Natural smoulder in cigarettes*; Combustion and Flame; 10; 161 - 164
103. R. R. Baker; 1976; *The kinetics of tobacco pyrolysis*; Thermochemica Acta; 17; 29 - 63
104. R. R. Baker; 1975; *Contributions to the draw resistance of a burning cigarette*; Beiträge zur Tabakforschung International; 8; 124 - 131

105. R. R. Baker; 1976; *Gas velocities inside a burning cigarette*; Nature; 264; 167 - 169
106. R. W. Jenkins, R. T. Bass, R. H. Newman and M. K. Chavis; 1977; *Cigarette smoke formation studies. Part 5. The effects of the cigarette periphery on mainstream smoke formation*; Beiträge zur Tabakforschung International; 9; 126 - 130
107. A. Egerton, K. Gugan and F. J. Weinberg; 1963; *The mechanism of smouldering in cigarettes*; Combustion and Flame; 7; 63 - 78
108. R. R. Baker; 1977; *Combustion and thermal decomposition regions inside a burning cigarette*; Combustion and Flame; 30; 21 - 32
109. R. R. Baker; 1981; *Product formation mechanisms inside a burning cigarette*; Progress in Energy and Combustion Science; 7; 135 - 153
110. R. R. Baker; 1984; *The effect of ventilation on cigarette combustion mechanisms*; Recent Advances in Tobacco Science; 10; 88 - 150
111. R. R. Baker; 1987; *Some burning problems in tobacco science*; International conference on the physical and chemical processes occurring in a burning cigarette; Winston-Salem, North Carolina; R.J. Reynolds Tobacco Co.; 1 - 61
112. R. R. Baker and D. P. Robinson; 1990; *Tobacco combustion - the last ten years*; Recent Advances in Tobacco Science; 16; 3 - 101
113. D. W. Eaker; 1990; *Dynamic behaviour and filtration of mainstream smoke in the tobacco column and filter*; Recent Advances in Tobacco Science; 16; 103 - 185
114. R. R. Baker; 1987; *A review of pyrolysis studies to unravel reaction steps in burning tobacco*; Journal of Analytical and Applied Pyrolysis; 11; 555 - 573
115. C. L. Browne, C. H. Keith and R. E. Allen; 1980; *The effect of filter ventilation on the yield and composition of mainstream and sidestream smoke*; Beiträge zur Tabakforschung International; 10; 2; 81 - 90
116. W. R. Johnson, R. W. Hale, S. C. Clough and P. H. Chen; 1973; *Chemistry of the conversion of nitrate nitrogen to smoke products*; Nature; 243; 223 - 225

117. T. B. Williams; 1980; *The Determination of Nitric Oxide in Gas Phase Cigarette Smoke by Non-dispersive Infrared Analysis*; Beiträge zur Tabakforschung International; 10; 2; 91 - 99
118. V. Norman, A. M. Ibrig, T. M. Larson and B. L. Moss; 1983; *The effect of some nitrogenous blend components on NO/NO<sub>x</sub> and HCN levels in mainstream and sidestream smoke*; Beiträge zur Tabakforschung International; 12; 2; 55 - 62
119. S. Umemura, M. Muramatsu and T. Okada; 1986; *A Study on Precursors of Nitric Oxide in Sidestream Smoke*; Beiträge zur Tabakforschung International; 13; 4; 183 - 190
120. S. S. Hecht, I. Schmeltz and D. Hoffmann; 1977; *Nitrogenous compounds in cigarette smoke and their possible precursors*; Recent Advances in Tobacco Science; 3; 59 - 93
121. O. T. Chortyk and W. S. Schlotzhauer; 1973; *Studies on the pyrogenesis of tobacco smoke constituents (a review)*; Beiträge zur Tabakforschung International; 7; 3; 165 - 178
122. R. A. Heckman and F. W. Best; 1981; *An investigation of the lipophilic bases of cigarette smoke*; Tobacco Science; 25; 33 - 39
123. M. P. Newell, R. A. Heckman and R. F. Moates; 1978; *Isolation and identification of new components in the ether-soluble portion of cigarette smoke condensate*; Tobacco Science; 22; 6 - 11
124. W. S. Schlotzhauer and O. T. Chortyk; 1987; *Recent Advances in studies on the pyrosynthesis of cigarette smoke constituents*; Journal of Analytical and Applied Pyrolysis; 12; 193 - 222
125. C. R. Enzell and I. Wahlberg; 1980; *Leaf composition in relation to smoking quality and aroma*; Recent Advances in Tobacco Science; 6; 64 - 122
126. I. Wahlberg and C. R. Enzell; 1984; *Tobacco cembranoids*; Beiträge zur Tabakforschung International; 12; 3; 93 - 104
127. H. R. Burton and G. Childs; 1975; *The thermal degradation of tobacco*; Beiträge zur Tabakforschung International; 8; 4; 174 - 180

128. H. R. Burton and G. Childs; 1977; *Thermal decomposition of tobaccos*; Beiträge zur Tabakforschung International; 9; 1; 45 - 52
129. M. Frenklach; 1988; *On the driving force of PAH production*; 22nd Symposium (International) on Combustion; Pittsburgh; The Combustion Institute; 1075 - 1082
130. M. Frenklach and H. Wang; 1990; *Detailed modeling of soot particle nucleation and growth*; Twenty-third Symposium (International) on Combustion; Pittsburgh; The Combustion Institute; 1559 - 1566
131. R. F. Severson, M. E. Snook, O. T. Chortyk and R. F. Arrendale; 1976; *A chromatographic analysis for polynuclear aromatic hydrocarbons in small quantities of cigarette smoke condensate*; Beiträge zur Tabakforschung International; 8; 5; 273 - 282
132. M. E. Snook, R. F. Severson, H. C. Higman, R. F. Arrendale and O. T. Chortyk; 1976; *Polynuclear aromatic hydrocarbons of tobacco smoke: isolation and identification*; Beiträge zur Tabakforschung International; 8; 5; 250 - 272
133. M. E. Snook, R. F. Severson, R. F. Arrendale, H. C. Higman and O. T. Chortyk; 1977; *The identification of high molecular weight polynuclear aromatic hydrocarbons in a biologically active fraction of cigarette smoke condensate*; Beiträge zur Tabakforschung International; 9; 2; 79 - 101
134. M. R. Guerin; 1987; *Formation and physico-chemical nature of sidestream smoke*; I. K. O'Neill, K. D. Brunnemann, B. Dodet and D. Hoffmann; Environmental Carcinogens, methods of analysis and exposure measurement, Vol. 9, passive smoking; Lyon, France; IARC; Chapter 2; 11 - 23
135. R. F. Arrendale, R. F. Severson and M. E. Snook; 1980; *Quantitative Determination of Naphthalenes in Tobacco Smoke by Gas Chromatography*; Beiträge zur Tabakforschung International; 10; 2; 100 - 105
136. I. Schmeltz, J. Tosk and D. Hoffmann; 1976; *Formation and determination of naphthalenes in cigarette smoke*; Analytical Chemistry; 48; 4; 645 - 650

137. G. M. Badger, J. K. Donnelly and T. M. Spotswood; 1965; *The formation of aromatic hydrocarbons at high temperatures. XXIV. The pyrolysis of some tobacco constituents*; Australian Journal of Chemistry; 18; 1249 - 1266
138. J. Lam, B. O. Pedersen and T. Thomasen; 1985; *Pyrolytic disintegration of selected tobacco constituents and pyrosynthetic formation of aromatic hydrocarbons from cleavage products formed by pyrolysis*; Beiträge zur Tabakforschung International; 13; 1; 1 - 9
139. W. S. Schlotzhauer, I. Schmeltz and S. F. Osman; 1970; *Evidence for the origin of monoalkanes in cigarette smoke*; Chemistry and Industry (London); 43; 1377 - 1378
140. J. C. Leffingwell; 1976; *Nitrogen compounds of leaf and their relationship to smoking quality and aroma*; Recent Advances in Tobacco Science; 2; 1 - 31
141. T. Miyake and T. Shibamoto; 1995; *Quantitative analysis by gas chromatography of volatile carbonyl compounds in cigarette smoke*; Journal of Chromatography A; 693; 376 - 381
142. J. T. Williamson, J. F. Graham and D. R. Allman; 1965; *The modification of cigarette smoke by filter tips*; Beiträge zur Tabakforschung International; 3; 3; 233 - 242
143. IARC; 1985; *Allyl compounds, aldehydes, epoxides, and peroxides. IARC monographs on the evaluation of carcinogenic risk of chemicals to humans*; Lyon, France; International Agency for Research on Cancer; p. 369
144. I. Schmeltz and D. Hoffmann; 1977; *Nitrogen-containing compounds in tobacco and tobacco smoke*; Chemical Reviews; 77; 3; 295 - 311
145. I. Schmeltz, A. Wenger, D. Hoffmann and T. C. Tso; 1979; *Chemical studies on tobacco smoke. 63. On the fate of nicotine during pyrolysis and in a burning cigarette*; Journal of Agricultural and Food Chemistry; 27; 3; 602 - 608
146. T. S. Osdene; 1976; *Reaction mechanisms in the burning cigarette*; N. J. Fina; Second Philip Morris Science Symposium; New York; Philip Morris; 41 - 59; Proceedings of the Second Philip Morris Science Symposium: The recent chemistry of natural products, including tobacco

147. T. H. Houseman; 1973; *Studies of cigarette smoke transfer using radioisotopically labelled tobacco constituents*; Beiträge zur Tabakforschung International; 7; 3; 142 - 147
148. K. D. Brunnemann and D. Hoffmann; 1991; *Analytical studies on N-nitroamines in tobacco and tobacco smoke*; Recent Advances in Tobacco Science; 17; 71 - 112
149. A. Wiernik, A. Christakopoulos, L. Johnson and I. Wahlberg; 1995; *Effect of air-curing on the chemical composition of tobacco*; Recent Advances in Tobacco Science; 21; 39 - 80
150. D. Hoffmann, K. D. Brunnemann, B. Prokopczyk and M. V. Djordjevic; 1994; *Tobacco-specific N-nitroamines and areca-derived N-nitroamines: chemistry, biochemistry, carcinogenicity and relevance to humans*; Journal of Toxicology and Environmental Health; 41; 1 - 52
151. R. E. Allen and D. G. Vickroy; 1976; *The characterisation of cigarette smoke from Cytrel smoking products and its comparison to smoke from flue-cured tobacco. III. Particulate phase-analysis*; Beiträge zur Tabakforschung International; 8; 7; 430 - 437
152. R. W. Jenkins; 1985; *Neutron activation analysis in tobacco and cigarette smoke studies: 2R1 cigarette composition, smoke transference and butt filtration*; Beiträge zur Tabakforschung International; 13; 2; 59 - 65
153. R. W. Jenkins; 1990; *A review of the uses of nuclear radiation in tobacco and smoke research*; Beiträge zur Tabakforschung International; 14; 6; 353 - 378
154. W. A. Pryor, D. G. Prier and D. F. Church; 1983; *Electron-Spin Resonance Study of Mainstream and Sidestream Cigarette Smoke: Nature of the Free Radicals in Gas-Phase Smoke and in Cigarette Tar*; Environmental Health Perspectives; 47; 345 - 355
155. D. F. Church and W. A. Pryor; 1985; *Free-Radical Chemistry of Cigarette Smoke and Its Toxicology Implications*; Environmental Health Perspectives; 64; 111 - 126
156. W. A. Pryor, B. J. Hales, P. I. Premovic and D. F. Church; 1983; *The radicals in cigarette tar: their nature and suggested physiological implications*; Science; 220; 425 - 427

157. G. Jeanty, J. Massé, P. Bercot and F. Coq; 1984; *Quantitative Analysis of Cigarette Smoke Condensate Monophenols by Reverse-Phase High-Performance Liquid Chromatography*; Beiträge zur Tabakforschung International; 12; 5; 245 - 250
158. C. R. Green, F. W. J. Conrad, K. A. Bridle and M. F. Borgerding; 1985; *A Liquid Chromatography Procedure for Analysis of Nicotine on Cellulose Acetate Filters*; Beiträge zur Tabakforschung International; 13; 1; 11 - 16
159. B. Gerstenberg and M. Speck; 1986; *Determination of Catechol in Cigarette Smoke Condensate by High-Performance Liquid Chromatography (HPLC) Analysis with an Automated Precolumn Sample Preparation*; Beiträge zur Tabakforschung International; 13; 5; 239 - 242
160. G. Zurek, A. Büldt and U. Karst; 2000; *Determination of acetaldehyde in tobacco smoke using N-methyl-4-hydrazino-7-nitrobenzofurazan and liquid chromatography / mass spectrometry*; Fresenius Journal of Analytical Chemistry; 366; 396 - 399
161. F. Omori, N. Higashi, M. Chida, Y. Sone and S. Suhara; 1999; *Internal Standard-based Analytical Method for Tobacco Smoke Vapor Phase Components*; Beiträge zur Tabakforschung International; 18; 4; 131 - 146
162. J.-Z. Dong and S. C. Moldoveanu; 2004; *Gas chromatography - mass spectrometry of carbonyl compounds in cigarette mainstream smoke after derivatization with 2,4-dinitrophenylhydrazine*; Journal of Chromatography A; 1027; 25 - 35
163. G. Holzer and J. Oro; 1976; *Gas chromatographic - mass spectrometric evaluation of exhaled tobacco smoke*; Journal of Chromatography; 126; 771 - 785
164. G. Gmeiner, G. Stehlik and H. Tausch; 1997; *Determination of seventeen polycyclic aromatic hydrocarbons in tobacco smoke condensate*; Journal of Chromatography A; 767; 163 - 169
165. S. B. Stanfill and D. L. Ashley; 2000; *Quantitation of flavour-related alkenylbenzenes in tobacco smoke particulate by selected ion monitoring gas chromatography - mass spectrometry*; Journal of Agricultural and Food Chemistry; 48; 1298 - 1306
166. D. F. Magin; 1980; *Gas chromatography of simple monocarbonyls in cigarette whole smoke as the benzyloxime derivatives*; Journal of Chromatography; 202; 255 - 261

167. E. J. Nanni, M. E. Lovette, R. D. Hicks, K. W. Fowler and M. F. Borgerding; 1990; *Separation and quantitation of phenolic compounds in mainstream cigarette smoke by capillary gas chromatography with mass spectrometry in the selected-ion mode*; Journal of Chromatography; 505; 365 - 374
168. H. Sakuma, M. Kusama, N. Shimojima and S. Sugawara; 1978; *Gas chromatographic analysis of the p-nitrophenylhydrazones of low boiling carbonyl compounds in cigarette smoke*; Tobacco Science; 22; 158 - 160
169. J. Holtzclaw, S. Rose, J. Wyatt, D. Rounbehler and D. Fine; 1984; *Simultaneous determination of hydrazine, methylhydrazine, and 1,1-dimethylhydrazine in air by derivatization/gas chromatography*; Analytical Chemistry; 56; 2952 - 2956
170. R. E. Baren, M. E. Parrish, K. H. Shafer, C. N. Harward, Q. Shi, D. D. Nelson, J. B. McManus and M. S. Zahniser; 2004; *Quad quantum cascade laser spectrometer with dual gas cells for the simultaneous analysis of mainstream and sidestream cigarette smoke*; Spectrochimica Acta Part A; 60; 3437 - 3447
171. Q. Shi, D. D. Nelson, J. B. McManus, M. S. Zahniser, M. E. Parrish, R. E. Baren, K. H. Shafer and C. N. Harward; 2003; *Quantum Cascade Infrared Laser Spectroscopy for Real-Time Cigarette Smoke Analysis*; Analytical Chemistry; 75; 5180 - 5190
172. K. M. Hafner; 2004; *Untersuchungen zur Bildung brennstoffabhängiger Stickstoffoxide bei der Abfallverbrennung mittels analytischer Messmethoden*; PhD thesis; Technische Universität München
173. T. Streibel, K. Hafner, F. Mühlberger, T. Adam, R. Warnecke and R. Zimmermann; 2005; *Investigation of NO<sub>x</sub> precursor compounds and other combustion by-products in the primary combustion zone of a waste incineration plant using on-line, real time mass spectrometry and Fourier-Transform Infrared Spectrometry (FT-IR)*; Analytical and Bioanalytical Chemistry; DOI: 10.1007/s00216-005-3340-z
174. F. Mühlberger; 2003; *Entwicklung von on-line-Analyseverfahren auf Basis der Einphotonenionisations-Massenspektrometrie*; PhD thesis; Technische Universität München

175. L. Cao, R. Zimmermann, A. Kettrup and H. Z. Wang; 2004; *Investigation of combustion/pyrolysis behaviour of polyvinyl chloride materials by on-line single photon ionization/resonance enhanced multi-photon ionization-time of flight mass spectrometry*; Chinese Journal of Analytical Chemistry; 32; 6; 699 - 704
176. L. Cao, F. Mühlberger, T. Adam, T. Streibel, H. Z. Wang, A. Kettrup and R. Zimmermann; 2003; *Resonance-Enhanced Multiphoton Ionization and VUV-Single Photon Ionization as Soft and Selective Laser Ionization Methods for On-Line Time-of-Flight Mass Spectrometry: Investigation of the Pyrolysis of Typical Organic Contaminants in the Steel Recycling Process*; Analytical Chemistry; 75; 21; 5639 - 5645
177. F. Mühlberger, J. Wieser, A. Ulrich and R. Zimmermann; 2002; *Single photon ionization (SPI) via incoherent VUV-excimer light: robust and compact time-of-flight mass spectrometer for on-line, real-time process gas analysis*; Analytical Chemistry; 74; 15; 3790 - 3801
178. F. Mühlberger, J. Wieser, A. Morozov, A. Ulrich and R. Zimmermann; 2005; *Single-Photon Ionization Quadrupole Mass Spectrometry with an Electron Beam Pumped Excimer Light Source*; Analytical Chemistry; 77; 7; 2218 - 2226
179. R. Dorfner, T. Ferge, C. Yeretjian, A. Kettrup and R. Zimmermann 2004; *Laser mass spectrometry as on-line sensor for industrial process analysis: Process control of coffee roasting*; Analytical Chemistry; 76; 5; 1368 - 1402
180. R. Dorfner; 2004; *Echtzeit-Analyse von flüchtigen Verbindungen in Kaffee-Röstgasen*; PhD thesis; Technische Universität München
181. J. B. Pallix, U. Schühle, C. H. Becker and D. L. Huestis; 1989; *Advantages of Single-Photon Ionisation over Multiphoton Ionisation for Mass Spectrometric Surface Analysis of Bulk Organic Polymers*; Analytical Chemistry; 61; 805 - 811
182. H. Koizumi; 1991; *Predominant decay channel for superexcited organic molecules*; Journal of Chemical Physics; 95; 5846 - 5852
183. Y. Hatano; 2001; *Interaction of VUV photons with molecules: Spectroscopy and dynamics of molecular superexcited states*; Journal of Electron Spectroscopy and Related Phenomena; 119; 2-3; 107 - 125

184. Y. Hatano; 1999; *Interaction of vacuum ultraviolet photons with molecules. Formation and dissociation dynamics of molecular superexcited states*; Physics reports; 313; 109 - 169
185. R. Feng, G. Cooper and C. E. Brion; 2002; *Dipole (e,e) spectroscopic studies of benzene: quantitative photoabsorption in the UV, VUV and soft X-ray regions*; Journal of Electron Spectroscopy and Related Phenomena; 123; 2-3; 199 - 209
186. D. M. P. Holland, D. A. Shaw, I. Sumner, M. A. Bowler, R. A. Mackie, L. G. Shpinkova, L. Cooper, E. E. Rennie and C. A. F. Johnson; 2002; *A time-of-flight mass spectrometry study of the fragmentation of valence shell ionised benzene*; International Journal of Mass Spectrometry and Ion Processes; 220; 31 - 51
187. E. E. Rennie, C. A. F. Johnson, J. E. Parker, D. M. P. Holland, D. A. Shaw and M. A. Hayes; 1998; *A photoabsorption, photodissociation and photoelectron spectroscopy study of C<sub>6</sub>H<sub>6</sub> and C<sub>6</sub>D<sub>6</sub>*; Chemical Physics; 229; 107 - 123
188. M. Yoshino, J. Takeuchi and H. Suzuki; 1973; *Absorption cross section and photoionization efficiencies of benzene and styrene vapor in the vacuum ultraviolet*; Journal of the Physical Society of Japan; 34; 4; 1039 - 1044
189. R. Feng, G. Cooper and C. E. Brion; 2002; *Dipole (e,e + ion) spectroscopic studies of benzene: absolute oscillator strengths for molecular and dissociative photoionization in the VUV and soft X-ray regions*; Journal of Electron Spectroscopy and Related Phenomena; 123; 2-3; 211 - 223
190. L. Cooper, L. G. Shpinkova, E. E. Rennie, D. M. P. Holland and D. A. Shaw; 2001; *Time-of-flight mass spectrometry study of the fragmentation of valence shell ionised nitrobenzene*; International Journal of Mass Spectrometry and Ion Processes; 207; 223 - 239
191. S. Tixier, G. Cooper, R. Feng and C. E. Brion; 2002; *Measurement of absolute dipole oscillator strengths for pyridine: photoabsorption and the molecular and dissociative photoionization in the valence shell (4-200 eV)*; Journal of Electron Spectroscopy and Related Phenomena; 123; 185 - 197

192. D. A. Shaw, D. M. P. Holland, M. A. MacDonald, M. A. Hayes, L. G. Shpinkova, E. E. Rennie, C. A. F. Johnson, J. E. Parker and W. von Niessen; 1998; *An experimental and theoretical study of spectroscopic and thermodynamic properties of toluene*; Chemical Physics; 230; 97 - 116
193. H. W. Jochims, H. Baumgärtel and S. Leach; 1996; *Photoionization quantum yields of polycyclic aromatic hydrocarbons*; Astronomy and Astrophysics; 314; 1003 - 1009
194. H. W. Jochims, E. Rühl, H. Baumgärtel, S. Tobita and S. Leach; 1997; *VUV peaks in absorption spectra and photoion yield curves of polycyclic aromatic hydrocarbons and related compounds*; International Journal of Mass Spectrometry and Ion Processes; 167/168; 35 - 53
195. J. C. Person and P. P. Nicole; 1970; *Isotope Effects in the Photoionization Yields and the Absorption Cross Sections for Acetylene, Propyne, and Propene*; Journal of Chemical Physics; 53; 5; 1767 - 1774
196. J. W. Au, G. Cooper, G. R. Burton and C. E. Brion; 1994; *An valuation of atomic and molecular mixture rules and group additivity concepts for the estimation of radiation absorption by long-chained, saturated hydrocarbons at vacuum UV and soft X-ray energies*; Chemical Physics; 187; 305 - 316
197. G. H. Ho, M. S. Lin, Y. L. Wang and T. W. Chang; 1998; *Photoabsorption and photoionization of propyne*; Journal of Chemical Physics; 109; 14; 5868 - 5879
198. I. Cacelli, V. Carravetta, R. Moccia and A. Rizzo; 1988; *Photoionization and photoabsorption cross section calculations in molecules: CH<sub>4</sub>, NH<sub>3</sub>, H<sub>2</sub>O and HF*; Journal of Physical Chemistry; 92; 979 - 982
199. R. Feng and C. E. Brion; 2002; *Absolute photoabsorption cross-sections (oscillator strengths) for ethanol (5-200 eV)*; Chemical Physics; 282; 419 - 427
200. R. Feng, G. Cooper and C. E. Brion; 2001; *Ionic photofragmentation and photoionization of dimethyl ether in the VUV and soft X-ray regions (8.5-80 eV) - absolute oscillator strengths for molecular and dissociative photoionization*; Chemical Physics; 270; 319 - 332

201. G. R. Wight, M. J. van der Wiel and C. E. Brion; 1977; *Dipole oscillator strengths for excitation, ionisation and fragmentation of NH<sub>3</sub> in the 5 to 60 eV region*; Journal of Physics B: Atom. Molec. Phys.; 10; 10; 1863 - 1873
202. I. Cacelli and V. Carravetta; 1996; *Differential photoionization cross section calculation of NH<sub>3</sub> in the random phase approximation*; Journal of Physics B: At. Mol. Opt. Phys.; 29; 3363 - 3371
203. D. Edvardsson, P. Baltzer, L. Karlsson, B. Wannberg, D. M. P. Holland, D. A. Shaw and E. E. Rennie; 1999; *A photoabsorption, photodissociation and photoelectron spectroscopy study of NH<sub>3</sub> and ND<sub>3</sub>*; Journal of Physics B: At. Mol. Opt. Phys.; 32; 2583 - 2609
204. K. Watanabe, F. M. Matsunaga and H. Sakai; 1967; *Absorption Coefficient and Photoionization Yield of NO in the Region 580-1350 Å*; Applied Optics; 6; 3; 391 - 396
205. K. Watanabe, F. F. mArmo and E. C. Y. Inn; 1953; *Photoionization cross section of nitric oxide*; Physical Review; 91; 5; 1155 - 1158
206. J. W. Au and C. E. Brion; 1997; *Absolute oscillator strengths for the valence-shell photoabsorption (2-200 eV) and the molecular and dissociative photoionization (11-80 eV) of nitrogen dioxide*; Chemical Physics; 218; 109 - 126
207. R. Feng, G. Cooper and C. E. Brion; 1999; *Absolute oscillator strengths for hydrogen sulphide II. Ionic photofragmentation and photoionization in the valence shell continuum regions (10 - 60 eV)*; Chemical Physics; 249; 223 - 236
208. W. C. Wiley and I. H. McLaren; 1955; *Time-of-Flight Mass Spectrometer with Improved Resolution*; Review of Scientific Instruments; 26; 12; 1150 - 1157
209. B. A. Mamyrin, V. I. Karataev, D. V. Shmikk and V. A. Zagulin; 1973; *The mass-reflectron, a new nonmagnetic time-of-flight mass spectrometer with high resolution*; Journal of Experimental and Theoretical Physics; 37; 45 - 48
210. P. D. Maker and R. W. Terhune; 1965; *Optical effects due to an induced polarization third order in the electric field strength*; Physical Review; 137, Number 3A; 801 - 818

211. C. R. Vidal; 1987; *Four-Wave Frequency Mixing in Gases*; L. F. Mollenauer and J. C. White; Tunable Lasers; Series Four-Wave Frequency Mixing in Gases; Berlin; Springer Verlag; 59; 56 - 113
212. G. C. Bjorklund; 1975; *Effects of Focusing on Third-Order Nonlinear Processes in Isotropic Media*; IEEE Journal of Quantum Electronics; QE-11, No. 6; 287 - 296
213. C. H. Becker; 1991; *On the use of single-photon ionization for inorganic surface analysis*; Fresenius Journal of Analytical Chemistry; 341; 3 - 6
214. N. Materer, R. S. Goodman and S. R. Leone; 1997; *Laser single-photon ionization mass spectrometry measurements of SiCl and SiCl<sub>2</sub> during thermal etching of Si(100)*; Journal of Vacuum Science and Technology; A 15(4), Jul/Aug 1997; 2134 - 2142
215. J. L. Trevor, L. Hanly and K. R. Lykke; 1997; *Laser Desorption/Vacuum Ultraviolet Photoionization of Alkanethiolate Self-assembled Monolayers*; Rapid Communications in Mass Spectrometry; 11; 587 - 589
216. J. G. Boyle, L. D. Pfefferle, E. E. Gulcicek and S. D. Colson; 1991; *Laser-driven electron ionization for a VUV photoionization time-of-flight mass spectrometer*; Review of Scientific Instruments; 62; 2; 323 - 333
217. A. H. Kung, J. F. Young and S. E. Harris; 1973; *Generation of 1182-Å radiation in phase-matched mixtures of inert gases*; Applied Physics Letters; 22; 301 - 303
218. A. H. Kung, J. F. Young and S. E. Harris; 1976; *Erratum: Generation of 1182-Å radiation in phase-matched mixtures of inert gases*; Applied Physics Letters; 28; p. 239
219. D. J. Butcher, D. E. Goeringer and G. B. Hurst; 1999; *Real-Time Determination of Aromatics in Automobile Exhaust by Single-Photon Ionization Ion Trap Mass Spectrometry*; Analytical Chemistry; 71; 2; 489 - 496
220. O. Kornienko, E. T. Ada, J. Tinka, M. B. J. Wijesundara and L. Hanley; 1998; *Organic Surface Analysis by Two-Laser Ion Trap Mass Spectrometry. 2. Improved Desorption/Photoionisation Configuration*; Analytical Chemistry; 70; 1208 - 1213
221. F. Mühlberger; 2002; *Entwicklung einer Vakuum-UV-Ionenquelle für die Massenspektrometrie an Umweltproben*; Diploma thesis; Technische Universität München

222. R. J. J. M. Steenvoorden, P. G. Kistemaker, A. E. Vries, L. Michalak and N. M. M. Nibbering; 1991; *Laser single photon ionization mass spectrometry of linear, branched and cyclic hexanes*; International Journal of Mass Spectrometry and Ion Processes; 107; 475 - 489
223. E. Nir, H. E. Hunziker and M. S. Vries; 1999; *Fragment-Free Mass Spectrometric Analysis with Jet Cooling/VUV Photoionization*; Analytical Chemistry; 71; 1674 - 1678
224. R. J. J. M. Steenvoorden, E. R. E. Hage, J. J. Boon, P. G. Kistemaker and T. L. Weeding; 1994; *Investigation of the Effects of Cooling After Laser Desorption Before Post-ionization*; Organic Mass Spectrometry; 29; 78 - 84
225. F. Mühlberger, R. Zimmermann and A. Kettrup; 2001; *A Mobile Mass Spectrometer for Comprehensive On-Line Analysis of Trace and Bulk Components of Complex Gas Mixtures: Parallel Application of the Laser-Based Ionization Methods VUV Single-Photon Ionization, Resonant Multiphoton Ionization, and Laser-Induced Electron Impact Ionization*; Analytical Chemistry; 73; 15; 3590 - 3604
226. D. J. Butcher; 1999; *Vacuum ultraviolet radiation for single-photoionization mass spectrometry: a review*; Microchemical Journal; 62; 354 - 362
227. L. W. Sieck; 1983; *Determination of molecular weight distribution of aromatic components in petroleum products by chemical ionisation mass spectrometry with chlorobenzene as reagent gas*; Analytical Chemistry; 55; 38 - 41
228. National Institute of Standards and Technology NIST; 2005; *NIST Chemistry WebBook*; <http://webbook.nist.gov/chemistry/>
229. K. Hafner, R. Zimmermann, E. R. Rohwer, R. Dorfner and A. Kettrup; 2001; *A Capillary-Based Supersonic Jet Inlet System for Resonance-Enhanced Laser Ionization Mass Spectrometry: Principle and First On-line Process Analytical Applications*; Analytical Chemistry; 73; 17; 4171 - 4180

230. H. J. Heger, R. Zimmermann, R. Dorfner, M. Beckmann, H. Griebel, A. Kettrup and U. Boesl; 1999; *On-line Emission Analysis of Polycyclic Aromatic Hydrocarbons down to pptv Concentration Levels in the Flue Gas of an Incineration Pilot Plant with a Mobile Resonance-Enhanced Multiphoton Ionization Time-of-Flight Mass Spectrometer*; Analytical Chemistry; 71; 46 - 57
231. R. Zimmermann, H. J. Heger, A. Kettrup and U. Boesl; 1997; *A Mobile Resonance-enhanced Multiphoton Ionization Time-of-Flight Mass Spectrometry Device for On-line Analysis of Aromatic Pollutants in Waste Incinerator Flue Gases: First Results*; Rapid Communications in Mass Spectrometry; 11; 1095 - 1102
232. S. Mitschke, T. Adam, T. Streibel, R. R. Baker and R. Zimmermann; 2005; *Application of time-of-flight mass spectrometry with laser-based photo-ionization methods for time-resolved on-line analysis of mainstream cigarette smoke*; Analytical Chemistry; 77; 8; 2288 - 2296
233. B. A. Williams, T. N. Tanada and T. A. Cool; 1992; *Resonance Ionization Detection Limits for Hazardous Emissions*; 24th Symposium (International) on Combustion; Pittsburgh; The Combustion Institute; 1587-1596
234. M. Blazsó; 1997; *Recent trends in analytical and applied pyrolysis of polymers*; Journal of Analytical and Applied Pyrolysis; 39; 1 - 25
235. S. Tsuge; 1995; *Analytical pyrolysis - past, present and future*; Journal of Analytical and Applied Pyrolysis; 32; 1 - 6
236. W. J. Irvin; 1982; *Analytical pyrolysis - a comprehensive guide*; J. Cazes; Chromatographic Science Series; New York; Marcel Dekker; 22
237. T. P. Wampler; 1999; *Introduction to pyrolysis-capillary gas chromatography*; Journal of Chromatography A; 842; 207 - 220
238. T. P. Wampler; 2004; *Practical applications of analytical pyrolysis*; Journal of Analytical and Applied Pyrolysis; 71; 1; 1 - 12
239. H. L. C. Meuzelaar, W. Windig, A. M. Harper, S. M. Huff, W. H. McClennen and J. M. Richards; 1984; *Pyrolysis mass spectrometry of complex organic materials*; Science; 226; 268 - 274

240. J. J. Morelli; 1990; *Thermal analysis using mass spectrometry: A review*; Journal of Analytical and Applied Pyrolysis; 18; 1; 1 - 18
241. J. J. Boon; 1992; *Analytical pyrolysis mass spectrometry: new vistas opened by temperature-resolved in-source PYMS*; International Journal of Mass Spectrometry and Ion Processes; 118 - 119; 755 - 787
242. T. P. Wampler; 1989; *A selected bibliography of analytical pyrolysis applications 1980 - 1989*; Journal of Analytical and Applied Pyrolysis; 16; 4; 291 - 322
243. H.-J. Schulten; 1984; *Relevance of Analytical Pyrolysis Studies to Biomass Conversion*; Journal of Analytical and Applied Pyrolysis; 6; 251 - 272
244. H. Wilcken; 1996; *Quality control of paints: Pyrolysis-mass spectrometry and chemometrics*; Analytica Chimica Acta; 336; 201 - 208
245. R. F. Severson, W. S. Schlotzhauer, R. F. Arrendale, M. E. Snook and H. C. Higman; 1977; *Correlation of polynuclear aromatic hydrocarbon formation between pyrolysis and smoking*; Beiträge zur Tabakforschung International; 9; 1; 23 - 37
246. H.-R. Schulten; 1986; *Pyrolysis-field ionization mass spectrometry - A new method for direct, rapid characterization of tobacco*; Beiträge zur Tabakforschung International; 13; 5; 219 - 227
247. I. Schmeltz, A. Wenger, D. Hoffmann and T. C. Tso; 1979; *Chemical studies on tobacco smoke. 63. On the fate of nicotine during pyrolysis and in a burnt cigarette*; Journal of Agricultural and Food Chemistry; 27; 602 - 608
248. I. Schmeltz, W. S. Schlotzhauer and E. B. Higman; 1972; *Characteristic products from pyrolysis of nitrogenous organic substances*; Beiträge zur Tabakforschung International; 6; 3; 134 - 138
249. M. A. Scheijen, B. B.-d. Boer and J. Boon; 1989; *Evaluation of a tobacco fractionation procedure using pyrolysis mass spectrometry combined with multivariate analysis*; Beiträge zur Tabakforschung International; 14; 5; 261 - 282
250. H. Im, F. Rasouli and M. Hajaligol; 2003; *Formation of nitric oxide during tobacco oxidation*; Journal of Analytical and Applied Pyrolysis; 51; 7366 - 7372

251. J. M. Halket; 1985; *Rapid characterization of tobacco by combined direct pyrolysis-field ionization mass spectrometry and pyrolysis-gas chromatography-mass spectrometry*; Journal of Analytical and Applied Pyrolysis; 8; 547 - 560
252. G. Grimmer, A. Glaser and G. Wilhelm; 1966; *Die Bildung von Benzo(a)pyren und Benzo(e)pyren beim Erhitzen von Tabak in Abhängigkeit von Temperatur und Strömungsgeschwindigkeit in Luft- und Stickstoffatmosphäre*; Beiträge zur Tabakforschung International; 3; 6; 415 - 421
253. R. R. Baker; 1975; *The formation of the oxides of carbon by the pyrolysis of tobacco*; Beiträge zur Tabakforschung International; 8; 1; 16 - 27
254. J. D. Green, J. Chalmers and P. J. Kinnard; 1989; *The transfer of tobacco additives to cigarette smoke*; Beiträge zur Tabakforschung International; 14; 5; 283 - 288
255. S. S. Stotesbury; 1999; *The pyrolysis of tobacco additives as a means of predicting their behaviour in a burning cigarette*; Beiträge zur Tabakforschung International; 18; 4; 147 - 163
256. S. J. Stotesbury, L. J. Willoughby and A. Couch; 2000; *Pyrolysis of cigarette ingredients labelled with stable isotopes*; Beiträge zur Tabakforschung International; 19; 2; 55 - 64
257. E. B. Sanders, A. I. Goldsmith and J. I. Seeman; 2003; *A model that distinguishes the pyrolysis of D-glucose, D-fructose, and sucrose from that of cellulose. Application to the understanding of cigarette smoke formation*; Journal of Analytical and Applied Pyrolysis; 66; 29 - 50
258. W. S. Schlotzhauer, R. F. Arrendale and O. T. Chortyk; 1985; *The rapid pyrolytic characterization of tobacco leaf carbohydrate material*; Beiträge zur Tabakforschung International; 13; 2; 74 - 80
259. J. Lam, B. O. Pederson and T. Thomson; 1985; *Pyrolytic disintegration of selected tobacco constituents and pyrosynthetic formation of aromatic hydrocarbons from cleavage products formed by pyrolysis*; Beiträge zur Tabakforschung International; 13; 1; 1 - 9

260. S.-F. Wang, B.-Z. Liu, K.-J. Sun and Q.-D. Su; 2004; *Gas chromatographic-mass spectrometric determination of polycyclic aromatic hydrocarbons formed during the pyrolysis of phenylalanine*; Journal of Chromatography A; 1025; 255 - 261
261. R. R. Baker and L. J. Bishop; 2004; *The pyrolysis of tobacco ingredients*; Journal of Analytical and Applied Pyrolysis; 71; 1; 223 - 311
262. R. R. Baker, E. D. Massey and G. Smith; 2004; *An overview of the effects of tobacco ingredients on smoke chemistry and toxicity*; Food and Chemical Toxicology; 42S; 53 - 83
263. R. R. Baker and J. Pereira da Silva; 2004; *The effect of tobacco ingredients on smoke chemistry. Part II: Casing ingredients*; Food and Chemical Toxicology; 42S; S39 - S52
264. R. R. Baker, J. Pereira da Silva and G. Smith; 2004; *The effect of tobacco ingredients on smoke chemistry. Part I: Flavourings and additives*; Food and Chemical Toxicology; 42S; S3 - S37
265. E.-J. Shin, M. R. Hajaligol and F. Rasouli; 2003; *Characterizing biomatrix materials using pyrolysis molecular beam mass spectrometer and pattern recognition*; Journal of Analytical and Applied Pyrolysis; 68 - 69; 213 - 229
266. N. Simmleit and H.-R. Schulten; 1986; *Differentiation of commercial tobacco blends by pyrolysis field ionization mass spectrometry and pattern recognition*; Fresenius Journal of Analytical Chemistry; 324; 9 - 12
267. R. Zimmermann, H. J. Heger and A. Kettrup; 1999; *On-Line monitoring of traces of aromatic-, phenolic- and chlorinated components in flue gases of industrial scale incinerators and cigarette smoke by direct-inlet laser ionization-mass spectrometry (REMPI-TOFMS)*; Fresenius Journal of Analytical Chemistry; 363; 720 - 730
268. R. Zimmermann, R. Dorfner and A. Kettrup; 1999; *Direct analysis of products from plant material pyrolysis*; Journal of Analytical and Applied Pyrolysis; 49; Elsevier; 257 - 266
269. S. N. Gilchrist; 1999; *5C. Oriental tobacco*; L. D. Davis and M. T. Nielsen; Tobacco - Production, Chemistry, and Technology; Oxford, U.K.; Blackwell Science; 154 - 164

270. G. K. Palmer and R. C. Pearce; 1999; *5B. Light air-cured tobacco*; L. D. Davis and M. T. Nielsen; Tobacco - Production, Chemistry, and Technology; Oxford, U.K.; Blackwell Science; 143 - 153
271. J. I. Seeman, M. Dixon and H.-J. Hausmann; 2002; *Acetaldehyde in mainstream tobacco smoke: formation and occurrence in smoke and bioavailability in the smoker*; Chemical Research in Toxicology; 15; 11; 1331 - 1350
272. R. S. Adhav, S. R. Adhav and J. M. Pelaprat; 1987; *BBO's Nonlinear Optical Phase-Matching Properties*; Laser Focus/Electro-Optics; 74; 88 - 100
273. K. Haider; 1985; *Pyrolysis field ionization mass spectrometry of lignins, soil humic compounds and whole soil*; Journal of Analytical and Applied Pyrolysis; 8; 317 - 331
274. R. J. Evans and T. A. Milne; 1987; *Molecular characterization of the pyrolysis of biomass. I. Fundamentals*; Energy & Fuels; 1; 2; 123 - 137
275. J. C. Leffingwell; 1999; *Basic chemical constituents of tobacco leaf and differences among tobacco types*; D. L. Davis and M. T. Nielsen; Tobacco: Production, Chemistry and Technology; Oxford, UK; Blackwell Science; 265 - 284
276. G. H. Bokelman and W. S. Ryan; 1985; *Analyses of bright and burley tobacco laminae and stems*; Beiträge zur Tabakforschung International; 13; 1; 29 - 36
277. T. Adam, T. Streibel, S. Mitschke, F. Mühlberger, R. R. Baker and R. Zimmermann; 2005; *Application of time-of-flight mass spectrometry with laser-based photoionization methods for analytical pyrolysis of PVC and tobacco*; Journal of Analytical and Applied Pyrolysis; 74; 454 - 464
278. F. Biasioli, F. Gasperi, E. Aprea, D. Mott, E. Boscaini, D. Mayr and T. D. Märk; 2003; *Coupling proton transfer reaction-mass spectrometry with linear discriminant analysis: a case study*; Journal of Agricultural and Food Chemistry; 51; 7227 - 7233
279. R. Fisher; 1936; *The use of multiple measurements in taxonomic problems*; Annals of Eugenics; 7; 179 - 188
280. R. O. Duda and P. E. Hart; 1973; *Pattern classification and scene analysis*; New York; John Wiley & Sons Inc; p. 482

281. F. Marini, A. L. Magri, F. Balestrieri, F. Fabretti and D. Marini; 2004; *Supervised pattern recognition applied to the discrimination of the floral origin of six types of Italian honey samples*; *Analytica Chimica Acta*; 515; 117 - 125
282. H. Yoshida, R. Leardi, K. Funatsu and K. Varmuza; 2001; *Feature selection by genetic algorithms for mass spectral classifiers*; *Analytica Chimica Acta*; 446; 485 - 494
283. W. J. Egan, R. C. Galipo, B. K. Kochanowski, S. L. Morgan, E. G. Bartick, M. L. Miller, D. C. Ward and R. F. Mothershead; 2003; *Forensic discrimination of photocopy and printer toners. III: Multivariate statistics applied to scanning electron microscopy and pyrolysis gas chromatography/mass spectrometry*; *Analytical and Bioanalytical Chemistry*; 376; 1286 - 1297
284. A. D. Shaw, A. diCamillo, G. Vlahov, A. Jones, G. Bianchi, J. Rowland and D. B. Kell; 1997; *Discrimination of the variety and region of origin of extra virgin olive oils using  $^{13}\text{C}$  NMR and multivariate calibration with variable reduction*; *Analytica Chimica Acta*; 348; 357 - 374
285. S. Krishnan, K. Samudravijaya and P. V. S. Rao; 1996; *Feature selection for pattern classification with Gaussian mixture models: A new objective criterion*; *Pattern Recognition Letters*; 17; 803 - 809
286. P. Malkavaara, R. Alen and E. Kolehmainen; 2000; *Chemometrics: An important tool for the modern chemist, an example from wood-processing chemistry*; *Journal of Chemical Information and Computer Science*; 40; 438 - 441
287. M. A. Sharaf, D. L. Illman and B. R. Kowalski; 1986; *Chemometrics*; P. J. Elving and J. D. Winefordner; *Chemical analysis*; New York; John Wiley & Sons; 82; 1 - 295
288. D. L. Massart, B. G. M. Vandeginste, S. N. DEming, Y. Michotte and L. Kaufman; 1988; *Chemometrics: a textbook*; Volume 2; B. G. M. Vandeginste and L. Kaufman; *Data handling in science and technology*; Amsterdam; Elsevier Science Publishers B. V.
289. J. W. Einax, H. W. Zwanziger and S. Geiß; 1997; *Chemometrics in environmental analysis*; S. Pauly and C. Clauß; Weinheim; VCH Verlagsgesellschaft mbH; p. 384

290. S. Wold and M. Sjöström; 1998; *Chemometrics, present and future success*; *Chemometrics and intelligent laboratory systems*; 44; 3 - 14
291. H. Günzler; 1998; *Analytiker Taschenbuch*; Berlin; Springer; 19; p. 360
292. D. L. Massart and L. Kaufman; 1983; *The interpretation of analytical chemical data by the use of cluster analysis*; P. J. Elving and J. D. Winefordner; *Chemical analysis - A series of monographs on analytical chemistry and its applications*; New York; John Wiley & Sons; 65; 1 - 231
293. B. Lavine and J. J.J. Workman; 2004; *Chemometrics*; *Analytical Chemistry*; 76; 12; 3365 - 3372
294. I. T. Jolliffe; 1986; *Principal component analysis*; Springer series in statistics; New York; Springer-Verlag
295. S. Wold; 1987; *Principal Component Analysis*; *Chemometrics and Intelligent Laboratory Systems*; 2; 37 - 52
296. R. G. Brereton; 2000; *Introduction to multivariate calibration in analytical chemistry*; *The analyst*; 125; 2125 - 2154
297. I. Duarte, A. Barros, P. S. Belton, R. Righelato, M. Spraul, E. Humpfer and A. M. Gil; 2002; *High-resolution nuclear magnetic resonance spectroscopy and multivariate analysis for the characterization of beer*; *Journal of Agricultural and Food Chemistry*; 50; 2475 - 2481
298. M. J. Martin, F. Pablos and A. G. Gonzalez; 1996; *Application of pattern recognition to the discrimination of roasted coffees*; *Analytica Chimica Acta*; 320; 191 - 197
299. R. Briandet, E. K. Kemsley and R. H. Wilson; 1996; *Discrimination of arabica and robusta in instant coffee by fourier transform infrared spectroscopy and chemometrics*; *Journal of Agricultural and Food Chemistry*; 44; 170 - 174
300. L. Maeztu, C. Sanz, S. Andueza, M. P. d. Peña, J. Bello and C. Cid; 2001; *Characterization of espresso coffee aroma by static headspace GC-MS and sensory flavor profile*; *Journal of Agricultural and Food Chemistry*; 49; 5437 - 5444

301. S. J. Haswell and A. D. Walmsley; 1998; *Multivariate data visualization methods based on multi-elemental analysis of wines and coffees using total reflection X-ray fluorescence analysis*; Journal of Analytical Atomic Spectrometry; 13; 131 - 134
302. K. Héberger, E. Csomós and L. Simon-Sarkadi; 2003; *Principal component and linear discriminant analyses of free amino acids and biogenic amines in Hungarian wines*; Journal of Agricultural and Food Chemistry; 51; 8055 - 8060
303. C. P. Bicchi, A. E. Binello, M. M. Legovich, G. M. Pellegrino and A. C. Vanni; 1993; *Characterization of Roasted Coffee by S-HSGC an HPLC-UV and Principal Component Analysis*; Journal of Agriculture and Food Chemistry; 41; 12; 2324 - 2328
304. K. Wada, H. Sasaki, M. Shimoda and Y. Osajima; 1987; *Objective evaluation of various trade varieties of coffee by coupling of analytical data and multivariate analyses*; Agricultural and Biological Chemistry; 51; 7; 1753 - 1760
305. M. J. Martin, F. Pablos and A. G. Gonzalez; 1998; *Discrimination between arabica and robusta green coffee varieties according to their chemical composition*; Talanta; 46; 1259 - 1264
306. R. M. Alonso-Salces, S. Guyot, C. Herrero, L. A. Berrueta, J. F. Drilleau, B. Gallo and F. Vicente; 2004; *Chemometric characterisation of Basque and French ciders according to their polyphenolic profiles*; Analytical and Bioanalytical Chemistry; 379; 464 - 475
307. L.-K. Ng, M. Hupe, M. Vanier and D. Moccia; 2001; *Characterization of cigar tobaccos by gas chromatographic/mass spectrometric analysis of nonvolatile organic acids: Application to the authentication of cuban cigars*; Journal of Agricultural and Food Chemistry; 49; 1132 - 1138
308. M. Cocchi, G. Foca, M. Lucisano, A. Marchetti, M. A. Pagani, L. Tassi and A. Ulrici; 2004; *Classification of cereal flours by chemometric analysis of MIR spectra*; Journal of Agricultural and Food Chemistry; 52; 1062 - 1067
309. C. Armanino and M. R. Festa; 1996; *Characterization of wheat by four analytical parameters. A chemometric study*; Analytica Chimica Acta; 331; 43 - 51

310. C. Cordella, I. Moussa, A.-C. Martel, N. Sbirrazzuoli and L. Lizzani-Cuvelier; 2002; *Recent developments in food characterization and adulteration detection: technique-oriented perspectives*; Journal of Agricultural and Food Chemistry; 50; 1751 - 1764
311. R. Bucci, A. D. Magrí, A. L. Magrí, D. Marini and F. Marini; 2002; *Chemical authentication of extra virgin olive oil varieties by supervised chemometric procedures*; Journal of Agricultural and Food Chemistry; 50; 413 - 418
312. A. Martinez and A. Kak; 2001; *PCA versus LDA*; IEEE Transactions on pattern analysis and machine intelligence; 23; 2; 228 - 233
313. F. Mühlberger, A. Ulrich and P. Wallenta; 2003; *Moleküle im Anflug: Anwendung inkohärenter Vakuum-Ultraviolet-Lichtquellen zur Fotoionisation in der Massenspektrometrie*; Laser + Photonik; 3; 12 - 13
314. G. Vilcins; 1975; *Determination of Ethylene and Isoprene in the Gas Phase of Cigarette Smoke by Infrared Spectroscopy*; Beiträge zur Tabakforschung International; 8; 4; 181 - 185
315. P. Ceschini and A. Lafaye; 1976; *Evolution of the Gas-Vapour Phase and the Total Particulate Matter of Cigarette Smoke in a Single Puff*; Beiträge zur Tabakforschung International; 8; 6; 378 - 381
316. M. E. Parrish, J. L. Lyons-Hart and K. H. Shafer; 2001; *Puff-by-puff and intrapuff analysis of cigarette smoke using infrared spectroscopy*; Vibrational Spectroscopy; 27; 29 - 42
317. S. Li, J. L. Banyasz, M. E. Parrish, J. Lyons-Hart and K. H. Shafer; 2002; *Formaldehyde in the gas phase of mainstream cigarette smoke*; Journal of Analytical and Applied Pyrolysis; 65; 137 - 145
318. M. E. Parrish, C. N. Harward and G. Vilcins; 1986; *Simultaneous Monitoring of Filter Ventilation and a Gaseous Component in Whole Cigarette Smoke Using Tunable Diode Laser Infrared Spectroscopy*; Beiträge zur Tabakforschung International; 13; 4; 169 - 181

319. M. E. Parrish and C. N. Harward; 2000; *Measurement of Formaldehyde in a Single Puff of Cigarette Smoke Using Tunable Diode Laser Infrared Spectroscopy*; Applied Spectroscopy; 54; 11; 1665 - 1677
320. S. Plunkett, M. E. Parrish, K. H. Shafer, D. Nelson, J. Shorter and M. Zahniser; 2001; *Time-resolved analysis of cigarette combustion gases using a dual infrared tunable diode laser system*; Vibrational Spectroscopy; 27; 53 - 63
321. S. Plunkett, M. E. Parrish, K. H. Shafer, J. H. Shorter, D. D. Nelson and M. S. Zahniser; 2002; *Hydrazine detection limits in the cigarette smoke matrix using infrared tunable diode laser absorption spectroscopy*; Spectrochimica Acta Part A; 58; 2505 - 2517
322. C. E. Thomas and K. B. Koller; 2001; *Puff-by-puff Mainstream Smoke Analysis by Multiplex Gas Chromatography-Mass-Spectrometry*; Beiträge zur Tabakforschung International; 19; 7; 345 - 351
323. K. A. Wagner, R. Higby and K. Stutt; 2005; *Puff-by-puff analysis of selected mainstream smoke constituents in the Kentucky Reference 2R4F Cigarette*; Beiträge zur Tabakforschung International; 21; 5; 273 - 279
324. E. L. Crooks and D. Lynn; 1992; *The measurement of intrapuff nicotine yield*; Beiträge zur Tabakforschung International; 15; 2; 75 - 86
325. S. Li, R. M. Olegario, J. L. Banyasz and K. H. Shafer; 2003; *Gas chromatography-mass spectrometry analysis of polycyclic aromatic hydrocarbons in single puff of cigarette smoke*; Journal of Analytical and Applied Pyrolysis; 66; 156 - 163
326. R. R. Baker and C. J. Proctor; 2001; *2001 - A smoke odyssey*; Coresta 2001; Xian, China; Smoke & Technology Groups' Meeting
327. T. Higenbottam, C. Feyeraand and T. J. Clark; 1980; *Cigarette smoke inhalation and the acute airway response*; Thorax; 35; 4; 246 - 254
328. J. F. Pankow; 2001; *A consideration of the role of gas/particle partitioning in the deposition of nicotine and other tobacco smoke compounds in the respiratory tract*; Chemical Research in Toxicology; 14; 11; 1465 - 1481
329. S. Mitschke; PhD thesis; available 2007; University of Augsburg

330. P. X. Chen and S. C. Moldoveanu; 2003; *Mainstream smoke chemical analyses for 2R4F Kentucky Reference Cigarette*; *Beiträge zur Tabakforschung International*; 20; 7; 448 - 458
331. A. Norman; 1999; *11 B. Cigarette design and materials*; L. D. Davis and M. T. Nielsen; *Tobacco. Production, Chemistry and Technology*; Oxford, UK; Blackwell Science; 353 - 387
332. C. Liu; 2004; *Glycerol transfer in cigarette mainstream smoke*; *Beiträge zur Tabakforschung International*; 21; p. 111
333. A. Rodgman; 2002; *Some studies of the effects of additives on cigarette mainstream smoke properties. II. Casing materials and humectants*; *Beiträge zur Tabakforschung International*; 20; 4; 279 - 299
334. U.S. Patent No. 5,803,081; 1998
335. U.S. Department of Health and Human Services; 2004; *11<sup>th</sup> report on carcinogens*; Public Health Service, National Toxicology Program
336. W. A. Pryor; 1997; *Cigarette Smoke Radicals and the Role of Free Radicals in Chemical Carcinogenicity*; *Environmental Health Perspectives*; 105; 4; 875 - 882
337. R. Cueto and W. A. Pryor; 1994; *Cigarette smoke chemistry: conversion of nitric oxide to nitrogen dioxide and reactions of nitrogen oxides with other smoke components as studied by Fourier transform infrared spectroscopy*; *Vibrational Spectroscopy*; 7; 97 - 111
338. C. D. R. Borland, A. T. Chamberlain, T. W. Higenbottam, R. W. Barber and B. A. Thrush; 1985; *A Comparison between the Rate of Reaction of Nitric Oxide in the Gas Phase and in Whole Cigarette Smoke*; *Beiträge zur Tabakforschung International*; 13; 2; 67 - 73
339. W. A. Pryor, M. Tamura and D. F. Church; 1984; *ESR spin-trapping study of the radicals produced in NOx/olefin reactions: A mechanism for the production of the apparently long-lived radicals in gas-phase cigarette smoke*; *Journal of the American Chemical Society*; 106; 5073 - 5079

340. S. L. Baum, I. G. M. Anderson, R. R. Baker, D. M. Murphy and C. C. Rowlands; 2003; *Electron spin resonance and trap investigation of free radicals in cigarette smoke: development of a quantification procedure*; *Analytica Chimica Acta*; 481; 1 - 13
341. K. Shinagawa, T. Tokimoto and K. Shirane; 1998; *Spin Trapping of Nitric Oxide in Aqueous Solutions of Cigarette Smoke*; *Biochemical and Biophysical Research Communications*; 253; 99 - 103
342. IARC; 1999; *Re-evaluation of some organic chemicals, hydrazine, and hydrogen peroxide. IARC monographs on the evaluation of carcinogenic risk of chemicals to humans*; Lyon, France; International Agency for Research on Cancer; p. 1589
343. IARC; 1987; *Overall evaluations of carcinogenicity. IARC monographs on the evaluation of carcinogenic risk of chemicals to humans*; Lyon, France; International Agency for Research on Cancer; p. 440
344. D. W. Bombick, B. R. Bombick, P. H. Ayres, K. Putman, J. Avalos, M. F. Borgerding and D. J. Doolittle; 1997; *Evaluation of the genotoxic and cytotoxic potential of mainstream whole smoke and smoke condensate from a cigarette containing a novel carbon filter*; *Fundamental and Applied Toxicology*; 38; 11 - 17
345. D. Turnbull, J. V. Rodricks and S. M. Brett; 1990; *Assessment of the potential risk to workers from exposure to 1,3-butadiene*; *Environmental Health Perspectives*; 86; 159 - 171
346. R. L. Melnick, R. C. Sills, J. H. Roycroft, B. J. Chou, H. A. Ragan and R. A. Miller; 1994; *Isoprene, an endogenous hydrocarbon and industrial chemical, induces multiple organ neoplasia in rodents after 26 weeks of inhalation exposure*; *Cancer Research*; 54; 20; 5333 - 5339
347. R. Snyder and C. C. Hedli; 1996; *An overview of benzene metabolism*; *Environmental Health Perspectives*; 104; Supplement 6; 1165 - 1171

348. Q. Lan, L. Zhang, G. Li, R. Vermeulen, R. S. Weinberg, M. Dosemeci, S. M. Rappaport, M. Shen, B. P. Alter, Y. Wu, W. Kopp, S. Waidyanatha, C. Rabkin, W. Guo, S. Chanock, R. B. Hayes, M. Linet, S. Kim, S. Yin, N. Rothman and M. T. Smith; 2004; *Hematotoxicity in workers exposed to low levels of benzene*; Science; 306; 1774 - 1776
349. International Program on Chemical and Safety, IPCS; 2005; Canadian Centre for Occupational Health and Safety; <http://www.inchem.org/pages/icsc.html>
350. IARC; 1986; *Tobacco smoking. IARC monographs on the evaluation of carcinogenic risk of chemicals to humans*; Lyon, France; International Agency for Research on Cancer; p. 421
351. F. Mühlberger, K. Hafner, S. Kaesdorf, T. Ferge and R. Zimmermann; 2004; *Comprehensive On-Line Characterization of Complex Gas Mixtures by Quasi-Simultaneous Resonance-Enhanced-Multiphoton Ionization, Vacuum-UV-Single-Photon Ionization and Electron Impact Ionization in a Time-of-Flight Mass Spectrometer: Setup and Instrument Characterization*; Analytical Chemistry; 76; 22; 6753 - 6764
352. J.-Z. Dong, J. N. Glass, B. T. Thompson, B. F. Price, J. H. Lauterbach and S. C. Moldeoveanu; 2000; *A Simple Technique for Determining the pH of Whole Cigarette Smoke*; Beiträge zur Tabakforschung International; 19; 1; 33 - 48
353. J. F. Pankow, A. D. Tavakoli, W. Luo and L. M. Isabelle; 2003; *Percent free base nicotine in the tobacco smoke particulate matter of selected commercial and reference cigarettes*; Chemical Research in Toxicology; 16; 1014 - 1018
354. M. Dixon, K. Lambing and J. I. Seeman; 2000; *On the Transfer of Nicotine from Tobacco to the Smoker. A Brief Review of Ammonia and "pH" Factors*; Beiträge zur Tabakforschung International; 19; 2; 102 - 113
355. S. W. Purkis, C. A. Hill and I. A. Bailey; 2003; *Current measurement reliability of selected smoke analytes*; Beiträge zur Tabakforschung International; 20; 5; 314 - 324
356. G. Vilcins and J. O. Lephardt; 1975; *Ageing processes of cigarette smoke: formation of methyl nitrite*; Chemistry and Industry; 22; 974 - 975

357. C. H. Sloan and J. E. Keifer; 1969; *Determination of NO and NO<sub>2</sub> in cigarette smoke from kinetic data*; Tobacco Science; 13; 180 - 182
358. R. R. Baker and R. A. Crellin; 1977; *The diffusion of carbon monoxide out of cigarettes*; Beiträge zur Tabakforschung International; 9; 3; 131 - 140
359. S. Li, J. L. Banyasz, R. M. Olegario, C. B. Huang, E. A. Lambert and K. H. Shafer; 2002; *The flame effect on benzo[a]pyrene in cigarette smoke*; Combustion and Flame; 128; 314 - 319
360. J. I. Seeman, S. W. Laffoon and A.J.Kassman; 2003; *Evaluation of relationships between mainstream smoke acetaldehyde and "tar" and carbon monoxide yields in tobacco smoke and reducing sugars in tobacco blends of U.S. commercial cigarettes*; Inhalation Toxicology; 15; 373 - 395
361. H.-J. Eberhardt; 1995; *Human smoking behaviour in comparison with machine smoking methods: A summary of the five papers presented at the 1995 meeting of the CORESTA Smoke and Technology Groups in Vienna*; Beiträge zur Tabakforschung International; 16; 4; 131 - 140
362. K. D. Brunnemann, J. Masaryk and D. Hoffmann; 1983; *The role of tobacco stems in the formation of N-nitroamines in tobacco and cigarette mainstream and sidestream smoke*; Journal of Agricultural and Food Chemistry; 31; 1221 - 1224
363. T. Yamamoto, Y. Suga, C. Tokura, T. Toda and T. Okada; 1985; *Effect of Cigarette Circumference on Formation Rates of various Components in Mainstream Smoke*; Beiträge zur Tabakforschung International; 13; 2; 81 - 87
364. R. W. Dwyer and S. G. Abel; 1986; *The Efficiencies of Cellulose Acetate Filters*; Beiträge zur Tabakforschung International; 13; 5; 243 - 253
365. R. R. Baker; 1989; *The viscous and inertial flow of air through perforated papers*; Beiträge zur Tabakforschung International; 14; 5; 253 - 260

- 
366. K. Formella, T. Braumann and H. Elmenhorst; 1992; *The influence of different filter parameters on the semivolatile composition of mainstream smoke*; Beiträge zur Tabakforschung International; 15; 3; 123 - 128
367. D. Hoffmann, M. V. Djordjevic and I. Hoffmann; 1997; *The changing cigarette*; Preventive Medicine; 26; 427 - 434

**Abbreviations**

1R4F, 2R4F	Research cigarette codes
AG	Aktiengesellschaft
AVG	Average
Bp	Boiling point
CORESTA	Centre de Coopération pour les Recherches Scientifiques Relatives au Tabac
DIN	Deutsche Industrie Norm
EI	Electron impact
ETS	Environmental Tobacco Smoke
Fig.	Figure
FTC	Federal Trade Commission
FV	Fischer-Value, Fisher-Ratio
FWHM	Full width at half maximum
GC	Gas chromatography
GmbH	Gesellschaft mit begrenzter Haftung
i.d.	Inner diameter
IARC	International Agency for Research on Cancer
IE	Ionisation energy
Inc.	Incorporation
IP	Ionisation potential
IR	Infrared spectroscopy
ISO	International Organisation for Standards
KTRDC	Kentucky Tobacco Research & Development Center
MCP	Multi Channel Plate
MS	Mass spectrometry
MSS	Mainstream smoke
$m/z$	mass-to-charge ratio
NFT	New filter type cigarette
o.d.	Outer diameter
OSHA	Occupational Safety and Health Administration
PC	Principal component
PCA	Principal component analysis

---

pCi	pico Curie
PhD	Doctorate thesis
ppb	Parts per billion
ppm	Parts per million
Py	Pyrolysis
REMPI	Resonance enhanced multiphoton ionisation
S/N	Signal to noise ratio
SPI	Single Photon Ionisation
SSS	Sidestream smoke
THG	Third harmonic generator
TKR	Thomas-Kuhn-Reiche sum rule
TOF	Time-Of-Flight
TPM	Total Particulate Matter
TSNA	Tobacco-specific nitroamine
TWA <sub>8</sub>	Permissible eight hour time weighted average concentration
UK	United Kingdom
USA	United States of America
UV	ultraviolet
V <sub>p</sub>	vapour pressure
VUV	Vacuum ultraviolet
WHO	World Health Organisation

## List of figures

Figure 1: Photograph of a Cambridge filter pad (diameter 44 mm) before (right) and after (left) the smoking of one cigarette

Figure 2: Different smoke streams occurring in a burning cigarette and contributing to mainstream, sidestream, and environmental tobacco smoke [97]

Figures 3 A, B, and C: Temperature of the coal (Fig. 3 A), temperature of the gas phase (Fig. 3 B) and oxygen contribution (Fig. 3 C) inside the burning zone of a cigarette halfway through a 2 s puff [98-103]

Figure 4: Illustration of combustion zone and pyrolysis/distillation zone inside the cigarette's burning zone, and other effects inside the tobacco rod influencing the composition and concentration of tobacco smoke [14]

Figure 5: Chemical structures of some important PAHs identified in tobacco smoke and expected yields in non-filter cigarettes [75, 134, 135]

Figure 6: Chemical structures of the most common tobacco alkaloids together with typical mainstream smoke yields of non-filter cigarettes [134, 143]

Figure 7: Some possible products of the pyrolysis and combustion of originally present nicotine in tobacco together with percentage fraction and separation in mainstream and sidestream smoke [145]

Figure 8: Formation of tobacco-specific nitroamines NNK, NNN, NAB, NAT, NNA, NNAL, iso-NNAL, and iso-NNAC from common tobacco alkaloids [150]

Figure 9: Photoabsorption oscillator strength of benzene as a function of the photon energy in the range from 4 to 56 eV [185]

Figure 10: Photoionisation cross section for the formation of  $C_6H_6^+$  from benzene in the range from 9 to 30 eV [186]

Figure 11: Time-of-flight spectra of benzene after ionisation with four different photon energies of 15.7, 22.4, 31.8, and 35.4 eV

Figure 12: Photoionisation cross sections for the formation of the  $C_6H_5^+$ ,  $C_6H_4^+$ ,  $C_4H_4^+$ ,  $C_4H_3^+$ ,  $C_4H_2^+$ , and  $C_3H_3^+$  fragments from benzene in the range from 13.8 to 30 eV [186]

Figure 13 A: Photograph of the SPI/REMPI/EI-TOFMS instrument which was used for all the experiments in this work

Figure 13 B: Sketch of the set-up of the SPI-TOFMS unit of the instrument

Figure 14: Ionisation potentials of certain classes of organic molecules as a function of their molecular weight [227]

Figure 15: Comparison of the signal intensities of the calibration gases of equal concentration normalised to the signal of benzene

Figure 16: Illustration of the experimental set-up of the SPI-TOFMS system coupled to the pyrolysis furnace

Figure 17: Outlet of the pyrolysis furnace with the quartz tube wrapped in heating mats and the transfer line of the SPI-TOFMS coupled orthogonally to the quartz tube

Figure 18: Inlet of the pyrolysis furnace and the quartz tube with the reaction gas line connected to the tube

Figure 19: Photograph of the quartz boat containing a tobacco sample taken before being pushed into the quartz tube of the pyrolysis furnace

Figures 20 A, B, and C: Conversion of time-resolved recorded mass spectra into averaged sum spectra including standard deviation

Figure 21: SPI sum spectra of Burley tobacco at 400 °C, 500 °C, 600 °C, 700 °C, 800 °C, 900 °C and 1000 °C in nitrogen

Figure 22: SPI sum spectra of Burley tobacco at 400 °C, 500 °C, 600 °C, 700 °C, 800 °C, 900 °C and 1000 °C in synthetic air

Figures 23 A, B, and C: Behaviour of primary (Fig. 23 A), secondary (Fig. 23 B), and tertiary components (Fig. 23 C) as a function of temperature from the pyrolysis of tobacco in nitrogen and air atmosphere by means of selected compounds and tobacco types

Figure 24: Thermal decomposition of nicotine in Burley tobacco in nitrogen in the temperature range from 400 °C to 1000 °C

Figure 25 A, B, C: Thermal behaviour of the possible nicotine pyrolysis products pyrroline (69  $m/z$ , Fig. 25 A), a nicotine fragment (84  $m/z$ , Fig. 25 B), and myosmine (146  $m/z$ , Fig. 25 C) in Burley tobacco in nitrogen in the temperature range from 400 °C to 1000 °C

Figure 26 A, B, C, and D: Thermal behaviour of the possible nicotine pyrolysis products pyrrol (67  $m/z$ , Fig. 26 A), methyl pyridine/aniline (93  $m/z$ , Fig. 26 B), styrene/pyridincarbonitrile (104  $m/z$ , Fig. 26 C), and vinylpyridine (105  $m/z$ , Fig. 26 D) in Burley tobacco in nitrogen in the temperature range from 400 °C to 1000 °C

Figure 27 A, B, C, D, E, and F: Thermal behaviour of the most stable possible nicotine pyrolysis products benzene (78  $m/z$ , Fig. 27 A), pyridine (79  $m/z$ , Fig. 27 B), benzonitrile (103  $m/z$ , Fig. 27 C), naphthalene (128  $m/z$ , Fig. 27 D), quinoline (129  $m/z$ , Fig. 27 E), and naphthalenecarbonitrile (153  $m/z$ , Fig. 27 F) in Burley tobacco in nitrogen in the temperature range from 400 °C to 1000 °C

Figure 28: Thermal behaviour of H<sub>2</sub>S (34  $m/z$ ) and methanethiol (48  $m/z$ ) as a function of temperature for the pyrolysis of Burley in nitrogen in the temperature range from 400 °C to 1000 °C

Figure 29: Averaged sum spectrum including standard deviation of the pyrolysis of Burley tobacco in nitrogen at 800 °C

Figure 30: Averaged sum spectrum including standard deviation of the pyrolysis of Virginia tobacco in nitrogen at 800 °C

Figure 31: Averaged sum spectrum including standard deviation of the pyrolysis of Oriental tobacco in nitrogen at 800 °C

Figure 32: Comparison of the content of nitrogen-containing substances from pyrolysis of Virginia, Burley and Oriental tobacco at 800 °C in nitrogen and air by means of  $\text{NH}_3$  (17  $m/z$ ) formed

Figure 33: Comparison of carbohydrate content for Virginia, Burley, and Oriental tobacco pyrolysed at 400 °C in nitrogen and air by means of furfural/dimethylfuran (96  $m/z$ ) formed

Figures 34 A, B, and C: Difference spectra between Burley and Oriental (Fig. 34 A), Burley and Virginia (Fig. 34 B) and Oriental and Virginia (Fig. 34 C) in nitrogen at 800 °C

Figure 35: Flow chart of the data pre-processing steps prior to Principal Component Analysis

Figures 36 A and B: Score (Fig. 36 A) and loading (Fig. 36 B) plots by using the  $m/z$  featuring the twenty five highest Fisher-Ratios for the Principal Component Analysis of the three tobacco types Burley, Oriental, and Virginia

Figures 37 A and B: Score (Figure 37 A) and loading (Fig. 37 B) plots by using the  $m/z$  featuring the three highest Fisher-Ratios for the Principal Component Analysis of the three tobacco types Burley, Oriental, and Virginia

Figure 38: Four different uptake mechanisms of smoke constituents in the humans' respiratory tract

Figure 39: Illustration of the experimental set-up of the smoking machine coupled to the SPI-TOFMS

Figure 40: Photograph of the modified smoking-machine connected to the Cambridge filter holder and the transfer line

Figure: 41: Processing of time-resolved mass spectra to quantified puff-by-puff resolved yields exemplarily shown for acetaldehyde

Figure 42: Comparison of gas phase and whole smoke by opposing two sum spectra of a completely smoked 2R4F cigarette

Figures 43 A and B: Successive smoking and cleaning puffs of the gas phase (Fig. 43 A) and whole smoke (Fig. 43 B) of the 2R4F cigarette, shown for acetaldehyde (44  $m/z$ )

Figure 44: Illustration of the three different approaches (A, B, and C) for the definition of 'whole cigarette' and the two approaches for the definition of 'single puff' (A' and B')

Figure 45: Quantitative, puff-by-puff resolved and total yields of hazardous substances analysed in the gas phase and whole smoke of the 2R4F research cigarette with cleaning puffs added to the smoking puffs

Figure 46: Quantitative, puff-by-puff resolved and total yields of hazardous substances analysed in the gas phase and whole smoke of the 2R4F research cigarette without cleaning puffs added to the smoking puffs

Figures 47 A, B, and C: Puff-resolved ratios of the compounds acetone (58  $m/z$ ; Fig. 47 C), toluene (92  $m/z$ ; Fig. 47 B), and butadiene (54  $m/z$ ; 47 A) in the vapour phase and the particulate phase of the 2R4F cigarette

Figure 48: Difference spectrum of the first and second puff of the 2R4F research cigarette

Figures 49 A and B: Fig. 49 A illustrates the score-plots of the three individual measurements and the mean of the scores. Fig. 49 B shows the mean only and the assigned puffs

Figures 50 A to D: Score-plots and loading-plots of first and second (Fig. 50 A and B) and first and third (Fig. 50 C and D) principal components of the 25 Fisher-Values from the first to the ninth puff

Figures 51 A to D: Score-plots and loading-plots of first and second (Fig. 51 A and B) and first and third (Fig. 51 C and D) principal components of the 25 Fisher-Values from the second to the ninth puff

Figure 52: Puff-by-puff resolved TPM yields of the four single tobacco types Oriental, Burley, Maryland, and Virginia as well as the 2R4F research cigarette

Figures 53 A and B: Comparison of two normalisation procedures shown for NO and acetaldehyde. On the left the total yields were divided by total tar and on the right by total TPM respectively

Figures 54 A to J: Quantitative puff-by-puff resolved and total absolute (top) and normalised (bottom) yields for each cigarette type

Figure 55: Qualitative puff-by-puff resolved and total absolute (top) and normalised (bottom) yields of  $\text{NH}_3$  (17  $m/z$ ) for each cigarette type

Figure 56 A to D: Difference spectra between first and second puff for all four single tobacco types Virginia (Fig. 56 A), Oriental (Fig. 56 B), Burley (Fig. 56 C), and Maryland (Fig. 56 D)

Figure 57: Puff-by-puff resolved and total TPM yields of the two cigarette types 'light' and 'NFT' as well as the 2R4F

Figures 58 A to J: Quantitative puff-by-puff resolved and total absolute (top) and normalised (bottom) yields for the three cigarette types

## List of tables

Table 1: Approximate chemical composition of whole mainstream smoke [63]

Table 2: Number of compounds identified in tobacco smoke addressed to different substance classes [63]

Table 3: List of biologically active agents in the mainstream smoke of non-filter cigarettes colloquially referred to as ‘Hoffmann list’ [85, 86]

Table 4: Three different rankings of smoke constituents by means of their carcinogenic potential in mainstream smoke [90, 94-96]

Table 5: Three different rankings of smoke constituents by means of their toxic but non-carcinogenic potential in mainstream smoke [90, 94-96]

Table 6: Technical specifications and properties of the used laser system and the VUV generation unit

Table 7: Relevant substance classes being ionisable by SPI with the VUV wavelength of 118 nm. Listed are the first species of each homologue row which have an IP below 10.49 eV. The IP of species belonging to the same homologue usually decreases with increasing molecular weight [228]

Table 8: Technical details and adjusted parameters of the transfer line sampling system

Table 9: Applied voltages and instrumental details of the time-of-flight mass spectrometer

Table 10: Detection limits of a variety of compounds. Presented are six different averages of mass spectra (1, 2, 3, 5, 10, and 100) which represent six different time resolutions

Table 11: Photoabsorption cross sections, photoionisation cross sections, photoionisation quantum yields, differences between the applied photon energy of 10.49 eV and the corresponding IPs, and the relative signal intensities of the standard compounds normalised to benzene [172]

Table 12: Assignment of observed tobacco masses to most possible chemical compounds in tobacco pyrolysis and cigarette smoke according to listed references

Table 13: Classification of observed tobacco masses as primary, secondary or tertiary component

Table 14: Growing, processing, and chemical properties of the tobacco types Virginia, Burley, and Oriental [13, 14, 269, 270, 275]

Table 15: Assignment of the twenty prevailing  $m/z$  of the difference spectrum Burley – Oriental

Table 16: Assignment of the twenty prevailing  $m/z$  of the difference spectrum Burley – Virginia

Table 17: Assignment of the twenty prevailing  $m/z$  of the difference spectrum Oriental – Virginia

Table 18: The  $m/z$  featuring the 25 highest Fisher-Values for the discrimination between Burley and Oriental

Table 19: The  $m/z$  featuring the 25 highest Fisher-Values for the discrimination between Burley and Virginia

Table 20: The  $m/z$  featuring the 25 highest Fisher-Values for the discrimination between Oriental and Virginia

Table 21: The  $m/z$  featuring the 25 highest Fisher-Values for the discrimination between Burley, Oriental, and Virginia

Table 22: Percentage composition of the University of Kentucky 2R4F research cigarette [330]

Table 23: Design parameters of the four single tobacco cigarettes and the Kentucky 2R4F research cigarette

Table 24: Design parameters of the 'light' cigarette and the 'New Filter Technology' (NFT) cigarette

Table 25: Chemical structures of the nine hazardous target molecules as well as some important physical and toxicological properties

Table 26: Total yields of diverse smoke constituents of the 2R4F research cigarette analysed by three different research groups

Tables 27 A and B: Averaged yield ( $\bar{m}$ ) and standard deviation (std) of the quantitative, puff-by-puff resolved compounds in  $\mu\text{g}$ , analysed in the gas phase (Table 27 B) and whole smoke (Table 27 A) of the 2R4F research cigarette by adding the cleaning puffs to the smoking puffs

Table 28: Pairwise and overall Fisher-Values for the puff-resolved smoking of the 2R4F cigarette

## Acknowledgment

Der praktische Teil der vorliegenden Arbeit wurde im Zeitraum von August 2002 bis September 2005 im Institut für Ökologische Chemie des GSF-Forschungszentrums für Umwelt und Gesundheit, Neuherberg, durchgeführt.

Herrn Prof. Dr. Antonius Kettrup danke ich sehr für die Aufnahme an seinem Institut.

Besonderer Dank gilt Herrn Prof. Dr. Ralf Zimmermann für die Aufnahme in seine Arbeitsgruppe, die interessante und vielseitige Themenstellung und die freundschaftliche Betreuung.

Herrn Prof. Dr. H. Parlar danke ich für die Übernahme des Koreferats.

Ich danke meinem ehemaligen Kollegen („Major“) Dr. Klaus Hafner für die Einarbeitung am Institut und die zahlreichen Diskussionen auch außerhalb der Wissenschaftswelt.

Besonderer Dank gilt auch Herrn Stefan Mitschke für die gute und erfolgreiche Zusammenarbeit am „Radikalprojekt“.

Herrn Dr. Thorsten Streibel danke ich herzlich für die vielseitigen und freundschaftlichen Gespräche und die angenehme Atmosphäre im Raum 21.

Herrn Dr. Fabian Mühlberger danke ich für die Hilfestellung bei technischen Problemen aller Art.

Desweiteren bedanke ich mich bei allen derzeitigen und ehemaligen Kollegen an der GSF, an der Universität Augsburg und am BifA für die hervorragende Stimmung in der Arbeitsgruppe („wo wir sind ist vorne“).

Herzlich bedanken möchte ich mich auch bei Dr. Richard R. Baker für die zahlreichen fachlichen Diskussionen, die Hilfe bei allen Fragen der Tabakchemie und das Korrekturlesen meiner Arbeit.

Ganz herzlicher Dank gilt meiner Freundin, meinen Eltern, meiner Schwester mit Familie und meinen Freunden für die seelische und moralische Unterstützung in allen Lebenslagen.

## List of publications

### I. Peer-reviewed scientific articles

1) T. Adam, E. Duthie, J. Feldmann

*Investigations into the use of copper and other metals as indicators for the authenticity of Scotch whiskies*

Journal of the Institute of Brewing; 108 (4), (2002) 459-464

2) L. Cao, F. Mühlberger, T. Adam, T. Streibel, H. Z. Wang, A. Kettrup, R. Zimmermann

*Resonance-enhanced multiphoton ionization and VUV-single photon ionization as soft and selective laser ionization methods for on-line time-of-flight mass spectrometry: Investigation of the pyrolysis of typical organic contaminants in the steel recycling process*

Analytical Chemistry; 75 (21), (2003) 5639-5645

3) T. Streibel, T. Adam, F. Mühlberger, L.Cao, R. Zimmermann

*Application of Time-of-Flight Mass Spectrometry with Laser-Based Photoionization Methods for Analytical Pyrolysis of PVC*

Organohalogen Compounds; (2004) 66

4) M. Fernandes-Whaley, F. Mühlberger, A. Whaley, T. Adam, R. Zimmermann, E. Rohwer, A. Walte

*On-line derivatization for resonance-enhanced multiphoton ionization time-of-flight mass spectrometry: Detection of aliphatic aldehydes and amines via reactive coupling of aromatic photo ionization labels*

Analytical Chemistry 77 (1), (2005) 1-10

5) T. Adam, T. Ferge, S. Mitschke, T. Streibel, R.R. Baker, R. Zimmermann

*Discrimination of three tobacco types (Burley, Virginia and Oriental) by pyrolysis single-photon ionisation–time-of-flight mass spectrometry and advanced statistical methods*

Analytical and Bioanalytical Chemistry; 381 (2), (2005) 487-499

- 6) S. Mitschke, T. Adam, T. Streibel, R.R. Baker, R. Zimmermann  
*Application of Time-of-Flight Mass Spectrometry with Laser-Based Photoionization Methods for Time-Resolved On-Line Analysis of Mainstream Cigarette Smoke*  
Analytical Chemistry; 77 (8), (2005) 2288-2296
- 7) T. Adam, T. Streibel, S. Mitschke, F. Mühlberger, R.R. Baker, R. Zimmermann  
*Application of time-of-flight mass spectrometry with laser-based photoionization methods for analytical pyrolysis of PVC and tobacco*  
Journal of Analytical and Applied Pyrolysis; 74 (1-2), (2005) 454-464
- 8) T. Streibel, K. Hafner, F. Mühlberger, T. Adam, R. Zimmermann  
*Resonance-enhanced multiphoton ionisation time-of-flight mass spectrometry for detection of nitrogen containing aliphatic and aromatic compounds: REMPI-spectroscopic investigation and on-line analytical application*  
Applied Spectroscopy; 60 (1), (2006) 72-79
- 9) T. Streibel, K. Hafner, F. Mühlberger, T. Adam, R. Warnecke, R. Zimmermann  
*Investigation of NO<sub>x</sub> precursor compounds and other combustion by-products in the primary combustion zone of a waste incineration plant using on-line, real time mass spectrometry and Fourier-Transform Infrared Spectrometry (FT-IR)*  
Analytical and Bioanalytical Chemistry; 384 (5), (2006) 1096-1106
- 10) T. Adam, S. Mitschke, T. Streibel, R.R. Baker, R. Zimmermann  
*Quantitative puff-by-puff resolved characterisation of selected toxic compounds in cigarette mainstream smoke*  
Chemical Research in Toxicology; 19 (4), (2006) 511-520
- 11) T. Adam, S. Mitschke, T. Streibel, R.R. Baker, R. Zimmermann  
*Puff-by-puff resolved characterisation of cigarette mainstream smoke by single photon ionisation (SPI) - time of flight mass spectrometry (TOFMS): Comparison of the 2R4F research cigarette and pure Burley, Virginia, Oriental and Maryland tobacco cigarettes*  
Analytica Chimica Acta; 572 (2), (2006) 219-229

12) T. Streibel, S. Mitschke, T. Adam, J. Weh, R. Zimmermann

*Thermal Desorption/Pyrolysis Coupled with Photo Ionisation Time-of-Flight Mass Spectrometry for the Analysis and Discrimination of pure tobacco samples*

submitted to Journal of Analytical and Applied Pyrolysis

## II. Poster presentations

1) CORESTA Congress; Kyoto, Japan; October 2004

*Application of laser ionization mass spectrometry for puff-resolved on-line characterization of organic compounds in cigarette smoke and off-gases from tobacco pyrolysis experiments*

S. Mitschke, T. Adam, T. Streibel, R.R. Baker, R. Zimmermann

2) 14. Anakon; Regensburg, Germany; February 2005

*Photoionisations-Massenspektrometrie für die Charakterisierung von organischen Spezies in Pyrolysegas von Tabak und Tabakrauch*

T. Streibel, T. Adam, S. Mitschke, R.R. Baker, R. Zimmermann

### III. Oral presentations and conference contributions

1) Colloquium Spectroscopicum Internationale CSI XXXIII; Granada; Spain;

10<sup>th</sup> September 2003

*On-Line Analysis Of Cigarette Smoke By Laser-Based Single-Photon-Ionization (SPI) And Resonance-Enhanced-Multiphoton Ionization (REMPI)*

2) 57<sup>th</sup> Tobacco Science & Research Conference TSRC; Norfolk, Virginia; USA;

23<sup>th</sup> September 2003

*On-Line Analysis Of Cigarette Smoke By Laser-Based Single-Photon-Ionization (SPI) And Resonance-Enhanced-Multiphoton Ionization (REMPI)*

3) American Health Foundation Cancer Center; Institute for Cancer Prevention; North White Plains, New York; USA; 26<sup>th</sup> September 2003

*On-Line Analysis Of Cigarette Smoke By Laser-Based Single-Photon-Ionization (SPI) And Resonance-Enhanced-Multiphoton Ionization (REMPI)*

4) Colloquium of the 'Institute of Ecological Chemistry' at the 'GSF Research Centre for Environment and Health'; Neuherberg, Germany; 20<sup>th</sup> January 2005

*Application of laser ionization mass spectrometry for puff-resolved on-line characterization of organic compounds in cigarette smoke and off-gases from tobacco pyrolysis experiments*

5) 59<sup>th</sup> Tobacco Science & Research Conference TSRC; Stone Mountain / Atlanta, Georgia; USA; 27<sup>th</sup> September 2005

*Puff-by-puff resolved analysis of cigarette mainstream smoke by laser based single photon ionization (SPI) – time-of-flight mass spectrometry (TOFMS)*

## Curriculum vitae

### Persönliche Daten

Name	Thomas Walter ADAM
Geburtsdatum	15. Dezember 1975
Geburtsort	Wasserburg am Inn
Nationalität	deutsch

### Schulausbildung

1982 – 1986	Grundschule in Haag in OB
1986 – 1995	Gymnasium in Wasserburg am Inn

### Studium

Sept. 1995 – Juli 1996	Sprachstudiums- (Goldsmith College, London) und Arbeitsaufenthalt in Hastings und London / England
Nov. 1996 – Juli 1998	Chemiestudium (Grundstudium) an der Universität Regensburg
Sept. 1998 – Aug. 1999	Chemiestudium an der University of Aberdeen / Schottland (Erasmus-Stipendiat)
Nov. 1999 – März 2001	Chemiestudium (Hauptstudium) an der Universität Regensburg
April 2001 – Dez. 2001	Diplomarbeit am Alfred-Wegener-Institut für Polar- und Meeresforschung in Bremerhaven (Titel: “Characteristion of size-fractionated aerosol particles from the East Atlantic and Spitsbergen”)
Aug. 2002 – Sept. 2005	Doktorarbeit im Institut für Ökologische Chemie des GSF-Forschungszentrum für Umwelt und Gesundheit, Neuherberg

